

Ebiloma, Godwin Unekwuajo (2017) *Identification of new lead compounds for the treatment of African trypanosomiasis*. PhD thesis.

<https://theses.gla.ac.uk/8340/>

Copyright and moral rights for this work are retained by the author

A copy can be downloaded for personal non-commercial research or study, without prior permission or charge

This work cannot be reproduced or quoted extensively from without first obtaining permission in writing from the author

The content must not be changed in any way or sold commercially in any format or medium without the formal permission of the author

When referring to this work, full bibliographic details including the author, title, awarding institution and date of the thesis must be given

Identification of new lead compounds for the treatment of African trypanosomiasis

Godwin Unekwuajo Ebiloma

**This thesis is submitted in fulfilment of the requirements for
the degree of Doctor of Philosophy**

**Institute of Infection, Immunity & Inflammation
College of Medical, Veterinary & Life Sciences
University of Glasgow**

January 2017

Abstract

African trypanosomiasis and leishmaniasis are caused by parasites which belong to the genera *Trypanosoma* and *Leishmania*, respectively. These diseases affect a large number of people in many parts of the world, and could be fatal if not properly treated. These diseases are also animal infective, where they also cause weight loss and significant number of deaths in domestic and wild animals, posing a restraint on agricultural outputs and economic prosperity, especially in resource poor communities. While these diseases can be treated with the available chemotherapy, this is faced with many challenges, including drug resistance, toxicity, high treatment cost and lack of guaranteed supply. Hence, there is a need for new treatment approaches. Here, we aim to examine the *in vitro* efficacy of purified natural compounds, and synthetic mitochondrion-targeting lipocations against these parasites, assay their toxicity to human cells *in vitro*, and investigate the mode of their antiparasite activities.

Natural products such as plant secondary metabolites serve as potent defence chemicals with an intrinsic multifunctional mode-of-action on plants pathogens, justifying their folkloric use as medicinal herbs, and their remarkable contributions to drug discovery. Consequently, we here report the results of the *in vitro* screening of extracts from seven selected medicinal plant species (*Centrosema pubescens*, *Moringa oleifera*, *Tridax procumbens*, *Polyalthia longifolia*, *Newbouldia laevis*, *Eucalyptus maculata*, and *Jathropha tanjorensis*), used traditionally to treat various parasitic infections in North central region of Nigeria, the isolation of their bioactive principles, and their mode of action.

The selected plants were extracted with hexane, ethyl acetate and methanol. Active principles were isolated by bioassay-led fractionation, testing for trypanocidal activity, and identified using NMR and mass spectrometry. EC₅₀ values for their activity against wild-type and multi-drug resistant *Trypanosoma brucei* were obtained using the viability indicator dye resazurin.

The result shows that crude extracts and isolated active compounds from *Polyalthia longifolia* and *Eucalyptus maculata*, in particular, display promising activity against drug-sensitive and multi-drug resistant *Trypanosoma brucei*. The EC₅₀ value of a clerodane (16 α -hydroxy-cleroda-3,13(14)-Z-dien-15,16-olide, HDK20) isolated from *Polyalthia longifolia* was as low as 0.38 μ g/mL, while a triterpenoid (3 β ,13 β -dihydroxy-urs-11-en-28-oic acid, HDK40) isolated from *Eucalyptus maculata* displayed an EC₅₀ of 1.58 μ g/mL. None of the isolated compounds

displayed toxicity towards Human Embryonic Kidney cells at concentrations up to 400 $\mu\text{g/mL}$. In addition, the isolated compounds were also active against *Leishmania mexicana*, as well as against *T. congolense*.

We further exploited various biochemical approaches to reveal the mode-of-action of HDK-20 and HDK-40 on Wild-Type *Trypanosoma brucei* trypomastigotes. Growth curves of *T. brucei* s427 wild-type grown in the continuous presence of HDK20 or HDK40 at concentrations $\geq \text{EC}_{50}$ showed the compounds were trypanocidal, and their effects were irreversible after a limited exposure time of 1 hour. Fluorescence microscopic assessment of DNA configuration revealed cell cycle defects after 8 hours of incubation with either compound: DNA synthesis could not be initiated, leading to a dramatic increase in cells with 1 nucleus and 1 kinetoplast (1N1K). DNA fragmentation became evident after 10 hours of incubation with compound HDK-20, visualised by flow cytometry and Terminal deoxynucleotidyl transferase dUTP Nick-End Labelling (TUNEL) assay. HDK-20 and HDK-40 also induced a fast and profound depolarisation of the parasites' mitochondrial membrane potential after 1 hour of incubation and this continued until a near complete depolarization was achieved after 12 hours. Intracellular ATP levels of the *T. brucei* were also measured and were found to be depleted by approximately 50% in treated cells. However untargeted metabolomic assessments of *T. brucei* cells did not reveal the targeting of any specific metabolic pathway.

Considering that lipophilic cations (LCs) can diffuse across biological membranes (and also cross the blood-brain barrier) to achieve therapeutic doses in tissues, we investigated a chemical strategy to boost the trypanocidal activity of 2,4-dihydroxybenzoate (2,4-DHB)- and salicylhydroxamate (SHAM)-based trypanocides with triphenylphosphonium and quinolinium LCs. The synthesized LC conjugates were active in the submicromolar to low nanomolar range against wild-type and multi-drug resistant strains of African trypanosomes (*T. brucei brucei* and *T. congolense*). This represents an improvement in trypanocidal potency of at least 200-fold, and up to >10,000-fold, compared with the non-LC coupled parent compounds 2,4-DHB and SHAM respectively. Selectivity over human cells ranged from >500 to >23,000. Mechanistic studies showed that the LC based inhibitors tested did not inhibit the cell cycle but affected parasite respiration in a dose-dependent manner. Mitochondrial functions were also studied for selected compounds, and we discovered that the compounds did inhibit mitochondrial function after 1

hour, and ATP generation was markedly reduced; suggesting that the trypanosome alternative oxidase (TAO) is the likely target of the two series of LC based inhibitors.

In order to carry out direct inhibition of TAO by our synthesized inhibitors, we expressed and purified the physiological form of TAO that does not include its N-terminal 25 amino acid mitochondrial targeting sequence (Δ MTS rTAO), and this was expressed in a haem deficient *E. coli* (FN102). This physiologically relevant rTAO enzyme was used to characterize the inhibitory efficacy of 32 cationic and non-cationic compounds and develop structure-activity relationships with these series of 2,4-DHB and SHAM derivatives. Kinetics of binding to Δ MTS rTAO determined by Lineweaver–Burk plot analysis, and Surface Plasmon Resonance (SPR) experiments indicated a non-competitive inhibition similar to the parent compounds. The inhibitors, which showed nanomolar IC_{50} values against Δ MTS rTAO in the same range as ascofuranone ($IC_{50} = 2$ nM) for the most potent compounds, also displayed *in vitro* efficacy against wild type and resistant strains of *T. brucei* and *T. congolense*. The cationic compounds were extremely potent trypanocides with EC_{50} values similar or lower than the reference drugs pentamidine and diminazene. Selectivity over human cells was >8 (for non-cationic compounds) and between >900 and $344,000$ for the cationic derivatives. As a whole, the data are consistent with TAO being the primary target of these inhibitors in the parasite cell.

Overall, we isolated several promising trypanocidal compounds from Nigerian medicinal plants; these showed low toxicity, no cross-resistance with current treatments, and were efficacious against kinetoplastid parasites including *L. mexicana* and both human-infective and veterinary *Trypanosoma* species. Both compounds showed a parasite-specific multi-target mechanism of action, which provides a biochemical explanation for their promising broad spectrum anti-parasite activity. We also conclude that effective mitochondrial targeting greatly potentiates the activity of TAO inhibitors. Hence, further structure activity relationship analysis is required to optimise these natural and synthetic lead compounds, while *in vivo* assays are ongoing to confirm their anti-trypanosome and anti-leishmania efficacies.

Table of Contents

Abstract.....	ii
Table of contents.....	v
List of Tables.....	xi
List of figures.....	xii
Acknowledgments.....	xv
Declaration.....	xvi
Abbreviations.....	xvii
 Chapter 1: Introduction.....	1
1.1 Trypanosomes and trypanosomiasis.....	2
1.1.1 Morphology and life cycle of <i>Trypanosoma brucei</i>	3
1.1.2 Human African Trypanosomiasis (HAT): The disease, pathology and clinical manifestation.....	7
1.1.3 Diagnosis, Treatment and control of HAT.....	10
1.1.4 African Animal Trypanosomiasis (AAT).....	12
1.1.5 Chemotherapy of African trypanosomiasis.....	14
1.1.6 Transporters involved in drug uptake and mechanisms of drug resistance in trypanosomes.....	21
1.2 <i>Leishmania</i> and leishmaniasis.....	26
1.2.1 Morphology and life cycle.....	26
1.2.2 Leishmaniasis: pathology and clinical manifestation.....	29
1.2.3 Treatment and control of leishmaniasis.....	30
1.3 Natural products in drug discovery.....	33
1.3.1 Natural products from fungi: Antibiotics.....	34
1.3.2 Natural products from plants: Secondary metabolites.....	36
1.3.3 Compounds derived from plants as anti-protozoal agents.....	37
1.3.4 Treatment of trypanosomiasis with natural products and their derivatives.....	38
1.3.5 Treatment of leishmaniasis with natural products and their derivatives.....	39
1.4 Mitochondrial biology of <i>T. b. brucei</i>	40
1.5 Trypanosome metabolism and drug targets.....	42
1.5.1 Divergent metabolism provides many potential drug targets in trypanosomes.....	42

1.5.2 The glycosome and glucose metabolism.....	43
1.5.3 The alternative oxidase in trypanosomes.....	46
1.5.4 TAO as a drug target – work done to date.....	47
1.6 Aims.....	51
Chapter 2: Materials and methods.....	52
2.1 Parasites, cell lines and cultures.....	53
2.1.1 <i>Trypanosoma brucei</i> and <i>Trypanosoma congolense</i> bloodstream forms (BSF).....	53
2.1.2 <i>Leishmania mexicana</i> promastigotes.....	54
2.1.3 Mammalian cell cultures.....	54
2.1.4 Bacterial strains.....	54
2.2 Preparation of stabilates.....	55
2.3 Materials.....	55
2.3.1 Growth media and chemicals.....	55
2.3.2 Phytochemical extraction materials and solvents.....	55
2.3.3 Test compounds and extracts.....	56
2.4 Phytochemical analysis.....	56
2.4.1 Plant collection and preparation of samples.....	56
2.4.2 Bioassay guided fractionation of crude extracts.....	58
2.4.3 Purification and characterization of promising extracts.....	58
2.4.4 Compound identification by Nuclear Magnetic Resonance (NMR) and Mass spectrometric based techniques.....	61
2.5 <i>In vitro</i> drug sensitivity assay using Resazurin (Alamar blue) dye.....	63
2.5.1 Drug sensitivity using Alamar Blue assay in bloodstream forms of <i>T. b. brucei</i>	63
2.5.2 Drug sensitivity using Alamar Blue assay in <i>L. mexicana</i> promastigotes.....	64
2.5.3 Assessment of cytotoxicity of test compounds on Human Embryonic Kidney cells and Human Foreskin Fibroblast cells using an improved protocol.....	65
2.6 Drug sensitivity assay using cell counts.....	65
2.7 Drug sensitivity assay using Propidium Iodide (PI).....	66
2.8 Determination of oxygen consumption rate.....	66
2.9 Determination of mitochondrial membrane potential (Ψ_m) using flow cytometry.....	67
2.10 Assessment of cell cycle (DNA content assay) using flow cytometry.....	67

2.11 Assessment of cell morphology and DNA configuration using fluorescence microscopy.....	68
2.12 TUNEL assay.....	69
2.13 ATP level determination.....	70
2.14 Metabolomic assessments of <i>T. b. brucei</i> cells treated with natural compounds.....	70
2.15 TAO over-expression.....	71
2.15.1 Extraction of Genomic DNA.....	71
2.15.2 Primer design for Polymerase Chain Reaction (PCR).....	72
2.15.3 Gradient PCR.....	72
2.15.4 Agarose Gel Electrophoresis of DNA.....	73
2.15.5 TAO gene amplification.....	73
2.15.6 Transformation of XL1 blue <i>E.coli</i>	73
2.15.7 PCR screening of colonies.....	73
2.15.8 Transfection of Blood Stream Form (BSF) <i>T. brucei</i> with <i>TbAOX</i> inserted into pHD1336.....	74
2.15.9 Real Time-PCR.....	75
2.16 Cloning, expression, and direct inhibitory studies of physiologic Trypanosome Alternative Oxidase (Δ MTS-TAO).....	75
2.16.1 Plasmid construction for recombinant TAO expression.....	75
2.16.2 SDS-PAGE of purified rTAO.....	76
2.16.3 Preparation of inner membrane-rich fraction.....	77
2.16.4 Membrane solubilisation.....	78
2.16.5 Purification of recombinant TAO.....	78
2.16.6 Preparation of Ubiquinol-1 (UQ ₁ H ₂) from Ubiquinone-1 (UQ ₁).....	79
2.16.7 Ubiquinol oxidase/TAO inhibitory assay.....	80
2.17 Surface Plasmon Resonance (SPR) binding analysis of enzyme-inhibitor complex.....	80
Chapter 3: Isolation of anti-parasitic compounds from Nigerian medicinal plants.....	81
3.1 Introduction.	82
3.2 Results.....	84
3.2.1 Antitrypanocidal activity and cross resistance studies of extracts using wild type and the Multi-drug resistant strains of <i>T. brucei</i>	84

3.2.2 <i>In vitro</i> selectivity of extracts: therapeutic index relative to Human Embryonic Kidney cells.....	85
3.2.3 Anti-Leishmanial activity of the primary plant extracts.....	87
3.2.4 Bioactivity-guided isolation of the active constituents from extracts.....	88
3.2.5 Trypanocidal activity of the purified active compounds.....	89
3.2.6 Cytotoxicity of the purified compounds.....	91
3.2.7 Activity of Purified compounds against <i>Trypanosoma congolense</i> and <i>Leishmania mexicana</i>	92
3.3 Discussion.....	93

Chapter 4: Investigations into the mode of action of selected natural compounds against *T. brucei*.....97

4.1 Introduction.....	98
4.2 Results.....	100
4.2.1 Effect of different concentrations of HDK20 and HDK40 on the growth curve of bloodstream form <i>T. brucei brucei</i> WT following long and limited exposures.....	100
4.2.2 Monitoring the speed of action (Time to kill) of HDK20 and HDK40 on Trypanosomes by using a propidium iodide based assay.....	102
4.2.3 Natural products cause cell cycle arrest in trypanosomes.....	103
4.2.4 Microscopical investigation of cellular morphology of <i>T. b. brucei</i> treated with purified natural compounds.....	105
4.2.5 Assessment of DNA breaks using TUNEL assay.....	106
4.2.6 Effects of purified natural compounds on mitochondrial membrane potential of <i>T. b. brucei</i> treated cells.....	108
4.2.7 Effects of purified natural compounds on ATP levels in <i>T. b. brucei</i>	110
4.2.8 Metabolomic assessments of <i>T. b. brucei</i> cells treated with sub-lethal doses of purified compounds.....	113
4.3 Discussion.....	119

Chapter 5: Evaluation of mitochondrion-targeting lipophilic cation conjugates of Salicylhydroxamate and 2,4-Dihydroxybenzoate as potential drugs against African trypanosomes.....126

5.1 Introduction.....	127
-----------------------	-----

5.2 Results.....	129
5.2.1 Assessment of trypanocidal activity of mitochondrion-targeting lipophilic cations on wild-type and multi-drug resistant trypanosome lines; determination of <i>in vitro</i> selectivity index.....	129
5.2.1.1 <i>In vitro</i> activity of lipophilic cation–TAO inhibitors on <i>T. brucei</i> (Lister s427) and <i>T. congolense</i> (strain IL3000) bloodstream forms.....	130
5.2.1.2 Assessment of cross-resistance with current anti-trypanosome drugs.....	134
5.2.1.3 Cytotoxic activity of lipophilic cation–TAO inhibitors on human cells and therapeutic index values.....	135
5.2.2 Analysis of structural determinants of the mitochondrial targeting inhibitors contributing to their trypanocidal activity.....	136
5.2.3 Monitoring the rate of trypanosome lysis induced by test compounds, using propidium iodide.....	138
5.3 Discussion.....	139
 Chapter 6: Investigation into the mode of action of mitochondria targeting lipophilic cations against <i>T. b. brucei</i> bloodstream form.....	141
6.1 Introduction.....	142
6.2 Results.....	143
6.2.1 Effects of TAO over-expression and aquaporin knockout in TAO activity against <i>T. b. brucei</i> bloodstream forms.....	143
6.2.2 Lipophilic cation–TAO inhibitors strongly affect the mitochondrial membrane potential (Ψ_m).....	150
6.2.3 Effects of lipophilic cation-TAO inhibitors on ATP levels in <i>T. b. brucei</i>	154
6.2.4 Effects of lipophilic cation-TAO inhibitors on oxygen consumption rate in <i>T. b. brucei</i>	156
6.2.5 Cell cycle analysis of lipophilic cation–TAO inhibitor exposed cells.....	160
6.3 Discussion.....	161
 Chapter 7: Direct inhibition studies with purified recombinant TAO lacking a mitochondria targeting signal.....	165
7.1 Introduction.....	166

7.2 Results.....	168
7.2.1 Complementation by rTAO of FN102 <i>E.coli</i> lacking a terminal oxidase.....	168
7.2.2 SDS-PAGE analysis of purified rTAO at various stages of purification and purification table for Δ MTS-TAO/ <i>fl</i> -TAO.....	172
7.2.3 Direct inhibitory studies with Δ MTS TAO: SAR studies with cationic and non-cationic inhibitors.....	173
7.2.4 Michaelis-Menten kinetics and double reciprocal Lineweaver-Burk plots for TAO inhibitors.....	179
7.2.5 Binding affinity of lipophilic cation–TAO inhibitor to TAO revealed by Surface Plasmon Resonance spectrometry (Biacore) experiments.....	182
7.3 Discussion.....	186
Chapter 8: General Discussion.....	191

List of Tables

Table 3.1 EC ₅₀ value, Resistance Factor (RF) and Selectivity Index (SI) of crude ethyl acetate (E), Hexane (H), and methanol (M) extracts from seven Nigerian medicinal plants.....	86
Table 3.2 Comparing the EC ₅₀ values of purified natural compounds for the different trypanosomes strains (s427 WT, B48 and AQP2/3KO, AQP1-3-KO, <i>TbAT1</i> -KO, and R0.8) used in this study.....	90
Table 4.1 General overview of the metabolome of treated cells at multivariate level.....	116
Table 4.2 Overview of differences in the intracellular metabolome after HDK20 or HDK40 treatment - univariate level.....	117
Table 4.3 Overview of the extracellular metabolome - univariate level (HDK20).....	118
Table 4.4 Overview of the extracellular metabolome - univariate level (HDK40).....	119
Table 5.1 EC ₅₀ values (μM) against Wild Type and Resistant Strains of <i>T. b. brucei</i> , <i>T. congolense</i> , and Cytotoxicity against Human Cells (CC ₅₀ , μM).....	131
Table 6.1 EC ₅₀ values (μM) of LC TAO inhibitors against BSF <i>T. b. b.</i> cell line over-expressing TAO, and glycerol (5 mM) potentiating effect on Wild type BSF <i>T. b. b.</i>	146
Table 6.2 EC ₅₀ values (μM) of LC TAO inhibitors against BSF <i>T. b. b.</i> cell line with double or triple knockouts of the aquaporin genes.....	148
Table 7.1 Purification and activity table for rTAO.....	173
Table 7.2 EC ₅₀ values (μM) against <i>T. b. brucei</i> WT and IC ₅₀ values of inhibition of rTAO (μM).....	175
Table 7.3 Summary table for TAO inhibitors' binding kinetics as revealed by SPR (BIAcore) experiments.....	185

List of Figures

Figure 1.1 Schematic diagram of <i>Trypanosoma brucei</i> in its intermediate bloodstream form, showing the major organelles.....	5
Figure 1.2 Life cycle of <i>Trypanosoma brucei</i>	6
Figure 1.3 Map of Africa showing the major subspecies of <i>Trypanosoma brucei</i> , the causative agents of HAT according to geographic distribution.....	9
Figure 1.4 Some of the chemical structures of substances known to be active against African trypanosomiasis.....	19
Figure 1.5 Chemical structures of the prodrug pafuramidine (DB289) and the active drug furamidine (DB75).....	20
Figure 1.6 Model showing the main transport proteins involve in the uptake of the commonly available anti-trypanocidal drugs.....	23
Figure 1.7 Schematic illustrations of the major intracellular organelles present in <i>Leishmania</i> promastigote (left) or the amastigote (right) forms.....	27
Figure 1.8 Sand fly and human stages of leishmaniasis.....	28
Figure 1.9 Bioactive molecules used for the treatment of leishmaniases.....	32
Figure 1.10 Structure of the natural product based antibiotics.....	35
Figure 1.11 structures of cordycepin, Quercetin, and proanthocyanidin.....	38
Figure 1.12 Schematic representation of glycolysis in the bloodstream-form of <i>T. brucei</i>	45
Figure 1.13 Structure of SHAM.....	48
Figure 1.14 Structure of ascofuranone.....	49
Figure 2.1 Drug dilution (doubly diluted) down two rows across the plate.....	64
Figure 3.1 Drug sensitivity assays with medicinal plant extracts against <i>T. brucei</i> s427WT and B48 cell lines.....	85
Figure 3.2 Effect of Nigerian plant extracts on <i>L. mexicana</i> promastigotes.....	87
Figure 3.3 Anti-kinetoplastid compounds isolated from <i>Polyalthia longifolia</i> (HDK - 20, 79 and 52) and <i>Eucalyptus maculata</i> (HDK-40)	88
Figure 3.4 Cytotoxicity assay of natural compounds on HEK 293-T cells, with 24 h cyto-adherence, 30 h incubation with drugs, and 24 h with sodium resazurin (alamar blue).....	92
Figure 3.5 Effects of purified natural compounds against three pathogenic protozoa.....	93

Figure 4.1 Structure of 16 α -hydroxycyclohexa-3,13(14)Z-dien-15,16-olide, HDK20, and 3 β ,13 β -dihydroxy-urs-11-en-28-oic acid, HDK40 and their <i>in vitro</i> EC ₅₀ against trypomastigotes of <i>T. b. brucei</i>	99
Figure 4.2 Growth curve assays of HDK20 and HDK40 treated cells.....	101
Figure 4.3 Results showing the speed of action of test compounds, HDK20 and HDK40 on trypanosomes.....	102
Figure 4.4 Cell cycle determination in <i>T. b. s427</i> WT using DAPI.....	104
Figure 4.5 DNA contents and mitochondrial examination of treated and untreated (ND) cells.....	106
Figure 4.6 DNA fragmentation of treated and untreated <i>T. b s427</i> cells following 12 hours of incubation with the test compounds (HDK20 and HDK40) or without the test compounds (untreated cells).....	107
Figure 4.7 Mitochondrial membrane potential (% ψ_m) of treated and untreated <i>T. b. s427</i> WT cells.....	109
Figure 4.8 Determination of ATP levels in trypanosomes.....	112
Figure 4.9 Data visualization of the Principal Component Analysis (PCA) of the intracellular metabolome of HDK20, and HDK40 treated cells.....	114
Figure 4.10 Data visualization of the Principal component analysis (PCA) of extracellular metabolome of HDK20, and HDK40 treated cells.....	115
Figure 5.1 Examples of 2,4-dihydroxybenzoate and salicylhydroxamate derivatives showing low micromolar activity against <i>T. brucei</i>	128
Figure 5.2 Design and general structure of the SHAM and 2,4-DHB conjugates.....	129
Figure 5.3 Comparing the trypanocidal efficacies of the DHB based inhibitors.....	133
Figure 5.4 Summary SAR of DHA-based trypanocides with triphenylphosphonium or quinolinium lipophilic cations (LC); or its dimer highlighting the unique structures on the scaffold that is responsible for the trypanocidal activity on wild-type trypanosomes.....	137
Figure 5.5 Viability assay for TAO25 and TAO24.....	138
Figure 6.1 Expression of TAO in <i>T. b. brucei</i> trypomastigotes.....	144
Figure 6.2 Histograms of TMRE fluorescence in populations of <i>T. b. brucei</i> trypomastigotes incubated with 0.005 μ M TAO25, Valinomycin (100 nM), 10 μ M troglitazone, or no test compound for the indicated duration.....	152

Figure 6.3 Mitochondrial membrane potential ($\% \Psi_m$) of treated and untreated <i>T. b. brucei</i> s427 WT cells.....	153
Figure 6.4 ATP concentrations in 10^7 <i>T. b. brucei</i>	155
Figure 6.5 Oxygen consumption assay of selected TAO inhibitors on <i>T. b. b</i> s427.....	157
Figure 6.6 Dose dependent oxygen consumption assay of TAO25 and TAO 29 on <i>T. b. b</i> s427, using the MitoXpress®-Xtra HS kit, which generates a fluorescence signal inversely proportional to the oxygen concentration.....	158
Figure 6.7 oxygen consumption assay of TAO inhibitors on aqp1-3 triple null trypanosomes , and on mammalian cells (HFF-T25).....	159
Figure 6.8 Percentage of cells at various cell division stages in populations treated or not treated with 0.005 μ M of TAO25.....	161
Figure 7.1 Summarized structures of the TAO inhibitors.....	168
Figure 7.2 Plasmid map showing the point of insertion of fl or Δ MTS-TAO in pETSUMO expression vector via the T – A cloning.....	169
Figure 7.3 Comparative studies of the complementation of haem deficient FN102 <i>E. coli</i> by full-length (fl) and Δ MTS-TAO.....	170
Figure 7.4 SDS-PAGE for the various purification steps involved in the purification of rTAO from FN102 <i>E. coli</i> mitochondria membrane.....	172
Figure 7.5 Comparative analysis of test compounds on TAO inhibition.....	178
Figure 7.6 TAO kinetic determinations in the presence of varying concentrations of inhibitors and substrate concentration (Q_1H_2).....	181
Figure 7.7 Binding kinetics of TAO22 and TAO29 into rTAO.....	184
Figure 7.8 On-Off rate map of TAO inhibitors.....	186

Acknowledgements

I thank God almighty for the gift of life, and the grace to start and complete this thesis.

I also want to thank my dear parents Dr Joseph Ebiloma & Mrs Racheal Ebiloma for all the sacrifices made towards my upbringing and towards attaining this height in my education, all of which I can never repay in equal measures.

I want to thank my beloved wife Rhoda for her support and understanding especially all the times (including weekends and holidays) that I have to be in the lab. These thanks also go to my dear son Barnabas (Barnnie).

The relationship between my supervisor Prof. Harry De Koning and I goes beyond the usual. Thank you for your teachings, love, and moral support. He was very professional; he completely understands the needs and challenges of international students. All of these and others led to the successful completion of this thesis. He is simply the best.

In addition, I want to thank other members of my supervisory team, and my assessors for their criticism and inputs.

The success story of this thesis will not be complete without mentioning the immense contributions by our collaborators: Dr Dardonville's lab of Instituto de Química Médica, Madrid; Prof kiyoshi's lab of Department of Biomedical Chemistry, Graduate School of Medicine, University of Tokyo; Prof Harada's lab of the Department of Applied Biology, Kyoto Institute of Technology, Kyoto, Japan; and to Prof Gray's lab of Strathclyde Institute of Pharmacy and Biomedical Sciences, University of Strathclyde, Glasgow. Thank you all for your corrections and suggestions especially allowing me to do part of this research in your lab.

Special thanks to Dr Anthonius Eze, Dr Olumide Ajibola, Dr Manal Natto, Dr Emmanuel Balogun, Dr Aysin Tulunay, and Prof John Igoli for the overwhelming support giving to this research. My thanks also goes to all the group members of Prof Harry De koning and Prof Mike Barrett, it was a wonderful experience been with you guys.

Finally, to my sponsors: Tertiary Education Trust Fund (TETFund), Nigeria; Kogi State University, Nigeria; and MacRobertson Travel Scholarship.

Author's declaration

I declare that the results presented in this thesis are my own work and that, to the best of my knowledge, it contains no material previously substantially overlapping with material submitted for the award of any other degree at any institution, except where due acknowledgment is made in the text.

Godwin Unekwuajo Ebiloma

January 2017

List of Abbreviations

AAT	African animal trypanosomiasis
ABC	ATP- binding cassette
ALA	Aminolevulinic acid
ANOVA	Analysis of variance
AOX	Alternative oxidase
AQP	Aquaglyceroporins
ATP	Adenosine triphosphate
AU	Artificial unit
BBB	Blood brain barrier
bp	Base pairs
BSF	Bloodstream form
cAMP	Cyclic adenosine monophosphate
CATT	Card agglutination trypanosomiasis test
CL	Cutaneous leishmaniasis
CNS	Central nervous system
CSF	Cerebrospinal fluid
DAPI	4,6-diamidino-2-phenylindole
DHB	Dihydroxybenzoate
DCL	Diffuse cutaneous leishmaniasis
DFMO	Alpha-difluoromethylornithine
DMEM	Dulbecco's modified eagle's medium
DMSO	Dimethyl sulphoxide
DNA	Deoxyribonucleic acid
<i>E. coli</i>	<i>Escherichia coli</i>
EC ₅₀	Effective concentration inhibiting 50% cell proliferation
EDTA	Ethylenediaminetetraacetic acid
FACS	Fluorescence activated cell sorting
FBS	Fetal bovine serum
FCS	Fetal calf serum
FDA	Food and drug administration
FDR	False discovery rate

G1	Gap 1
GIT	Gastrointestinal tract
h	Hour
HAPT	High-affinity pentamidine transporter
HAT	Human African Trypanosome
HCL	Hydrochloric acid
HEK	Human embryonic kidney
HEPES	4-(2-hydroxyethyl)-1-piperazineethanesulfonic acid
HFF	Human foreskin fibroblasts
HIV	Human immunodeficiency virus
HMG-CoA	3-hydroxy-3-methyl-glutaryl-coenzyme A
HMI9	Hirumi medium 9
HOMEM	Haemoflagellate-modified minimal essential medium
IC ₅₀	50% inhibitory concentration
IV	Intravenous
K	kinetoplast
K _a	Constant of association
K _d	Constant of dissociation
kD	kilodalton
kDNA	kinetoplast DNA
K _i	Constant of inhibition
KO	knockout
L	Litre
LAPT	Low affinity pentamidine transporter
LC	Lipophilic cation
LC-MS	Liquid chromatography - mass spectrometry
MCL	Mucocutaneous leishmaniasis
MMP	Mitochondrial membrane potential
MTS	Mitochondrial Targeting Signal
N	Nucleus
NAD	Nicotinamide adenine dinucleotide
NECT	Nifurtimox Efflornitine Combination Therapy
ND	Not determined

nM	Nanomolar
NMR	Nuclear Magnetic Resonance
NMT	N-myristoyltransferase
NTD	Neglected tropical disease
ODC	Ornithine decarboxylase
ORF	Open reading frame
P2	Aminopurine transporter 2
PAGE	Polyacrylamide gel electrophoresis
PAO	Phenyl Arsine Oxide
PBS	Phosphate-buffered saline
PCA	Principal component analyses
PCR	Polymerase chain reaction
PI	Propidium iodide
qPCR	Quantitative polymerase chain reaction
rpm	Revolutions per minutes
RNA	Ribonucleic acid
SAR	Structure activity relationship
SDS	Sodium dodocyl sulphate
SHAM	Salicylhydroxamate
SI	Selectivity index
SPR	Surface Plasmon Resonance
SUMO	Small ubiquitin-related modifier
TAO	Trypanosome alternative oxidase
TLC	Thin layer chromatography
TMRE	Tetramethylrhodamine ethyl ester
TPP	Triphenyl phosphonium
TUNEL	Terminal deoxynucleotidyl transferase dUTP nick end labeling
ULP	Ubiquitin-like-specific protease
UV	Ultraviolet
VL	Visceral leishmaniasis
VSG	Variable surface glycoprotein
WHO	World Health Organisation
WT	Wild type

CHAPTER ONE: Introduction

Chapter 1: Introduction

1.1 Trypanosomes and trypanosomiasis

Trypanosomatids, including *Trypanosoma* and *Leishmania* species are uniflagellated protists. Together with the biflagellated bodonids, trypanosomes are categorized as kinetoplastids, which are characterized by the presence of a single mitochondrion possessing a large amount of DNA (kDNA) in a distinct organelle, known as the kinetoplast.

Trypanosomes are unicellular flagellated parasitic protozoa which belong to the Genus *Trypanosoma*, of the Trypanosomatidae Class, and of the Protozoa Kingdom. There are many trypanosomes species and subspecies already described in literature.

Some species of trypanosomes infect a diversity of different vertebrates, including humans. Most of these species are transmitted by insect vectors such as the tsetse fly - which transmits *Trypanosoma brucei gambiense* and *T. b. rhodesiense*, causing Human African Trypanosomiasis (HAT), as well as other species including *T. b. brucei*, *T. congolense* and *T. vivax*, which cause African Animal trypanosomiasis (AAT). However, other *Trypanosoma* species have alternative modes of transmission. For example, through the faeces of an infected triatomine bug, commonly known as 'kissing bugs', among several names, depending on the geographical area, in which case it is called Chagas disease, also known as American trypanosomiasis. This is a life-threatening disease caused by *Trypanosoma cruzi* which is endemic in 21 countries in the Americas (Barreto-de-Albuquerque *et al.*, 2015). Some *Trypanosoma* species such as *Trypanosoma equiperdum* are transmitted by direct contact of the host with the pathogen itself, *i. e.* without an intermediate host or vector. However, the majority of *Trypanosoma* species are spread by blood-feeding invertebrates serving as intermediate hosts, but there are differences in pathology among the various species. They are generally found in the mid-gut of an invertebrate host, but usually occupy the bloodstream when they invade the mammalian host.

The name *Trypanosoma* is derived from two Greek words *trypano* (borer) and *soma* (body) due to their corkscrew-like movement (Gerasimos and Kent, 2014). Except for *T. equiperdum*, and the insect parasites such as all species of Crithidia (insect-to-insect transmission), all other pathogenic trypanosomatids are heteroxenous (they need more than one obligatory host to complete their life cycle) or are transmitted by animal vectors. *Trypanosoma* are a group of single-celled flagellates

that are transmitted by insects (Sternberg, 2004) and they parasitize vertebrates. A basic distinction between parasites with different localizations of their development inside the insect vector, and the mode of transmission, necessitated a subdivision of the genus *Trypanosoma* into two sections: *Salivaria* and *Stercoraria*. Salivarian trypanosomatids including *T. brucei* spp., *T. congolense* and *T. vivax* complete their life-cycle in the salivary glands of the insect and are transmitted to the host through saliva following a bite of an infected insect. *T. cruzi*, on the other hand, belongs to the *Stercoraria* since their development occurs inside the hindgut of the vector (triatomine bug) and transmission to the host is through faeces (Edmundo, 2002). In addition, transmission of both *Trypanosoma* types can also occur via blood transfusion, use of contaminated needles or via the congenital route (Barret *et al.*, 2003). In addition, although most *Trypanosoma* parasites reside in the blood and tissue fluids of their hosts, *T. cruzi* lives intracellular following entry into their host. The ‘trypanosomiasis’ therefore are made up of a group of important animal and human vector-borne parasitic diseases, specifically American (Chagas’ disease, *T. cruzi*) and African (sleeping sickness, *T. brucei*) trypanosomiasis.

Several *Trypanosoma* species and subspecies are of economic importance on the African continent where they cause the human and animal forms of the disease, HAT and AAT (or nagana) respectively, in which case are a hindrance to human welfare, both affecting cattle rearing and agricultural development in several resource poor communities in Africa.

Two subspecies of *Trypanosoma brucei* infect humans, with each causing slightly different pathologies but whichever case, it is called HAT. *Trypanosoma brucei gambiense* is found in central and western Africa where it causes a relatively chronic form of the disease which may develop over a number of years. *Trypanosoma brucei rhodesiense* on the other hand is found in southern and east Africa where it causes an acute illness which could lead to death within weeks or months. These two forms of sleeping sickness are usually fatal if left untreated (Rodenko *et al.*, 2015; Alkhaldi *et al.*, 2016), although there are emerging, sporadic reports of long-term asymptomatic cases (Jamonneau *et al.*, 2012).

1.1.1 Morphology and life cycle of *Trypanosoma brucei*

Trypanosoma brucei is a distinctive unicellular eukaryotic organism measuring between 8 and 50 µm in length. *T. brucei* has an elongated body with a streamlined and narrowing shape. The cell

organelles including mitochondria, nucleus, endoplasmic reticulum, Golgi apparatus and ribosomes are all enclosed by the plasma membrane (Figure 1.1). It also possesses a distinctive organelle called the kinetoplast, made up of many DNA molecules (mitochondrial DNA) which functions as a single large mitochondrion. In *T. brucei*, the kinetoplast is situated close to (and attached to) the basal body by which it is indistinguishable under the microscope. A single flagellum running towards the anterior end emanates from the basal body. The flagellum is anchored to the parasites' cell membrane along its body surface by an undulating membrane. At the anterior end, only the tip of the flagellum is free (Gerasimos and Kent, 2014). There is also a thick coat of variant surface glycoprotein (VSG) (Figure 1.1) at the cell surface of the bloodstream form (BSF); an equal dense coat of procyclins replaces this VSG when *T. brucei* differentiates into the procyclic stage in the midgut of the tsetse fly (Ferrante and Allison, 1989).

VSG is known to be involved in several mechanisms involved in evading the immune response system of the host which includes preventing complement activation (Sternberg, 2004) as well as the decrease in antibody titres against VSG, which is believed to take place by the endocytosis of antibody-VSG complexes, which is subsequently followed by proteolysis of antibody followed by the recycling of VSG back to the surface of the parasite (Engstler *et al.*, 2007). VSG is an immunodominant antigen, and is capable of stimulating both the T-cell-dependent and -independent B-cell responses, which depends on its conformation (Mansfield, 1994).

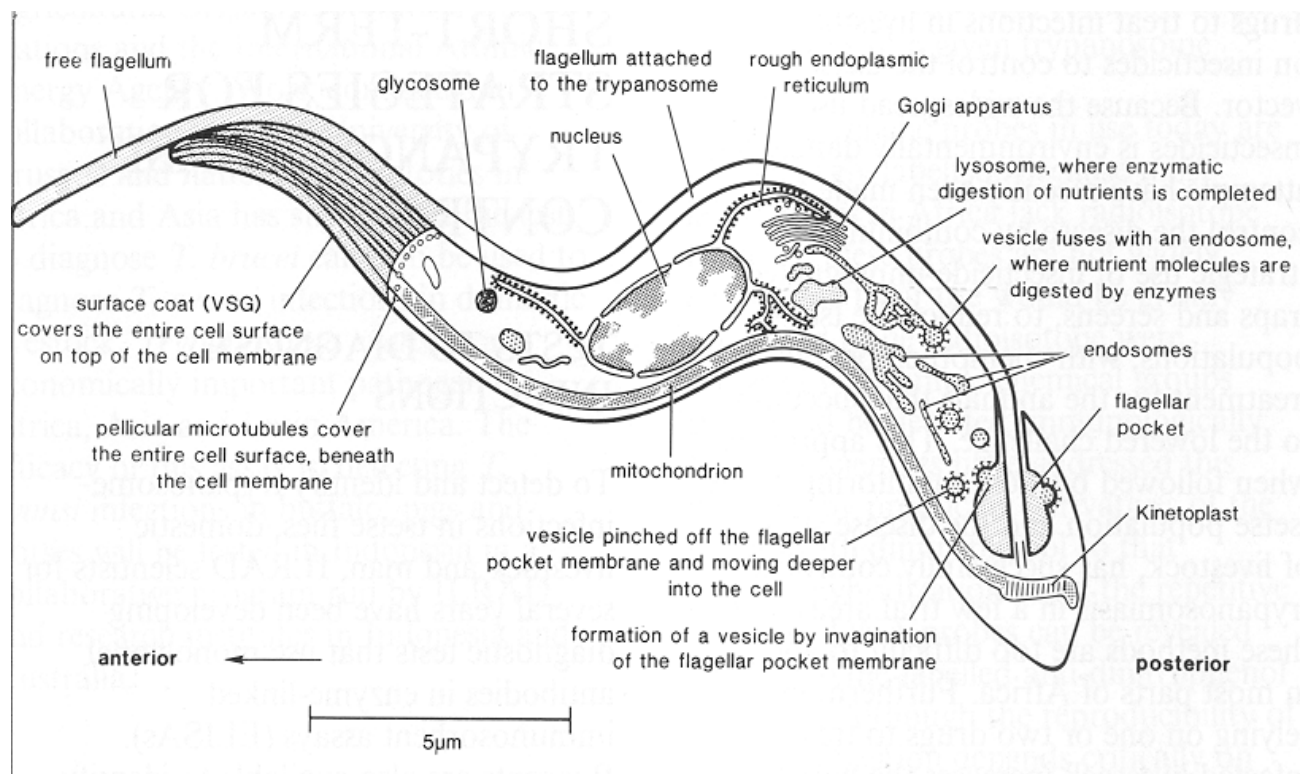


Figure 1.1 Schematic diagram of *Trypanosoma brucei* in its intermediate bloodstream form, showing the major organelles. The arrow in the figure shows the direction of parasite movement. Adapted from: <http://agsavet.blogspot.co.uk/2011/12/trypanosomiasis.html>

Trypanosomatids display more than a few different stages of cellular organisation. Among others, *T. brucei* adopt the following two major forms at various stages of their life cycle:

The epimastigote is the main insect stage of *T. brucei* and it is found in the salivary glands of the tsetse fly (vector) (Figure 1.2). Lying anterior to the nucleus at this stage is the kinetoplast and basal body, a long flagellum is also attached along the parasite's cell body. The flagellum originates from the centre of the parasite's cell body (Stuart *et al.*, 2008).

The form present in the mammalian hosts is called trypomastigote. The basal body and kinetoplast at this stage are posterior of the nucleus.

The name flagellum is derived from the Greek word 'mastig' which meaning whip, this refers to the parasite's whip-like motion of the flagellum (Stuart *et al.*, 2008). There are two unique structures on the flagellum of trypanosomes, a distinctive flagellar axoneme located parallel to the paraflagellar rod, and a lattice structure of proteins which is exclusive to the kinetoplastida, dinoflagellates, and euglenoids (Gerasimos and Kent, 2014).

Also extending from the basal body of the kinetoplast is a cytoskeletal structure. The flagellum is attached to the cytoskeleton of the trypanosome's main cell body by four specific microtubules that run parallel to the flagellar tubulin in the same direction.

Trypanosomes flagellar functions as an attachment to the fly gut in the procyclic phase and locomotion by oscillations along its attached flagellum and cell body. There are additional functions, specifically in cell division and driving the very fast rate of VSG endocytosis/turnover/recycling (Gerasimos and Kent, 2014).

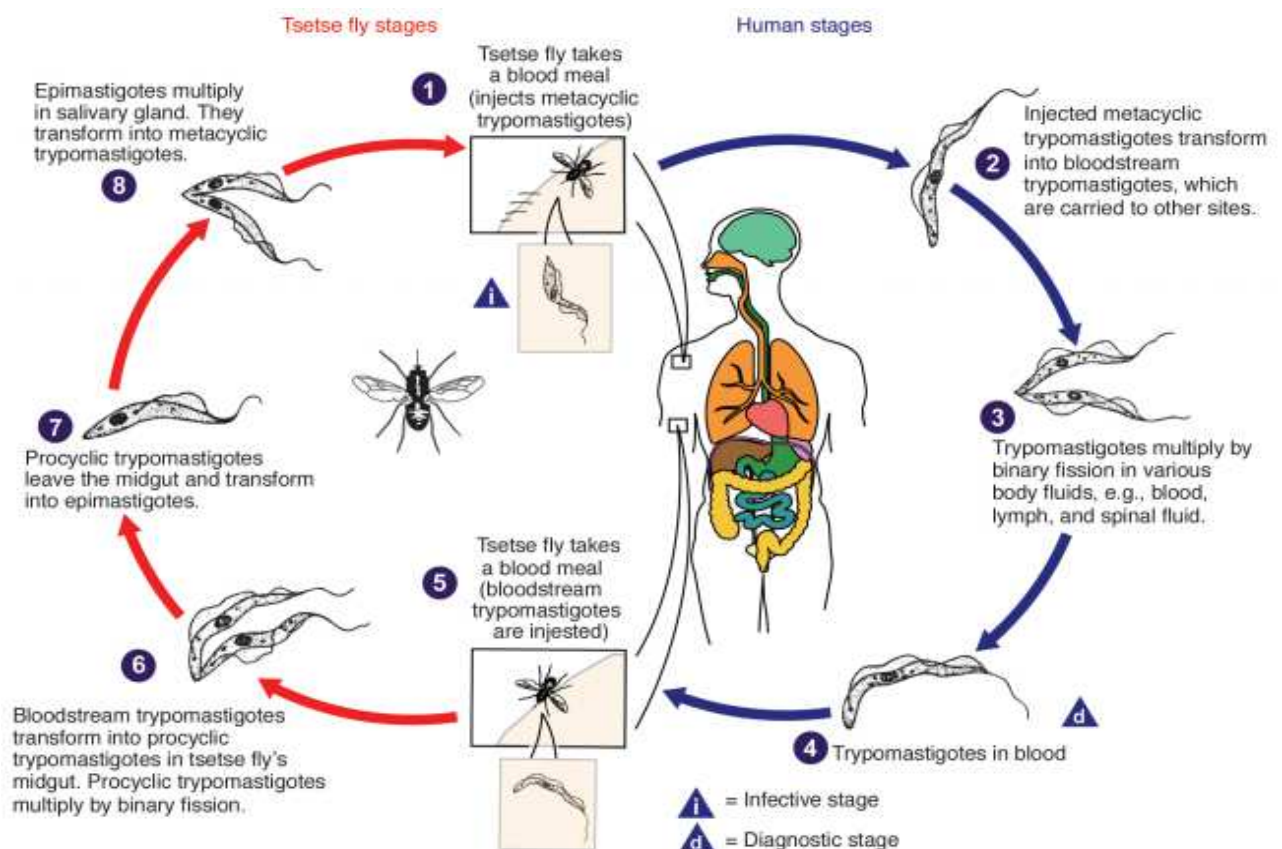


Figure 1.2 Life cycle of *Trypanosoma brucei*. Image credit: Centres for Disease Control Public Health Image Library.

In the life cycle of *T. brucei* (Fig. 1.2), an infected tsetse fly of the genus *Glossina* injects metacyclic trypomastigotes into the skin tissue of a mammalian host during a blood meal from the mammalian host. The parasites gain access to the lymphatic system and then pass into the host's bloodstream. They transform into bloodstream trypomastigotes when inside the host, they are transported to other sites throughout the body, and they reach other body fluids (e.g., lymph, and spinal fluid) then continue the cell division by binary fission. The entire duration of the life cycle of African Trypanosomes is characterized by extracellular stages. The tsetse fly becomes infested

with the bloodstream trypomastigotes once taking a blood meal on an infected mammalian host. The parasites change into procyclic trypomastigotes in the fly's midgut, where it then multiplies by binary fission, it leaves the insect's midgut and transforms into epimastigotes. When the epimastigotes reaches the insect's salivary glands, it continues its division via binary fission. The cycle in the fly normally takes about 3 weeks. Although humans are the primary reservoir for *T. b. gambiense*, this species can also be found in animals. Wild animals are the key reservoir of *T. b. rhodesiense*.

1.1.2 Human African Trypanosomiasis (HAT): The disease, pathology and clinical manifestation.

Human African trypanosomiasis (HAT) is also known as sleeping sickness, and it is a parasitic disease spread by the bite of an infected 'Glossina' insect, known as tsetse fly. HAT commonly comes in two forms: West African and East African. Both forms are caused by a protozoan parasite belonging to the genus *Trypanosoma*; HAT has resurfaced over the past few decades as a key threat to human health and wellbeing in many parts of Africa. *Trypanosoma brucei gambiense* is a subspecies of trypanosomes that is identified as the causative agent of sleeping sickness in West Africa while *Trypanosoma brucei rhodesiense* is known to be the cause of sleeping sickness in East Africa (Williams, 1996). There are distinctive differences between the clinical features and biology of *T. b. rhodesiense* and *T. b. gambiense* diseases, which perhaps is due to an increased adaptation of *T. b. gambiense* parasite to humans (Kennedy, 2004).

The discovery of HAT was made in 1910 following an earlier discovery of AAT in 1894. Since these discoveries, several peaks of epidemics have overwhelmed the African continent (Cox, 2004). Eventhough an obvious reduction in the prevalence of HAT was noticed between 1949 and 1965, the disease resurfaced over the past few decades becoming one of the causes of mortality and morbidity in humans (Kennedy, 2006). Many factors are responsible for this resurgence, these include: the parasites acquiring drug resistance, socio-economic upheavals (especially (civil) war) which in turn lead to disruption of disease monitoring and control; inadequate financial provision of important resources to the disease in the time of peace; changes to climate and vegetation; movements of animal reservoirs; the appearance of novel virulent parasite strains; and changes in host disease vulnerability (Atouguia and Kennedy, 2000; Kuzoe, 1993). Many of these itemised

factors may operate at the same time, and there have been many substantial epidemics and focal emergences of HAT in several regions of Africa in the past few years (Kennedy, 2004).

According to the World Health Organization, in 2006, 60 million people in 36 countries were at risk of contracting HAT, while about 500,000 people were reported to be infected with the disease, and at least 70,000 new cases were reported annually. However, with sustained control efforts from stakeholders, the number of new cases was drastically reduced. In 2009 the number of reported cases nosedived below 10,000 for the first time in 50 years, and in 2014 about 3796 cases were recorded (WHO, 2016). This significant gain notwithstanding, HAT still signifies an impediment to the welfare of humans, affecting about one-third of the total land area of Africa (Fig. 1.3), and as long as the disease is not completely eradicated, it is likely to resurge once control measures are once more relaxed.

Transmission of HAT takes place via the inoculation of metacyclic trypomastigotes, which are the infective form of the parasite, into the skin of the host by the bite of an infected vector, the tsetse fly. This leads to an inflammatory nodule or ulcer known as a 'trypanosomal chancre' which is a local skin lesion and may occur between 1–2 days following the bite (Cecchi *et al.*, 2009). After this time, parasites move to the draining lymph nodes where they reach the bloodstream, thereby initiating the haemolymphatic stage of HAT (Kennedy, 2006). Metacyclic trypomastigotes then change into bloodstream trypomastigotes and spread to other sites right through the body; they also invade other blood fluids and continue cell division via binary fission. The haemolymphatic stage is characterized by fever, headache and malaise (Kuzoe, 1993). Most people usually realise their infection only when stage-two symptoms begin to appear and they may not seek out treatment until then. In more acute *rhodesiense* infection, pulmonary oedema, pancarditis and congestive heart failure can lead to fatalities even at this early stage (Cecchi *et al.*, 2009). A distinctive sign of *gambiense* infection is a widespread lymphadenopathy which develops after a number of weeks, this is usually visible around the neck region and it is known as Winterbottom's sign (Kennedy, 2006). Parasites can be detected in lymph, blood, and other tissue samples at this stage. However, they are more often than not below the detection level, particularly in infection with *gambiense* (Kuzoe, 1993); this makes detection of HAT at the early stage very difficult. When tsetse flies feed on the blood of an infected mammalian host, they become infected with the bloodstream trypomastigotes that they ingest. In the midgut of the fly, bloodstream trypomastigotes change into procyclic trypomastigotes then start multiplying by binary fission.

They leave the midgut of the insect, transform into epimastigotes, and get into the salivary glands, then divide by binary fission and change into metacyclic trypomastigotes. The complete life cycle in the tsetse fly lasts about three weeks (Stuart *et al.*, 2008).

In the early stage of HAT, during the process of trypanosome proliferation parasites invade the host's bloodstream and lymphatic system where they cause symptoms that include headache, fever, chills, and lymphadenopathy. At this stage, activation of the immune system becomes evident as seen in the enlargement of the lymph node, splenomegaly, and hepatomegaly. If left untreated, the parasites can transcend the blood-brain barrier where they invade the central nervous system (CNS) in just a few weeks. The patient progresses to the CNS stage, where the symptoms of this stage include serious headaches, progressive mental deterioration, insomnia, tremors, and psychiatric manifestations. If the disease is still left untreated, it may end in somnolence, seizures, coma and, eventually, death (Stuart *et al.*, 2008).

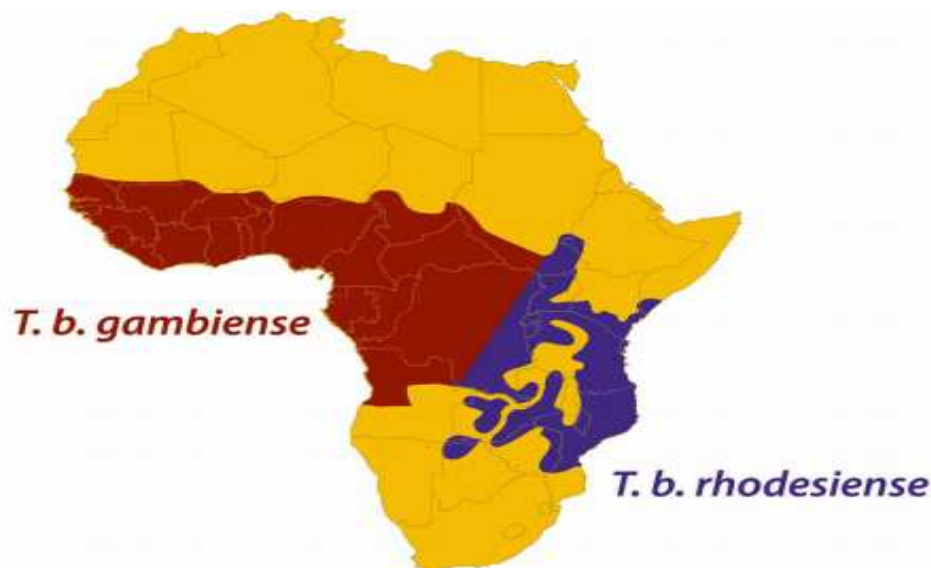


Figure 1.3. Map of Africa showing the major subspecies of *Trypanosoma brucei*, the causative agents of HAT according to geographic distribution. Transmission of HAT presently take place at a low level in most of the countries in tropical Africa, at least about 50 million people are at risk with sporadic epidemic outbreaks. The regions with humans infected with *T.b. gambiense* are shown in red while the areas with *T. b. rhodesiense* are shown in blue. (<http://www.dpd.cdc.gov/>).

The transmission of HAT is caused as a result of infection with the morphologically identical subspecies *T. b. gambiense* present in West and Central Africa and *T. brucei rhodesiense* present in East and Southern Africa (fig. 1.3). More than 90% of all HAT reported cases are believed to

be caused by *T. brucei gambiense* (Barrett *et al.*, 2003; Sternberg, 2004). *T. b. rhodesiense* on the other hand accounts for fewer than 10% of all reported cases of HAT; nevertheless, it is responsible for the most deadly form of the disease as progression to the late stage of the disease happens in a matter of weeks, often leading to death within 3 months (Cecchi *et al.*, 2009; Simarro *et al.*, 2009).

1.1.3 Diagnosis, Treatment and control of HAT

Diagnosing HAT is commonly centred on both investigative and clinical data sets. A characteristic clinical manifestation (e.g. detection of trypanosomes in the blood), put into context the geographical region where HAT is identified to be prevalent, is obviously a significant diagnostic hint. However, the broad-spectrum nature of various clinical features linked to HAT makes it difficult to diagnose the infection and distinguish it from other tropical infections such as typhoid, malaria, HIV, tuberculosis, toxoplasmosis, leishmaniasis, viral encephalitis, or hookworm infections (Atouguia and Kennedy, 2000). A specific challenge is that antimalarial treatment for fever-like symptoms can in fact reduce the fever that is caused by HAT, therefore mystifying and delaying accurate diagnosis; indeed the two infections may also occur simultaneously. Precise diagnosis, especially at the hemolymphatic stage of HAT, would normally include using stained thin and thick films to confirm the presence of trypanosomes in patients' peripheral blood (Atouguia and Kennedy, 2000; Truc *et al.*, 2002). Despite the fact that detecting parasites in the blood is often a success in infection with *T. rhodesiense*, since parasitaemia is permanent, it is very difficult using this method in infection with *T. gambiense*, where a few parasites are observed in the peripheral circulation other than at times of cyclic parasitaemia. Therefore, diagnosis of *T. gambiense* infection is critically based on serologic tests. Presently an antibody-detecting card agglutination trypanosomiasis test (CATT) which is rapid, simple, and easy to perform is commonly used for the serological diagnosis of *T. gambiense* (Truc *et al.*, 2002).

The treatment of HAT at the moment is based on five key drugs, which are pentamidine, suramin, melarsoprol, eflornithine (difluoromethylornithine, or DFMO), and nifurtimox. However, it should be noted that majority of these trypanocides were developed within the first half of the twentieth century, actually most of these drugs most likely would not have passed the present high safety standards (Fairlamb, 1990). Early-stage of HAT is treated with an intravenous (IV)

injection of suramin in *T. rhodesiense* infection at a dose of 4-5 mg/kg (test dose), then 20 mg/kg/day with a maximum dose of 1 g per injection, at a rate of one injection per week for five weeks or with 4 mg/kg intramuscular injections of pentamidine once a day for seven consecutive days in the case of *T. gambiense* infection (Docampo and Moreno, 2002). This treatment is effective only at this stage and prevents the disease from progressing.

Melarsoprol is a trivalent organic arsenical known to have the ability to cross the blood-brain barrier (Atouguia and Kennedy, 2000; Legros *et al.*, 2002), and because of that it is used for treating late-stage disease in both forms of HAT, although it is presently being phased out for *gambiense* HAT. Precise treatment protocols differ significantly between different places and also depending on the parasite strain. Usually, a regimen of 3-4 i.v. doses is administered on a daily bases for a period of 3 - 4 weeks (Legros *et al.*, 2002). Normally, patients are followed up every 6 months for a total of 2 years with CSF examination and clinical evaluation. However, this strategy is difficult to execute as a routine practice in the field. While about 80-90% of all patients are cured using the standard treatment protocol (Atouguia and Kennedy, 2000), there is increasing evidence of drug resistance, for instance, the treatment failure rate was put at 30% among patients receiving treatment in Northern Uganda (Legros *et al.*, 1994; Legros *et al.*, 2002). Nevertheless the main challenge using melarsoprol is the serious post-treatment reactive encephalopathy (PTRE) which follows treatment in up to 10% of all cases, and has a fatality rate of about 50% (Pepin and Milord, 1994). Consequently the overall death rate from melarsoprol treatment is approximately 5%, which is still unacceptably high.

Eflornithine (difluoromethylornithine [DFMO]) an inhibitor of ornithine decarboxylase initially developed as an anticancer drug is used as a monotherapy for treating late stage of HAT. Different open studies showed its efficacy however, studies against placebo were difficult due to ethics (Pepin *et al.*, 1987). DFMO was at first unavailable due to some production problems and high pricing. It is now used for the treatment of *T. b. gambiense* in several countries where it showed its potency and appeared safer than melarsoprol (Franco *et al.*, 2012). DFMO is also used in combination with Nifortimox (Nifurtimox Eflornithine Combination Therapy, NECT). NECT is currently the preferred treatment for late stage *gambiense* due to its reduced toxicity and relative efficacy however; it is not used against *rhodesiense* disease (Franco *et al.*, 2012).

Control of HAT would involve eliminating the vector but this is difficult because of the large area occupied by the tsetse fly vector. However, a committed effort aimed at controlling HAT like the one which led to the recent decline in HAT incidence will require an increased public health awareness strategy that will significantly reduce, and eventually eliminate the human-tsetse fly contact by spraying insecticides, using sophisticated fly traps in the infected areas, and using molecular genetics strategies like the exchange of vulnerable insect phenotypes with an engineered refractory ones to reduce transmission of HAT (Aksoy, 2003). Additionally, a combination of political will and stability, and a significant increase in funding will be needed to improve infrastructure, a better surveillance strategy and screening humans and domestic animals in areas at risk of HAT infection. Also, a more effective treatment regimen is required for treating human disease and of animal reservoirs.

1.1.4 African Animal Trypanosomiasis (AAT)

African animal trypanosomiasis (AAT) is a parasitic disease caused by trypanosomes, and results primarily in anaemia and severe weight loss, which leads to great economic losses in livestock and reduced agricultural output. In most cases it is fatal if left untreated (Acha, 2013). AAT is commonly found mostly in those areas of Africa where its vector, the tsetse fly, is present. One organism, *Trypanosoma vivax*, is reported to have established itself in South America, and it is spread by biting flies that act as mechanical vectors (Batista *et al.*, 2009; Davila and Silva, 2009). Protecting livestock from trypanosomiasis is very hard to achieve in the endemic regions, as bites from the primary vector, the tsetse flies as well as other insects would have to be prevented, or the transmission cycle broken by successfully treating every infected animal.

About 50 million heads of cattle are being threatened by African animal trypanosomiasis (AAT) per year, resulting in about 3 million deaths a year (Acha, 2013); this has a serious impact on the production of cattle in sub-Saharan Africa. AAT is known to be caused by a variety of species: *T. b. brucei*, *T. congolense*, *T. evansi*, and *T. vivax*, cause “nagana” in cattle while *T. equiperdum* is known to cause “dura” in horses (Raper *et al.*, 2001; Picozzi *et al.*, 2008). Numerous classical parasitological and molecular approaches have been put to use in order to characterize representative strains of *T. evansi*, and *T. equiperdum* and these have in fact shown to be definite petite mutants of *T. brucei*. Interestingly, these trypanosomes have lost all (akinetoplastidy, Ak) or part (dyskinetoplastidy, Dk) of their kinetoplast DNA (kDNA); consequently, they were

considered as two subspecies, *T. brucei evansi*, and *T. brucei equiperdum* respectively, that recently arose spontaneously (Gibson *et al.*, 2001; Lai *et al.*, 2008).

T. congolense can be grouped into three types, which are called the kilifi, savannah, and the forest types. Other *Trypanosoma* species such as *T. godfreyi* and *T. simiae* can also cause AAT (Asbeck *et al.*, 2004). There are some trypanosome infections in Africa that are not known to be classified as any of the currently recognized species (Hamilton *et al.*, 2008). Co-infections can take place with more than one species of trypanosome.

All domestic animals can be infected with trypanosomes; the disease has been reported in goats, cattle, sheep, camels, cats, pigs, dogs, water buffalo, horses, donkeys, alpacas, llamas and other animal species (Doko *et al.*, 1997; Gow *et al.*, 2007; Dietmar, 2008). In most parts of Africa where the disease exist, cattle are the major species known to be affected. This is likely to be due to the feeding preference of tsetse flies; in effect, because of the size differentials in grazing animals, cattle can ‘shield’ other domestic animals like sheep, pigs and goats from the tsetse fly bites. In addition, over 30 species in the wild, in game reserves or in zoos, including ruminants like the antelopes and African buffalos, white-tailed deer, duikers, lions, leopards, as well as wild equidae, warthogs, elephants, capybaras, nonhuman primates and a range of rodents’ species are also known to be at risk of AAT (Brown, 2008; Gustave *et al.*, 2015). The DNA of *T. vivax* has been observed by PCR in monitor lizards (*Varanus ornatus*) and crocodiles in Africa, but it is not clear at the moment whether *T. vivax* can become established in reptiles or it is simply inoculated momentarily by insects (Desquesnes and Dia 2004; Njiokoua *et al.*, 2004). Experimental infections have been reported in laboratory animals like rats, mice, rabbits, and guinea pigs (Albright and Albright, 1981). The preferences for a suitable host by each species of trypanosome differ, but *T. congolense*, *T. b. brucei*, and *T. vivax* have a broad range of hosts among domesticated animals (Davila and Silva, 2009). Though *T. suis* and *T. godfreyi* infections occur in pigs however, *T. simiae* appears to be dominant in pigs’ infection (Njiokou *et al.*, 2004), nevertheless, it has also been reported in camels, cattle, and horses by PCR (Pinchbeck *et al.*, 2008; Salim *et al.*, 2011).

The major clinical symptoms of AAT are weight loss, anaemia, an intermittent fever, and lymphadenopathy. Animals become increasingly emaciated, Milk yield decreased in dairy animals (Dietmar, 2008). In addition, neurological symptoms, diarrhoea, dependent oedema, cardiac

lesions, appetite loss, keratitis, lacrimation, and other clinical symptoms have also been reported (Njiokoua *et al.*, 2004). Also, there is an established effect on reproduction like premature births, perinatal losses, abortions and testicular damage in male animals. Deaths are also very common in animals that are chronically infected, and animals that are said to have clinically recovered may relapse when they are stressed (Sekoni, 1994). Trypanosomes can also cause immunosuppression in animals, and coexisting infections may increase the severity of this disease (Thumbi *et al.*, 2014; Olifiers, 2015). Also reported among African cattle infected with *T. vivax* is acute hemorrhagic syndrome (Desquesnes and Dia, 2004). More often than not, affected animals will have enlarged lymph nodes coupled with signs of severe anaemia, and they will develop widespread mucosal and visceral haemorrhages, mainly in the gastrointestinal tract (GIT). This syndrome can be rapidly fatal (Gutierrez *et al.*, 2006; Magona *et al.*, 2008; Olifiers, 2015).

Morbidity and mortality is known to vary with the animal breed, the strain and the inoculating dose from the infecting organisms (Jones and Davila, 2001). It has been reported that some breeds of small ruminants and African cattle on the basis of their genetics are resistant to developing clinical trypanosomiasis; this phenomenon is known as trypanotolerance (Dietmar, 2008; Ilboudo *et al.*, 2014 Yaro *et al.*, 2016). Known trypanotolerant breeds of cattle in Africa include West African Shorthorn (also known as Muturu, Laguna/ Lagune, Baoule, Samba/ Somba or Dahomey cattle, Namchi) and the N'Dama breed of cattle (Yaro *et al.*, 2016).

1.1.5 Chemotherapy of African trypanosomiasis

HAT is particularly problematic to treat due to the unacceptable toxicity and the intricate administration of the chemotherapies presently available for treatment. Besides, resistance to current drugs by trypanosomes is another threat to chemotherapy.

A few drugs are at the moment registered for use in treating HAT: pentamidine, melarsoprol, suramin, eflornithine, and nifurtimox eflornithine combination therapy (NECT). NECT is really the current recommended treatment for late stage *T. b. gambiense* HAT. However, none of these drugs are absolutely safe as all of them have certain degree of toxicity. Pentamidine and suramin are used in the first or early stage of *T. b. gambiense* and *T. b. rhodesiense* infections respectively. Meanwhile three key drugs are used to treat AAT: diminazene aceturate (DA), homidium salts (chloride or bromide), and isometamidium chloride (ISM).

1.1.5.1 Pentamidine

Pentamidine (PMD) is an aromatic diamidine that is soluble in water, and was introduced in 1937. It is the first choice of drug for treating early-stage of HAT caused by *T. b. gambiense*. Pentamidine (Fig. 1.4) is reasonably well tolerated. It is administered by intramuscular injection (i/m), with the most frequently reported adverse events been site pain, transient swelling, abdominal pain, gastrointestinal complications, and hypoglycaemia. The use of PMD may, nevertheless, be circumscribed owing to pancreatic or renal function in immune deficient patients, cardiac dysrhythmias and hypotension, acute deterioration of bone marrow, or induction of abortion when used in pregnancy (Steverding, 2010).

Several researches have concentrated on the mode of action of PMD; however, none seems to convincingly define the target (Soeiro *et al.*, 2008). PMD, being an aromatic diamidine, is a compound that belongs to a class of the DNA minor groove binders. It is thought that formation of complexes between diamidines and DNA may prevent transcription, and/or may act through inhibition of DNA-dependent protein complexes.

1.1.5.2 Melarsoprol

Melarsoprol is used for treating HAT, and is an extremely toxic compound that contains arsenic and displays very strong reactivity with thiols (Gurib-Fakim, 2006).

Melarsoprol (Fig. 1.4) was formulated in 1949 for the treatment of HAT. Up until 1990, the only chemotherapy existing for treating the late stage of both west and east African HAT was melarsoprol. To the current date, it remains the only chemotherapy that is effective (and licensed) for treating second-stage of HAT caused by *T. b. rhodesiense*. However, toxicity remains a key issue with the use of melarsoprol. The most important side effects is the encephalopathic syndrome which take place in about 8.0% of *T. b. rhodesiense* and 4.7% of *T. b. gambiense* patients, with an unacceptable high fatality rate (Steverding, 2010). Exfoliative dermatitis and cardiotoxicity are the other side effects that are serious and, in the latter case, potentially life-threatening. Treatment regimens are usually long and will normally need hospitalisation. Besides, melarsoprol-resistant trypanosomes are well reported from a growing list of countries. In more than a few areas, treatment failures reached 30% in treated patients (Steverding, 2010).

Though the mode of action of melarsoprol has been comprehensively studied, it still remains vague. Melarsoprol is unstable in plasma of patients and is quickly metabolised to melarsen oxide

(Keiser and Burri, 2000). It has been suggested that trivalent arsenicals like melarsoprol have a greater affinity for sulfhydryl-containing agents like intracellular thiol in the cell, plus dihydrolipoate and the closely neighbouring cysteine residues of several proteins. For instance trypanothione has been shown to form a stable adduct with the aromatic arsenical drug melarsen oxide [p-(4,6-diamino-s-triazinyl-2-yl) aminophenyl arsenoxide] (Fairlamb *et al.*, 1989).

1.1.5.3 Suramin

Suramin is a sulphonated naphthylamine (Fig. 1.4) that was developed in 1916, and it is used for treating the early-stage of HAT caused by *T. b. rhodesiense*. It causes certain unwanted side effects especially allergic reactions and urinary tract diseases. There are several hypotheses that have been put forward for suramin's mechanism of action, but none of these have been proven (Zoltner *et al.*, 2016).

It has been shown that suramin inhibits the glycolytic enzymes, including 6-phosphogluconate dehydrogenase, which is an enzyme present in the pentose-phosphate pathway, as well as dihydrofolate reductase and thymidine kinase (Keiser and Burri, 2000). However, suramin has six negative charges which it uses for binding via an electrostatic interaction with positively charged areas of several enzymes; therefore suramin may elicit its trypanocidal action via several targets. Thus, the pertinent question is how it selectively enters trypanosomes rather than host cells.

1.1.5.4 Eflornithine

Eflornithine, also called α -difluoromethylornithine, DFMO, (Fig. 1.4) was approved for use in 1990; it still remains one of the newest drugs used for treating HAT. Although it was originally developed for use as an anticancer drug, it was later discovered to be active against the late-stage of HAT caused by *T. b. gambiense*, particularly in patients that were not responding to treatment with melarsoprol. Eflornithine is an irreversible inhibitor of the enzyme ornithine decarboxylase (ODC) - the initial enzyme in the biosynthetic pathway of polyamine (Oredsson *et al.*, 1980). The result of ODC inhibition is the reduction in the synthesis of the polyamines spermidine and putrescine; because of that it results in the loss of the distinctive and very important antioxidant metabolite trypanothione. These metabolic changes prevent parasite cell division and the drug treatment therefore must rely on an active immune system to eliminate the cell-cycle arrested forms from the host's system (Steverding, 2010).

A major shortcoming of eflornithine use is the difficult nature of the regimen. For instance, because of the short half-life of the drug in plasma, it is necessary to administer four i.v. infusions per day, lasting for two weeks. The most common side effect is bone marrow suppression which leads to leucopenia, anaemia, thrombocytopenia, gastrointestinal symptoms.

1.1.5.5 Nifurtimox-eflornithine combination therapy (NECT)

Nifurtimox-eflornithine combination therapy (NECT) was recently (2009) approved for use in treating late-stage HAT caused by *T. b. gambiense*. NECT comprises of a basic co-administration of intravenous eflornithine and oral nifurtimox (Yun *et al.* 2010).

Nifurtimox is a derivative of nitrofurantoin that was formulated in the 1960s. Its anti-trypanosomal activity was experimentally reported and ever since 1967 it has been put to use for treating trypanosomiasis (Chagas' disease) caused by *Trypanosoma cruzi* in Latin America. NECT is now the present day treatment for late-stage of HAT (Zoltner *et al.*, 2016). This is because it is more effective and less toxic than melarsoprol, it is easier to administer and cheaper than eflornithine monotherapy: just two injections a day are administered over a 10 days period (Yun *et al.* 2010). The biological relevance for this treatment most probably lies in the ability of eflornithine to deplete the level of trypanothione and the capability of nifurtimox to produce reactive oxygen species in trypanosomes, however, the mechanism of action of nifurtimox is not well understood.

1.1.5.6 Diminazene aceturate

Diminazene aceturate (DA) (Figure 1.4) is structurally an aromatic diamidine that was obtained from the experimental drug Surfen. DA is sold as an aceturate salt and is made up of two amidinophenyl moieties joined by a triazene bridge: p,p-diamidinodiazaminobenzene diacetate tetrahydrate.

When trypanosomes take up DA, it is mainly associated with the kinetoplast DNA (kDNA), where it binds specifically and interacts with sites that are rich in adenine-thymine (A-T) base pairs. DA has a significantly greater affinity towards the 5'-AATT-3' than it has for the 5'-TTAA-3' regions of DNA. It has been established that DA binds to the minor groove of double stranded DNA via hydrogen-bond and electrostatic forces (Peregrine and Mamman, 1993). Consequently, DA inhibits the biosynthesis of RNA primers, leading to the build-up of replicating intermediates and consequent prevention of kDNA replication.

Moreover, DA has been shown to inhibit mitochondrial type II topoisomerases in trypanosomes and blocks DNA replication (Roy, *et al* 2010). There have been proposals for its use in human patients, but its safety and potential for cross-resistance with melarsoprol (with P2 transporter being the primary uptake route) remain a serious concern and it is highly unlikely that funding for clinical trials could be obtained, especially since DA does not cross the blood-brain barrier, and can not be used against late stage trypanosomiasis.

1.1.5.7 Homidium salts

Homidium is chemically 3,8-diamino-5-ethyl-6-phenylphenanthridinium (Figure 1.4). Homidium is commonly known by its bromide salt (ethidium bromide) or its chloride salt called Novidium[®]. Homidium is known to be active against *T. vivax* and *T. congolense* infections in cattle. In the field, homidium is basically used as a curative drug; but a prophylactic effect, which varies from 2 to 19 weeks, has also been reported (Dolan *et al.*, 1990; Stevenson *et al.*, 1995). Homidium was extensively used in the 1960s, however, the parasite soon developed resistance, which spread. In addition, it was highly mutagenic and, consequently, its use has been significantly reduced (Stevenson *et al.*, 1995). The recommendation is really to discontinue its use in treating animals. This is reasonable seeing the level of precautions taken by laboratory technicians when staining DNA with this compound (ethidium bromide). Phenanthridinium drugs exert their trypanocidal activity through the inhibition of nucleic acid synthesis. The drugs intercalate with DNA, thereby inhibiting DNA and RNA polymerases (Ullu *et al.*, 2010). However, other biochemical mechanisms are involved in the anti-trypanosome activity of these drugs, these including selective cleavage of kDNA minicircles, membrane transport, the modulation of glycoprotein biosynthesis, and lipid metabolism (Roy *et al.*, 2010).

1.1.5.8 Isometamidium chloride

Isometamidium (ISM) is a phenanthridinium salt which is chemically known as 8-[(m-amidinophenyl-azo) amino]-3-amino-5-ethyl-6-phenylphenanthridinium chloride hypochloride (Figure 1.4) and differs from homidium by an additional moiety of m-amidinophenyl-azo-amine. This means ISM is essentially diminazene coupled to homidium (Delespaux and de Koning, 2007).

ISM is cationic drug which is amphiphilic, and is sold as a dark reddish-brown powder. ISM product comprises 30% of a mixture of its two isomers and a little amount of a bis-compound and 70% of ISM and homidium (as Novidium® and Ethidium®). ISM is used in aqueous solution mostly by deep intra muscular route.

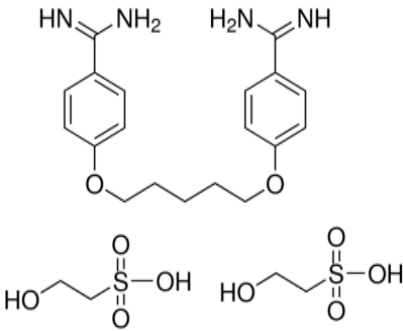
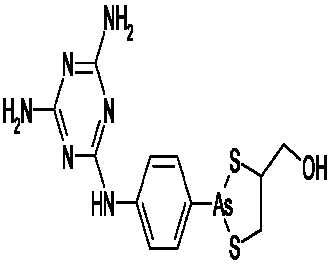
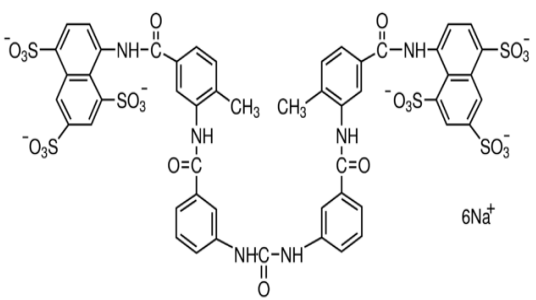
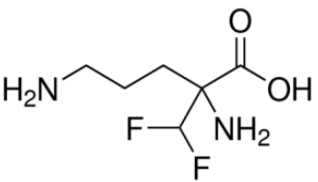
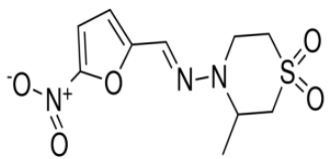
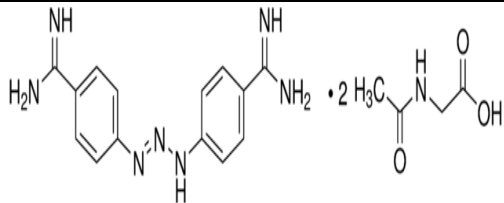
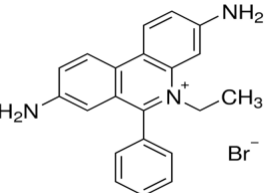
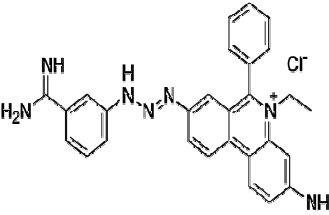
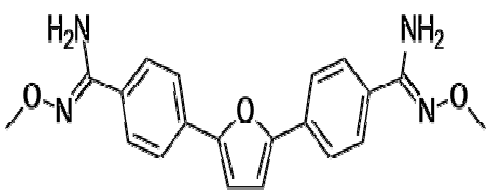
 <p>Pentamidine isethionate salt</p>	 <p>Melarsoprol</p>	 <p>Suramin sodium salt.</p>
 <p>Eflornithine</p>	 <p>Nifurtimox</p>	 <p>Diminazene aceturate.</p>
 <p>Homidium (ethidium bromide)</p>	 <p>Isometamidium chloride</p>	 <p>Pafuramidine</p>

Figure 1.4 Some of the chemical structures of substances known to be active against African trypanosomiasis.

1.1.5.9 Drugs in development

Pafuramidine/furamidine (DB289/DB75) was designed for the treatment of HAT and has got to advanced clinical trials (phase III). Pafuramidine is an amidoxime prodrug (Figure 1.5) which is converted by cytochrome P₄₅₀ to its active diamidine derivative, furamidine. Because

Pafuramidine can cross the intestinal epithelium and accumulates to a significant level in the blood, it can be administered through an oral route. Uptake of pafuramidine occurs primarily through the P2 transporter (Ward *et al.*, 2011).

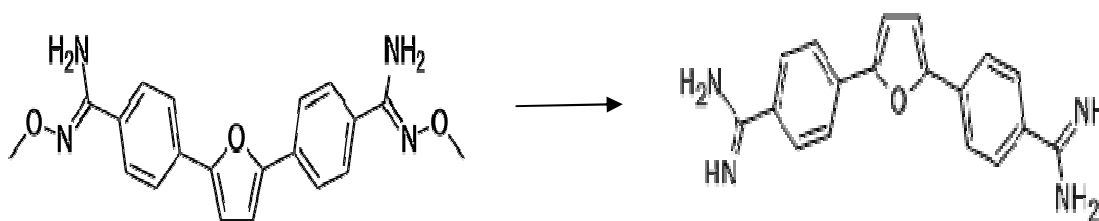


Figure 1.5 Chemical structures of the prodrug pafuramidine (DB289) and the active drug furamidine (DB75).

However the active compound, furamidine is only effective in treating first stage of HAT, but ineffective against the late stage. Initially, there were reported minor side effects such as fever and intermittent pruritis, but unfortunately, pafuramide failed at the end of the trials due to serious concerns of nephrotoxicity in patients (Brun *et al.*, 2010).

Fexinidazole, and oxaborole SCYX-7158 are also molecules currently in clinical development for use as trypanosomiasis drugs (Grewal *et al.*, 2016).

SCYX-7158 is reported to be orally active, and the pharmacokinetic and biological properties suggest that this compound is efficacious and safe to treat the neurological stage of HAT (Jacobs *et al.*, 2011).

On the other hand, pharmacokinetic data of fexinidazole shows that the *in vivo* killing activity is caused by its sulfone and sulfoxide metabolites. Fexinidazole and its metabolites however need up to 48 h of exposure to induce maximal trypanocidal activity *in vitro*. The *in vitro* and *in vivo* trypanocidal activities of fexinidazole as well as its two main metabolites offer proof that this compound has the prospects to be an effective oral chemotherapy for both the *T. b. rhodesiense* and *T. b. gambiense* forms of HAT and both stages of the disease (Kaiser *et al.*, 2011).

1.1.6 Transporters involved in drug uptake and mechanisms of drug resistance in trypanosomes.

The phenomenon of drug resistance was first discovered in trypanosomes by Paul Ehrlich and co-workers (Ehrlich, 1907). Consequently, Paul Ehrlich was the first to conduct an experiment to determine a *T. brucei* mechanism of drug resistance. Using acridine dyes while carrying out vital staining reactions, he discovered that sensitive trypanosomes stained more readily than drug-resistant ones. As a result of these results, Ehrlich propounded the ‘chemoreceptor’ hypothesis, suggesting that drugs act through specific receptors, also that a reduction of affinity of the individual receptor is responsible for drug resistance. Following this finding, Hawking studied trypanamide resistance in trypanosomes using chemical quantification of arsenic in trypanosomes and in post-incubation medium. He submitted that only the trypanamide-susceptible trypanosomes absorbed the drug (Hawking, 1936).

More recently, reduced import of pentamidine was observed in a multidrug-resistant *T. b. brucei* (Carter *et al.*, 1995), and isometamidium-resistant *T. congolense* field isolates were observed to accumulate less isometamidium than the susceptible ones (Sutherland *et al.*, 1991). There was also a decreased accumulation of DFMO but increased ornithine accumulation in procyclic DFMO-resistant *T. b. brucei* than in the drug-sensitive ones, suggesting at least two mutations, as excess ornithine did not inhibit DFMO uptake (Phillips and Wang, 1987); rather, passive diffusion is believed to be responsible for trypanosomal DFMO uptake (Bitonti *et al.*, 1986).

The recurring link of drug resistance with reduced drug uptake highlights the significance of drug transport in African trypanosomes. Either increased drug export or decreased drug import (chemoreceptor hypothesis) is responsible for the reduction of net drug uptake. Any of these mechanisms suggest mutations in specific transporters since most anti-trypanosomal drugs do not diffuse freely across the plasma membrane. Identifying specific drug transporters as well as finding out whether such transporters are mutated in the drug-resistant types is a worthwhile strategy to elucidating the mechanisms of drug resistance in trypanosomes at the molecular level. This mutation could involve loss of a drug importer, overexpression of a drug exporter or a drug transporter changing specificity for substrate. Examples are discussed below.

1.1.6.1 Reduced drug import is the mechanism for resistance associated with purine transporters in trypanosomes.

Carter and Fairlamb performed an *in vitro* screen of various metabolites and nutrients for their ability to block melarsen-induced killing of bloodstream forms *T. b. brucei*, this they did in order to ascertain the transporter that facilitates melarsoprol uptake in trypanosomes (Carter and Fairlamb, 1993). Of all the various physiological compounds studied, only adenosine and adenine protected trypanosomes, signifying that the arsenical is taken up through an adenine nucleoside/nucleobase transporter. This transporter was named P2 (Figure 1.6), and melarsen competitively inhibited it as was determined by an *in vitro* transport assays on trypanosomes (Carter and Fairlamb, 1993). Other trypanosomal nucleoside and purine base uptake systems have been studied (de Koning and Jarvis, 1997a,b, 1999; Goldberg *et al*, 1998; de Koning *et al.*, 1998), but none of them was able to transport clinical trypanocides.

It was afterwards discovered that pentamidine uptake was also through the P2 transporter (Carter *et al.*, 1995; de Koning, 2001); this provided a rationale for the repeated incidence of cross-resistance involving diamidines and melaminyl arsenicals in *T. brucei* species (Fairlamb *et al.*, 1992; Pospichal *et al.*, 1994).

1.1.6.2 LAPT1 and HAPT1 are also involved in pentamidine transport and resistance in trypanosomes

Only a marginal level of pentamidine resistance was conferred on trypanosomes by loss of the *TbAT1* gene alone. This means a non-P2 transport mechanism is also involved in pentamidine uptake, as demonstrated by *TbAT1* negative trypanosomes retaining sensitivity to modest concentrations of pentamidine *in vitro* (Bridges *et al.*, 2007; Teka *et al.*, 2011). Two adenosine-insensitive transporters for pentamidine have been reported: a low-affinity pentamidine transporter (LAPT1) and a high affinity pentamidine transporter (HAPT1) (Figure 1.6) (De Koning, 2001). Although diminazene, a diamidine, is structurally related to pentamidine, it is not a good substrate for LAPT1 or HAPT1 (Matovu *et al.*, 2003; Bridges *et al.*, 2007; Munday *et al.*, 2015). Studies have also revealed recently that HAPT1 similarly contributed to the *in vitro* uptake of the arsenical melarsen oxide by *TbAT1*^{-/-} trypanosomes, despite the relatively low affinity of the transporter for this drug (Bridges *et al.*, 2007; Munday *et al.*, 2015).

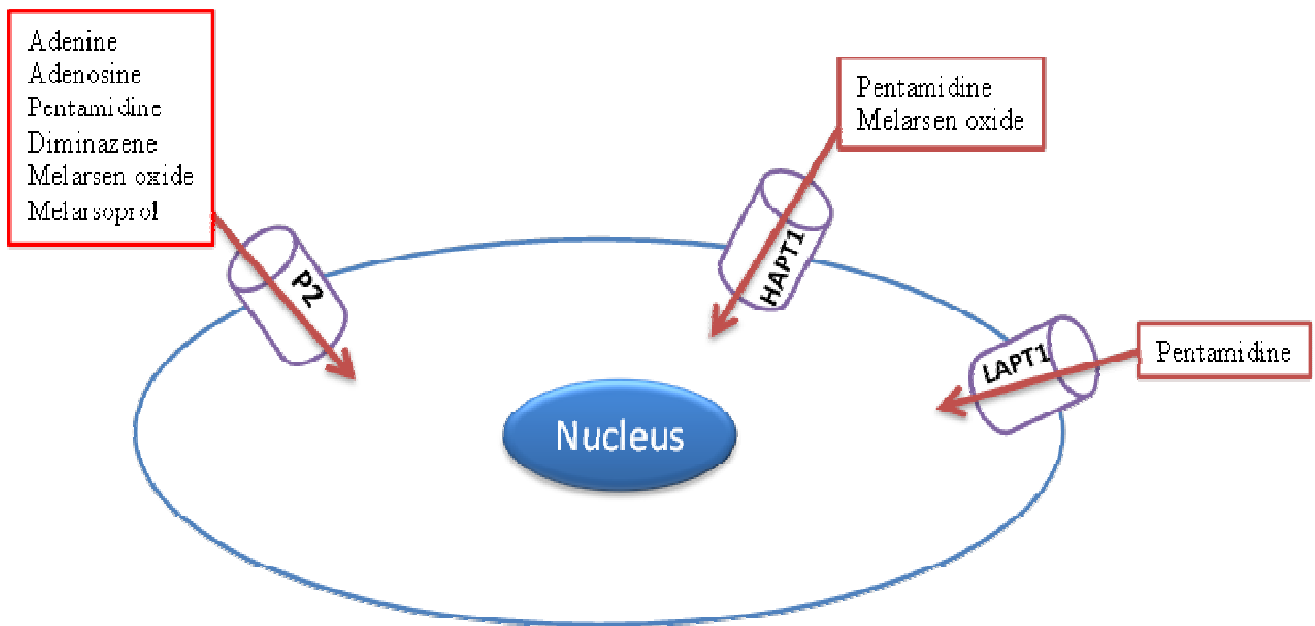


Figure 1.6 Model showing the main transport proteins involve in the uptake of the commonly available anti-trypanosomal drugs. LAPT (Low affinity pentamide transporter); HAPT (High affinity pentamide transporter); P2 (Purine transporter protein).

1.1.6.3 Loss of *Trypanosoma brucei* aquaporin 2 (*TbAQP2*) is also responsible for melarsoprol-pentamidine cross resistance

Using an RNAi library screen, *T. brucei* aquaporins 2 and 3 were identified to be candidate resistance genes for melarsoprol-pentamidine cross resistance. These two genes are near-identical, sharing 83% sequence identity, and are arranged on chromosome 10 in a tandem array (Alsford *et al.*, 2012; Munday *et al.*, 2015). It was revealed that *TbAQP2* was responsible for arsenical and pentamidine sensitivity/resistance when these two genes were individually expressed in *aqp2*–*aqp3* double null cells (Baker *et al.*, 2012).

The sensitivity of trypanosomes to cymelarsan and pentamidine was however restored upon re-expressing *TbAQP2* in B48 cells, re-establishing the lost HAPT1 activity, establishing the surprise identity of HAPT1 as an aquaporin channel (Munday *et al.*, 2015). The B48 cell line, a derivative of *T. brucei brucei*, which had the *TbAT1* gene deleted through homologous recombination, was shown to have additionally lost the HAPT1 activity after passage in increasing pentamidine concentrations, was shown to have a recombined mutant AQP2 locus instead of the wild-type allele (Bridges *et al.*, 2007). Recently, it has been shown that there is a

correlation between mutations in the AQP2 locus and melarsoprol treatment failure in central Africa (Graf *et al.*, 2015).

1.1.6.4 Increased drug export is responsible for the ABC transporters associated drug resistance in Trypanosomes.

The ABC transport proteins are large membrane bound proteins having distinctive ATP-binding cassettes, two of them per transporter. Substrates range from whole proteins to inorganic ions (Higgins, 1992). Substrate translocation coupled to ATPase activity enables active transport to occur. Many ABC transport proteins can serve as a detoxification efflux pump that can lead to drug resistance (Mäser *et al.*, 2003).

Members of the ABC transporter super family are the main transport proteins involved in drug export.

Mäser and Kaminsky (1998) characterised three *T. brucei* ABC transporter genes: *TbABC1*, *TbABC2*, and *TbABC3*. All the three genes were expressed in both the procyclic and bloodstream forms, but to date it is unclear whether they contribute significantly to clinical levels of drug resistance; however, in *Leishmania* and *Plasmodium* species the evidence for involvement of ABC transporter in drug resistance is much stronger (Mäser and Kaminsky, 1998).

1.1.6.5 Alternative mechanisms for drug resistance also exist in Trypanosomes.

There is information in literature regarding alternative mechanisms for drug resistance in trypanosomes, unconnected to drug transport.

A pentamidine-resistant *T. b. brucei* BSF cell line has been reported with unchanged drug uptake and a P2 transporter that was fully functional (Berger *et al.*, 1995), although only one such report has been made and there has been no other confirmation of such a mechanism.

In addition to the loss of P2 transporter, a reduced lipoic acid content was reported to be associated with melarsen resistance in *T. b. brucei* (Fairlamb *et al.*, 1992). Also, *T. b. brucei* procyclics selected for high-level resistance to DFMO showed not only a reduced DMFO uptake and increased ornithine uptake, but also increased levels of ODC mRNA, although the gene copy number of ODC was unaffected (Bellofatto *et al.*, 1987; Mäser *et al.*, 2003).

Another drug been investigated for mechanism of resistance is Isometamidium (ISM), and was reported to have other mechanism of resistance. Transport of ISM into the parasite is energy dependent. From the cytoplasm, ISM crosses into the mitochondrion of the cell by the same energy dependent process (Delespaux *et al.*, 2008). Development of resistance could therefore be due to: alteration of a potential transporter situated in the mitochondrial inner membrane, reduced diffusion across mitochondrial membranes, or increased export of the drug through a transporter which is situated in the cytoplasmic membrane or it could possibly be a combination of these processes. It was recently shown that ISM-resistant trypanosomes have a much-reduced mitochondrial membrane potential due to a mutation in the gamma subunit of the F_0F_1 ATPase, and this greatly reduces the accumulation of the drug in the mitochondrion (Eze *et al.*, 2016).

A totally different cause of drug resistance in trypanosomes is the failure to undertake programmed cell death (apoptosis). Damage which is caused by drugs may not kill the parasites directly but would activate apoptosis. DNA-binding drugs can induce apoptosis which could also be applicable to diamidines. However, there is no direct evidence so far that this potential mechanism is involved in actual drug resistance in protozoa.

A more important one is the nitroreductase that activates nitro compounds such as benznidazole and nifurtimox in trypanosomes. A single point mutation in this gene can lead to a substantial level of resistance to nitro drugs (Wilkinson *et al.*, 2008; Mejia *et al.*, 2012).

Different mechanisms of drug resistance are not mutually exclusive but are rather often multifactorial (Campos *et al.*, 2014). Mechanisms like increased drug export, reduced drug import, and other mechanisms go together and can mutually lead to a higher resistance level. For instance, resistance to sinefungin of more than one thousand-fold has been observed for a *T. b. brucei* field isolate that is multidrug-resistant (Kaminsky and Zweygarth, 1989). Conversely, modest changes in the susceptibility of drug, as explained above, may yet be important to the effect of drugs on trypanosomes.

1.2 *Leishmania* and leishmaniasis

Leishmaniasis is a disease caused by an obligate intracellular protozoan parasite belonging to the genus *Leishmania*. Transmission of the protozoa parasite is achieved through the bite of an infected tiny insect vector (about 2 – 3 millimetre-long) known as *Lutzomyia* sandfly in the new world and the *phlebotomine* sandfly in the old world. Although leishmaniasis is mostly a zoonotic disease affecting predominantly domestic animals, about 20 species of *Leishmania* are known to be pathogenic in humans however; the taxonomic importance of a number of them is disputed (Rogers and Bates 2007). These include the *L. mexicana* complex with three main species (*L. mexicana*, *L. venezuelensis*, *L. amazonensis*), the *Leishmania donovani* with 3 other species (*L. infantum*, *L. donovani*, *L. chagasi*), *L. major*; *L. aethiopica*; *L. tropica*; and the subgenus *Viannia* having four main species (*L. (V.) peruviana*, *L. (V.) guyanensis*, *L. (V.) braziliensis*, *L. (V.) panamensis*). These species are indistinguishable morphologically; however they can be distinguished by molecular methods, monoclonal antibodies, or isoenzyme analysis (Singh *et al.* 2014).

Clinical infection caused by *Leishmania* comes in three main forms: visceral leishmaniasis, cutaneous leishmaniasis, and mucocutaneous leishmaniasis. However, asymptomatic cases have been reported in endemic areas, which act as the main reservoir for re-infection (Singh, Hasker *et al.*, 2014). Usually, *Leishmania* infection follows two distinct transmission cycles: a strictly anthroponotic cycle, which is characteristically seen in densely populated urban areas with humans being the host; and a zoonotic cycle, with dogs as the host being the main animal reservoir, which can also include other mammals.

1.2.1 Morphology and life cycle.

Leishmania is a unicellular protist belonging to a class known as the Kinetoplastida. All kinetoplastids are flagellated at some stage in their life cycle, and also have a distinctive DNA-containing organelle called a kinetoplast, which is present inside their mitochondrion, at the base of the flagellum (Figure 1.7). The kinetoplast consists of many circular copies of kinetoplast DNA (kDNA), performing the same role as the mitochondrial genome in higher eukaryotes.

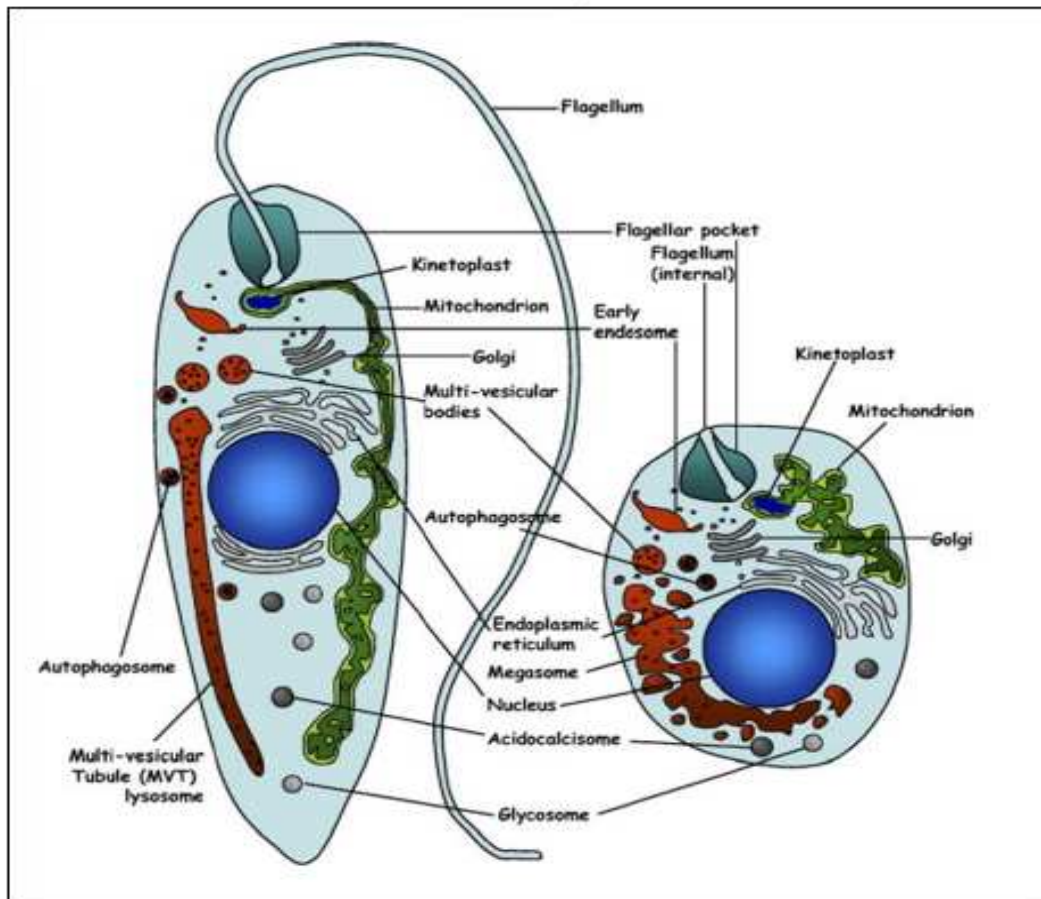


Figure 1.7 Schematic illustrations of the major intracellular organelles present in *Leishmania* promastigote (left) or the amastigote (right) forms. The anterior end of the cell is marked by the flagellar pocket (Besteiro *et al.*, 2007).

Leishmania has a life cycle which is digenetic, and alternates between the mammalian host and the sand fly vector (Figure 1.8). When an infected female sand fly feeds on a blood meal of a suitable host, the parasite (metacyclic promastigotes) is introduced into the host's skin. Metacyclic promastigotes are the extracellular, non-dividing, and infectious stage (Bates, 2007). Impaired uptake of the host blood results in the insect trying to feed with increased frequency, thereby increasing the likelihood of transmitting the parasite (Rogers and Bates 2007). The parasite is therefore introduced into the skin of the host, as are the pro-inflammatory salivary constituents. The resident phagocytic cells inside the skin tissues of the host are then invaded by the parasites.

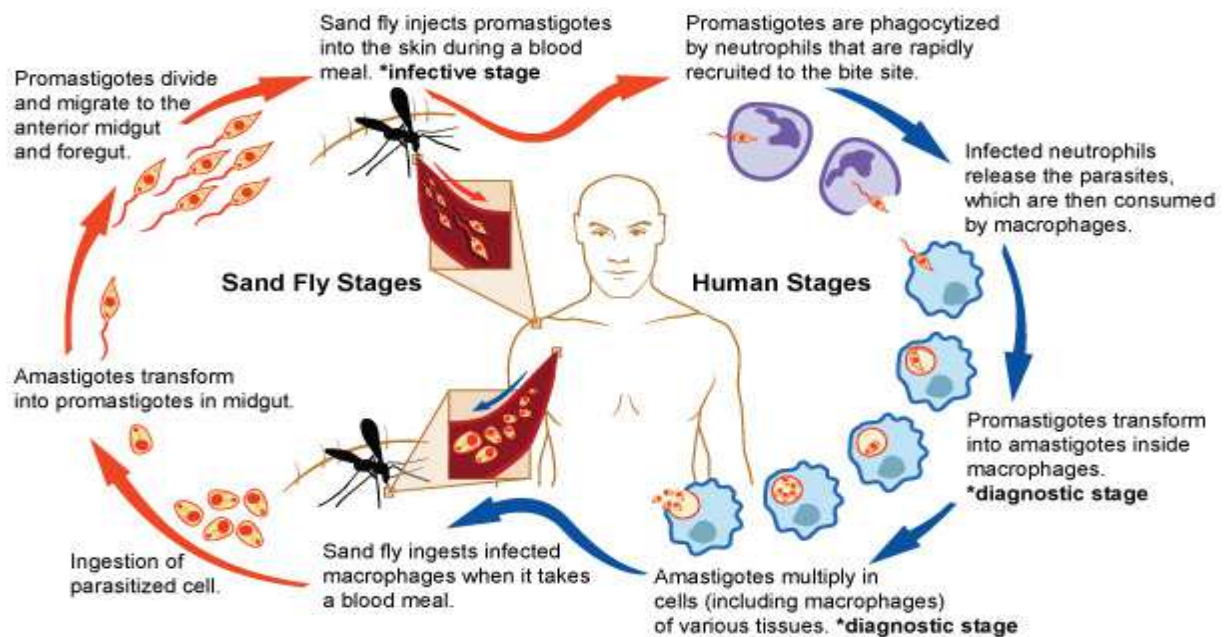


Figure 1.8 Sand fly and human stages of leishmaniasis. The vectors that spread *Leishmania* are the sand flies, when they feed on the host blood they inject infective promastigotes. The promastigotes then invade macrophages of the host via receptor-mediated endocytosis, they then transform into amastigotes and start multiplying by binary fission. The cycle continues as sand flies get infected when they ingest infected cells as they take a parasite-containing blood from an infected host. The amastigotes then transform into promastigotes, then develop to an infective metacyclic promastigotes inside the midgut of the sand fly (Image credit NIAID, <http://www.niaid.nih.gov/topics/leishmaniasis/pages/lifecycle.aspx>).

Once the parasite gets inside the host cell, it differentiates into the non-flagellated obligate intracellular form known as amastigote. The parasites carry on multiplying through mitotic cell division, as intracellular amastigote, and re-invade other phagocytic cells, waiting to be picked up in the blood meal of the next sand fly.

Once inside the midgut of sand fly, the amastigote further differentiates into the early procyclic promastigotes, which rapidly multiply by cell division, at the same time attaching itself to the inside wall of the insect's midgut. This attachment to the midgut wall by the parasite is made possible by lipophosphoglycan (LPG) which covers the cell surface of the parasite (Pimenta *et al.* 1994). This attachment to the midgut wall prevents the parasite from being expelled like the digested blood meal as part of the sand fly's excrement. The parasite further differentiates into the replicating promastigote form; it then moves further to the midgut anterior and continues replicating. This stage is followed by differentiation into the metacyclic promastigotes that infect mammals.

1.2.2 Leishmaniases: pathology and clinical manifestation

The obligate intracellular protozoa parasite belonging to the genus *Leishmania* is the cause of leishmaniases. It has a broad range of clinical symptoms: cutaneous, diffuse cutaneous, mucocutaneous, and visceral.

1.2.2.1 Cutaneous leishmaniasis (CL)

The most common form of leishmaniases is the cutaneous form (50-75% of all cases). It is caused by *Leishmania* species such as *L. mexicana*, *L. major*, *L. braziliensis*, *L. tropica*, and *L. panamensis*. They usually affect the exposed parts of the body such as legs, face, neck, and arms. The infection can cause large number of lesions – at times up to 200 – resulting in severe disabilities which always lead to patients having permanent scars, a stigma which can lead to social discrimination (Bates, 2007).

1.2.2.2 Diffuse cutaneous leishmaniasis (DCL)

L. aethiopica is the causative agent of this form of leishmaniasis and causes chronic and dispersed skin lesions similar to those of leprosy. Treatment often fails since it mostly takes place in patients having a reduced cell-mediated immune response (Singh *et al.* 2014).

1.2.2.3 Mucocutaneous leishmaniasis (MCL)

L. braziliensis is the causative agent of the mucocutaneous forms of leishmaniasis and can result in partial or the total damage of mucous membranes of the mouth, nose, and throat cavities as well as surrounding tissues. Secondary fungi and bacteria infections are also common (Rogers and Bates 2007).

1.2.2.4 Visceral leishmaniasis

Visceral leishmaniasis is also known as dumdum or kala azar fever. This form of leishmaniasis is caused by *L. infantum*, *L. donovani*, and *L. chagasi*. It is associated with considerable weight loss, irregular bouts of fever, swelling of the liver and spleen, and anaemia. It is the most serious form of leishmaniasis and if not treated, the death rate can be as high as 100% in developing countries (Singh *et al.* 2014).

1.2.3 Treatment and control of leishmaniasis

The chemotherapy presently available for treating leishmaniasis is far from ideal. Pentavalent antimonials remain the first-line drug treatment; however, resistance to these drugs is extensive in India. Nevertheless, clear progress has been made with miltefosine, amphotericin B, and paromomycin, but treatment challenges remain a serious issue.

1.2.3.1 Pentavalent antimonials

Pentavalent antimonials are the first-line treatment drug for cutaneous leishmaniasis (CL), and visceral leishmaniasis (VL). These drugs include meglumine antimoniate and sodium stibogluconate. They were made available for the first time in 1945 and continue to be effective but the variable efficiency against CL and VL and the condition for up to 28 days of parenteral administration are the main limiting factors to the drug's usefulness (Yesilova, *et al.*, 2016). Also, the occurrence of significant levels of resistance, which are most serious in India, makes the drug outdated in these areas. They also have serious side effects such as renal toxicity, pancreatitis, and cardiac problems. Their mode of action is understood to be via the inhibition of glycolytic enzymes and other metabolic pathways (Yesilova, *et al.*, 2016). The cause of antimonial resistance in India has recently been identified as a mutation in the *L. donovani* AQP1 gene (Imamura *et al.*, 2016).

1.2.3.2 Amphotericin B

The anti-fungal, polyene macrolide antibiotic amphotericin B (Figure 1.9) has been demonstrated to be very effective for treating antimonial-resistant *L. donovani* visceral leishmaniasis and cases

of mucocutaaneous leishmaniasis. However, it is an unpleasant drug due to the requirement for a 4 h infusion administration, and its high toxic side-effects. Nevertheless, lipid-associated preparations of this drug have been formulated which reduced the nature of the drug and also prolonged the plasma half-life. The most tested of these drugs is Ambisome[®] (liposome formation), which since has been given approval by FDA but then again high cost has restricted its use. Amphotericin B interacts with ergosterol, and in so doing changes the composition and permeability of the membrane, killing the parasite (Ordonez-Gutierrez *et al.*, 2007).

1.2.3.3 Pentamidine

The use of this diamidine (Pentamidine) has been limited by its toxicity, as it needs to be given at higher dosage to treat leishmaniasis than African trypanosomiasis. Consequently, it is only used as a second-line drug via the intramuscular route of administration. Due to the unacceptable side-effects elicited by the use of pentamidine, including hypoglycaemia, and hypotension, this drug is suggested for use in: (i) leishmaniasis resistant to antimony (ii) when severe cardiac or hepatic toxicity arises in the course of antimonial therapy (iii) when antimonials are contraindicated (Croft *et al.*, 2005).

1.2.3.4 Miltefosine

The first effective oral treatment of visceral leishmaniasis is with miltefosine (Figure 1.9), and it is one of the most recent progresses made in anti-leishmanial drug discovery. Miltefosine is an alkylphosphocholine which was initially developed as an anticancer agent. It is likewise active against cutaneous leishmaniasis. The mode of action of miltefosine is by changing the sterol and phospholipid structure of the parasites membrane. Its main constraint is teratogenicity; consequently pregnancy is a contra-indication for this treatment (Sindermann and Engel, 2006).

1.2.3.5 Paromomycin

Paromomycin (Figure 1.9) was initially formulated as an oral aminoglycoside for the treatment of intestinal infections and had previously shown effectiveness as a topical treatment for cutaneous leishmaniasis in 1985, and as a parenteral chemotherapy for visceral leishmaniasis in 1990.

However, it took until 2005 for the phase III clinical trials against visceral leishmaniasis to be finished – reflecting the inadequate funding sources (Croft, *et al.*, 2002).

1.2.3.6 Allopurinol and azoles

The purine analogue allopurinol (Figure 1.9) was recognized for its anti-leishmanial efficacy over 30 years ago, because it was extensively used for other clinical conditions, and has good oral bioavailability it moved into clinical trials for leishmaniasis. But unfortunately, the outcome was disappointing. At the moment, allopurinol is only part of a maintenance treatment for canine leishmaniasis. Azoles, like fluconazole, ketoconazole, and itraconazole have gone through a number of trials for visceral leishmaniasis and cutaneous leishmaniasis but presented an unsatisfactory efficacy in the end (Martinez *et al.*, 1997; de Macedo-Silva *et al.*, 2013).

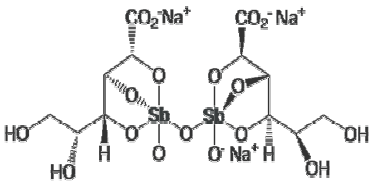
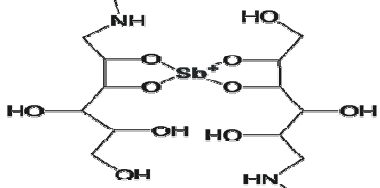
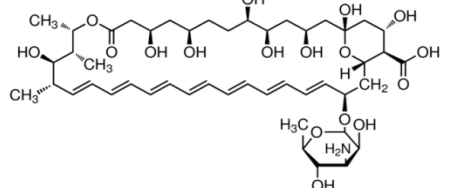
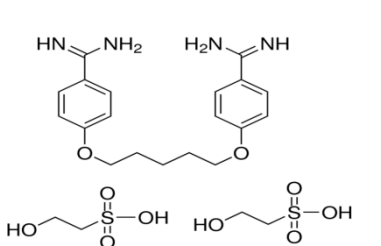
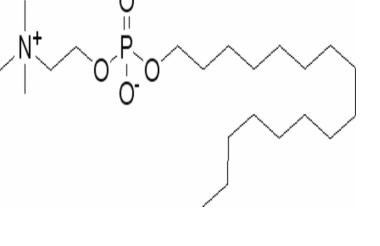
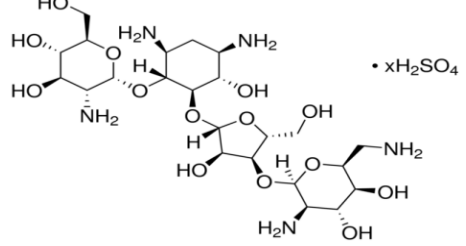
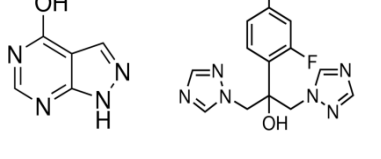
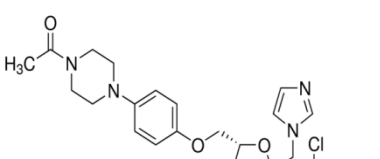
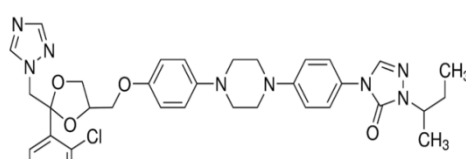
 <p>Sodium stibogluconate</p>	 <p>Meglumine antimoniate</p>	 <p>Amphotericin B</p>
 <p>Pentamidine</p>	 <p>Miltefosine</p>	 <p>Paromomycin</p>
 <p>Allopurinol (left) and fluconazole (right).</p>	 <p>Ketoconazole</p>	 <p>Itraconazole</p>

Figure 1.9 Bioactive molecules used for the treatment of leishmaniases.

1.2.3.7 Drugs in development

Several potential drugs are right now at different stages of development. An oral chemotherapy that might be effective on visceral leishmaniasis is a derivative of 8-aminoquinoline called sitamaquine, which causes oxidative stress in *Leishmania donovani* promastigotes by targeting succinate dehydrogenase, but then again resistant *Leishmania* lines have previously been reported (Loiseau *et al.*, 2011). However, 2-substituted quinolines were found to be effective against these resistant lines, which suggest that the 8-aminoquinoline and 2-substituted quinolin perhaps are affecting different targets in *L. donovani* (Loiseau *et al.*, 2011). Bisphosphonates like pamidronate and risedronate have also been reported for their anti-leishmanial efficacies in experimental animals. Their major target is believed to be the farnesyl pyrophosphate synthase, an important enzyme in the biosynthesis of isoprenoids (Shakya *et al.*, 2011). The search for more active drugs against leishmaniasis is ongoing.

1.2.3.8 Control of leishmaniasis

Vector control may be beneficial under certain circumstances but are not appropriate in all epidemiological situation and need infrastructure and vigilance beyond the ability of several endemic nations. The disease can be stopped by preventing sandfly bites through the use of insecticides or insect repellents. Vaccination still remains the best option for control of all types of the leishmaniasis.

1.3 Natural products in drug discovery

The historical source of disease treatments has been natural products such as plants, animals, and minerals. However, antique wisdom remains the source of contemporary medicine and a vital basis of future medicine and therapeutics.

In contrast to the typical combinatorial chemistry, natural products continue to offer a unique structural diversity, presenting the prospects for discovering mostly new low molecular weight lead compounds. Not more than 10% of global biodiversity has yet been explored for possible biological activity (Cragg and Newman, 2005), consequently, countless quantities of beneficial

natural leads with a tremendous diversity of structures and pharmacological activities await discovery.

The prospect for using natural products in combating diseases can be understood with traditional medicines. Historically, natural products have played a significant part in combating and preventing human diseases throughout the world. The first annals were found in cuneiform inscribed on clay tablets, and date from around 2600 BC, from Mesopotamia (Purvis, 2000). According to WHO, two thirds of the world's population continue to depend largely on traditional medicine for their health care needs. Natural product medicines originate from several organism types including plants, bacteria, fungi, sponges, protists, and other invertebrates present in various environments such as rain forests, hot springs, and deep seas.

1.3.1 Natural products from fungi: Antibiotics

For thousands of years now, micro and macro fungi have been playing a major role in human life. They were used, and continue to be used for various needs. For instance, yeast is being used for the preparation of alcoholic beverages, mushrooms are used as food, and some are used as medications in traditional medicine, while others are for cultural purposes. With the present improvements in microbiology, their usage has been extended to antibiotics, enzymes, biological control, and other pharmacologically active products (Lorenzen and Anke, 1996).

Fungi are more normally found in the environment, some of them have part of their life cycle residing in various tissues of plants without producing any noticeable sign of infection (Tan and Zou, 2001). They can be seen inhabiting grasses, trees, herbaceous plants where they reside within the intercellular space of plant stem, roots and leaves, algae and petioles, without affecting the host organism. These fungi are altogether known as endophytes. New bioactive molecules obtained from these fungal sources have produced many important leads for the pharmaceutical industry (Cragg and Newman, 2005).

One of the well-known natural product breakthroughs obtained from a fungus is undoubtedly penicillin (Figure 1.10), obtained from the fungus *Penicillium notatum*, which was discovered in 1929 by Fleming. Old strategies for identifying β -lactams were in use up until 1968, when it was decided that all the β -lactams of natural origins had been discovered. However, the case was

different with the 1970's introduction of some new methods of screening, the production of β -lactams supersensitive bacterial strains, β -lactamases inhibition tests and sulphur containing metabolites specificity led to the discovery of new structural classes of antibiotic (carbapenems, norcardicins, monobactams, imipenem and aztreonam) (Fabbretti and Gualerzi, 2011).

Polypores are macro fungi and are of the phyla Ascomycota and Basidiomycota (basidiomycetes); they produce many pharmacologically active molecules. Around 75% of all tested polypores have strong antimicrobial activities, and may therefore create a possible basis for the development of new antibiotics (Zjawiony, 2004).

Edmund Kornfeld in 1953 isolated vancomycin, a glycopeptide antibiotic made in *Amycolatopsis orientalis* cultures, and was active against a broad spectrum of gram-positive microorganisms such as *Streptococci* and *Staphylococci* and against gram-negative bacteria such as, fungi and mycobacteria and as a result FDA in 1958 approved it for use in the treatment of chronic infections and against susceptible organisms in patients hypersensitive to penicillin (Butler, 2004).

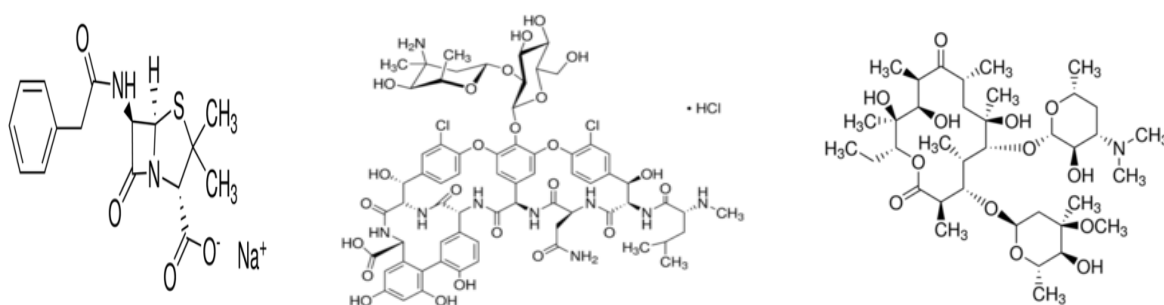


Figure 1.10 Structure of the natural product based antibiotics: Penicillin G sodium salt (left), vancomycin hydrochloride (middle), and erythromycin (right).

The antibacterial drug, erythromycin (Figure 1.10) which is a macrolide antibiotic was isolated from the microorganism *Saccharopolyspora erythraea*. Erythromycin has a wide range of activities against gram-positive *bacilli* and *cocci* and is used for respiratory tract infections (Dewick, 2002; Butler, 2004).

1.3.2 Natural products from plants: Secondary metabolites

The synthesis and breakdown of carbohydrates, proteins, nucleic acids, and fats, which are indispensable to all living organisms, is termed primary metabolism and the molecules involved in these pathways are called *primary metabolites*. The mechanism with which a living organism synthesizes molecules known as *secondary metabolites* (or natural products) is frequently found to be exclusive to a particular living organism or is simply an expression of the distinctiveness of the species and this is termed *secondary metabolism* (Maplestone *et al.*, 1992). These secondary metabolites are normally not critical for the development, growth, or reproduction of a living organism but are synthesized either to act as a likely mechanism for the survival of the organism by defending it against herbivores, protecting their reproductive elements, protecting it from disease-causing microorganisms (bacteria, fungi, nematodes or viruses), preventing other plants from growing and competing with it, or could be a result of a general adaption of the organism to its surrounding environment (Dewick, 2002; Colegate and Molyneux, 2008).

The biosynthesis of secondary metabolites is the result of the basic processes associated with photosynthesis, glycolysis and citric acid cycle to produce biosynthetic intermediates which, eventually, leads to the biosynthesis of secondary metabolites, which are generally referred to as natural products (Dewick, 2002). It can however be seen that even though the number of the precursor molecules are limited, the diversity of new secondary metabolites is virtually unlimited. The most significant precursor molecules used for synthesizing secondary metabolites are the ones obtained from the intermediates: Shikimic acid, Acetyl coenzyme A (acetyl-CoA), 1-deoxyxylulose-5-phosphate, mevalonic acid. They play a significant role in many biosynthetic pathways, involving several different reactions and mechanisms (e.g., decarboxylation, alkylation, Claisen, aldol and Schiff base formation (Dewick, 2002).

It is therefore hypothesized that the secondary metabolic pathways make use of the acetate, amino acids and shikimate pathways to make intermediates also called *shunt metabolites*, which adopt an alternate biosynthetic pathway resulting in the biosynthesis of secondary metabolites (Sarker *et al.*, 2006). Natural causes (such as environmental changes or viruses) or unnatural causes (such as radiation or chemicals) may be the reason for this alteration in the biosynthetic pathways, which could be an adaptation strategy or to make the organism live longer (Sarker *et al.*, 2006). It is this distinctive biosynthesis of important natural products, synthesized by so many marine and

terrestrial organisms that bring about the typical chemical structures that have an assortment of biological activities.

Natural products from plants are useful against various groups of disease-causing organisms such as fungi, bacteria, and viruses. Therefore these natural compounds from plants like phenolics, quinones, terpenes, alkaloids, saponins, and their derivatives are quite beneficial for human consequent of their anti-parasitic activities and highly selective mechanisms of action. In addition to direct use of natural product from plants such as quinine, morphine, etc., the scaffolds of many of these metabolites have been effectively utilized to create pharmacologically more active molecules.

1.3.3 Compounds derived from plants as anti-protozoal agents

A number of well-established anti-protozoal drugs are natural products or derived from them. These include those from microorganisms such as amphotericin B and paramomycin for treating leishmaniasis; as well as those obtained from plants such as artemisinin and quinine used for treating malaria. The bark of *Cinchona* species have been used for centuries by the natives in the Amazon area for treating fevers particularly malaria. It was not until 1820 that the French pharmacists, Pelletier and Caventou isolated the active compound quinine from the bark of *Cinchona officinalis*. In those early days, the curative agent for malaria was quinine but afterward synthetic derivatives (amodiaquine, chloroquine, mefloquine and primaquine) have been developed (Dias *et al.*, 2012). Regardless of the long history of usage, first as plant extract preparations and later on as a pure compounds, malaria treatment, to an extent, is still depend on quinine, particularly cerebral malaria.

The anti-plasmodial activities in the extracts of *Artemisia annua*, was discovered in 1969. *Artemisia annua* is another plant that was long used for treating fevers in Chinese folkloric medicine. The successful isolation of the active compound artemisinin one year later from *Artemisia annua* represented one of the most important discoveries in the fight against infections caused by protozoan parasites. Presently, a number of semisynthetic artemisinin derivatives have been approved and registered for use (artesunate, artemether, and dihydroartemisinin) (Chris and Jay, 2014).

1.3.4 Treatment of trypanosomiasis with natural products and their derivatives

Several compounds isolated from natural source have been shown to inhibit the growth of trypanosomes *in vitro* with EC₅₀ values in the submicromolar range and for some of these products this activity seems to be quite selective. But there is as yet a paucity of information in the literature regarding their experimentally determined mode of action.

Cordycepin (Figure 1.11-A) is a metabolite produced by the fungus known as *cordyceps militaris*. Cordycepin was initially used with deoxycoformycin (DCF), which is a potent inhibitor of the enzyme adenosine deaminase. DCF prevents the inactivation of cordycepin *in vivo*, and was used for treating certain forms of malignant tumours in human subjects, but it is not considered safe enough for the treatment of sleeping sickness together with cordycepin (Cuadros *et al.*, 2000), although coadministration of these compounds was found to be effective against late-stage infections in mice experimentally infected with *T. b. gambiense* and *T. b. rhodesiense* (Salcedo *et al.*, 2003).

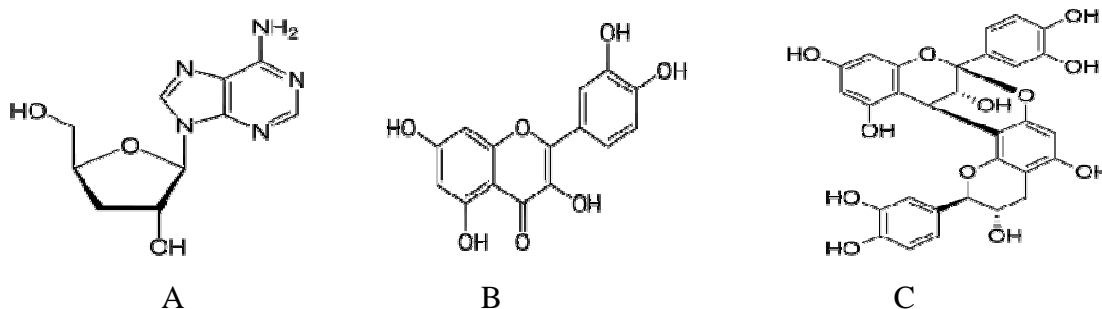


Figure 1.11 structures of cordycepin (A), Quercetin (B), and proanthocyanidin (C)

The mechanisms responsible for the anti-trypanosomal activities were experimentally studied and found that cordycepin causes apoptosis in trypanosomes; secondary necrosis was observed afterwards upon propidium iodide aided measurement of DNA degradation, also observed was the translocation of plasma membrane phosphatidylserine to the outer leaflet from the inner leaflet (Salcedo *et al.*, 2003).

Quercetin (Figure 1.11-B) and its derivatives are polyphenolic flavonoids commonly found in plants such as tea, onions, biloba, and ginkgo. Quercetin has been reported to directly promote *T. b. gambiense* death via apoptosis (Mamani-Matsuda *et al.*, 2004).

A proanthocyanidin (Figure 1.11-C) has been purified from *Kola acuminata* nut and was reported to have anti-*T. brucei* properties *in vitro* in a mouse model (Alvarez-Miranda *et al.*, 2003). Ultrastructural alterations were seen using an electron microscopy, and these were reported to be caused by the rupture of plasma membranes and the release of cellular contents.

1.3.5 Treatment of leishmaniasis with natural products and their derivatives

There is significant progress with leishmanial research in recent time but an effective, safe, inexpensive, and true antileishmanial drug is still missing. Several molecules especially of plant origins have displayed potential as anti-leishmanial lead.

A bis-naphthoquinone, diospyrin extracted from the bark of the plant *Diospyros montana* (Ebenaceae), was shown to exhibit a substantial level of activity against *L. donovani* promastigotes (de Araújo *et al.*, 2014). The mode of action of this compound is thought to be via binding to topoisomerase I, thereby inhibiting the enzyme's catalytic activity, or through stabilization of topoisomerase I-DNA binary complex.

The monoterpene linalool, purified from the plant *Croton cajucara* (Euphorbiaceae), also displayed strong anti-leishmanial potentials with an IC₅₀ of 28 nM against promastigotes and an IC₅₀ of 143 nM against intracellular amastigotes of *L. amazonensis* (Usta *et al.*, 2009). *In vitro* experiments in mouse macrophages show that treating with 15 ng/mL of the essential oil to already infected macrophages of mice lowered the association between parasites and macrophages by about 50% coupled with an elevated production of nitric oxide. Further treatment with linalool for 1 h resulted in a 100% complete elimination of intracellular amastigotes, and promastigotes, at the same time exhibiting no toxicity to the murine macrophages. The mode of action was reported to be likely through the destruction of the kinetoplast, and swelling of the mitochondrial followed by disintegration of the parasite (Usta *et al.*, 2009).

Also, the diterpene ribenol, an ent-manoyl oxide derivative purified from the plant *Sideritis varoi* (Lamiaceae), as well as a 15-monomethyl ester of dehydropinifolate purified from the stem bark of another plant, *Polyalthia macropoda* (Annonaceae), were reported to have *in vitro* activity against *L. donovani* promastigotes (Garcia-Granados *et al.*, 1997).

In addition, the triterpene betulinaldehyde isolated from the stem of the plant *Doliocarpus dentatus* (Dilleniaceae), and ursolic acid purified from the bark of the plant *Jacaranda copaia*, both had activity against *L. amazonensis* amastigotes (Takahashi *et al.*, 2004).

Furthermore, the saponin, mimengoside-A, purified from *Buddleja madagascariensis* (Loganiaceae) leaves (Ding *et al.*, 1992), had activity against *L. infantum* promastigotes. Another saponin, muzanzagenin, isolated from *Asparagus africanus* (Liliaceae) roots, was active against promastigotes of *L. major*.

Flavonoids can also have a significant level of antileishmanial activity, which is thought to be through the inhibition of polyamine biosynthetic enzymes. Therefore, they remain promising candidates to be developed as drugs used for treating all forms of leishmaniasis (Muzitano *et al.*, 2006). Consequently, the flavonoids 8-prenylmucronulatol, smiranicin and glyasperin H, all purified from the plant *Smirnowia iranica*, was reported to inhibit the growth of promastigotes of *L. donovani*. These compounds' mode of action was reported to be perhaps via the induction of kinetoplastid DNA cleavage and arrest of the cell cycle in the G₀/G₁ phase which is mediated by topoisomerase II, leading to a programmed cell death in both promastigotes of *L. donovani* and intracellular amastigotes (Singh, *et al.*, 2008).

Many of these isolated compounds were reported to have immuno-modulatory properties coupled with anti-leishmanial activity, which makes them even more beneficial. This is because leishmaniasis is associated with a compromised immune response.

1.4 Mitochondrial biology of *T. b. brucei*

Most of the existing data concerning *T. brucei* mitochondrial function or structure is obtained from the parasite's procyclic form, while relatively little is known regarding the mitochondrion of the bloodstream form (Schneider *et al.*, 2007). In *T. brucei* procyclics the mitochondrion performs a significant function in the synthesis of cellular ATP through substrate level and oxidative phosphorylation, (Bringaud *et al.*, 2012; Schneider *et al.*, 2007), however, it is also believed to contribute to the pentose phosphate pathway, cellular redox balance maintenance (Bringaud *et al.*, 2012), metabolism of carbohydrate, biosynthesis and conversion of amino acids, nucleotides and lipids.

The structure of the mitochondria of *T. brucei* is made up of a matrix, mitochondrial inner membrane; mitochondrial intermembrane space; and a mitochondrial outer membrane (Panigrahi *et al.*, 2008), which is identical to other eukaryotes' mitochondria. The *T. brucei* mitochondrion, however, contains other features that differ from that of other eukaryotes. For instance, *T. brucei* has a single tubular mitochondrion which stretches all over the entire length of the cell. *T. brucei* can alter the structure and function of its mitochondrion as a response to the different environment of the host, as well as the substrates availability, that the trypanosomes meet in the course of their life cycle (Fenn and Matthews, 2007). The tubular shape of the mitochondrion can also be branched, and depending on the *T. brucei* life cycle stage, it may in fact form a cellular network (Schneider, 2001).

In procyclic forms of *T. brucei* most of the cellular ATP is obtained through degradation of proline, as well as substrate level and oxidative phosphorylation that occur in the parasite mitochondrion (Schneider *et al.*, 2007; Bringaud *et al.*, 2012). In addition, the mitochondrion also has a well established mitochondrial respiratory chain, which is concerned with the task of maintaining the cellular redox balance and ATP synthesis through an ATP synthase (complex V) which is situated on the inner membrane of the mitochondria (van Hellemond *et al.*, 2005). The mitochondrion of *T. brucei* procyclics is very much branched to enhance the function of its membrane surface, which is in line with its role in producing ATP (Schneider, 2001). This is in contrast to the parasite's bloodstream form (BSF), where the single mitochondrion has little or no branching at all as it is reduced into a simple tubular structure (Schneider, 2001). The bloodstream form of the parasite is completely dependent on the compartmentalised glycolytic pathway and the glycosomes for its cellular ATP provision considering that it resides in the glucose-rich human bloodstream (Lamour *et al.*, 2005). The joint action of an ATP synthase and a mitochondrial alternative oxidase (TAO) is what maintains the redox balance in BSF of *T. brucei* (Schnauffer *et al.*, 2005). The mitochondrion of *T. brucei* BSF also lacks a functional cytochrome c, respiratory chain, and TCA cycle. (van Hellemond *et al.*, 2005).

1.5 Trypanosome metabolism and drug targets

There are two ways by which the metabolic activity of trypanosomes may affect its host: by producing toxic metabolites or depleting the host's essential nutrients, which the parasite requires for growth and proliferation. There are many biochemical pathways present in a trypanosome, some of which are very essential for the parasite survival.

Studies on various biochemical pathways present in trypanosomes have been done using NMR, HPLC, and conventional biochemical techniques and enzymology. The pathways most studied inclined towards carbohydrate metabolism (Haanstra *et al.*, 2008), or the variations in oxidative pathways (trypanothione synthesis) accompanying the developmental cycle of the parasites (Xiao *et al.*, 2009). Consequently, the detailed analyses of some metabolic pathways like mitochondrial functions and glycolysis have made other areas of trypanosome biochemistry somewhat understudied. However, the application of metabolomics and systems biology to these challenges is beginning to cover some of these gaps. The differences in the end products of the metabolism of glucose, the development of an active cytochrome system in procyclics for which it is absent in the bloodstream form, the difference in sensitivity to cyanide between the bloodstream and procyclic forms, and the existence of the glycerophosphate oxidase pathway in the bloodstream form are all important pieces of information, and the knowledge of the parasites metabolism at each stage of their life cycle is key to the development of effective inhibitors capable of killing the parasite without harming the host (Abubakar *et al.*, 2016).

1.5.1 Divergent metabolism provides many potential drug targets in trypanosomes

Trypanosomes possess a range of biochemical distinctiveness, some of them are found to be pharmacologically important (Oppenheimer, 1985). Their single mitochondrion has a genome which is structured into a system of more than a thousand DNA circles which is catenated and of variable sizes, known as kinetoplast DNA; therefore they are called kinetoplastids. This unique characteristic of the kinetoplastids makes mitochondrial replication a likely chemotherapeutic target (Shapiro and Englund, 1995). The presence of trypanothione as part of the parasite's redox metabolic pathway is another distinctive characteristic of kinetoplastids. Trypanothione is a covalent network of two glutathiones joined together by a spermidine (Fairlamb *et al.*, 1985). The protein trypanothione reductase and its substrate trypanothione constitute a critical defence against free radicals and oxidative stress (Penketh and Klein, 1986). The existence of spermidine

in trypanothione draws pharmacological attention to the biosynthesis of polyamines (Bacchi and Yarlett, 1993), specifically to ornithine decarboxylase and S-adenosylmethionine decarboxylase. Purine salvage is another anti-trypanosomal chemotherapeutic target, considering that trypanosomes cannot synthesise purines *de novo*, instead they depend completely on the uptake of exogenous purine nucleosides and nucleobases from their host's milieu (Fish *et al.*, 1982). Other distinctive features of trypanosomes, and consequently possible drug targets, are the editing of mitochondrial RNA, trans-splicing of mRNA (Simpson *et al.*, 2003), acidocalcisomes (Vercesi *et al.*, 1994), and the glycosomes (Opperdoes and Borst, 1977).

1.5.2 The glycosome and glucose metabolism

Glycosomes were first discovered in *Trypanosoma brucei*. Most of the enzymes involved in glycolysis are contained in these organelles; this is why they are called glycosomes. Compartmentation of glycolysis within these organelles in trypanosomes is very unique because in other organisms glycolysis is essentially cytosolic.

Glycosomes belong to the family of organelle called peroxisome, though initially there were various disagreements on this affiliation because catalase, being the hallmark peroxisomal enzyme, is absent in glycosomes of trypanosomes and more so that because of the near complete glycolytic role of the glycosomes in *T. brucei*; glycolytic enzymes make up approximately 90% glycosomal enzymes in the bloodstream form of these parasites (Hannaert, 2011), consistent with glucose being the sole carbon source for the parasites at this life cycle stage.

When *T. brucei* is being introduced into the mammalian bloodstream by the bite of an infected tsetse fly, it finds a basically constant environment within the bloodstream, which is very rich in glucose, enabling it to proliferate quickly. Therefore it is able to produce all its ATP via aerobic glycolysis or, rather by anaerobic glycolysis at places where the oxygen tension is low. The major part of the glycolytic pathway has been sequestered inside glycosomes and has been shown to be essential for glycolysis, ATP production and growth of the bloodstream-form of the trypanosomes and this has been shown to provide them with a distinctive mechanism for rapidly switching from aerobic to anaerobic glycolysis (Albert *et al.*, 2005). Anaerobic glycolysis does not allow them to make enough ATP to support growth; however, it permits trypanosomes to overcome short periods of anaerobiosis (Caceres *et al.*, 2010).

Energy metabolism, particularly glycolysis, is regarded as a key chemotherapeutic target in *T. brucei* for the reason that, when residing in the host bloodstream, the trypanosome is completely dependent on the utilization of glucose from blood and body fluids, which it converts to pyruvate for its energy (ATP) needs (Figure 1.12). Furthermore, glycolysis in the trypanosomes is distinctive because it is compartmentalised, and several of its glycolytic enzymes show some distinctive kinetic and structural features, that are likely adaptations to this tight packaging of substrate and enzymes (Verlinde *et al.*, 2001). In contrast to glycolysis in other organisms including the mammalian host where the enzymes involved in glycolysis are situated in the cytosol, the seven glycolytic enzymes metabolizing glucose and converting it to 3-phosphoglycerate are present in the glycosomes. However, the last three glycolytic enzymes are localized in the cytosol (Fig. 1.12). Consequently a good number of the *T. brucei* glycolytic enzymes have so far been confirmed by RNAi as good chemotherapeutic targets (Albert *et al.*, 2005; Caceres *et al.*, 2010).

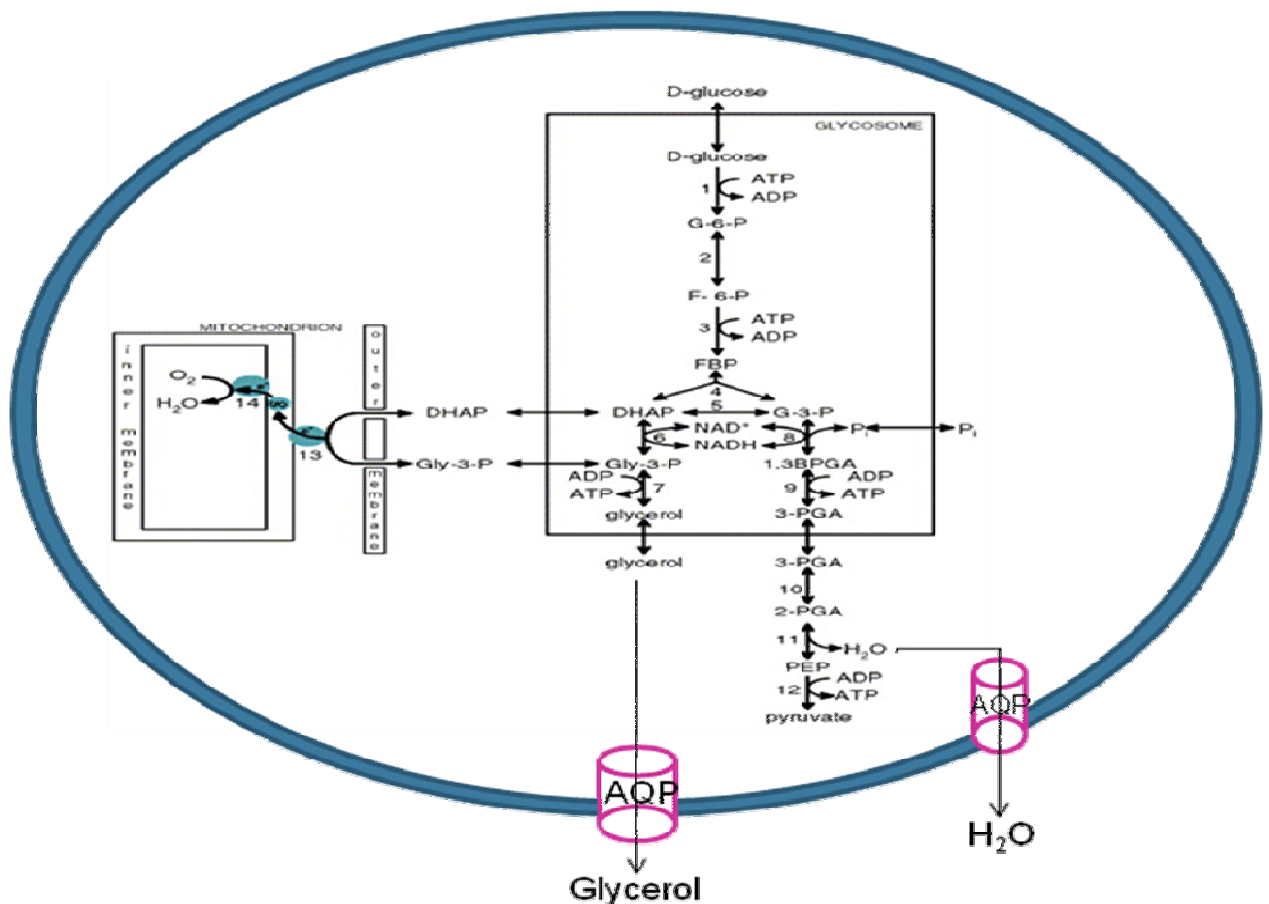


Figure 1.12 Schematic representation of glycolysis in the bloodstream-form of *T. brucei*. Under aerobic conditions, glucose is converted into pyruvate. Under anaerobic conditions equimolar amounts of glycerol and pyruvate are produced. Abbreviations: 1,3BPGA, 1,3-bisphosphoglycerate; DHAP, dihydroxyacetone phosphate; F-6-P, fructose 6-phosphate; FBP, fructose 1,6-bisphosphate; G-3-P, glyceraldehyde 3-phosphate; G-6-P, glucose 6-phosphate; Gly-3-P, glycerol 3-phosphate; PEP, phosphoenolpyruvate; 3-PGA, 3-phosphoglycerate; Pi, inorganic phosphate; UQ, ubiquinone pool; AQP, aquaglyceroporin channel. Enzymes are: 1, hexokinase; 2, glucose-6-phosphate isomerase; 3, phosphofructokinase; 4, aldolase; 5, triosephosphate isomerase; 6, glyceraldehyde-3-phosphate dehydrogenase; 7, glycerol kinase; 8, glyceraldehyde-3-phosphate dehydrogenase; 9, glycosomal phosphoglycerate kinase; 10, phosphoglycerate mutase; 11, enolase; 12, pyruvate kinase; 13, FAD-dependent glycerol-3-phosphate dehydrogenase; 14, alternative oxidase.

Inside the glycosome, the glycosomal NADH, obtained as a product of the catalytic reaction of glyceraldehyde 3-phosphate dehydrogenase, is re-oxidised to NAD^+ followed by transfer of electrons to molecular oxygen through a glycerol 3-phosphate oxidase (GPO) system present inside the mitochondria. A glycerol 3-phosphate dehydrogenase, which is dependent on NADH and present in the glycosome is involved in this process, it is a putative transport protein situated in the glycosomal membrane where glycerol-3-phosphate (G-3-P) is exchanged for

dihydroxyacetone phosphate (DHAP). The mitochondrial GPO is a system consisting of a glycerol 3-phosphate dehydrogenase which is FAD-linked, ubiquinone and a terminal oxidase, called the trypanosome alternative oxidase (TAO) which is located in the inner mitochondrial membrane (Hannaert, 2011). Since mammalian cells do not have TAO, this indispensable re-oxidation machinery of *T. brucei* might be explored as a chemotherapeutic target.

1.5.3 The alternative oxidase in trypanosomes

African trypanosomes can use distinct metabolic systems quite different from that of their hosts to adapt and survive the low oxygen tension inside their host. Rather than using the available oxygen within their host to synthesize ATP, they prefer to employ anaerobic metabolic pathways (Nakamura *et al.*, 2010).

For instance, procyclic forms of *Trypanosoma brucei* found in the infected tsetse fly vector synthesise ATP by oxidative phosphorylation. But once the trypanosomes enters the mammalian bloodstream, both the oxidative phosphorylation and cytochrome respiratory pathway vanish and are substituted with the trypanosomal alternative oxidase (TAO), which begins to functions as the only terminal oxidase, with a task of re-oxidizing the NADH (produced during glycolysis) back to NAD^+ (Shiba *et al.*, 2013).

Because no cytochrome system is found in the long-slender bloodstream form, this form of the parasite instead utilizes the cyanide-insensitive glycerol-3-phosphate oxidase system to re-oxidize the NADH produced during glycolysis. This specialized system specifically oxidizes the glycerol-3-phosphate produced in glycosomes by using the electron transport system present in the inner mitochondrial membrane which consists of a glycerol-3-phosphate dehydrogenase, ubiquinone, and a terminal oxidase known as Trypanosome Alternative Oxidase (TAO) (Ingrid *et al.*, 2013). This is a non-protonmotive ubiquinol oxido-reductase that catalyzes the 4-electron reduction of molecular oxygen to water. Genes encoding alternative oxidase were initially thought to be the exclusive reserve of higher plants, yeast, algae, slime molds, free-living amoebae, nematodes, and eubacteria (Shiba *et al.*, 2013).

The alternative oxidase (TAO) of the long slender bloodstream form of *T. brucei* is totally different in structure compared with the cyanide-sensitive cytochrome C oxidase present in

mammalian (and procyclic) mitochondria (Lukeš *et al.*, 2005). In comparison with other alternative oxidases (AOX), TAO contains two atoms of bound iron rather than haem as the prosthetic group. It also has a characteristic cyanide-insensitive ubiquinol activity that can be inhibited by salicylhydroxamic acid (SHAM) (Kido *et al.*, 2010). It is a mitochondrial inner membrane protein, contains four α -helices and has a mass of 30-38 kDa, with a catalytic site that contains the binuclear iron centre, which is coordinated by two helices, containing a conserved Glu or Asp residue (Nihei *et al.*, 2002).

TAO is considered a good chemotherapeutic target for drug development against trypanosomes because this unique oxidase is very essential for their respiration and survival since it re-oxidises cytosolic NADH, and because this protein is not found in the mammalian host but present in the obligate parasite, trypanosomes, and is critical for its survival.

1.5.4 TAO as a drug target – work done to date

The trypanosome alternative oxidase (TAO) has been genetically and pharmacologically validated to be critical for the survival of the parasite bloodstream form (Shiba *et al.*, 2013; Saimoto *et al.*, 2013). Following this validation, there have been significant attempts to identify a potent inhibitor of this interesting enzyme.

1.5.4.1 Salicylhydroxamic acid (SHAM) as a TAO inhibitor

Salicylhydroxamic acid (SHAM) (Figure 1.13) was the first inhibitor of TAO to be discovered (Oppendoes *et al.*, 1976). SHAM is a potent and irreversible inhibitor of urease in plants and bacteria; therefore it is usually used for treating urinary tract infections. Although SHAM is similar to urea, it is not hydrolysed by the urease present in the urinary tract. However, it is metabolized to salicylamide when administered orally which then exerts analgesic, anti-inflammatory and antipyretic effects (Oppendoes *et al.*, 1976).

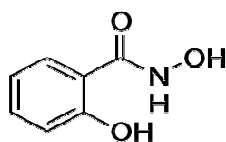


Figure 1.13 Structure of SHAM.

Salicylic hydroxamic acid (SHAM) has been comprehensively studied as an inhibitor of the cyanide-insensitive alternative oxidase present in the respiration system of plants. SHAM is known to inhibit the alternative oxidase (AOX) enzyme in plants and some fungi mitochondrial electron transport chain system, where it inhibits the enzyme by blocking the mainly uninhibited electron flow through the AOX. The AOX acts as a short circuit in the normal electron transport chain where it dissipates electrons with a rather-reduced translocation of protons therefore diminishing the generation of ATP by oxidative phosphorylation (Bonner *et al.*, 1986; Juszczuk *et al.*, 2003). But when AOX is inhibited by SHAM, electrons will be forced through the cytochrome pathway and more specifically via cytochrome IV, thus allowing the operation of the cytochrome pathway with no AOX activity to be studied (Juszczuk *et al.*, 2003).

Following the interesting discovery of an identical cyanide-insensitive alternative oxidase system in the various *Trypanosoma* species, investigators assessed the potency of SHAM as an inhibitor of *Trypanosoma* respiration. As the AOX pathway in *Trypanosoma* species is found to be the exclusive electron transport pathway, SHAM would totally shut down the oxygen consumption of this organism. The inhibitory potential of SHAM against the trypanosome alternative pathway has been reported against trypanosomes, crude inner membrane extracts, and against purified TAO. SHAM was reported to give an IC₅₀ (half-maximal inhibition of trypanosome respiration) at a concentration of 15 μ M (Evans and Brown, 1973; Oppendoes *et al.*, 1976). At this time in the research, the promising *in vitro* experimental results suggested that it was likely to have therapeutic potential that could be developed into a drug for treating *Trypanosoma* infections.

Regrettably, *in vivo* research using SHAM alone to treat trypanosome-infected animals was found not to have much therapeutic effect (Oppendoes *et al.*, 1976). However, the efficacy was improved when glycerol was co-administered with SHAM (Evans and Brightman, 1980; Nihei *et al.*, 2002). Taking into consideration the structure of SHAM, it could be deduced why the *in vivo* activity was insufficient. Unlike many cationic trypanocides, such as diamidines (Stewart *et al.*, 2005),

choline analogues (Ibrahim *et al.*, 2011) and bisphosphonium salts (Alkhaldi *et al.*, 2016), SHAM is not expected to accumulate sufficiently in the mitochondria of trypanosomes because of the very negative mitochondrial inner membrane potential. Therefore a good *in situ* inhibitor of TAO would have a functional group to give a dispersed positive charge around the molecule in order to enhance rapid accumulation of the inhibitor inside the mitochondria (Alkhaldi *et al.*, 2016). In combination with glycerol, SHAM was trypanocidal because the glycerol via mass action would inhibit glycerol-3-phosphate dehydrogenase- the key enzyme in the glycerol-producing pathway (Yabu *et al.*, 2006), thus blocking the trypanosome's final route to ATP production (Figure 1.12). In the presence of a respiratory inhibitor such as SHAM, as well as under certain anaerobic conditions, glycerol-3-phosphate (G-3-P) begins to build-up inside the glycosome, this will normally be converted to glycerol through a reverse action of an enzyme known as glycerol kinase (Ohashi-Suzuki *et al.*, 2011). Nevertheless, once glycerol concentration in the medium reaches several millimolar, mass action will cause the enzyme to reverse the reaction and start producing glycerol-3-phosphate from glycerol consequently, anaerobic glycolysis taking place inside the glycosome will ultimately stop, leading to respiratory arrest, energy deprivation and inevitable death of the parasite (Yabu *et al.*, 2006; Ohashi-Suzuki *et al.*, 2011). Another reason for the poor *in vivo* result observed using SHAM as a TAO inhibitor was its low aqueous solubility, as this limits its bioavailability.

1.5.4.2 Ascofuranone as a TAO inhibitor.

Ascofuranone (Figure 1.14) is a prenylphenol antibiotic which was isolated from a phytopathogenic fungus, *Ascochyta visiae* (Yabu *et al.*, 2006). The chemical structure of ascofuranone is made up of three distinct moieties: an aromatic ring, a linker and a furanone ring.

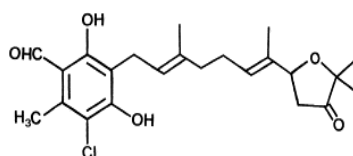


Figure 1.14 Structure of ascofuranone.

Ascofuranone was tested for its inhibitory properties on the mitochondrial electron transport system of the ascomycetous yeast, *Hansenula anomala*, and was reported for its selective inhibition of the enzyme succinate dehydrogenase and external NADPH dehydrogenase (Sakajo *et*

al., 1993). Eventually, ascofuranone was found to inhibit the *Trypanosoma brucei* alternative oxidase in the sub-nanomolar range, and is now one of the lead compounds in an effort to produce drugs which specifically targets this enzyme for use in the treatment of trypanosomiasis. The compound has also been found effective in both *in vitro* cell culture and in infections in mice (Yabu *et al.*, 2006).

Ascofuranone was reported to strongly inhibit both glucose-dependent cellular respiration and the glycerol-3-phosphate-dependent mitochondrial O₂ utilization in long slender bloodstream forms (BSF) of *Trypanosoma brucei brucei* (Minagawa *et al.*, 1997; Nihei *et al.*, 2003). This observed inhibition was thought to be the result of inhibition of the mitochondrial electron transport system, which is made up of the glycerol-3-phosphate dehydrogenase (EC 1.1.99.5) and TAO. Ascofuranone was found to noncompetitively block the reduced coenzyme Q1-dependent uptake of O₂ in the mitochondria with respect to ubiquinol ($K_i = 2.38$ nM). Consequently, the susceptible site action was suggested to be the ubiquinone redox machinery linking these two enzyme activities (Minagawa *et al.*, 1997). Unfortunately, this interesting observation was, as with SHAM, not reproduced in a mouse model. Nevertheless, ascofuranone in combination with glycerol potentially blocked energy production, and completely inhibited the *in vitro* and *in vivo* growth of the parasite (Yabu *et al.*, 1998).

In order to elucidate not only the mechanism of TAO inhibition by ascofuranone but also the inhibitor-enzyme interaction, derivatives of ascofuranone were recently designed and synthesized, and the structure-activity relationship has been evaluated. Saimoto *et al.* (2013) identified the pharmacophore of AF that interacts with TAO base on structure-activity relationship. The comprehensive inhibitory profiles of these analogues implicated the 1-formyl and 6-hydroxyl groups, as contributing to intramolecular hydrogen bonding and/or may serve as donor for hydrogen-bonding, and that these were responsible for the direct interaction with TAO.

1.5.4.3 Ascofuranone derivatives as inhibitors of TAO

For drug development, structural adjustments are often necessary to increase the pharmacological potential and the manufacturing process of a drug candidate after absorption, distribution, metabolism, elimination and then toxicity studies have been carried out. The identification of the charge distribution and steric features on a test compound that is required to guarantee the best

interactions with an exact biological target, thereby blocking (or in some cases triggering) its biological reaction could open the door to the optimisation of an initial lead compound into a novel drug. As part of that process of optimisation, it may be highly advantageous to change the innate physical properties of the compound, and design a compound with a simple structure (to reduce the cost of synthesis), and, for instance, optimise water solubility for an effective *in vivo* absorption. Information from the study of structure activity relationship (SAR) would therefore be an essential component of the design of a promising candidate drug.

Structure activity relationship (SAR) has been performed on ascofuranone in order to establish a link between the chemical (3-dimensional) structure of ascofuranone and the observed biological activity. This enabled the determination of the chemical group(s) responsible for inducing the intended biological effect on TAO. This has allowed the modification of the effect or the potency of ascofuranone by modifying its chemical structure (Nakamura *et al.*, 2010; Saimoto *et al.* 2013).

As stated above, the chemical structure of ascofuranone is made up of three distinct moieties: an aromatic ring, a linker and a furanone ring (Figure 1.14). Chemical modifications of the functional groups at these three moieties have been performed.

Many Ascofuranone derivatives have been tested for their inhibitory activity against TAO. Saimoto *et al.* (2013) carried out SAR studies on ascofuranone and revealed the following: (i) the furanone ring on AF is not needed for inhibition of TAO; (ii) the 3-chloro and/or 2-methyl groups are contributory to the conformation of the enzyme-bound molecule; (iii) only one isoprene in juxtaposition with the aromatic ring of AF is recognized by TAO; (iv) The direct interaction between TAO and AF is consequent of the intramolecular hydrogen bonding and/or the 6-hydroxyl and 1-formyl groups' hydrogen-bonding donor activity (Saimoto *et al.*, 2013).

1.6 Aims

The aims of this work is to develop novel and efficient therapeutic leads by investigating the anti-trypanosomal efficacies of selected tropical plants and their active constituents, and of synthetic trypanosome alternative oxidase inhibitors, establish their selective toxicity *in vitro*, and investigate the mechanism of their anti-parasite activity.

Chapter 2: Materials and methods

2.1 Parasites, cell lines and cultures

2.1.1 *Trypanosoma brucei* and *Trypanosoma congolense* bloodstream forms (BSF)

A number of different strains of *Trypanosoma brucei brucei* bloodstream form (BSF) were used in this study: (1) Wild type *T. b. brucei*, strain Lister 427 (s427; MiTat 1.2/BS221); (2) An s427-WT derived *TbAT1* knockout (*tbat1*^{-/-}), which had both the *TbAT1*/P2 transporter coding alleles in the s427-WT strain deleted; this was achieved by a consecutive replacement of both alleles of *TbAT1* gene with resistance markers for the antibiotics neomycin and puromycin resulting in resistance to diminazene aceturate and some degree of resistance to a number of other trypanocides such as melarsen oxide and pentamidine (Matovu *et al.*, 2003); (3) A multidrug resistant strain, B48 which was derived from a *TbAT1*-KO strain after increasing exposure to pentamidine and lacks both the *TbAT1*/P2 transporter and the high affinity pentamidine transporter (HAPT1) (Bridges *et al.*, 2007); (4) The pentamidine-resistant Aquaporin 2/3 double null, and Aquaporin 1-3 triple null (*aqp2/aqp3*, *aqp1-3* null strains respectively); *aqp2/aqp3* null was obtained by the knockout of the aquaporin genes specifically implicated in pentamidine – melarsoprol cross-resistance in field isolates (Alsford *et al.*, 2012); (5) *T. brucei* cell line (R0.8), which upon increasing exposure became resistant to 0.8 μ M of compound A (CpdA), which is resistant to inhibitors of cAMP phosphodiesterases (PDEs) such as CpdA, and cross-resistant to membrane permeable cAMP analogues (Gould *et al.*, 2013); (6) A Trypanosome Alternative Oxidase (TAO) over-expressing cell line obtained from *T. b. b* s427 WT by over-expressing the TAO gene under blasticidin pressure, which should result in reduced sensitivity to TAO inhibitors.

All *T. b. brucei* strains were used only as bloodstream trypomastigotes, and cultured in standard Hirumi's Modified Iscove's medium 9 (HMI-9), supplemented with 10% heat inactivated Fetal Bovine Serum (FBS), 14 μ L/L β -mercaptoethanol, and 3.0 g sodium hydrogen carbonate per litre of medium (pH 7.4). Parasites were cultured in vented flasks at 37 °C in a 5% CO₂ atmosphere and were passage every 3 days (Yang *et al.*, 2015; Rodenko *et al.*, 2015). Bloodstream forms of *T. congolense* savannah-type strain IL3000 were cultured exactly as described by Coustou *et al.* 2010.

2.1.2 *Leishmania mexicana* promastigotes

Leishmania mexicana promastigote (MNYC/BZ/62/M379 strain) were grown in haemoflagellate-modified minimal essential medium (HOMEM) (Gibco[®], Life technologies, Ghent, Belgium) (pH 7.4) supplemented with 10% heat-inactivated fetal calf serum (FCS) at 25 °C. The medium was sterilized using a 0.22 µm filter prior to use and stored at 4 °C. The parasites were passaged three times a week in 10 ml of HOMEM with 10% Fetal Calf Serum (FCS).

2.1.3 Mammalian cell cultures

Human Embryonic Kidney (HEK) cells - 293T, or Human Foreskin Fibroblast (HFF) cells were grown in a standard culture that comprised 500 ml Dulbecco's Modified Eagle's Medium-DMEM (Sigma), 5 mL Penicillin/Streptomycin (Gibco), 5 mL L-Glutamax (200 mM, Gibco), and was supplemented with 50 mL new-born Calf Serum (NBCS) (Gibco). All components were mixed in sterile conditions and filtered with a 0.22 µm filter into a 500 mL sterile bottle, and stored at 4 °C. The cells were cultured and incubated at 37 °C + 5% CO₂ and were passaged three times a week when reaching 80-85% confluence in passage ratio in the vented flasks, and removal of the adherent cells was achieved with the help of 0.25% Trypsin-EDTA solution. The culture flasks were horizontally placed to expose a larger surface area in order to enable cell adherence, which is crucial for cell growth as a monolayer.

2.1.4 Bacterial strains

Routine cloning of *T. b. brucei* genomic sequences was done using the XL1 blue strain of *Escherichia coli* (*E. coli*). Top 10 *E. coli* and a kanamycin resistant-haem deficient FN102 *E. coli* were respectively used for the cloning and expression of recombinant TAO. These *E. coli* cells were stored as glycerol stabulates at -80 °C until used. The bacteria cells were grown in luria broth (LB) (sigma) that was complemented with 100 µg/mL of ampicillin (sigma) at 37 °C under an overnight vigorous shaking (250 rpm).

2.2 Preparation of stabilates

Stabilates were made from either genetically engineered cells or when necessary from the routinely used strains. Usually, a cell suspension of 2×10^6 cells/mL is made in HMI-9 supplemented with 10% FCS, and diluted 1:1 with HMI-9 containing 30% of glycerol. The prepared stabilates were aliquoted into cryo-vials and transferred to a -80 °C freezer and stored for between 24 - 48 h prior to transfer to liquid nitrogen for long-term storage. Stabilates were brought out of liquid nitrogen when needed and allowed to thaw at room temperature. Cells were harvested by centrifugation at a speed of $3000 \times g$ for 10 minutes at 21 °C to remove the glycerol, and the cells were then re-suspended in HMI-9 supplemented with 10% FCS.

2.3 Materials

2.3.1 Growth media and chemicals

Dulbecco's Modified Eagle's Medium, 0.25% Trypsin-EDTA solution, and Propidium iodide were all acquired from Sigma-Aldrich. L-Glutamax (200 mM), New-borne Calf Serum, Penicillin/Streptomycin, HOMEM medium and New-born Calf Serum were purchased from GIBCO. Heat-inactivated Fetal Calf Serum (FCS) was bought from Biosera. Alamar blue (Resazurin sodium salt) was purchased from Trek Diagnostics (UK), while Troglitazone was from Biomol.

2.3.2 Phytochemical extraction materials and solvents

The following materials were purchased: TLC grade silica gel coated aluminum sheet (Pre-coated Silica gel PF₂₅₄, Merck, Germany); *p*-Anisaldehyde (Sigma-Aldrich, UK); Dragendorff's reagent (Sigma-Aldrich, UK); Silica gel 60 PF₂₅₄ containing gypsum for preparative TLC (Merck, Germany); TLC grade silica gel 60H (Merck, Germany) for vacuum liquid chromatography; Lipophilic Sephadex[®] (LH-20100, Sigma-Aldrich, UK); Column grade silica gel (Silica gel 60, mesh size 0.063-0.200 mm, Merck, Germany).

Dichloromethane, *n*-Hexane, Ethyl acetate, Methanol, *n*-Butanol, and Acetone were all of HPLC grade, while Acetic acid was of Analytical grade.

Solvents listed above were used at different stages of extraction, analytical TLCs, and chromatographic separations. They were purchased in 2.5 L glass bottles from Fisher Scientific UK Ltd. All the solvents were either stored at room temperature or transferred to 500 mL solvent bottles for routine use.

Deuterated (99.9%) solvents (CDCl_3 , DMSO-d_6 , and Acetone-d_6) were bought from Sigma-Aldrich UK Ltd, and were used for NMR analysis of fractions.

2.3.3 Test compounds and extracts.

All extracts and purified natural compounds were soluble in DMSO, therefore were dissolved in DMSO at 20 mg/mL, and the stock solutions were stored at -20°C until use.

TAO inhibitors numbering from TAO-01 to TAO-53 were synthesized and supplied by Dr Christophe Dardonville of the Instituto de Química Médica, CSIC, Madrid, Spain. The inhibitors were soluble in DMSO, therefore were dissolved in DMSO at 20 mM, and the stock solutions were stored at -20°C until use.

2.4 Phytochemical analysis

Phytochemical analysis of the selected medicinal plants was conducted at the laboratory of Prof. Alexander Gray of Strathclyde Institute of Pharmacy and Biomedical Sciences, University of Strathclyde, Glasgow. This was carried out as reported below.

2.4.1 Plant collection and preparation of samples.

Following the method of Adewale *et al.*, 2011, ethnopharmacological method was used to collect the plants used in this research between the month of January and February from Anyigba, Kogi State, Nigeria. This involved engaging traditional healers via interviews in order to establish which plant/part of the plant preparations are in common uses and how it was administered. This research area is located on latitude $7^\circ 15' - 7^\circ 29' \text{N}$ and longitude $7^\circ 11' - 7^\circ 32' \text{E}$ with an altitude of 420 – 426 m above sea level. Plants were authenticated by taxonomists at the Herbarium section of the department of biological sciences, Kogi State University, Nigeria. The plants were confirmed to be:

Plant A – *Centrosema pubescens*; Plant B – *Moringa oleifera*; Plant C – *Tridax procumbens*;
Plant D – *Polyalthia longifolia*; Plant E – *Newbouldia laevis*; Plant F – *Eucalyptus maculata*;
Plant G – *Jatropha tanjorensis*.

Following authentication of the plant materials, the leaves of the plants were air dried to a consistent weight in the laboratory. The plants were ground to a fine power using a grinder (IKA® Werke GmbH & Co. KG, Germany) before extraction.

The powdered dry leaves (20 g) from plants used in this study were weighed into a thimble and placed in a soxhlet apparatus. The plant material was extracted consecutively using solvents of increasing polarity starting with *n*-hexane and followed by ethyl acetate and methanol (3.5 L each). Each extraction stage was carried out to exhaustion. All extracts obtained were evaporated at 40 °C. Recovery of solvent and concentration of the extracts was carried out under vacuum using a rotary evaporator connected to a condenser. Residual solvents were further allowed to evaporate under the fume hood before samples were freeze dried in a freeze dryer. The hexane, ethyl acetate, and methanol extracts obtained were labelled as below, then stored at -20 °C prior to analysis.

Samples were labelled accordingly as:

HDK-AE; HDK-AH; HDK-AM = Ethyl acetate, Hexane, and Methanol fractions from plant A respectively.

HDK-BE; HDK-BH; HDK-BM = Ethyl acetate, Hexane, and Methanol fractions from plant B respectively.

HDK-CE; HDK-CH; HDK-CM = Ethyl acetate, Hexane, and Methanol fractions from plant C respectively.

HDK-DE; HDK-DH; HDK-DM = Ethyl acetate, Hexane, and Methanol fractions from plant D respectively.

HDK-EE; HDK-EH; HDK-EM = Ethyl acetate, Hexane, and Methanol fractions from plant E respectively.

HDK-FE; HDK-FH; HDK-FM = Ethyl acetate, Hexane, and Methanol fractions from plant F respectively.

HDK-GE; HDK-GH; HDK-GM = Ethyl acetate, Hexane, and Methanol fractions from plant G respectively.

2.4.2 Bioassay guided fractionation of crude extracts

Following the exhaustive extraction of the plant materials, 21 crude extracts, itemised above, were collected and tested for their anti-trypanosome activity using a standard laboratory strain of

Trypanosoma brucei wild type s427 and the multi-drug resistant strain B48. As a selection criterion, only crude extracts having their EC₅₀ below 15 µg/mL were selected for further purification. In addition to this criterion, samples showing reduced sensitivity to B48 relative to the wild type were excluded. The crude extracts which met these selection criteria were carried further for isolation of their active principles.

2.4.3 Purification and characterization of promising extracts

Extracts that met the established selection criteria used in this work were further subjected to purification using a combination of the several methods outlined below.

2.4.3.1 Thin layer chromatography

Thin layer chromatography plate, which is an aluminium sheet coated with silica gel (Merck KGaA, Darmstadt Germany), was used for the separation of compounds. Thin layer chromatography (TLC) was used to i) screen the plant material for the presence of compounds; ii) determine the best eluting system for column chromatography iii) monitor fractions during column chromatography and iv) for preliminary analysis of compounds. Plant extracts, fractions or pure compounds were dissolved in an appropriate solvent and spotted approximately 1cm above the bottom edge of a TLC plate. The crude extract was also spotted to serve as control against the possibility of spotting artefacts. Spots were applied as bands to allow for an easy and accurate visualisation and the bands were kept as narrow as possible to minimise the overlapping of compounds. Solvent combinations of *n*-hexane/dichloromethane, *n*-hexane/ethyl acetate or ethyl acetate/methanol were used as mobile phases depending on the expected polarity of the sample under analysis.

Plates were first examined under UV light using short ($\lambda=254$ nm) and long wavelengths ($\lambda=366$ nm). Short UV is useful to detect aromatic compounds while compounds with conjugated double bonds were visible under long UV light. The essence of subjecting the TLC plate to UV light (long and short wavelength) is to be able to identify and hence distinguish compounds based on their UV properties.

Then, plates were sprayed with anisaldehyde-sulphuric acid to trigger an oxidation reaction between anisaldehyde, sulphuric acid, air, heat, and the compound(s). In addition, vanillin-

sulphuric acid reagents, which allow visualisation of most compounds (phenols, terpenes, sterols, pigments and sugars), was also used. Dragendroff's reagent was used for alkaloids. Various colours were observed after spraying with anisaldehyde-sulphuric acid or vanillin-sulphuric acid reagent and heating for 1-2 minutes with a heat gun. Alkaloids were detected as orange spots against a yellow background after treating with Dragendroff's reagent (Sherma and Fried, 2006). A combination of the relative mobility of compounds on TLC plate, UV property, and reaction with anisaldehyde-sulphuric acid spray was used as the bases for fraction combination for NMR.

2.4.3.2 Anisaldehyde-sulphuric acid spray.

Anisaldehyde-sulphuric acid was used for the detection of sugars, steroid, and terpenes on TLC. A solution of 0.5 ml anisaldehyde in 50 ml glacial acetic acid and 1 ml 97% sulphuric acid was prepared fresh before use.

2.4.3.3 Treatment of Chromatogram

TLC plates were heated to 100 - 105 °C until maximal visualization of the spots appeared. The background was brightened by the presence of water vapour. Lichen constituents, phenols, terpenes, sugars and steroids turned violet, blue, red, grey or green respectively upon heating.

2.4.3.4 Vacuum liquid chromatography

Vacuum liquid chromatography (VLC) was performed in a sintered glass funnel attached to a water pump. Silica gel 60H (TLC grade) was loaded onto the funnel and vacuum was applied to compress silica gel to a hard layer. The least polar solvent was allowed to run through the column to check whether the column was homogenously packed.

Samples were dissolved in an appropriate solvent, absorbed on a small amount of silica gel 60 (mesh size 0.063-0.200 mm) and dried in the hood to achieve a free flowing powder. The powder was loaded and packed as a uniform thin layer on the top of the compressed silica gel column and the thin layer was covered with filter paper to prevent distortion of the arrangement when solvent is added. The column was eluted starting with the least polar solvent (*n*-hexane) followed by ethyl

acetate/*n*-hexane mixtures of increasing polarity and finally with mixtures of ethyl acetate and methanol. The column was allowed to dry completely between fractions to improve resolution and separation of compounds. Each fraction was collected, and evaporated to dryness at 40 °C under vacuum using a rotary evaporator. The dried fractions were resuspended in dichloromethane and checked by TLC. Finally, they were pooled according to similar chemical profiles (Pattaraporn *et al.*, 2014).

2.4.3.5 Size exclusion chromatography

For non-polar fractions, Sephadex[®] was soaked in a solution of 5% *n*-hexane in dichloromethane or 50% dichloromethane in methanol for several hours. The slurry was then poured and packed in a glass chromatography column of appropriated size containing about 10-15 mL of solvent allowed to freely drip in order to prevent air bubbles. Samples were dissolved in a small volume of the solvent used for the mobile phase. The concentrated sample was loaded at the top of the column. Elution was done with 5% *n*-hexane in dichloromethane or 50% dichloromethane in methanol. If needed, elution was continued with 100% dichloromethane or 100% methanol, respectively. For relatively polar fractions, Sephadex[®] was soaked in methanol and the column was then eluted with the same solvent. When the column had finish running, Sephadex[®] was washed with water then methanol and kept dried for re-use.

2.4.3.6 Silica gel chromatography

Open Column Chromatography was performed on silica gel 60 (mesh size 0.063-0.200 mm). The column was packed using the wet packing technique. Silica gel 60 was made into slurry using the least polar solvent of the eluting system and then poured and packed in a glass chromatography column of appropriate size. Air bubbles were eliminated by tapping and allowing the tap to run while packing. Excess solvent was allowed to run through and the column was left to settle down. Samples were dissolved in a suitable solvent and adsorbed on a small amount of silica gel 60 (mesh size 0.063-0.200 mm), then loaded at the top of the column. Dry silica gel, or a cotton plug, or filter paper was applied over the sample to prevent any distortion when the solvent drops came from the solvent reservoir. Elution was carried out either isocratically (using a solvent system that

does not change composition during the run) or using a gradient. The collected fractions were analyzed by TLC and pooled according to similar chemical profiles.

2.4.4 Compound identification by Nuclear Magnetic Resonance (NMR) and Mass spectrometric based techniques.

1D and 2D ^1H - and ^{13}C -NMR experiments were carried out on a JEOL (JNM LA400) 400 MHz and a Bruker 500 or 400 MHz instruments. NMR tubes (5 mm) purchased from Wilmad-labglass were used for routine NMR experiments. Samples were dissolved in 0.6 mL of NMR grade deuterated chloroform and taken in NMR tubes. Before the tube was inserted into the spinner, it was thoroughly wiped with a clean wipe to remove any grease or solvent on the outside of the NMR tube which could contaminate the spinner and may cause the spinner to fail to grip the tube properly. The identification of pure compounds was first carried out by one dimensional ^1H and ^{13}C NMR spectroscopy. Spectra obtained for known compounds were identified following comparison with published spectral data. Further 2D experiments were carried out when necessary to accurately assign proton and carbon chemical shifts and determine relative stereochemistry in some cases.

2.4.4.1 ^1H -NMR

^1H -NMR experiments were carried out for all compounds isolated and were used as the primary means of structural identification. It provided information on the protons present in each molecule, their chemical shifts, multiplicity (coupling information) and estimated numbers from the integration. The spectra obtained were also used to assess the purity of any isolated compounds, and to determine the relative molar ratio of any components present as a mixture.

2.4.4.2 ^{13}C NMR

This gave information on the number and type of carbons present in a compound. The spectra obtained were either broad band-decoupled or J-modulated. In broad band-decoupled spectra, the ^1H nuclei are irradiated during the ^{13}C acquisition so all protons were fully decoupled from the ^{13}C nuclei. When this was done each distinct ^{13}C environment in the molecule gave rise to a

separate singlet signal. In the J-modulated experiment, the carbons were distinguished according to the extent of their proton attachments (C, CH, CH₂ and CH₃).

2.4.4.3 Correlation spectroscopy (COSY)

This 2D experiment gave ¹H-¹H coupling in the molecule and also revealed all coupling relationships in one experiment using a suitable pulse sequence. The proton shifts were plotted on both axes with the contour plotted along the diagonal of the square, and the correlations were shown as cross peaks with the diagonal corresponding to the ordinary ¹H spectrum. Thus, the cross peaks refer to the spin-spin coupled protons.

2.4.4.4 Nuclear Overhauser Enhancement spectroscopy (NOESY)

The NOESY experiment was performed in order to determine compound structure and their relative stereochemistry. In this experiment, all correlations between protons showing Nuclear Overhauser Effect (NOE) were recorded two-dimensionally. The NOESY spectrum was used to measure ¹H-¹H interactions arising from (through space) dipolar coupling. The spectrum obtained was similar to the COSY spectrum (scalar through bonds coupling), but the NOESY spectrum showed cross-peaks representing NOE correlations.

2.4.4.5 Heteronuclear Multiple Bond Correlation (HMBC)

The spectra obtained from this experiment revealed heteronuclear shift correlations via long-range couplings. The proton spectrum was arranged on one axis while the carbon was on the other, and the correlations were displayed as cross peaks. Unless otherwise stated, the HMBC experiment carried out for different samples in the present study used a time delay of 0.00625 s (e.g. $J_{CH} = 8$ Hz). Since this pulse programme uses ¹H-¹³C polarization transfer, the detection was about four times more sensitive than the ¹³C NMR experiment.

2.4.4.6 Heteronuclear Single Quantum Correlation (HSQC)

Heteronuclear Single Quantum Correlation (HSQC) is a 2D ¹H-¹³C experiment which was carried out to show one-bond (¹J) direct correlations. The pulse sequence applied in this experiment uses a time delay set to ^{1/2}J where J is the value similar to that of one-bond ¹H-¹³C coupling. In the

HSQC spectrum, the ^1H and ^{13}C (also called DEPT) spectrum was plotted along the abscissa and ordinate respectively. The cross-peaks indicated proton and carbons that were directly connected to each other.

2.4.4.7 Compound identification by Mass spectrometry

Mass spectrometry was used to identify the amount and type of chemicals present in our sample by measuring the mass-to-charge ratio and abundance of gas-phase ions. High (and low) resolution electron impact mass spectra were recorded on a JEOL 505HA spectrometer using direct probe at elevated temperature (110-160 °C) at 70 eV. Positive ion and negative ion mode Electrospray Ionisation (ESI) experiments were performed on a Thermo Finnigan LCQ-Deca Iontrap or Orbitrap HRESI mass spectrometer (mass analyser set up at 100,000 ppm, externally calibrated at 3 ppm). According to the polarity, samples were dissolved in acetonitrile, methanol or water (HPLC grade) or in a binary mixture of these solvents to get a concentration of 100 µg/mL. Sample solution (10-20 µL) was injected along with a direct infusion of 0.1% formic acid in acetonitrile: water (90:10) at a flow rate of 200 µL/min.

2.5 *In vitro* drug sensitivity assay using Resazurin (Alamar blue) dye

The sensitivity of the various class of compounds tested in this work was carried out using the parasite viability dye, resazurin which in the presence of a viable cell is reduced to a pink fluorescent compound called resorufin. Alamar blue was used in various assays as reported below.

2.5.1 Drug sensitivity using Alamar Blue in bloodstream forms of *T. b. brucei*

The drug susceptibilities of bloodstream form trypanosomes *T. brucei* s427 and B48 were determined using the resazurin (Alamar blue) assay. This involves adjusting cell density to the desired concentration of 2×10^5 cells/mL of which 100 µL was added to all of the wells in the plate having a 100 µl serially diluted test compound (200 µM top concentration) in HMI-9 + 10% FBS, then incubating trypanosomes and test compound for a period of 48 hours followed by the addition of 20 µl filter-sterilised resazurin solution prepared by adding 25 mg resazurin sodium salt to 200 mL PBS. This was followed by further 24 hours incubation. Standard drugs including

pentamidine and diminazene aceturate were used as positive control. Fluorescence was measured in the 96-well plates with a FLUOstar Optima (BMG Labtech, Durham, NC, USA) at wavelengths of 544 nm for excitation, 590 for emission, and a gain of 1250. EC₅₀ values were calculated by non-linear regression using an equation for a sigmoidal dose-response curve with variable slope (GraphPad Prism 5.0, GraphPad Software Inc., San Diego, CA, USA).

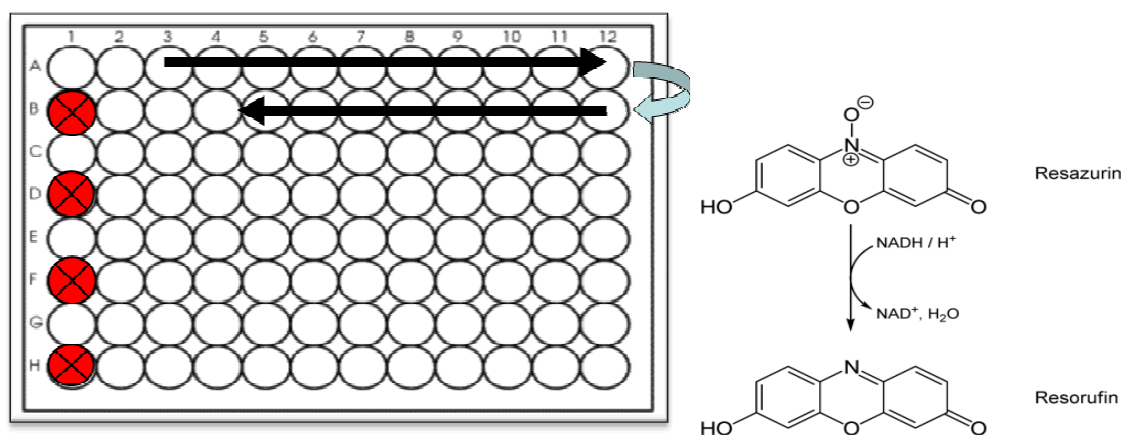


Figure 2.1 Drug dilution (doubly diluted) down two rows across the plate. The red well is the drug free well.

2.5.2 Drug sensitivity using Alamar Blue in *L. mexicana* promastigotes

The drug sensitivity assay in *L. mexicana* was carried out using a method similar to the one used for bloodstream form trypanosomes and was determined using the viability dye resazurin, which involves performing a serial dilution of drug such that there is 100 µL in each well as shown above (Figure 2.1). To each well, 100 µL of a 2×10^6 cells/mL suspension is to be added to give a final cell density of 1×10^5 /well. Because of the difficulty associated with counting *Leishmania* on a haemocytometer, due to their rapid motility, the cells were fixed in 1% formaldehyde and this was achieved by taking 50 µl of culture and adding this to 400 µl of the media (HOMEM, pH 7.4) and 50 µl of 1% formaldehyde, making a 10% culture dilution after which the count was multiplied by the dilution factor of 10 to get the actual cell density. After adjustment of the cell density to exactly 2×10^6 cells/ml, 100 µl of the suspension was added to all wells in the plate, each already containing 100 µl of the serially diluted drugs (or medium in the no-drug controls). The plate was incubated for a period of 72 hours, at 25 °C and 5% CO₂ followed by the addition of 20 µl resazurin. This was followed by further 48 hours incubation. Pentamidine was used as a standard drug. Fluorescence was measured in the 96-well plates with a FLUOstar Optima (BMG Labtech, Durham, NC, USA) at wavelengths of 544 nm for excitation, 590 for emission, and a

gain of 1250. EC₅₀ values were calculated by non-linear regression using an equation for a sigmoidal dose-response curve with variable slope (GraphPad Prism 5.0, GraphPad Software Inc., San Diego, CA, USA).

2.5.3 Assessment of cytotoxicity of test compounds on Human Embryonic Kidney (HEK) 293T cells or Human Foreskin Fibroblast (HFF) cells using an improved protocol

Toxicity of drugs to mammalian cells was carried out using Human Embryonic Kidney (HEK) Cells (strain 293T) or Human Foreskin Fibroblast (HFF) cells according to our improved protocol (Rodenko, *et al.*, 2015), with slight modifications. Briefly, HEK or HFF cells were grown in a culture containing 500 mL Dulbecco's Modified Eagle's Medium (DMEM) (Sigma), 50 mL New-born Calf Serum (NBCS) (Gibco), 5 mL Penicillin/Streptomycin (Gibco) and 5 mL L-Glutamax (200 mM, Gibco). Mammalian cells were incubated at 37 °C/5% CO₂ and were passaged when they reached 80 - 85% confluence in vented flasks. For the assay, cells were suspended at a density of 3×10^5 cells/mL, of which 100 µL was added to each well of a 96-well plate. The plate was incubated at 37 °C + 5% CO₂ for 24 hours to allow cell adhesion. Serial drug dilutions were prepared in a separate sterile plate and 100 µL was transferred to the wells containing the cells; PAO was used as positive control. The plate was then incubated at 37 °C/5% CO₂ for an additional period of 30 h followed by the addition of 10 µL of resazurin solution (125 mg/L in PBS) and a final incubation at 37 °C/5% CO₂ for 24 hours. The plate was read in a FLUOstar OPTIMA fluorimeter at wavelengths 530 nm for excitation and 590 nm for emission. The data were analysed using GraphPad Prism 5.0, and plotted to a sigmoid curve with variable slope to determine EC₅₀ values. The selectivity index was calculated as EC₅₀ (HEK)/EC₅₀ (trypanosomes).

2.6 Drug sensitivity assay using cell counts

Compounds of varying concentrations were tested on trypanosomes for determination of *in vitro* cell growth using cell counts. Trypanosomes at their mid logarithmic phase of growth were taken from cultures and cell density was determined using a haemocytometer. The cell density was adjusted to 2×10^5 with fresh HMI-9 medium. After predetermined periods of exposure to the test compound, cell counts were taken in triplicate, for each concentration of the compounds, typically

for up to 32 hrs. The experiment was repeated two more times and the average counts were used for plotting the growth curve against time in hours.

2.7 Drug sensitivity assay using a Propidium Iodide (PI)

This procedure was used to monitor the effects of the test compounds on trypanosome survival in real time (Rios Martinez *et al.*, 2015). Trypanosomes become fluorescent when the plasma membrane is breached and PI enters the cell and binds to nucleic acids (Gould *et al.*, 2008). In this method, 100 μ L of HMI-9 was added to each well of a 96-well plate and 100 μ L solution of test compounds at different concentrations, also in HMI-9, was added to the first column; wells receiving only media served as drug free controls. To each well was added 100 μ L of HMI-9 containing 1×10^7 trypanosomes and 18 μ M of PI. Wells containing the same final concentration of PI (9 μ M) in HMI-9 but no cells served to record background fluorescence. The plates were incubated in a FLUOstar OPTIMA fluorimeter (BMG Labtech) at 37 °C with 5% CO₂ atmosphere, and the fluorescence was recorded at 544 nm excitation and 620 nm emission for 6 hrs.

2.8 Determination of oxygen consumption rate.

The Oxygen Consumption Rate Assay Kit (Cayman chemicals, Ann Arbor MI, USA), designed to measure extracellular oxygen consumption in mammalian cells, was adapted to trypanosomes following the manufacturer's protocol, but with substantial modifications. Cells were seeded in a sterile 96-well flat bottom tissue culture plate at a seeding density of 8×10^4 cells/well (i.e. 5×10^5 cells/mL) in 150 μ L of HMI-9 and test compounds were added in 10 μ L to the appropriate wells, immediately prior to measurement; three blank wells received culture medium only. Glucose Oxidase Stock Solution (10 μ L, provided by the kit), was added to a control well to deplete all oxygen from the medium, and 10 μ L of SHAM was added to another control well (50 μ M final concentration). Finally, 10 μ L of the probe solution was added to every well except the blank wells; all reagents used had been freshly prepared. Using a repeating pipette, every well was gently overlaid with 100 μ L of mineral oil (provided in the assay kit) pre-warmed to 37 °C. The plate was immediately read kinetically for 120 minutes using a fluorimeter set at 37 °C and at a wavelength of 380 nm for excitation and 650 nm for emission. Gain was adjusted so that the

fluorescent signal of probe in 21% O₂ (air saturated) buffer was equal to 20% of the maximum measureable signal.

2.9 Determination of mitochondrial membrane potential (Ψ_m) using flow cytometry

Fluorescence Activated Cell Sorting technology (FACS) was employed in the determination of the change in mitochondrial membrane potential (MMP) due to exposure of trypanosomes to the test compounds by using tetramethylrhodamine ethyl ester (TMRE) (Denninger *et al.*, 2007). The cell density was adjusted to 1×10^6 cells/mL with and without test compounds for the start of the experiment. 1 mL of sample was transferred at each time point into a microfuge tube and centrifuged at 4500 rpm for 10 min at 4 °C. The pellet was re-suspended in 1 mL PBS containing 200 nM of TMRE, followed by incubation at 37 °C for 30 min. The suspension was placed on ice for at least 30 minutes before analysis by a Becton Dickinson FACS Calibur using a FL2-height detector and CellQuest and FlowJo software (Ibrahim *et al.*, 2011). Valinomycin (100 nM) and troglitazone (10 μ M) were employed as negative (mitochondrial membrane depolarisation) and positive (mitochondrial membrane hyperpolarisation) controls respectively (Denninger *et al.*, 2007). Mitochondrial membrane potential was determined at 0, 1, 4, 8 and 12 h.

2.10 Assessment of cell cycle (DNA content assay) using flow cytometry

Fluorescence Activated Cell Sorting Technology (FACS) was also used to study the effects of test compounds on DNA content in *Trypanosoma brucei brucei* s427 WT. Cell density was adjusted to 1×10^7 cells/mL with and without test compounds for the duration of the experiment. 1 mL of sample was transferred at each time point into microfuge tubes and centrifuged at $1620 \times g$ for 10 min at 4 °C, washed once in PBS containing 5 mM of EDTA and re-suspended and fixed in 1 mL of 70% methanol and 30% PBS/EDTA. The tube with the cells was left at 4 °C overnight in the dark, and the samples were subsequently washed once with 1 mL PBS/EDTA, re-suspended in 1 mL PBS/EDTA containing 10 μ g/mL propidium iodide and incubated at 37 °C for 45 minutes. RNase A (10 μ g/mL) was added before the samples were analysed by a Becton Dickinson FACSCalibur using the FL2-Area detector and CellQuest software. The data obtained were analysed using FlowJo software (FlowJo LLC, Ashland, OR, USA).

2.11 Assessment of cell morphology and DNA configuration using fluorescence microscopy

The configuration of nuclei and kinetoplast DNA of treated and untreated *T. brucei* was visualised using a vectashield mounting medium with the dye 4,6-diamidino-2-phenylindole (DAPI) (Vector Lab. CA, USA), which fluoresces when bound to DNA, while the mitochondrial integrity was examined using the Mito-Tracker Orange CMTMRos staining dye (ThermoFisher Scientific, UK), which is a cationic fluorophore that accumulates in the mitochondria due to the highly negative mitochondrial membrane (Gile *et al.*, 2015).

First, a stock solution of 100 μ M was made by adding 10 μ L of a 1 mM Mito-tracker stock to 90 μ L DMSO. From this solution, 1 μ L was added to 1 mL of sample at each time point to make a final concentration of 100 nM of Mito-tracker. The sample was then incubated at 37 °C and 5% CO₂ for 5 minutes. The incubated sample was washed in filter-sterilized 1 \times PBS and spun at 2,600 rpm for 10 minutes. After the final wash step, the sample was re-suspended in 1 mL of 1 x PBS. 50 μ L of the re-suspended cells were spread onto a glass microscope slide, and were left to air dry, the cells were then fixed in methanol overnight at -20 °C. The following day, the slides were rehydrated using 1 mL of PBS and allowed to rehydrate for 10 minutes after which it was then allowed to evaporate but not completely. A drop of Vectashield antifade mounting medium with DAPI (Vector Laboratories, USA) was added to the slides and spread by a coverslip; the coverslip was then applied and the edges were sealed with nail varnish.

Slides were observed for cell morphology under the Delta Vision core microscope using softWoRx software, while DNA configuration was assessed using a Zeiss Axioplan microscope using Hamamatsu digital camera and Openlab software. A total of 500 cells per slide were counted for each sample using a cell counter, and scores for DNA configuration were given following these groups: 1N1K, 1N2K, 2N2K (Early) and 2N2K (Late), where N is nuclear DNA; and K is kinetoplast DNA.

2.12 TUNEL assay

Fragmentation of parasite DNA after exposure with various compounds was evaluated by TUNEL assay using the APO-BrdU TUNEL Assay Kit (Invitrogen) for the detection of DNA fragmentation, following the manufacturer's protocol. The cell density of the parasites was adjusted to 1×10^6 cells/mL and the cells were incubated with or without the test compounds for the period of the experiment. After the incubation period the cells at first underwent fixation such that 1×10^7 cells were suspended in 500 μ L of PBS, followed by the addition of 5 mL of 1% (w/v) paraformaldehyde in PBS to the sample and then placed on ice for 15 minutes. After this, the sample was centrifuged at 2000 rpm for 5 minutes, and then the cells were washed twice in 5 mL PBS, before re-suspending them finally in 500 μ L PBS. Eventually, 5 mL of ethanol (70%) was added to the sample before storing at -20 °C. Before analysis by flow cytometry, the sample was centrifuged for 5 minutes at 2000 rpm in order to remove the ethanol. The cells were re-suspended in 1 mL of wash buffer, followed by centrifugation for 5 minutes at 2000 rpm; this step was repeated to remove any residual ethanol.

Following the wash step, 50 μ L of DNA-labelling solution (31.25 μ L dH₂O, 10 μ L of the reaction buffer, 8 μ L of BrdUTP, and 0.75 μ L of Terminal deoxynucleotidyl transferase (TdT) enzyme were added and then incubated at 37 °C for one hour (with an intermittent shaking of the sample every 15 min). At the end of the incubation period, 1 mL of the rinse buffer was added and the sample was spun for 5 minutes at 2000 rpm; this step was repeated, with the supernatants removed each time. After this, 100 μ L of the antibody staining solution (95 μ L of the rinse buffer and 5 μ L of the Alexa Fluor 488 dye-labelled anti-BrdU antibody) was added to the sample and then incubated at room temperature for 30 minutes in the dark. Finally, 500 μ L of propidium iodide/RNase (also provided by the kit) was added to the sample and the sample was then incubated for 30 minutes at room temperature with the sample protected from light. The sample was analysed by flow cytometry using both FL3- width and Anti-BrdU FITC detectors and cell Quest software. The data obtained were analysed with FlowJo (10) software.

2.13 ATP level determination

Intracellular ATP was measured using an ATP Determination Kit (Invitrogen), which contains Luciferase (recombinant firefly) and Luciferin, following the manufacturer protocol. Briefly, culture containing 1×10^7 cells of both treated and untreated parasites were taken and centrifuged for 10 minute at 2800 rpm (4 °C). The resulting pellets were washed twice in 200 μ L of 50 mM Tris-HCl, pH 7.4, containing 0.1 mM Dithiothreitol (DTT). The cells were then lysed by sonication on ice (twice for 10 seconds separated by 30 seconds) using a Soniprep 150 with amplitude at 8 micron. After this, it was centrifuged at 14000 rpm for 10 min at 4 °C. The resultant supernatant was frozen in liquid nitrogen and stored at -80 °C. Cellular ATP levels were measured using the contents provided in the kit. The standard reaction solution was prepared for a 10 mL volume master mix [8.9 mL dH₂O, 0.5 mL 20 \times reaction buffer, 0.1 mL of 0.1 M DTT, and 2.5 μ L firefly luciferase (5 mg/mL), 0.5 mL of 10 mM D-luciferin]. After this, 90 μ L reaction solution from the master mix was added to each well and the background luminescence was recorded using a FLUOstar OPTIMA fluorimeter; then 10 μ L of each sample was added to the well and incubated for 15 min at 28 °C and the luminescence was recorded. A standard curve was made using serial dilution of varying concentrations of ATP (0.5 μ M – 500 pM) to calculate the ATP concentrations in the samples.

2.14 Metabolomic assessments of *T. b. brucei* cells treated with natural compounds.

Bloodstream form *T. brucei* was seeded at the same cell density (2×10^5 /mL) in 75 cm² flasks (one for the drug treatment, and another for the negative control) two days before the experiment in order to have a mid-log phase culture. The cells were treated with the appropriate compounds at concentration equal to half their EC₅₀ for 10 h at 37 °C, and 5% CO₂. Samples of 1×10^8 cells were taken at the end of the incubation period, transferred to a 50 mL falcon tube, and quenched by rapidly cooling the cells to 4 °C by submerging tube in a dry ice/ethanol bath. During the cooling process, the samples were continuously stirred to avoid freezing and cell lysis; the tubes were then wiped and placed on ice. Next, the samples were spun at 1250 $\times g$ for 10 minutes at 4 °C, after which 10 μ L of the supernatant was taken from each sample, transferred to a microfuge tube and kept in a freezer at -80°C. This supernatant sample was eventually mixed with 200 μ L CMW for spent medium analysis. The supernatant having been mostly removed, (keeping the tube on ice) a

small volume was left in which the cells were re-suspended. This was transferred to a microfuge tube and centrifuged at 4500 rpm for 5 minutes at 4 °C, after which the last of the supernatant was carefully and completely removed. The pellet was washed in 1 mL PBS at 4 °C and centrifuged at 4500 rpm, for 5 minutes at 4 °C and this step was repeated for 20 seconds in order to remove any PBS left.

The pellet was then re-suspended in 200 µL of extraction solvent (Chloroform: Methanol: Water, CMW, 1:3:1) at 4 °C and was vigorously mixed in order to break up the pellet. The samples including the CMW solvent sample in microfuge tube (200 µL) and the fresh medium sample (10 µL medium + 200 µL CMW) were left on the shaker in the cold room (4 °C) for 1 hour at maximum speed. After this period of shaking, the samples were centrifuged at 13,000 rpm, for 10 min at 4 °C, and the supernatants (CMW extracts) were removed (180 µL) and transferred to MS vials, making sure no part of the pellet went into the sample.

About 10 µL from each sample was collected (with the exception of the ‘no fresh medium’ and CMW solvent samples) into the same microfuge tube and was used as quality control (QC). Argon (Ar) was added to each sample before sealing and the samples were eventually stored at -80°C until analysis by LCMS.

2.15 TAO over-expression

This was done with the aim of cloning the TAO gene into the pHD1336 plasmid in order to over-express it in *T. b* s427 WT, creating a tool for the validation or otherwise of the proposed mechanism of action of the designed TAO inhibitors.

2.15.1 Extraction of Genomic DNA

Genomic DNA (gDNA) was obtained from *T. b* s427WT, and performed using standard gDNA extraction kit (NucleoSpin®) according to the method below.

The trypanosome culture was spun at 2600 rpm for 10 minutes after which cell pellets were re-suspended in PBS buffer in the wash step and spun at 2600 rpm for 10 minutes before re-suspending the cell pellets in 500 µL of the NTE buffer (provided in the kit), 25 µL of 10% SDS, and 50 µL of 10 mg/mL RNase A. This mixture was then incubated at 37 °C for 5 minutes after

which 25 μ L of 20 mg/mL Pronase was added to the sample, which was then incubated overnight at 37 °C.

The next day, 600 μ L of phenol: chloroform: isoamyl alcohol (25:24:1) was added to the sample. The tube was then spun at 12,000 rpm for 5 minutes and the clear supernatant was removed and dispensed into a separate sterile centrifuge tube, followed by the addition of the same volume of the same mixture and was centrifuged. Once more the upper phase was transferred to a new sterile tube and 600 μ L of chloroform was added, and then centrifuged at 12,000 rpm for 5 minutes. The upper phase was then taken and transferred to a sterile polystyrene tube after which 2.5 mL of absolute ethanol was added to the sample in order to precipitate the DNA, the tube was centrifuged at 12,000 rpm for 5 minutes. The DNA obtained was washed with 70% ethanol. The tube was then centrifuged at a maximum speed and the DNA pellet was air-dried in the microbiological safety cabinet before it was resuspended in 50 μ L TE buffer and the DNA sample was quantified with a nanoDrop then was stored until use at 4 °C.

2.15.2 Primer design for Polymerase Chain Reaction (PCR)

Primers were designed for 5' and 3' ends of the *TbAOX* gene with HindIII and BamHI as restriction sites:

Forward- HDK560: GCGC AAGCTT ATGTTTCGTAACCACG

Reverse-HDK561: GCGGATCC TACACATGTTTGTTTACATT

2.15.3 Gradient PCR

Gradient PCR was performed to determine the TAO primers' annealing temperature (T_m). *T. b* 427 WT genomic DNA (gDNA) was used as template. This involves the use of: 10 μ L GC buffer, 2 μ L of 10 mM dNTPs, 2 μ L forward primer, 2 μ L reverse primer, 0.5 μ L gDNA, 0.5 μ L phusion polymerase, and 33 μ L H₂O. Next, 10 μ L of the 150 μ L master mix was added to 12 PCR tubes. Gene amplification was performed using a PCR machine.

2.15.4 Agarose Gel Electrophoresis of DNA

Agarose gels were prepared for the analysis of PCR products. Briefly, 1% agarose was dissolved in 1 × TAE buffer and the solution was boiled until it became clear, signifying that the agar was dissolved in the TAE buffer. After cooling the solution until it became lukewarm, SYBR[®] safe was added. The gel was run at 110 Volts and the bands were observed under the UV transilluminator. The size of the TAO gene was noted.

2.15.5 TAO gene amplification

The TAO gene was amplified using PCR method similar to the one highlighted above, from *T. b* 427 WT genomic DNA (gDNA) using a primer annealing temperature of 69.7 °C. The PCR product was PCR-cleaned and DNA was quantified using a Thermo-Fisher Scientific NanoDrop - a spectrophotometer that calculates the absorbance of a very small sample across different wavelengths. Double digest for TAO and for the vector pHD1336 was performed using HindIII and BamHI as restriction endonucleases. This was followed by ligation of the TAO gene into the pHD1336 backbone.

2.15.6 Transformation of XL1 Blue *E.coli*

In order to transform ligations into XL1 blue *E.coli*, aliquot of competent XL1 blue cells were defrost on ice. Then, 10 µL of ligation product was put into a 1.5 mL microfuge tube followed by the addition of 50 µL of XL1 blue cells. It was incubated on ice for 30 minutes and then heat shocked at 42 °C for 45 seconds after which it was put back on ice for 2 minutes. This was followed by the addition of 100 µL of LB broth, and incubated at 37 °C for 1 hour with shaking. Cells were spread using a sterile spreader on pre-heated (at 37 °C for 30 minutes) ampicillin containing Agar plates (100 µg/mL amp). It was then incubated at 37 °C overnight.

2.15.7 PCR screening of colonies

Colonies on plate were screened the next day using PCR. Bacterial colonies from the agar plate were picked with a sterile 200 µL pipette tip, and were streaked onto a new LB agar plate (numbering each colony) and then using the residual bacteria for a PCR reaction, dipping the tip

into the reaction mix. The new agar plate was then put into an incubator set at 37 °C while the PCR was carried out as follows:

The lead was set to 112 °C for a hot start PCR; the denaturation temperature step was set at 95 °C for 3 minutes; start cycle: x35; annealing temperature step; Gradient step: 48.5 °C for 30 seconds; extension step: 72 °C for 1 min. 40 seconds; End cycle; A further extension step of 72 °C for 5 min.; Storage: 10 °C.

Samples were then run on 1% agarose gel to determine the positive and negative colonies. Overnight cultures of positive colonies were grown by adding 5 µL of 100 mg/mL ampicillin to 5 mL LB broth, followed by the addition of a streak of the correct bacteria. These were kept in the shaker overnight. The following day, DNA was isolated from the colonies by miniprep, followed by a test digest to excise the insert from the vector. Samples yielding the correct sized dropout band were then sent for sequencing. Linearization of pHD1336 carrying the TAO insert was done using NotI incubated at 37 °C for 4 hour after which the digest was purified using standard PCR cleanup kits (NucleoSpin®).

2.15.8 Transfection of Bloodstream form (BSF) *T. brucei* with TAO inserted into pHD1336

Transfection was carried out on 5×10^6 BSF *T. brucei* cells using cells with a density of around 1×10^6 Cells/mL. The number of cells needed was worked out and the cells were spun at $1500 \times g$ for 10 minutes after which the supernatant was removed completely. Then, 10 µg of digested DNA was transferred to an electroporation cuvette. Cell pellets were resuspended in 100 µL T-cell buffer and added to the cuvette with the DNA. It was zapped in the Amaxa electroporation machine using the X-001 programme on the machine, after which the electroporated parasites were transferred immediately into 10 mL pre-warmed HMI-9 medium where they were allowed to recover for 6-18 hours at 37 °C, and 5% CO₂. Three 50 mL tubes were then set up and labelled D1, D2, and D3 respectively. This was followed by the addition of 23 mL, 33 mL, and 12 mL of HMI-9 to D1, D2, and D3 respectively. Also, 23 µL, 33 µL, and 12 µL of blasticidin (5 µg/mL) was added to D1, D2, and D3 respectively. After this, 1 mL of culture was added to D1, 3 mL of D1 was transferred to D2 and 12 mL of D2 was transferred to D3. This ended up with a plate of: 1/24 dilution, 1/288 dilution, and 1/576 dilution respectively. From each of D1, D2, and D3, 200 µL was transferred into separate 96 well plates, which were labelled appropriately. After this, 10 mL of fresh HMI-9 media was added to the remaining culture in the flask and 19 µL of blasticidin (5 mg/mL) was added. Both plates and culture flask were incubated at 37 °C and 5% CO₂.

2.15.9 Real Time-PCR

This was performed on transfectants, empty vector and wild type controls using a method previously described (Ali *et al.*, 2013). Briefly, complementary DNA (cDNA) for the TAO gene was synthesized using a Reverse Transcriptase (RT) kit (Primerdesign, UK). The cDNA for each of the samples was diluted 1:10 before using them for Real Time-PCR. Amplification of the cDNA was performed using a 7500 Real Time PCR System (Applied Biosystems). The dissociation curve was used to ensure the amplification of only one product, while samples without RT or cDNA were used as controls. The constitutively expressed gene GPI8 (Lillico *et al.*, 2003; Capewell *et al.*, 2011) was used as endogenous control. This uses primer sequences of 5'-TCTGAACCCGCGCACTTC and 5'-CCACTCACGGACTGCGTTT (Ali *et al.*, 2013). For TAO, the Δ CT method was used for relative quantification (RQ) using WT cells in HMI-9 as an internal control or a calibrator. All data was analysed using Real-Time PCR systems software (Applied Biosystems 7500 SDS). Primers used for the amplification of TAO were 5'-CGAAGTGGCTCGCGTGTA and 5'-TGATGAGGTCGCGGAATGT. The entire experiment was carried out on three independent occasions, beginning with cell culture and RNA isolation.

2.16 Cloning, expression, and direct inhibitory studies of physiologic Trypanosome Alternative Oxidase (Δ MTS-TAO)

In this section the direct inhibitory studies of recombinant TAO (rTAO) using the novel designer TAO inhibitors is described. However, because the full length TAO (*fl*-TAO) doesn't exist physiologically in trypanosomes, considering that the mitochondrial targeting signal (MTS) is cleaved upon transportation of TAO into the mitochondria, it was therefore imperative to target the physiological form of TAO (Δ MTS-TAO) and carry out direct inhibitory studies with the potential inhibitors. Over-expression of *N*-His₆ SUMO-TAO without mitochondrial targeting signal (Δ MTS) was carried out in haem-deficient FN102 cells.

2.16.1 Plasmid construction for recombinant TAO expression

A previous plasmid construct, pTAO, which contains the cDNA for TAO from *T. brucei brucei* TC221 as previously described by Nihei *et al.* (2002; 2003), was used as template for the

amplification of TAO using 5'-AGCCGTAACCACGCATCGAGG-3' and 5'-CTTGTGTTGAAGCAGAGAATGAGCGC-3' as sense and antisense cloning primers, respectively, for full length TAO, while 5'-AGCGACGCCAAAACACCTGTGTGGG-3' and 5'-CTTGTGTTGAAGCAGAGAATGAGCGC-3' primer pair was used to amplify the gene segment lacking the MTS coding sequence (Δ MTS-TAO). Pfu Ultra II Fusion HS DNA polymerase (Stratagene, Ca, USA) was used for the initial PCR amplifications followed by Taq DNA polymerase for the addition of 3' A-overhangs. Following the manufacturer's procedure, gel-purified PCR product (TAO) containing the 3' A-overhang was inserted into pET SUMO expression plasmid (Thermo-Fisher), and used for the chemical transformation of One Shot TOP10 *E. coli* cells. Colonies of transformants were grown on 50 μ g/mL Kanamycin-supplemented Luria-Broth (LB) plates. Construct-positive clones were confirmed by colony PCR and were then selected for liquid culture in LB media for the amplification of vector construct. TOYOBO Magnetic Extractor kit (Osaka, Japan) was used for plasmids extraction, and were subjected to further confirmation by sequence analyses. The NHis₆SUMO-tagged TAO was further sub-cloned into pET101 (Invitrogen) which contained a carbenicillin resistance cassette. Following PCR and gene analyses, the correct construct was used to transform a haem-deficient FN102 protein expression *E. coli* host having a Kanamycin resistance gene. The construct-positive colonies were selected under carbenicillin and Kanamycin pressure, and selected for storage and expression experiments.

2.16.2 SDS-PAGE of purified rTAO

SDS-PAGE was carried out following the method described in Balogun *et al.* 2013 with slight modifications. Bacterial lysate, membrane fractions, flow-through, and peak fractions from a TALON column were subjected to discontinuous SDS-PAGE. The stacking and separating gels were at 4% and 12% (w/v) acrylamide, respectively. Samples were mixed in a 1:1 (v:v) with 2 \times SDS PAGE loading buffer [4% (w/v) SDS, 125 mM TrisHCl, pH 6.8, 0.2% (w/v) bromophenol blue (Nacalai tesque), 15.8% (v/v) glycerol, and 10% (v/v) β -mercaptoethanol] and heated for 5 min at 95 $^{\circ}$ C. Protein preparations were then loaded into wells of a 1.0 mm thick gel and run alongside a lane containing broad-ranged Precision Plus Protein Standards (BIO-RAD, Hercules, CA, USA) in 1 \times Tris-glycine running buffer [0.1% (w/v) SDS, 14.3 g/L glycine, and 3.0 g/L Trizma-base]. The gel was run at 20 A per gel for about 90 min and stained for 25 minutes in GelCode Blue Safe Protein Stain (Thermo Fisher Scientific) and de-stained in milli-Q water on a

see-saw shaker with regular change of the milli-Q water after every 20 minutes until bands visibly appeared. Gel documentation was performed by scanning, using a colour imager (GT-7600U, Epson).

2.16.3 Preparation of inner membrane-rich fraction

Membrane samples were prepared following a method similar to the one described by Kido *et al.* (2010) with some modification. Briefly, glycerol stock of NHis₆SUMO-TAO-pET101/FN102 was streaked onto an LB plate containing 100 µg/mL carbenicillin, 50 µg/mL Kanamycin, and 50 µg/mL ALA (aminolevulinic acid) using a sterilized platinum rod spreader under sterile conditions. The plates were then incubated at 37 °C overnight. From the many colonies that appeared, a single colony of the strain (FN102) carrying the cDNA for *T. b. brucei* full-length or ΔMTS TAO was used to prepare a pre-culture in 100 mL of Luria Broth medium containing 10 mg carbenicillin, 5 mg kanamycin, and 5 mg 5-aminolevulinic acid (ALA) for 5 – 6 hours at 37 °C in a shaking incubator at 250 rpm for maximum aeration.

When the optical density (OD₆₀₀) was about 0.6, the pre-culture was transferred to centrifuge tubes. The tubes were centrifuged at 8000 rpm for 3 minutes at 4 °C. The supernatant was discarded and the pellets were re-suspended with 20 mL of fresh culture media, and then centrifuged at 8000 rpm at 4 °C for 3 minutes. This wash process was repeated 2 more times to remove residual 5-aminolevulinic acid in the pellets. The pellets were aerobically grown on a larger scale at 30 °C in a total volume of 6 L of S-medium containing, 0.2% (w/v) glucose, 50 g tryptone peptone, 25 g casamino acid, 25 g yeast extract, 15 g KH₂PO₄, 52 g K₂HPO₄, 12.5 g (NH₄)₂SO₄, 3.25 g trisodium-citrate.2H₂O, 0.25 g MgSO₄·7H₂O, 0.125 g FeCl₃, 0.125 g FeSO₄·7H₂O, 0.5 g carbenicillin, and 0.25 g Kanamycin. The 600 mL of the prepared culture was dispensed into 10 flasks for maximum aeration and growth. The initial OD₆₀₀ of the culture was 0.02.

Expression of soluble and active TAO was made possible by induction with 25 µM of the inducer, isopropyl β-D-thiogalactopyranoside (IPTG) when optical density at 600 nm (OD₆₀₀) reached 0.3, and post-induction growth was for 12 hours at 20 °C, after which the cells were harvested by centrifugation at 8000 rpm at 4 °C for 5 minutes. Pellets were re-suspended in 50 mM Tris–HCl (pH 7.5) containing 0.1 mM phenylmethane sulfonyl fluoride (PMSF), 40% (w/w)

sucrose, and protease inhibitor cocktail (Sigma). The cells were broken by a French press with a pressure of 150 - 200 megapascal. Unbroken cells were removed by centrifugation at 8000 ×g for 10 minutes in a Beckman Optima, L-90K ultracentrifuge (USA). Inner membranes of NHis₆SUMO-TAO-pET101/FN102 were fractionated in 40% sucrose after ultracentrifugation at 200,000 ×g for 1 hour at 4 °C in a Beckman Optima, L-90K (30 mL of 20% sucrose lysate was overlaid on 30 mL of 50 mM Tris–HCl pH 7.5 containing 40% (w/w) sucrose per ultracentrifuge tube). The buoyant rich inner membranes were fractionated and the inner membrane pellets was separated by further ultracentrifugation at 200,000 ×g for 1 hour (Beckman Optima, L-90K, USA). The brown coloured inner membrane pellet was re-suspended in 50 mM Tris–HCl (pH 7.5) containing 20% (w/w) sucrose.

2.16.4 Membrane solubilisation

The buoyant rich inner membranes were treated with solubilisation buffer (6 mg/mL protein in 50 mM Tris-HCl, 14% (w/v) n-octyl-β-D-glucopyranoside (OG), 2 M MgSO₄·7H₂O, 20% (v/v) glycerol, pH 7.3) at 4 °C (in the cold room); the membrane sample was maintained at 4 °C throughout the solubilisation process. The solubilized membranes were ultracentrifuged at 42,000 rpm for 1 hour at 4 °C. The total protein content and the quinol oxidase activities of the samples were determined at various stages i.e. before centrifugation, in the supernatant, and in the pellet.

2.16.5 Purification of recombinant TAO

Purification of rTAO was done by means of a hybrid batch/column procedure using TALON metal affinity resin containing Co²⁺ metal ion which has a strong affinity for/interacts and binds to the histidine tag on SUMO-TAO. This was carried out according to the manufacturer's instruction. Briefly, 4 mL of TALON metal affinity resin was equilibrated in a batch set-up with 100 mL of equilibration buffer (50 mM Tris–HCl containing 20% (v/v) glycerol, 1.4% (w/v) OG, 0.1 mM MgSO₄, pH 7.3). OG extract (20 ml) was mixed with the TALON resin for 20 minutes at 4 °C. The resin was washed twice with 100 mL of wash buffer containing a low concentration of imidazole (0.1 mM imidazole, 20 mM Tris–HCl, 0.04% (w/v) n-dodecyl-β-D-maltopyranoside (DM), 20% (v/v) glycerol, 50 mM MgSO₄, pH 7.3) and the resin-bound rTAO was transferred to a column for additional washing with 20 mL of second wash buffer (20 mM Tris–HCl, 0.1 mM imidazole, 0.04% (w/v) DM, 50 mM MgSO₄, 20% (v/v) glycerol pH 7.3; flow rate 1 mL/min) and

protein elution. Finally, rTAO was eluted with elution buffer containing a higher amount of imidazole (80 mM imidazole, 20 mM Tris-HCl, 0.04% (w/v) DM, 160 mM NaCl, 50 mM MgSO₄, 20% (v/v) glycerol pH 7.3; at a flow rate of 1 mL/min). Fractions (2 mL each) were collected in the cold room.

2.16.6 Preparation of Ubiquinol-1 (UQ₁H₂) from Ubiquinone-1 (UQ₁)

The quality of Ubiquinol-1 [2,3-Dimethoxy-5-methyl-6-(3-methyl-2-butenyl)-1,4-benzoquinol] is critical to the overall study of TAO kinetics. This is due to the ability of ubiquinol-1 to quickly re-oxidize to either the partially reduced (semiquinone or ubisemiquinone) form, or the fully oxidized (ubiquinone) in the presence of molecular oxygen. Because of this, the following procedure was carefully followed with all precautions duly observed.

Three bottles of UQ₁ [2,3-Dimethoxy-5-methyl-6-(3-methyl-2-butenyl)-1,4-benzoquinone] corresponding to 10 mg/bottle were emptied into 3 mL of absolute ethanol, then transferred to a separating funnel containing 15 mL of a 0.25 M sucrose, 0.1 M sodium phosphate buffer (pH 7.5). This was followed by the addition of 2 mL of the first separating solvent, cyclohexane, the mixture was subjected to N₂ (g) bubbling. An equal volume of the second separating solvent, ethanol (2 mL) was added to the mixture and transferred to a clamped separating funnel. This was followed by the addition of 1 spatula of the reducing agent Dithionite, and the separating funnel with its content was subjected to N₂ flushing. The mixture was vigorously mixed until the hexane part became clear, and a phase separation appeared in ~ 2 – 3 minutes. After the lower phase (ethanol phase) had been let down the funnel, the upper phase (hexane phase) was collected with a Pasteur pipette into a pre-weighed (W1) clean 20 mL Pyrex Eggplant type flask.

Because the ubiquinol (UQ₁H₂) produced would still be trapped in the aqueous phase, and to exhaustibly extract the UQ₁H₂, the ethanol phase was returned to the separating funnel after which 2 mL of fresh hexane was added to it, and it was mixed vigorously and left until a phase separation appeared. The hexane phase was collected and added to that previously collected in the pre-weighed (W1) clean 20 mL Pyrex Eggplant type flask followed by N₂ flushing. This process was repeated three more times to exhaustibly extract the trapped UQ₁H₂. The content of the Pyrex Eggplant type flask (UQ₁H₂ in hexane) was vacuum dried in a rotary evaporator set at 40 °C until the content became syrupy and there was no more hexane left. The flask was re-weighed (W2)

and the weight of UQ₁H₂ was calculated as W₂ – W₁. This was followed by the addition of 2 mL acidified ethanol (1% hydrochloric acid in ethanol) to recover the ubiquinol from the flask. The concentration was determined spectrophotometrically at 290 nm after which the spectrophotometric values were fitted to Beer-Lambert's law using an extinction coefficient of 5.0 mM⁻¹.cm⁻¹.

Aliquots were made in 5 mL amber bottles, and were deoxygenated with N₂ flushing and were stored at -20 °C until required.

2.16.7 Ubiquinol oxidase/TAO inhibitory assay

The Ubiquinol oxidase activity of purified TAO was measured by recording the absorbance change of ubiquinol-1 at 278 nm on a double beam-dual wavelength spectrophotometer (Shimadzu spectrophotometer UV-3000, Japan) over 2 minutes. Reactions were initiated by the addition of ubiquinol-1 ($\epsilon_{278}=15,000 \text{ M}^{-1} \text{ cm}^{-1}$) after 2 min of pre-incubation at 25 °C in the presence of rTAO and 50 mM Tris–HCl (pH 7.4) in a total reaction volume of 1 mL. For TAO kinetics/inhibitor assays, the reaction was initiated by the addition of varying concentration of ubiquinol-1 after 2 min pre-incubation at 25 °C in the presence of fixed amounts of rTAO and varying concentrations of Ubiquinol-1 and the inhibitor, all in a 50 mM Tris–HCl (pH 7.4) buffer containing 0.05%(w/v) octaethylene glycol-monododecylether detergent.

2.17 Surface Plasmon Resonance binding analysis of enzyme-inhibitor complex

Surface plasmon resonance (SPR) binding experiments were performed in order to study the molecular interactions between the inhibitors and the TAO enzyme, according to the method described by Drescher *et al.* 2009. Briefly, the test compounds were in the mobile phase and the recombinant TAO was fixed on a thin gold film. In the experiment, recombinant TAO was immobilized by an amine-coupling reaction onto a sensor chip (Biacore, Piscataway, NJ, USA) and was inserted into the flow chamber of the Biacore T200 (Biacore, Uppsala, Sweden). Addition of the flow-through analyte (the test compound) to the chamber resulted in the binding of the compound to the immobilized recombinant TAO, thereby producing a change in refractive index at the gold surface which was then quantified with precision. The sensorgram obtained was fitted to a 1:1 binding model, and the binding affinities were obtained from the ratio of rate constants, producing a rather straightforward characterization of the rTAO-inhibitor interaction.

Chapter 3: Isolation of anti-parasitic compounds from Nigerian medicinal plants.

3.1 Introduction

African trypanosomiasis and Leishmaniasis as a global health challenge is compounded by the lack of vaccines, making chemotherapy the only suitable alternative at the moment (La Greca and Magez, 2011). In addition, existing antiparasitic drugs are hampered by toxic side effects and the emergence of resistance (Delespaux and De Koning, 2007; Fairlamb *et al.*, 2016). However, natural products have been identified as highly promising starting points for the discovery of anti-protozoan agents (e.g. Salem and Werbovetz, 2006; Omar *et al.*, 2016; Siheri *et al.*, 2016; Dike *et al.*, 2016), and indeed have a long and distinguished history as essential drugs in the fight against tropical disease (e. g. Tu 2011). Indeed, over the period 1981-2002, 61% of all new chemical entities approved for infectious diseases were natural compounds or directly derived thereof (Newman *et al.*, 2003).

Natural products derived from plants have played an important role in the control of diseases caused by the protozoal parasites, a classical example is malaria caused by *Plasmodium falciparum*. Current malaria treatment relies heavily on plant-derived products, including the sesquiterpene lactone artemisinin (Wells, 2011), and the alkaloid quinine (Moyo *et al.*, 2016). The success stories of artemisinin, isolated from the Chinese wormwood plant (*Artemisia annua*) and of quinine, isolated from the bark of cinchona trees (*Cinchona officinalis*), both used traditionally as antimalarial therapies, justify drug discovery based on ethnopharmacological usage, as these drugs were discovered following an intensive screening of hundreds of plants traditionally used for treating malaria (Tu, 2011). These achievements notwithstanding, unfortunately, fewer efforts have been put into investigating extracts from various plants traditionally used for treating the kinetoplastid diseases like trypanosomiasis and leishmaniasis despite the undesirable side effects and effectiveness of the currently available drugs.

Centrosema pubescens, *Moringa oleifera*, *Tridax procumbens*, *Polyalthia longifolia*, *Newbouldia laevis*, and *Eucalyptus maculata* (Appendix A) thrive well in Nigeria where they grow in the wild except for *Moringa oleifera*, which is cultivated for food and for medicinal use. *Newbouldia laevis* is mostly used in northern Nigeria for boundary demarcation, while *Polyalthia longifolia* commonly called “‘mast tree” is used as an ornamental plant. These plants (studied in this work) are highly valued and are also used for treating various infections caused by the protozoan parasites including species of *Trypanosoma*, *Leishmania*, and *Plasmodium*, especially the strains

that resists existing chemotypes (Alli *et al.*, 2011; Abubakar *et al.*, 2012; Nwodo *et al.*, 2015; Bankole *et al.*, 2016). Because these plants grow on many soil types, are abundant in the wild, and only their leaves are used, their utilization as herbal remedies pose no danger to biodiversity.

The development of an effective chemotherapy based on a local resource will ensure new drugs that will combat existing problems of drug resistance and toxicity and provide additional economic driver for farmers, thus increasing economic activity and contributing to a reduction in poverty in resource poor communities where these diseases affect man and livestock. Hence, in this study, we investigate the potentials of selected herbs traditionally used for treating infections caused by trypanosomatid parasites in northern Nigeria.

Although leaves from the various plant species studied herein are traditionally used in northern Nigeria against various protozoan infections, but unfortunately none of the herbal preparations from these plants have been standardized for use, nor extensively investigated for their toxicity on mammalian cells, and their activity against protozoan parasites has not been scientifically validated. In search of improved and non-toxic active antiprotozoal principles that are not cross-resistant with current anti-parasitics, the results of the *in vitro* screening of extracts from seven selected medicinal plant species used traditionally to treat kinetoplastid infections in Nigeria, and the isolation of their bioactive principles is reported, with the aim of investigating the efficacies of the medicinal plant extracts, and of compounds isolated therefrom, against kinetoplastid parasites, assess cross-resistance to existing chemotherapy, and assay their toxicity against mammalian cells *in vitro*.

In order to achieve this aim, plants used locally to treat trypanosomiasis and other tropical fevers were obtained and extracted with hexane, ethyl acetate and methanol. Active principles were isolated by bioassay-led fractionation, testing for trypanocidal activity, and identified using NMR and mass spectrometry. EC₅₀ values for their activity against wild-type and multi-drug resistant *Trypanosoma brucei* were obtained using the fluorescent viability indicator dye resazurin. The results are presented below.

3.2 Results

3.2.1 Antitrypanocidal activity and cross resistance studies of extracts using wild type and the multi-drug resistant strains of *T. brucei*.

A total of 21 dried extracts from the leaves of the seven plants studied in this work were screened against protozoan parasites. Extracts were selected for further purification according to a slightly modified version of the protocol of Dua *et al.* 2011. The trypanocidal activity of the primary extracts was tested at a starting concentration of 400 µg/mL. None of the methanol fractions showed measureable activity, probably because all the active ingredients had already been extracted by the earlier hexane and ethyl acetate washes. Another notable observation was that most of the extracts did not show reduced activity against the multi-drug resistant strain B48, and are therefore not cross-resistant with first-line trypanosomiasis drugs such as pentamidine, melarsoprol, diminazene and Cymelarsan. The one exception was the hexane extract of plant A, which was in fact significantly more active against B48 ($P < 0.001$; Fig. 3.1).

The trypanocidal activities of the hexane (H) and ethyl acetate (E) extracts with EC_{50} values < 100 µM are depicted in Figure 3.1, and a full list is given in Table 3. 1. Of particular interest were those with an EC_{50} value below 15 µg/mL, being the hexane extract of plant D (HDK-DH, 2.4 ± 0.1 µg/mL), and the ethyl acetate extracts of plants E (HDK-EE, 4.2 ± 0.7 µg/mL) and F (HDK-FE, 12.3 ± 0.3 µg/mL); these were selected for further purification.

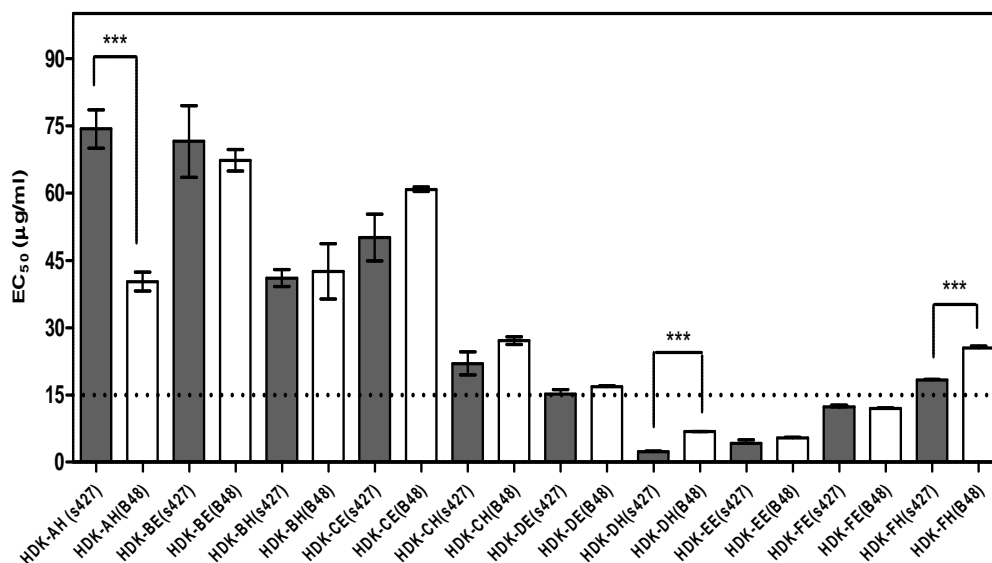


Figure 3.1 Drug sensitivity assays with medicinal plant extracts against *T. brucei* s427WT and B48 cell lines following 72 hours of exposures to extracts. The figure shows all the EC₅₀ values from hexane (H), ethyl acetate (E) and methanol (M) extracts that could be obtained using the protocol described in the Methods section. When not shown the EC₅₀ value was >400 µg/mL, which is equal to the highest concentration on the plate. The hexane fraction of *Centrosema pubescens* (HDK-AH) was more active against multi-drug resistant strain B48 than against wild type s427; no other significant differences ($p < 0.05$) between the two strains were observed. Bars represent the average EC₅₀ values and SEM of at least three independent determinations. *** $P < 0.001$ by Student's unpaired t-test. The dotted line identifies the fractions with EC₅₀ values ≤ 15 µg/ml.

3.2.2 *In vitro* selectivity of extracts: therapeutic index relative to Human Embryonic Kidney cells

All 21 crude extracts from the seven medicinal plants were tested on Human Embryonic Kidney (HEK) 293-T cells *in vitro*, using a modified, and more sensitive, resazurin assay, involving a total incubation period of 78 hours. The result showed that at high doses extracts HDK-CH, HDK-DH, HDK-EE, and HDK-FH displayed a cytostatic, rather than cytotoxic, activity against HEK cells ($EC_{50} < 100$ µg/ml), whereas other extracts displayed less toxicity (Table 3.1). Indeed, no EC₅₀ value could be obtained for 11 out of 21 extracts, using a top concentration of 400 µg/mL. The selectivity index (SI), defined as the *in vitro* EC₅₀ value of the extract against the host cell divided by the EC₅₀ value against the target cell, reached >20 but could not be determined where either EC₅₀ value could not be obtained due to either low efficacy or low toxicity.

Table 3.1 EC₅₀ value, Resistance Factor (RF) and Selectivity Index (SI) of crude ethyl acetate (E), Hexane (H), and methanol (M) extracts from seven Nigerian medicinal plants.

Fractions	<i>T. b.</i> s427 WT (µg/mL)	<i>T. b.</i> B48 (µg/mL)	RF	HEK (293T) cells (µg/mL)	SI
HDK-AE	92.2 ± 2.1	ND	ND	>500	>5.4
HDK-AH	74.3 ± 4.2	40.3 ± 2.1	0.54 ³	386 ± 24	5.2
HDK-AM	233 ± 11	ND	ND	>500	>2
HDK-BE	71.5 ± 8.0	67.3 ± 2.4	0.94	492 ± 37	6.9
HDK-BH	41.0 ± 1.9	42.6 ± 6.2	1.04	>500	>12
HDK-BM	>250	ND	ND	>500	≥2
HDK-CE	50.1 ± 5.2	60.8 ± 0.5	1.22	198 ± 12	4.0
HDK-CH	22.0 ± 2.6	27.1 ± 0.8	1.23	80.0 ± 17	3.6
HDK-CM	222 ± 5	ND	ND	>500	>2
HDK-DE	15.2 ± 1.0	16.9 ± 0.2	1.11	114 ± 3	7.5
HDK-DH	2.4 ± 0.1	6.8 ± 0.1	2.9 ³	50.9 ± 2.2	21.6
HDK-DM	129 ± 18	ND	ND	>500	>3.9
HDK-EE	4.2 ± 0.7	5.4 ± 0.1	1.28	56.2 ± 1.9	13.3
HDK-EH	98.5 ± 1.1	ND	ND	>500	>5
HDK-EM	150 ± 10	ND	ND	>500	>3.3
HDK-FE	12.3 ± 0.3	12.0 ± 0.1	0.98	246 ± 17	20.1
HDK-FH	18.4 ± 0.1	25.4 ± 0.5	1.38 ³	86.9 ± 9.9	4.7
HDK-FM	141 ± 16	ND	ND	>500	>2.8
HDK-GE	>500	ND	ND	378 ± 17	<1
HDK-GH	>500	ND	ND	>500	ND
HDK-GM	>500	ND	ND	>500	ND
Pentamidine	3.4 ± 0.5 ¹	1040 ± 180 ¹	305	ND	ND
PAO ²	ND	ND	ND	118 ± 6 ¹	ND

Results were expressed as average EC₅₀ of at least three independent determinations. Extracts HDK-CH, HDK-DH, HDK-EE, and HDK-FH were cytostatic rather than cytotoxic at high doses on HEK cells. Values are average of EC₅₀ values of 4 independent determinations, expressed in µg/mL. ¹EC₅₀ values for pentamidine and PAO are given in nM. ²PAO, phenylarsine oxide. ³P<0.001, Student's unpaired t-test, comparing WT and B48. ND, not determined.

3.2.3 Anti-Leishmanial activity of the primary plant extracts

In order to determine the *in vitro* anti-leishmania activity of extracts from the selected plants, the extracts were tested on *Leishmania mexicana* (M379) promastigotes (Fig. 3.2). The result revealed that hexane extracts from *Tridax procumbens* and *Polyalthia longifolia* (HDK-CH and HDK-DH) gave the best activity against *L. mexicana in vitro* (EC_{50} values of 16.8 and 17.2 $\mu\text{g/mL}$ respectively), while hexane extracts from *Moringa oleifera* (HDK-BH), *Newbouldia laevis* (HDK-EH), *Eucalyptus maculata* (HDK-FH), and ethyl acetate fractions of *Tridax procumbens* (HDK-CH) and *Polyalthia longifolia* (HDK-DH) all displayed moderate anti-leishmanial activity *in vitro* (EC_{50} 50-70 $\mu\text{g/mL}$). Extracts not included in figure 3.2 were inactive against *L. mexicana* under our experimental condition. There is only moderate correlation between the antileishmanial and antitrypanosomal activities of these extracts, but, importantly, extract HDK-DH displayed the strongest activity against both of the parasites.

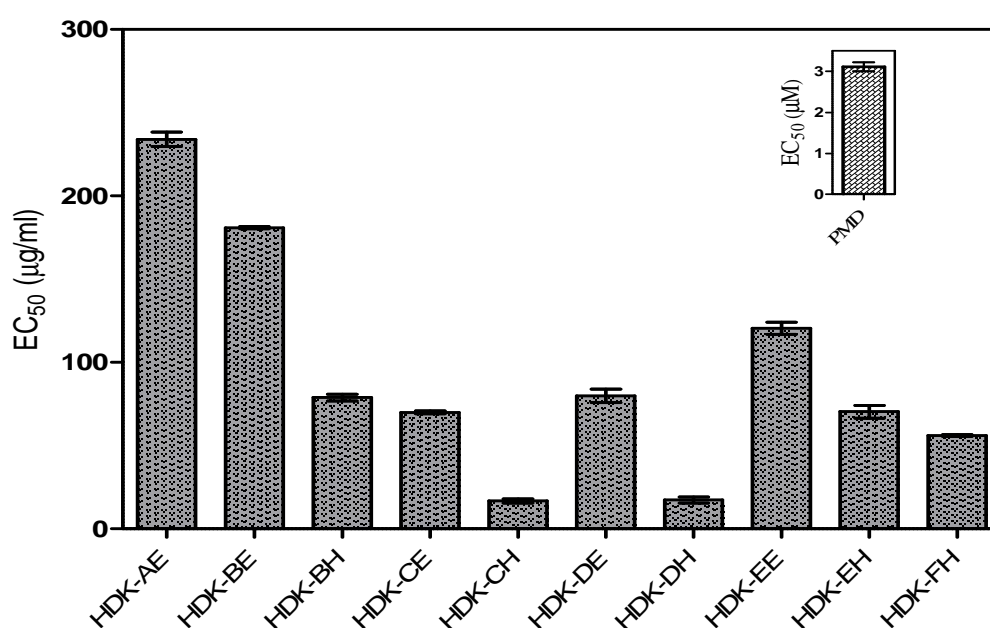


Figure 3.2 Effect of Nigerian plant extracts on *L. mexicana* promastigotes using a top/starting concentration of 400 $\mu\text{g/mL}$. The data shown are the average $EC_{50} \pm \text{SEM}$ of three separate experiments. Inset: pentamidine (PMD), a standard drug, was used as internal control.

3.2.4 Bioactivity-guided isolation of the active constituents from extracts

Between 150 - 200 fractions were collected from the column for each extract selected for fractionation, and the isolation of active compound was guided by the activity of each fraction. Progress of purification was monitored with NMR and mass spectrometric techniques.

After column chromatography the HDK-DH crude extracts yielded a fraction that was very active against trypanosomes. This was followed by further purification on a Sephadex column, which gave a pure and active compound, analyzed by ^1H and ^{13}C -NMR (Appendix B). Nuclear Overhauser Experiments, HMBC, HQSC, and COSY were then carried out to determine the exact structure and relative stereoisomer. Mass spectrometry was also performed to confirm the structure and its purity. The result was a clerodane-type diterpenoid with an α,β -unsaturated lactone ring in the side chain identified as clerodane (16- α -hydroxy-cleroda-3-13(-14)-Z-dien-15,16-olide; HDK-20).

In addition, polyalthialdioc acid (HDK-79) and Kolavenic acid (HDK-52) were also isolated pure from other fractions of the crude hexane extract of plant D, *Polyalthia longifolia* (Figure 3.3).

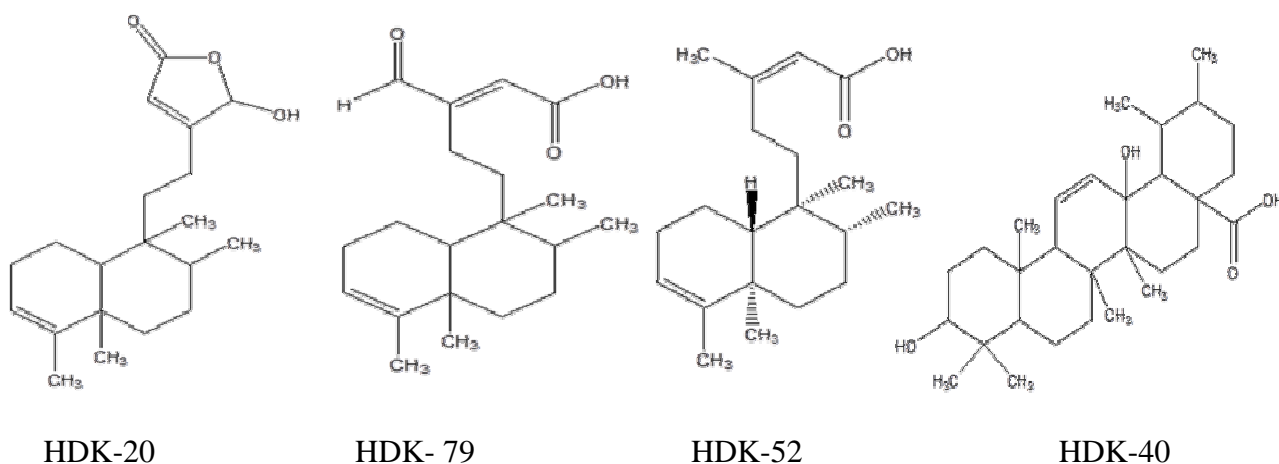


Figure 3.3 Anti-kinetoplastid compounds isolated from *Polyalthia longifolia* (HDK - 20, 79 and 52) and *Eucalyptus maculata* (HDK-40). HDK-20 is 16- α -hydroxy-cleroda-3-13(-14)Z-dien-15,16-olide; HDK-79 is kolavenic acid; HDK-52 is polyalthialdioc acid; and HDK-40 is 3 β ,13 β -dihydroxy-urs-11-en-28-oic acid.

Fractionation of extract HDK-FE yielded a series of compounds, including triterpenes, aromatics (xanthenes), cinnamate/chalcone types, aliphatics, and triterpenoids. Some of these were found in combination in the fractions, or with other impurities. However, the active fraction on trypanosomes was, after chemical analyses, identified as an ursane type triterpenoid ($\text{C}_{30}\text{H}_{48}\text{O}_4$;

HDK-40) with a molecular weight of 472.36 g/mol. Signals for seven skeletal methyl groups, of which two were doublets and five were singlets, were contained in the ^1H -NMR spectrum. The presence of 30 carbon atoms in its ^{13}C -NMR, coupled with the signal from the ^1H -NMR spectrum was suggestive of the fact that this compound was an ursane-type triterpenoid. Furthermore, analyses of the ^1H -NMR spectrum of this compound revealed two olefinic protons and a secondary hydroxyl group whose splitting pattern and chemical shift were characteristic of a 3β -equatorial hydroxy in the nucleus of a typical ursane-type triterpenoid.

In addition, two active compounds were identified from the crude extract of HDK-EE. The NMR and mass spectrometry analyses revealed them to be pheophytin A and B (HDK-28 and HDK-23 respectively) with molecular formula $\text{C}_{55}\text{H}_{74}\text{O}_5\text{N}_4$ and $\text{C}_{55}\text{H}_{72}\text{N}_4\text{O}_6$ and molecular masses of 870 and 885.18 g/mol respectively.

3.2.5 Trypanocidal activity of the purified active compounds

The isolated natural compounds were tested on wild-type s427 trypanosomes as well as a panel of s427-derived cell lines adapted to high levels of resistance of current and experimental classes of trypanocides. B48 is highly resistant to virtually all diamidines and melaminophenyl arsenicals; AQP2/3-KO lacks the AQP2/AQP3 genetic locus and is moderately resistant to pentamidine and melarsoprol; *Tb*AT1-KO is somewhat resistant to pentamidine and highly resistant to diminazene; R0.8 is highly resistant to inhibitors of cAMP phosphodiesterases TbrPDEB1 and B2 (Gould *et al.*, 2013), an important class of new therapeutic leads against trypanosomiasis (Shakur *et al.*, 2011; Gould *et al.*, 2011). The results are presented in the table below.

Table 3.2 Comparing the EC₅₀ values of purified natural compounds for the different trypanosomes strains (s427 WT, B48, AQP2/3KO, AQP1-3-KO, TbAT1-KO, and R0.8) used in this study.

Compounds	s427 WT	B48			AQP2/3-KO			AQP1-3-KO			TbAT1-KO			R0.8		
	EC50 (µg/ml)	EC50 (µg/ml)	RF	t-test	EC50 (µg/ml)	RF	t-test	EC50 (µg/ml)	RF	t-test	EC50 (µg/ml)	RF	t-test	EC50 (µg/ml)	RF	t-test
HDK-20	0.38 ± 0.05	0.40 ± 0.005	1.1	0.76	0.42 ± 0.02	1.1	0.53	0.46 ± 0.02	1.2	0.23	0.37 ± 0.009	1.0	0.82	0.48 ± 0.01	1.2	0.069
HDK-23	1.58 ± 0.09	1.86 ± 0.092	1.2	0.092	2.70 ± 0.08	1.7	0.0006	3.32 ± 0.04	2.1	2.3E-5	2.43 ± 0.071	1.5	0.0040	2.13 ± 0.24	1.3	0.044
HDK-28	25.0 ± 2.8	28.8 ± 4.2	1.2	0.46	22.8 ± 0.4	0.9	0.55	21.59 ± 0.41	0.9	0.35	26.9 ± 0.71	1.1	0.58	24.3 ± 0.7	0.9	0.70
HDK-40	1.58 ± 0.03	1.55 ± 0.012	1.0	0.40	1.39 ± 0.16	0.9	0.0046	1.194 ± 0.11	0.8	0.024	1.75 ± 0.022	1.1	0.020	1.68 ± 0.01	1.06	0.020
HDK-52	12.3 ± 0.5	10.1 ± 0.5	0.8	0.026	6.86 ± 0.04	0.6	0.0002	3.40 ± 0.21	0.3	1.0E-4	9.64 ± 0.78	0.8	0.029	14.2 ± 0.4	1.1	0.007
HDK-79	3.57 ± 0.16	5.2 ± 0.4	1.5	0.0059	5.54 ± 0.18	1.6	0.0011	6.29 ± 0.32	1.8	0.0024	4.81 ± 0.19	1.3	0.015	4.4 ± 0.3	1.2	0.019
¹ PMD (µM)	0.003 ± 0.0004	0.77 ± 0.013	232	1.3E-8	0.046 ± 0.02	15.5	7.8E-6	0.072 ± 0.0029	24.2	1.1E-6	0.0074±0.001	2.5	0.0021	0.0072 ± 0.0001	2.3	0.0019
² DA (µM)	0.23 ± 0.04	2.14 ± 0.24	9.3	4.5E-6	ND	--	--	ND	--	--	2.06 ± 0.74	9.0	3.8E-5	ND	--	--
³ NPD-001 (µM)	0.029 ± 0.005	ND	--	--	ND	--	--	ND	--	--	ND	--	--	3.53 ± 0.16	122	1.6E-6

Multi-drug resistant strains of *T. b. brucei* are not cross-resistant with the purified compounds. ¹PMD = Pentamidine, a known trypanocidal agent; ²DA, diminazene aceturate; ³NPD-001 is a trypanocidal phosphodiesterase inhibitor. RF = Resistance factor. An RF value of ~ 1 indicates no prospect for cross resistance; RF value well above one indicates possibility of cross resistance; RF value below 1 indicates increased sensitivity. P-values (p<0.05) were calculated using the unpaired Student's t-test. ND, not determined.

Compound HDK-20 displayed the highest activity against s427-WT trypanosomes, with an EC_{50} value of 0.38 ± 0.05 , corresponding to approximately 1 μ M. HDK-23, HDK-40 and HDK-79 also displayed activity below 5 μ g/mL, but the activity of HDK-52 was rather disappointing at 12.3 μ g/mL. HDK20, HDK-79 and HDK-52 are closely related compounds from the same plant, *Polyalthia longifolia*, and most likely metabolites of each other. Clearly, the sidechain appears to have a large impact on the trypanocidal activity with the closed β -lactone highly effective; this gives a potential starting point for derivatization towards even higher anti-parasitic activity. Testing of all purified compounds on our panel of drug resistant trypanosome lines identified only minor variations in sensitivity, which although statistically significant in some cases, were always well below even a 2-fold difference from EC_{50} value against the wild-type control (Table 3.2), in contrast to very high levels of resistance to the control drugs. As the resistance mechanisms for these drug classes are now well understood both in the lab strains here and in field isolates (Graf *et al.*, 2003) we can conclude with confidence that the natural compounds reported here are not cross-resistant with key trypanocide classes such as the diamidines, melaminophenyl arsenicals and PDE inhibitors. Indeed, HDK-52 was significantly more active against all the resistant strains of *T. brucei* than the wild type.

3.2.6 Cytotoxicity of the purified compounds

The purified compounds were tested for their effects on human embryonic kidney (HEK) cells, using the same protocol as used for the crude extracts, so as to determine whether the antiprotozoal activity is the result of general toxicity or is more specifically antiprotozoal. The toxicity assays showed that the natural compounds that have an effect on *T. brucei* have almost no inhibitory activity on HEK cell growth and viability. Selectivity indices (SI, EC_{50} of HEK cells / EC_{50} of parasites) for trypanosomes are not shown as none of the compounds tested were toxic to HEK cells at the highest concentration tested (200 μ g/mL) (Fig. 4). However, this means that SI values range between >8 for HDK-28 and >526 for HDK-20. We conclude that the purification increased not only the activity of the plant extracts but also dramatically improved the selectivity of the product.

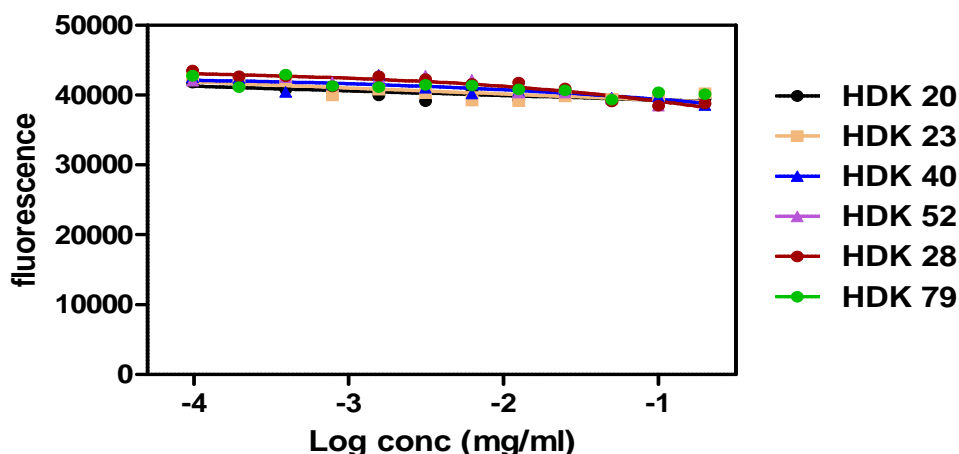


Figure 3.4 Cytotoxicity assay of natural compounds on HEK 293-T cells, with 24 h cyto-adherence, 30 h incubation with drugs, and 24 h with sodium resazurin (alamar blue). None of the isolated compounds displayed sigmoidal curves, showing that they were not toxic to mammalian cells at concentrations >200 mg/mL after 78 hours of incubation with the test compounds. The experiment shown was representative of three independent repeats with identical outcomes.

3.2.7 Activity of Purified compounds against *Trypanosoma congolense* and *Leishmania mexicana*.

The purified compounds were next tested against *T. congolense* in order to determine their prospects of being developed and used as veterinary drugs to treat animal African trypanosomiasis (AAT or nagana), a condition that causes billions of dollars in economic losses in sub-Saharan Africa (Giordani *et al.*, 2016). Most of the compounds were somewhat less potent against *T. congolense* than against *T. brucei* under the assay conditions, but displayed a similar order of potency: HDK-20 >> HDK-40 > HDK-52 = HDK-79. In addition, the compounds were tested against *L. mexicana* promastigotes. As for the other two protozoan species, HDK-20 was the most potent of the compounds tested, and the order against *L. mexicana* was HDK-20 >> HDK-52 > HDK-40 > HDK-79. Figure 3.5 displays the EC₅₀ values against all three pathogens side-by-side. The level of anti-parasite activity for HDK-20 makes this a promising lead compound against kinetoplastid pathogens.

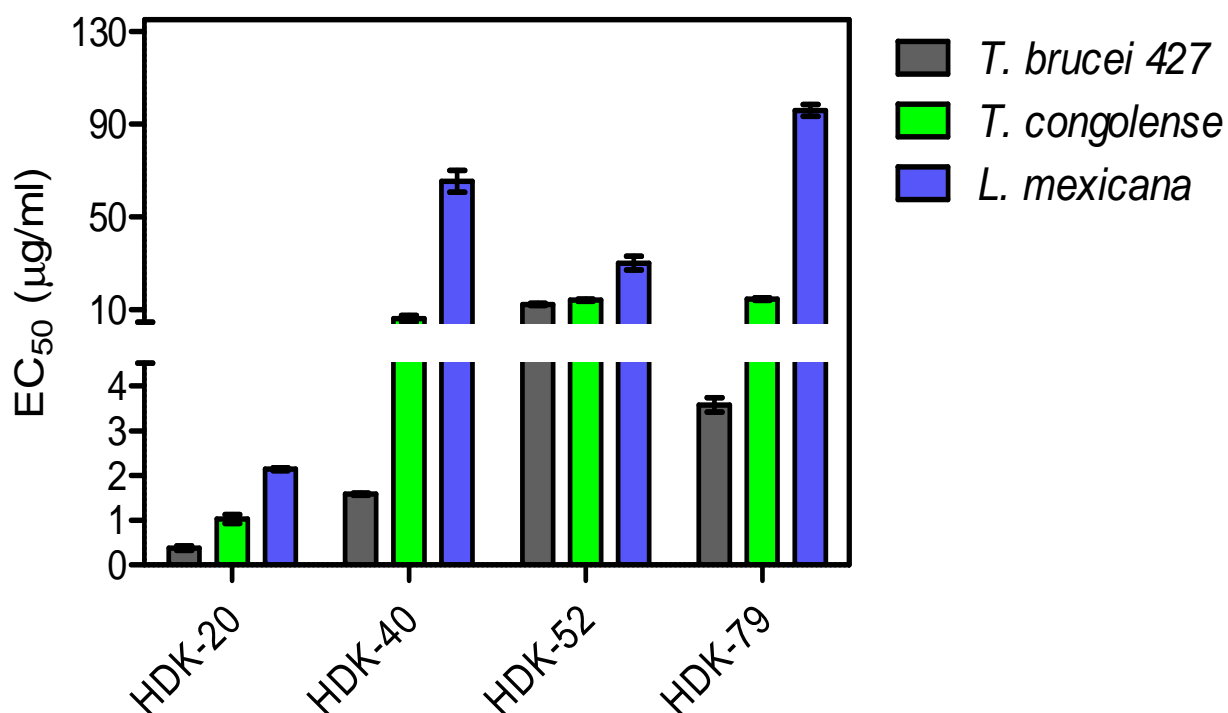


Figure 3.5 Effects of purified natural compounds against three pathogenic protozoa: bloodstream forms of *T. brucei* s427 and *T. congolense* strain IL3000, and promastigotes of *L. mexicana* strain M379, using a top/starting concentrations of 200 µg/ml. EC₅₀ values shown are the average and SEM of 4 independent determinations.

3.3 Discussion

There is an increased interest in the antiprotozoal screening of plant extracts related to traditional therapy (Ndjakou Lenta *et al.*, 2007; Osorio *et al.*, 2007) apparently due to their very low toxicity, the stability of natural compounds, and their reported reduced prospects for resistance or cross resistance to existing drugs (Nour *et al.*, 2009). We report here on the antiprotozoal activity of the extracts of seven Nigerian medicinal plants.

Several of the crude ethyl acetate and hexane extracts displayed promising activity, whereas the methanol extracts were markedly less active. The low activity of the methanol extracts may simply be the result of the plants material already having been extracted with hexane and ethyl acetate, or genuinely indicate that the less polar solutes from these plants have the best anti-protozoal activity. The polar compounds extracted by methanol generally display less cellular penetration than

hydrophobic ones (Orsi and Essex, 2010), and this may contribute to the lack of *in vitro* anti-parasite activity.

The extracts of *C. pubescens*, *M. oleifera*, *T. procumbens* and *J. tanjorensis* (plants A, B, C and G, respectively) did not display any significant *in vitro* anti-trypanosomal activity under our experimental design. However, these plants may contain compounds with other anti-protozoal or antibacterial activities, for which we did not test in the current study. Furthermore, the plants may in fact contain anti-trypanosomal compounds, but perhaps only in low amounts at the time of gathering the material. It must also be remembered that in the traditional usage the plant preparations are taken orally and may be activated *in vivo*.

It has previously been reported that Nigerian medicinal plants contain active anti-parasite constituents (Ene *et al.*, 2014; Igoli *et al.*, 2011). However, the plants that we report on here have not previously been investigated for their anti-kinetoplastid activities, nor have their active compounds been identified before now. The only exception is a report that methanol extracts of *P. longifolia* leaves (our plant D) inhibit the growth of *L. donovani* promastigotes, with an IC₅₀ value of 4.18 µg/mL (Pal *et al.*, 2011). In our screens, too, *P. longifolia* displayed the most promising anti-leishmanial activity, with the crude hexane extract displaying a similar IC₅₀ against *L. mexicana* promastigotes. *P. longifolia* leaf extracts have also been reported to possess activity against pathogenic fungi such as *Candida albicans*, and against gram-positive bacteria, particularly *Staphylococcus aureus*, but not against gram-negative strains (Chanda and Nair, 2010).

The second-most promising medicinal plant in our study was *E. maculata* (plant F), with both the ethyl acetate and hexane extracts displaying anti-trypanosomal EC₅₀ values below 20 µg/mL; this was apparently attributable to the presence of the ursane type triterpene HDK-40, isolated from the ethyl acetate extract. Several previous studies reported anti-infectious activities of *Eucalyptus* species. Extracts of *E. maculata* leaves with methanol-dichloromethane were previously shown to have activity against gram-positive bacteria (Takahashi *et al.*, 2004). Extracts from *E. sideroxylon* and *E. torquata* similarly displayed activity against gram-positive bacteria, and some fungi (Ashour, 2008), and, the ethyl acetate fraction from *E. camaldulensis* displayed a 100% growth inhibition against the protozoan *Trichomonas vaginalis* *in vitro* at a concentration of 12.5 mg/mL (Hassani *et al.*, 2013).

Extracts of *N. laevis* (plant E) have been reported to exercise anti-diabetic (ethanolic extract of leaves; Kolawole and Akanji, 2013), bactericidal (methanolic leaf extract; Usman and Osuji, 2007), analgesic and anti-inflammatory (ethanolic flower extract; Usman *et al.*, 2008) activities but we are not aware of any studies regarding their anti-protozoan activities. Here, we report the anti-kinetoplastid activity of *N. laevis* and attribute its activities to the presence of pheophytin, a compound that was previously isolated from *Loniera hypoglauca* in a screen for activity against hepatitis C virus, and was shown to inhibit its NC3 serine protease (Wang *et al.*, 2009). We found both pheophytin A and B to exhibit a good level of anti-trypanosomal activity, but pheophytin B was approximately 15-fold more potent than pheophytin A.

Our initial NMR data revealed the presence of some common classes of active compounds in these plants under study, including terpenoids, aromatics, and pheophytins (Salem and Werbovets, 2006; Wink, 2012). We attribute the remarkable anti-kinetoplastid activity of *Polyalthia longifolia* extracts and their isolated compounds observed in this study to the presence of clerodane diterpenes, of which the closed lactone form, HDK-20, was more active against the kinetoplastids than the aldehyde or carboxylic acid moieties on the scaffold. HDK-20 and HDK-79 have previously been described in extracts of *P. longifolia*, with antifeedant (Phadnis *et al.*, 1988) and anti-inflammatory properties (inhibition of NO production by macrophages; Wu *et al.*, 2014).

Wink (2008) reported that lipophilic secondary metabolites like the terpenoids have detergent-like properties which can disrupt biological membranes, alter their fluidity and inhibit the function of membrane proteins, including those involved in cellular signaling and transport. Although, we observed no major differences in activity against our cell lines with altered drug transport (B48, AQP2/3-KO, AT1-KO) or cAMP signaling (R0.8), HDK-52 consistently displayed a significantly higher activity against transporter mutants than against the wild-type, a situation that was reversed for HDK-79, and both were somewhat less effective against clone R0.8 as well. However, we do not propose that chemical disruption of the lipid bilayer can be the main mode of action of these compounds, as this would fail to explain the considerable selectivity *vis-à-vis* the *Leishmania mexicana* or human cells.

The active principles isolated in this work could be potentially developed to treat either human or animal African trypanosomiasis (HAT and AAT, respectively). Whereas HAT, commonly known as sleeping sickness, is a devastating, fatal disease, its disease burden is steadily declining (Simarro

et al., 2015) while AAT continues to cause huge economic losses, and places serious limitations on agriculture in sub-Saharan Africa – not just for cattle rearing (beef, dairy) but also for draught power for ploughs, carts, etc. The main AAT pathogens are *Trypanosoma congolense* and *Trypanosoma vivax* (Giordani *et al.*, 2016), and we therefore also tested some of the active principles on *in vitro* cultures of *T. congolense*. Interestingly, the same order of potency for these compounds applied for both *T. brucei* and *T. congolense*, with HDK-20 again being by far the most active agent. Together with the similarly potent activities against multi-drug resistant trypanosome lines, this appears to indicate that the clerodane diterpenes may have general utility against African trypanosomes. This is important, as African livestock may be infected by any of several *Trypanosoma* species and any drug must be able to act on all of them, as identification of (sub)-species for individual animals is currently impracticable. Although the bio-assay fractionation was guided by activity against *T. brucei*, the extracts and their isolated compounds were also tested on *L. mexicana*, as the plants are considered to have broad activity against protozoan infections. The anti-*Leishmania* efficacy of some of these plants (hexane extracts of *T. procumbens* and *P. longifolia*) and their purified compounds (HDK-20), affirms their continuous use in folkloric medicine, and we propose that at least some of the plants are good prospects for new drugs against kinetoplastid diseases.

Chapter 4: Investigations into the mode of action of natural compounds against *T. brucei*.

4.1 Introduction

Medicinal chemists have been able to synthesize a good number of synthetic chemo-types, which are being used for treating many but by no means all protozoan parasites. A particular problem remains with drugs against parasites causing the ‘neglected tropical diseases’. One of the major problems is that the most of these drugs are old, causing parasitic strains to become resistant to these drugs (Rodenko *et al.*, 2015). Unfortunately, the development of new and efficient anti-protozoan drugs has not received much attention or funding from the pharmaceutical industry for the reason that most of these diseases occur in resource-poor communities where the people suffering from these diseases cannot afford to pay for the high price of the drugs, but rely heavily on subsidized or donated drugs (Wink, 2012). Consequently, investing in drug development against especially tropical parasitic diseases is rather a risky venture. The search for anti-parasitics from natural sources especially from secondary metabolites derived from plants is a good alternative to synthetic drugs considering that medicinal plants have been used for centuries for treating infectious diseases.

Medicinal plants are a rich source of drug candidates and leads, and like synthetic compounds, could be exploited as anti-protozoan agents that could solve the present problem of drugs’ inefficiencies (Schmidt *et al.*, 2012; Wink, 2012). Some of the drugs in use today for tropical infections were originally from plant materials previously used for treating these same infections, which account for their long usage as traditional herbal remedies (Maya *et al.*, 2007). The success story of the alkaloid artemisinin, isolated from the Chinese anti-malarial wormwood plant (*Artemisia annua*), and quinine from the bark of cinchona trees (*Cinchona officinalis*) are classic examples (Willcox, 2011). Several plant-derived natural products from diverse structural classes including various flavonoids, alkaloids, quinonoids and terpenoids have been studied as anti-kinetoplastid candidates against some parasite, sometimes targeting specific metabolic pathways such as nucleic acid biosynthesis, biomembranes, and cytoskeletal proteins and enzymes (Wink, 2007).

Natural products have played a significant role in the development of new chemotherapies. For instance in the years 1981 to 2006, 1,184 new drugs were developed and registered for use, out of which 28% were of natural origin. Another 24% of all the new drugs registered within this period had functional groups with pharmacological activity (pharmacophores) derived from natural

products (Newman and Cragg, 2007). Therefore, a good starting point for drug discovery, and in particular to find anti-parasitic natural lead compounds would be traditional medicinal plants, such as those from Nigeria, that have been used to treat various types of infectious diseases. Although there have been many promising developments to identify leads against tropical protozoan parasites using various plant extracts the translation of these results into actual drug candidates has not occurred. In most cases the active principles of these plant extracts remain unknown due to a lack of research facilities and funding. Moreover, the specific mechanism of action of these reported bioactive extracts or bioactive principle is rarely determined if at all [e.g., triptolide; curcumin (Corson and Crews, 2007)]. However, a comprehensive understanding of the interaction of a drug lead with its molecular target is especially helpful for the process of drug development, for the reason that it allows the use of medicinal chemistry approaches for optimization, and in some cases a more suitable clinical trial design. This is crucial to the development of new and efficient chemotherapy that will replace the current inefficient ones.

Using *in vitro* models of *Trypanosoma brucei*, ethnopharmacological/bioassay guided fractionation approach was used towards the identification of new lead compounds and evaluate their potency, based on extracts from traditional medicinal plants from Nigeria. We have shown (see chapter three) that neither the crude extracts, nor the active compounds isolated from them, are toxic to human cells. However, promising activity was found against a drug sensitive wild type strain of *Trypanosoma brucei* (s427-WT) and a multi-drug resistant strain, B48, which lacks both the *TbAT1/P2* transporter and the high affinity pentamidine transporter (HAPT). Therefore this chapter reports the mode-of-action of two of the most promising isolated compounds (16 α -hydroxycyclohexa-3,13(14)*Z*-dien-15,16-olide [HDK20; figure 4.1(A)], and 3 β ,13 β -dihydroxy-urs-11-en-28-oic acid [HDK40; figure 4.1(B)] on *T. brucei*.

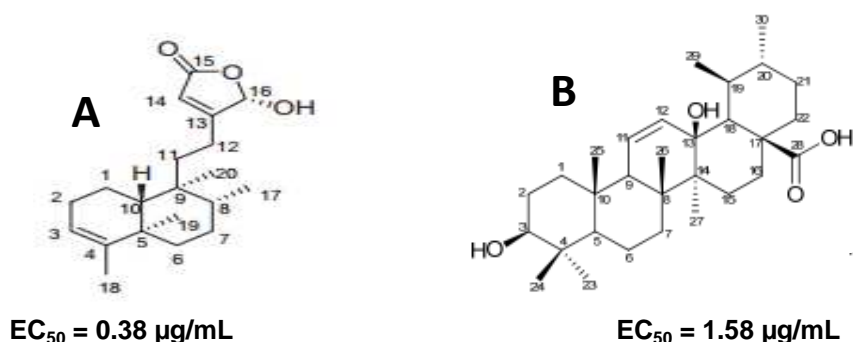


Figure 4.1 Structure of 16 α -hydroxycyclohexa-3,13(14)*Z*-dien-15,16-olide, HDK20 (A), and 3 β ,13 β -dihydroxy-urs-11-en-28-oic acid, HDK40 (B), and their *in vitro* EC₅₀ against trypomastigotes of *T. b. brucei*.

4.2 Results

4.2.1 Effect of different concentrations of HDK20 and HDK40 on the growth of bloodstream form *T. brucei brucei* WT following long and limited exposures.

The effect of test compounds HDK20 and HDK40 on trypanosome (s427 WT) proliferation was studied after exposure of a limited duration. For some drugs like the diamidines (i.e. pentamidine) trypanosomes need only to be exposed for a short period (1-3 hours); although this drug acts very slowly, cell death does occur hours after the exposure would have ceased (Barrett *et al.*, 2007). This means that its early effects are irreversible and trypanosomes will not recover once this effect is initiated. For the translation into *in vivo* activity, a short minimum exposure time for a drug is desirable and may reduce potential toxic effects associated with keeping compounds at peak circulation levels for longer. Obviously pharmacological data is crucial in the assessment of potential trypanocides, with key implications for any course of therapy.

Consequently, the effects of limited exposure of trypanosomes to the test compounds were carried out.

The initial seeding density was 2×10^5 cells/mL, the cells were treated with the appropriate test compound concentrations (Figure 4.2 panel B and D) except for the drug-free control. The cultures were first incubated at 37 °C and 5% CO₂ for a brief period of 1 hour, after which the cells were washed with fresh media by centrifuging at 2400 rpm, re-seeded (2×10^5 cells/mL) in fresh HMI-9 media, and samples were taken and counted at each time point. The counting was performed in triplicate and the average values obtained were plotted against time using GraphPad prism 5 software.

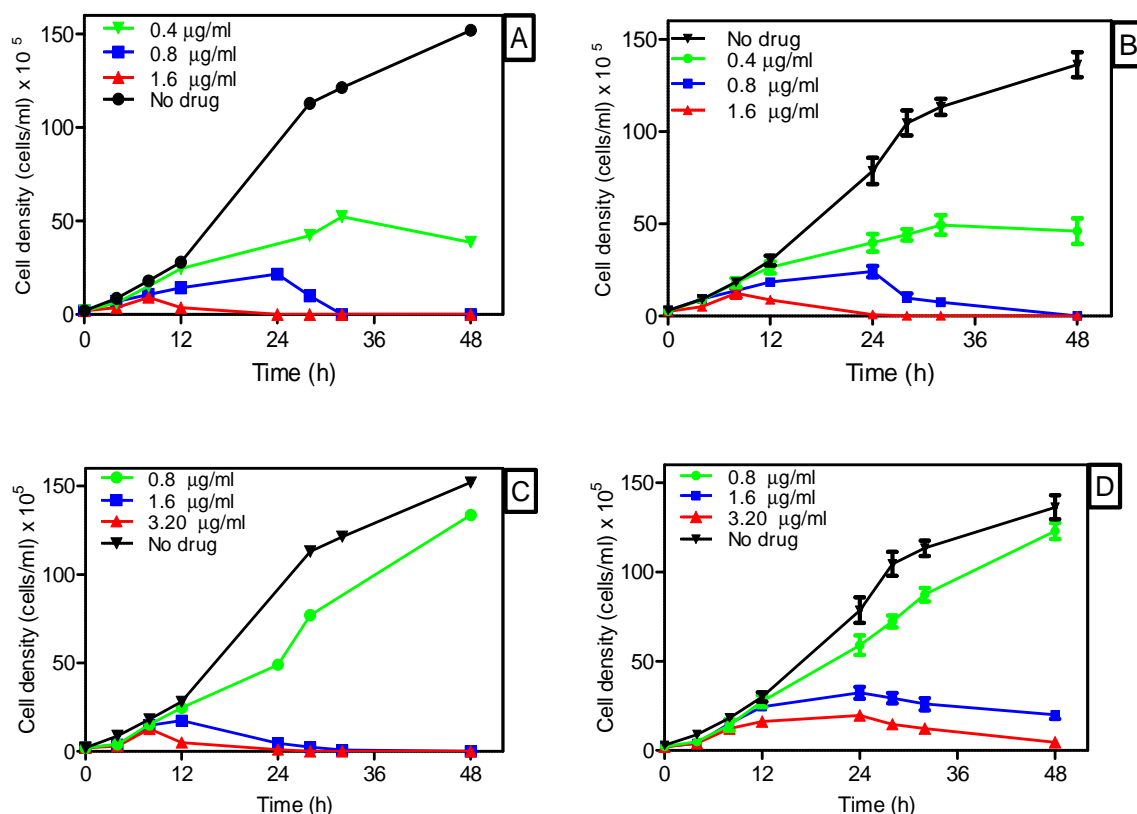


Figure 4.2 Growth curve assays of HDK20 and HDK40 treated cells: Growth curve of *T. brucei* wild-type s427 grown in the continuous presence of HDK20 or HDK40 at indicated concentrations, or untreated (no drug) (panels A and C respectively); and growth curve showing the effect of test compounds on trypanosome proliferation after a limited exposure (1 hour) to the same concentrations of HDK20 and HDK40 (Panels B and D respectively). Seeding density was 2×10^5 cells/mL, incubations were at 37 °C and 5% CO₂. In panels B and D, the cells were treated with the appropriate concentrations, the cells were washed with fresh media by centrifuging at 2400 rpm after 1 hours of exposure and were re-seeded at 2×10^5 cells/mL in fresh HMI-9 media, and samples were taken and counted at each time point. Microscopic cell counts were performed in triplicate using a haemocytometer, and the values obtained were plotted against time using GraphPad Prism 5 software.

The result shows that the growth pattern of cells with long time exposure were similar to those with limited exposure to HDK20 (Fig. 4.2). However, the time to achieve a complete clearance of trypanosomes from the culture was somewhat extended for this test compound at 0.8 µg/mL. For HDK40, the compound seemed rapidly trypanocidal in the continuous presence of the two higher concentrations, but following the wash after 1 h, the effect appeared to be a long-term growth arrest.

These results show that, over the duration of this experiment, the effects of HDK20 and HDK40 on trypanosomes are irreversible after a limited exposure time (1 h).

4.2.2 Monitoring the speed of action (Time to kill) of HDK20 and HDK40 on Trypanosomes by using a propidium iodide based assay.

The rationale for this assay is to examine the speed of action of the test compounds (HDK20 and HDK40) on wild type trypanosomes in real time. The principle of the assay is that cells become fluorescent as propidium iodide (PI) begins to enter them and become bound to nucleic acids. As PI is not taken up by intact *T. brucei*, this can only occur when the plasma membrane is breached as a result of loss of cellular integrity. Correspondingly, the effects of varying concentrations of the test compounds on the cell viability or membrane permeabilization were monitored over a 6-hour period.

The parasites were incubated with and without the test compounds in HMI-9 medium, which has 10% FBS, at 37 °C with 5% CO₂. Propidium iodide concentration was at 9 µM, and the fluorescence was measured over 6 hours at 544 nm for excitation and 620 nm for emission. Separate traces (background fluorescence were recorded in the absence of cells and these were subtracted from those presented herein.

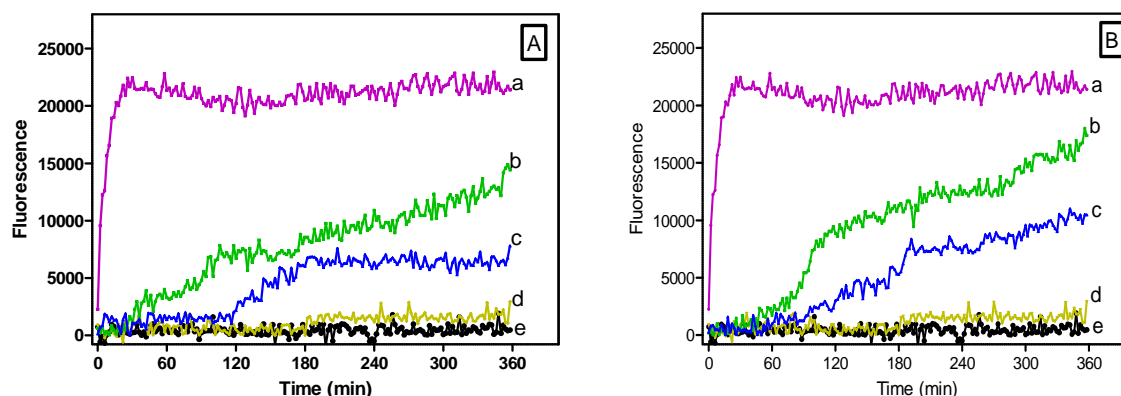


Figure 4.3 Results showing the speed of action of test compounds, HDK20 (panel A) and HDK40 (panel B) on trypanosomes. The result presented here shows Propidium Iodide (PI) permeabilization of cells caused by the two test compounds on the bloodstream form of *T. b. brucei* in a dose dependent fashion. The parasites were incubated with and without the test compounds in HMI-9 medium, which has 10% FBS at 37 °C with 5% CO₂. Propidium iodide concentration was at 9 µM, and the fluorescence was measured over 6 hours at 544 nm for excitation and 620 nm for emission. Digitonin, a compound known to cause rapid cell permeabilisation was used as positive control. Separate traces (background fluorescence

were recorded in the absence of cells and these were subtracted from those presented herein. a = digitonin treated cells; b = $4 \times EC_{50}$; c = $2 \times EC_{50}$; d = cells + PI (untreated); e = media + PI (no cells). Note that the experiments with HDK20 and HDK40 were performed at the same time, allowing the positive (digitonin) and negative control traces to be used in both panels.

Figure 4.3 shows that both compounds disrupted the plasma membrane architecture leading to loss of membrane integrity, consequently affecting cellular viability during 6 hours of incubation at concentrations of $2\times$ and $4\times$ their EC_{50} values, and there is a significant difference between treated and untreated trypanosomes ($0.4 \mu\text{g/mL}$ and $1.0 \mu\text{g/mL}$ for HDK20 and HDK40, respectively).

Trypanosomes treated with $0.8 \mu\text{g/mL}$ of HDK20 started becoming significantly fluorescent after approximately 2-3 hours of incubation; however, when this concentration was doubled ($1.6 \mu\text{g/mL}$), the cells became significantly fluorescent as early as 1-2 hours after the start of the incubation.

This period of increasing fluorescence was also similar for the HDK40 treated cells. None of the treated groups reached the maximum fluorescence as does the digitonin treated cells, reflecting a slow entry of PI into cells - either only part of the population became permeable to PI or the cells became increasingly permeable over the course of the experiment.

This result showed that HDK20 and HDK40 at concentrations above their EC_{50} cause a permeabilisation of the plasma membrane of trypanosomes leading to loss of membrane integrity. This experiment does not elucidate whether the cell membranes become permeable as a result of a loss of viability, or the other way around, where the perturbation of the cell membrane causes the cell death.

4.2.3 Natural products cause cell cycle arrest in trypanosomes

Some compounds purified from natural sources elicit their activity by inhibiting progression of the cell cycle, for instance by binding to a protein required for cell division, or by intercalating with DNA. Thus, an understanding of cell cycle events may help in deciphering the mode of action for anti-parasite compounds. Consequently, in this study, and following on from the cell viability (alamar blue) assay reported in chapter three, an attempt was made to study the effect of these test compounds on cell cycle progression in trypanosomes using a wild-type strain of *Trypanosoma brucei* s427 (1×10^7 cells/mL). Cells were stained with DAPI following incubation

with the test compounds at a concentration close to its EC₅₀, and viewed under a fluorescent microscope at various time points within the incubation period and the result was presented as percentage of 500 cells, and scores for DNA configuration given as 1N1K, 1N2K, 2N2K (Early: no cell division furrow) and 2N2K (Late, cell division furrow apparent), where N is nucleus; and K is kinetoplast.

The result showed that upon fluorescence microscopic examination of DNA configuration, cell cycle defects were noticed after 8 hours of incubation with the natural compounds: DNA synthesis could not be initiated, leading to a dramatic increase in the percentage of cells with just 1 nucleus and 1 kinetoplast, with a concomitant decrease in cells in all stages of the cell division process (see fig. 4.4).

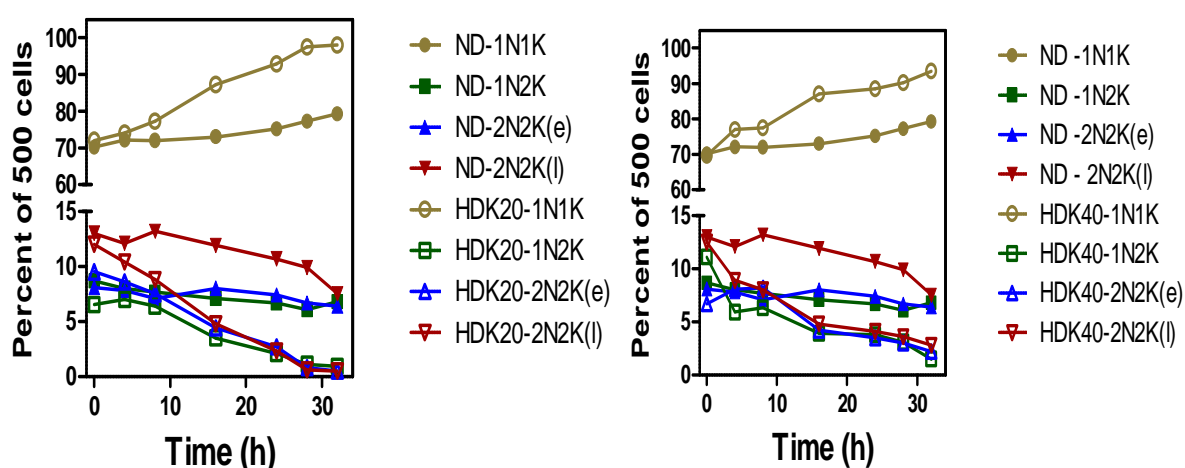


Figure 4.4 Cell cycle determination in *T. b. s427* WT using DAPI. Fixed cells prepared on slides were viewed under a fluorescence microscope after 32 hours of incubation with 0.2 µg/mL (HDK20) or 0.5 µg/mL (HDK40) and the untreated control (ND, no drug) were incubated without the test compounds. Values were expressed as percentage of 500 counted cells. N = nuclear DNA; K = kinetoplast DNA; e = early stage; L = late stage. Open symbols represents treated cells while filled symbols represent untreated cells. Note that because the incubations with both compounds were performed in parallel, the same control cell population was used in both panels.

HDK20 and HDK40 exhibited similar effects on the cell cycle of *T. brucei*, although at the concentrations chosen, the effect of HDK20 developed somewhat faster than that exhibited by HDK40. Both compounds caused the near-disappearance of the 2N2K-early and 2N2K-late cell cycle stages from the cell population after 28 hours of incubation. On the other hand, there was a

corresponding steady increase in the population of cells with 1N1K for the HDK20 treated cells from 8 hours of incubation and from 10 hours of incubation for the HDK40 treated cells (Fig. 4.4).

This result showed that the cell cycle might be a target for the trypanocidal activity of the test compounds or at least may be contributing to the efficacies of these compounds. The apparent cell cycle arrests induced by the continuous exposure to low concentrations of the compounds for up to 32 h are consistent with the growth inhibition depicted in Figure 4.2.

4.2.4 Microscopical investigation of cellular morphology of *T. brucei* treated with purified natural compounds

Microscopical investigation of cellular morphology of *T. brucei* treated with purified natural compounds was carried out after the cells were incubated with the purified compound and sample were taken at various time points, then incubating the samples at each time point with mitotracker,[®] and then staining the prepared slide with DAPI. Viewing was with the aid of a fluorescence microscope.

The result revealed that the cell population incubated with HDK-20 (0.4 µg/mL) had one nucleus and one kinetoplast (1N1K) DNA after 8 hours of incubation; however, DNA fragmentation became evident after 10 hours of incubation with compound HDK-20 (0.4 µg/mL). Although the mitochondrion of the cells remained normal throughout the experiment, cells treated with HDK 20 appear swollen after 12 hours of incubation, and in some cells the nucleus appeared to have fragmented.

The Untreated (control) cells remained normal throughout the period of the experiment as shown in figure 4.5. The kinetoplast DNA also appears to be normal in both the treated and control groups, and there were no monster cells found in the population to the extent that would suggest inhibition of cytokinesis.

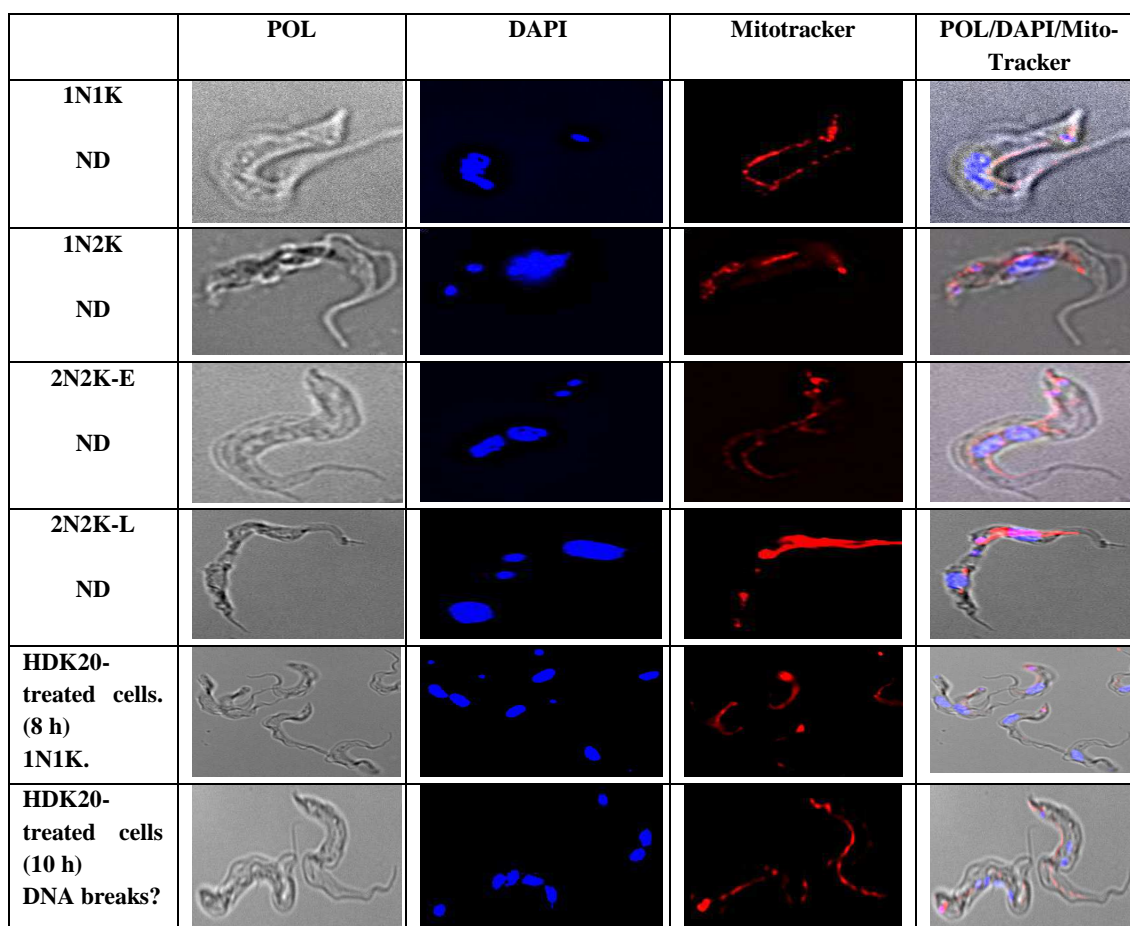


Figure 4.5 DNA contents and mitochondrial examination of treated and untreated (ND) cells.

Images of *T. brucei* s427 wild type showing DNA breaks following 10 hours of incubation with or without the test compound (HDK20, 0.4 $\mu\text{g/mL}$), and these images were taken with the aid of a fluorescent microscope. Treated cell population had 1N1K after 8 hours of incubation, and nuclear DNA fragmentation was noticed after 10 hours of incubation. N = nuclear DNA; K = kinetoplast DNA; e = early stage; L = late stage; ND = untreated control. DAPI = 4',6-diamidino-2-phenylindole; POL = Polarized light or bright field.

4.2.5 Assessment of DNA breaks using TUNEL assay

Cell cycle defects may lead to apoptosis or programmed cell death, and the latter is known to be linked with DNA fragmentation. The microscopic examination of cells treated with HDK 20 revealed cell cycle defect after 8 hours of incubation: DNA synthesis could not be initiated, leading to a dramatic reduction of cells with more than 1 nucleus or kinetoplast, and DNA fragmentation became evident after 10 hours of incubation with compound HDK-20 (0.4 $\mu\text{g/mL}$). Consequently, a TUNEL assay was used to study DNA fragmentation upon incubation with 0.3 $\mu\text{g/mL}$ HDK20 or 1 $\mu\text{g/mL}$ HDK40, and phleomycin (2 $\mu\text{g/mL}$) was used as a positive control (Sleigh, 1976), while the

negative control was drug free. Phleomycin, which is a mixture of copper-containing glycopeptides first isolated from *Streptomyces verticillus*, is known to bind to DNA where it induces DNA breakage either via enzymatic or non-enzymatic mechanisms (Sleigh, 1976).

Fragmentation of parasites DNA after exposure with the aforementioned compounds was evaluated by TUNEL assay using the APO-BrdU TUNEL Assay Kit (Invitrogen) for the detection of DNA fragmentation following the manufacturer protocol. The cell density of the parasites was adjusted to 1×10^6 cells/mL, the suspension was incubated with or without the test compounds for 12 h, and the results show that the drug-free culture was significantly different ($p < 0.05$) from the cells treated with HDK20 and HDK40 (Figure 4.6).

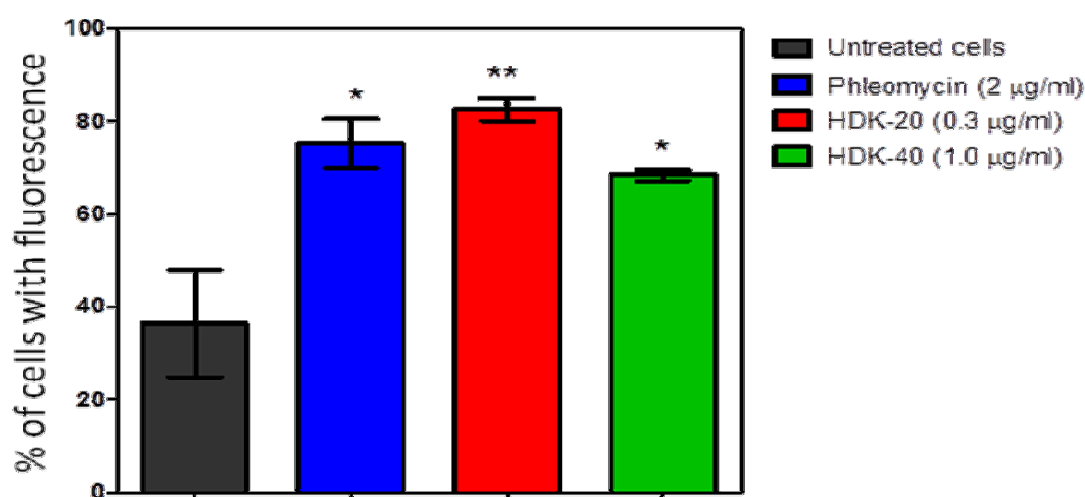


Figure 4.6 DNA fragmentation of treated and untreated *T. b* s427 cells following 12 hours of incubation with the test compounds (HDK20 and HDK40) or without the test compounds (untreated cells). Phleomycin (2 µg/ml) was used as a positive control. ** $p < 0.01$; * $p < 0.05$, and the result represent an average of three independent determinations using a flow cytometer and flowJo 10.0 software. The result revealed increase of cells with high fluorescence (Br-dU incorporation) after 12 hours incubation with HDK20 and up to 70% with such levels of fluorescence in HDK40 treated cells, which was similar to that observed with the phleomycin-treated control. The dot plot and histograms are presented in appendix D and E respectively.

The result showed a strong increase in Br-dU fluorescence in cells after 12 hours incubation with HDK20 and a slightly lower increase in cells treated with HDK40. Although the positive control (Phleomycin treated) exhibited a strong effect on the cell population, the cells treated with 0.3 µg/mL HDK20 appeared to have undergone an even more marked DNA fragmentation after 12 h

(Figure 4.6, also see appendix D and E) at the concentrations used, whereas there was no significant difference ($p < 0.05$) between the phleomycin treated and the HDK40 treated cells.

4.2.6 Effects of purified natural compounds on mitochondrial membrane potential of *T. b. brucei* treated cells.

HDK20 and HDK40 affected the cell cycle progression of *T. brucei* cells in this study leading to an apparent accumulation of cells in the G₁ phase of cell cycle and accumulation of 1N1K cells. A direct causal effect has been previously reported between the mitochondria membrane potential and cell cycle progression in *T. brucei* cells (Alkhalidi *et al.*, 2016). Consequently, we examined whether these compounds affect the mitochondrial function in *T. brucei* and whether this is connected with the cell cycle defects observed earlier.

In this study, Fluorescence Activated Cell Sorting (FACS) was employed for the determination of the change in mitochondrial membrane potential (MMP) due to exposure of trypanosomes to the test compounds using tetramethylrhodamine ethyl ester (TMRE) (Denninger *et al.*, 2007). A cell density of 1×10^6 cells/mL with and without test compounds was used for the start of the experiment, and 1 mL of sample was transferred at each time point into a microfuge tube and centrifuged at 4500 rpm for 10 min at 4 °C. The pellet was re-suspended in 1 mL PBS containing 200 nM of TMRE, followed by incubation at 37 °C for 30 min. The suspension was placed on ice for at least 30 minutes before analysis by a Becton Dickinson FACS Calibur using a FL2-height detector and CellQuest and FlowJo software (Ibrahim *et al.*, 2011). Valinomycin (100 nM) and troglitazone (10 µM) were employed as negative (mitochondrial membrane depolarisation) and positive (mitochondrial membrane hyperpolarisation) controls respectively (Denninger *et al.*, 2007). Mitochondrial membrane potential was determined at 0, 1, 4, 8 and 12 h.

The values given are the percentage of cells having fluorescence greater than 100 arbitrary units (AU), a value set to approximately 50% for the untreated cells, so that a shift to a higher fluorescence indicates hyperpolarisation (increased Ψ_m), while a shift to a lower fluorescence is indicative of a decreased Ψ_m (depolarization) (Denninger *et al.*, 2007; Alkhalidi *et al.*, 2016). The result was presented as histograms of TMRE fluorescence (See Appendix F).

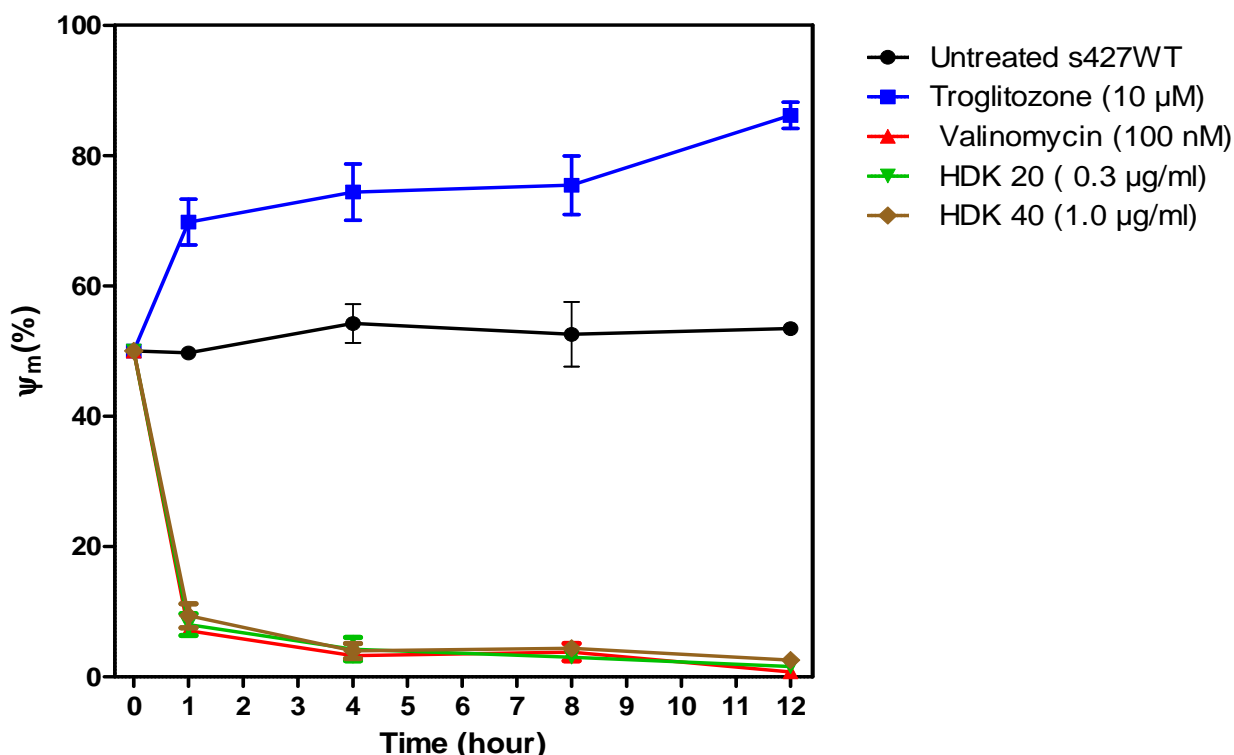


Figure 4.7 Mitochondrial membrane potential (% ψ_m) of treated and untreated *T. b.* s427 WT cells.

The analysis was measured with a flow cytometer using *T. b. b.* (bloodstream-form) incubated with 200 nM tetra-methylrhodamine (TMRE). Troglitazone (10 μ M) was used as mitochondrial membrane hyperpolarization control, while valinomycin (100 μ M) was used as mitochondrial membrane depolarization control. The results shown here are the averages of three independent experiments; and the error bars represent standard errors. A shift to a higher fluorescence indicates hyperpolarisation (increased Ψ_m), while a shift to a lower fluorescence is indicative of a decreased Ψ_m (depolarization)

The result shown above is a summary of the mitochondrial potential (Ψ_m) following 12 hours of incubation with or without the test compounds and read at 0, 1, 4, 8 and 12 h. As expected, there was no change in the mitochondrial potential for untreated cells for the duration of the experiment (12 h). However, valinomycin induced a very rapid and strong depolarisation of the mitochondrial membrane after just 1 hour of incubation, whereas troglitazone caused a clear hyperpolarisation of the mitochondrial membrane (Fig. 4.7).

Compounds HDK-20 and HDK-40, even at relatively low concentrations (0.3 μ g/mL and 1.0 μ g/mL, respectively) induced a fast and profound depolarisation of the parasites' mitochondrial membrane potential after 1 hour of incubation and continued until a near complete depolarization was achieved after 12 hours.

These results indicate that both HDK20 and HDK40 induced a depolarisation of mitochondrial membrane potential as an early effect on the parasites.

4.2.7 Effects of purified natural compounds on ATP levels in *T. b. brucei*

The previous section described that HDK20 and HDK40 caused depolarisation of the mitochondrial membrane potential of *T. brucei* s427 WT and it is well understood that the oligomycin-sensitive ATP synthase present in the mitochondrial membrane of bloodstream form (BSF) *T. b. brucei* is responsible for the maintenance of its mitochondrial membrane potential (Brown *et al.*, 2006). It is conceivable that a reduction in cellular ATP levels leads to the reduced mitochondrial membrane potential by denying the F₀F₁ ATPase the ATP it needs to pump H⁺ across the inner mitochondrial membrane. Consequently, these compounds were tested at the same concentrations as that of the mitochondrial membrane potential above in order to study their effect on ATP production.

Intracellular ATP level was measured using an ATP Determination Kit (Invitrogen) following the manufacturer protocol. ATP was determined using recombinant firefly luciferase and alongside its substrate D-luciferin in the cell. This assay is based on luciferase activity which requires ATP as a co-enzyme in an enzymatic reaction to produce a luminescent light (emission maximum was approximately 560 nm at pH 7.8). The luciferase assay was found to be very sensitive (the luminometer could detect as little as 0.1 picomole of ATP). Known amounts of an ATP standard (provided by the kit), prepared as a serial dilution were made and used to plot a standard curve which was eventually used to quantify *in vivo* ATP levels.

Accordingly, *Trypanosoma brucei* cultures containing 1×10^7 cells of both treated and untreated parasites were taken at each time points and centrifuged for 10 minute at 2800 rpm (4 °C) and the pellets was used for the assay using the assay kits and following the manufactures manual.

A standard curve was prepared using different concentrations of ATP (10 nM – 1 μ M) to calculate the ATP concentrations in the samples by imputing the luminescence obtained from the test well in the straight line equation generated from the standard curve shown in Fig 4.5A.

The result showed that intracellular ATP levels of the *T. brucei* treated with HDK20 and HDK40 were found to be severely depleted (Fig. 4.8 B). Although the intracellular ATP level in the HDK20

and HDK40 treated cells trended down after just one hour of incubation, this became statistically significant after 2 hours of incubation with both test compounds.

Oligomycin is a well-known inhibitor of ATP synthase. It was used in this study as a positive control to prevent phosphorylating respiration of trypanosomes by inhibiting the trypanosomes ATP synthase thereby blocking its proton channel (F_o subunit), which in most mitochondria is essential for the phosphorylation of ADP to ATP (energy generation) (Brown *et al.*, 2006), but in BSF generates the mitochondrial membrane potential. As the oligomycin treated (control) cells had the lowest ATP content it shows that the membrane potential is essential for ATP production. The fact that oligomycin induced a much more rapid depletion of ATP, compared to that exhibited by HDK20 and HDK40, seems to indicate that these test compounds do not directly inhibit the F_oF_1 ATPase.

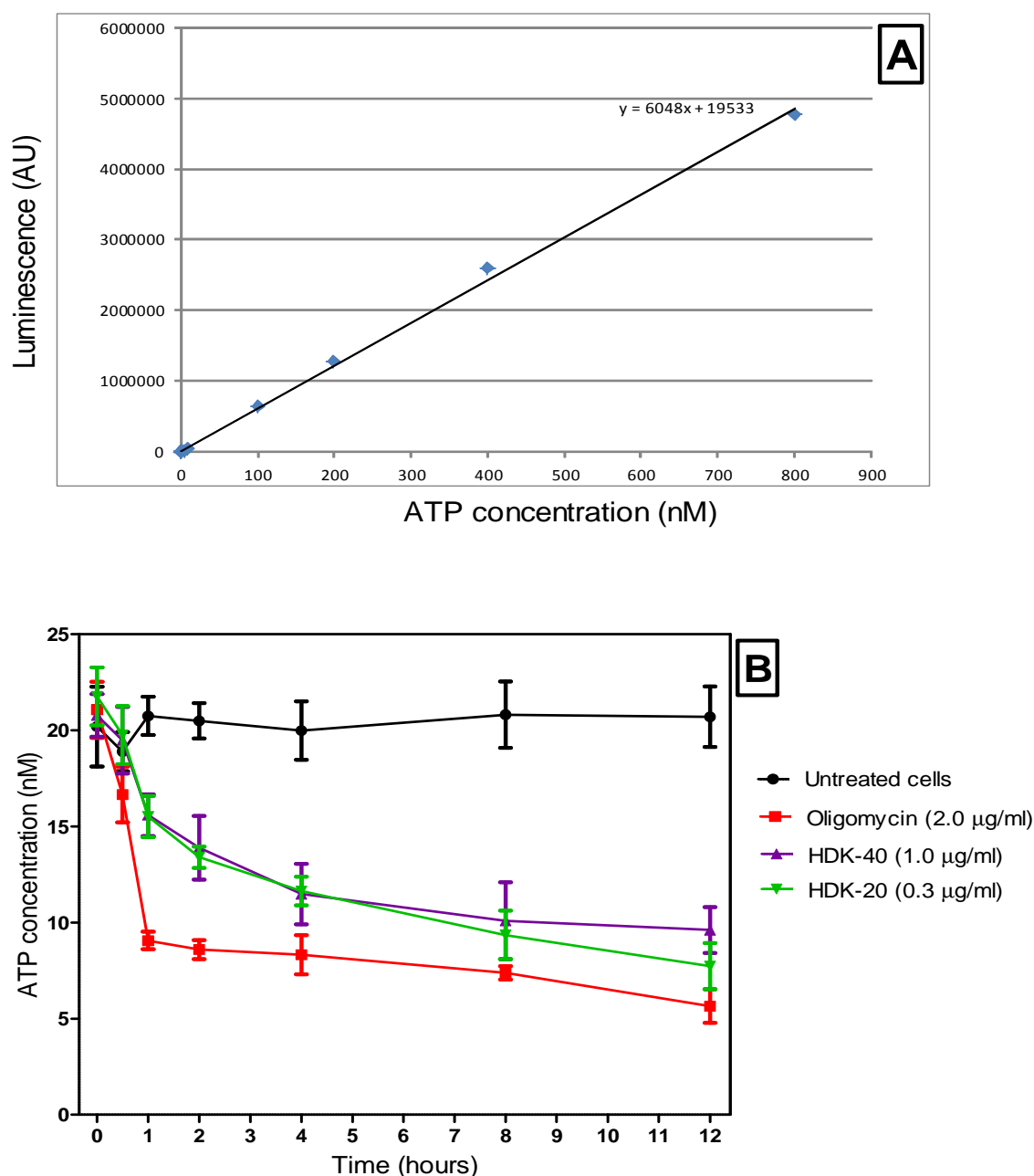


Figure 4.8 Determination of ATP levels in trypanosomes. (Panel-A) ATP standard curve determined in parallel and under the same assay condition as that of the test samples, the luminescence gotten expressed as artificial units were plotted against ATP concentrations (10 nM – 1 µM) to generate an equation for a straight line from which the ATP concentrations in the test samples were extrapolated by fitting their luminescence to this equation; (Panel-B) ATP concentrations in treated and untreated 10^7 *T. b. brucei* cells using 50 mL extraction buffer. Incubation was for a period of 12 hours with samples taken at each time point. The results shown here are the averages of four independent experiments; and the error bars represent standard errors.

ATP concentration in the oligomycin treated control was reduced to 8 nM after 1 hours of incubation compared to HDK20 and HDK40 treated cells which had an intracellular ATP concentration of 16 nM under our experimental conditions (Fig. 4.8 B). However the ATP concentration in the oligomycin treated cells then remained steady until after 8 hours of incubation before it fell further to a concentration of 6 nM. Meanwhile the HDK20 and HDK40 treated cells exhibited a steady decline in ATP concentration for the duration of the experiment, but had the lowest value of intracellular ATP levels of 10 nM and 13 nM respectively. The untreated cells had a rather steady intracellular ATP concentration throughout the experiment.

This result show that HDK20 and HDK40 deplete the *T. brucei* intracellular ATP concentration corresponding to their effect on mitochondria membrane potential described in the previous section. From the timelines of the two sets of experiments it appears that the loss of mitochondrial membrane potential precedes the reduction in ATP levels, and thus, like oligomycin causes the low ATP levels. Much less clear is how these two (unrelated) compounds cause such a dramatic collapse of Ψ_m . Usually, compounds with such effects are cationic and accumulate in the mitochondrion, but it is unlikely that either HDK20 or HDK40 are charged.

4.2.8 Metabolomic assessments of *T. b. brucei* cells treated with sub-lethal doses of purified compounds.

The biochemical investigation into the mode of action of a biologically active compound has in the past involved time-consuming assays on single enzyme activities. However, the use of a modern metabolomics platform can rapidly give insight into a multitude of biochemical pathways that could potentially be involved in the cellular perturbations induced by the test compound.

Metabolomics is a comparatively new technology that allows for the identification of hundreds of metabolites from a single sample, usually a cell extract or a sample of growth medium. In principle, if a drug inhibits an enzyme then it is expected that the substrate of this enzyme should build-up and its concentration should rise within the system, while the concentration of the product of the enzymatic reaction should fall. Also, if the drug perturbs the cell membrane by altering its integrity, then it is expected that this loss of plasma membrane integrity would result in build up of intracellular metabolites within the culture media relative to the untreated culture.

We also analysed the spent media, and directly compared the metabolite changes between the untreated control group and trypanosomes incubated with the test compounds (HDK20 and HDK40), as indicators for metabolic changes that cause perturbations in nutrient uptake or metabolite efflux (Fig 4.10). It was obvious from a global overview of data visualization of the principal component analysis (PCA) of the extracellular metabolome that there is a clear-cut separation of the treated replicates from that of untreated ones, and most of the replicates except 3SA and 4SC clustered together.

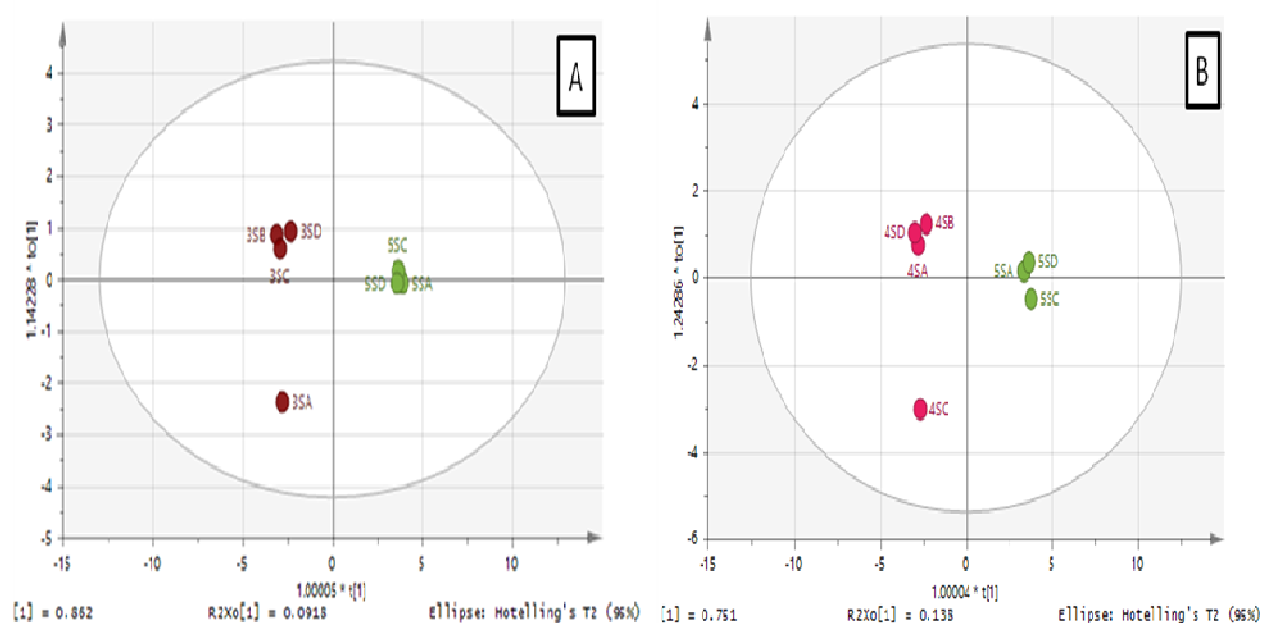


Figure 4.10 Data visualization of the Principal component analysis (PCA) of extracellular metabolome of HDK20 (3S, A-D) (Panel-A), and HDK40 (4S, A-D) (Panel-B) following 10 hours of incubation of the cells with the respective compounds at concentration equal to half their EC_{50} . The untreated cells (5S, A-C) were used as control and were incubated and subjected to the same experimental condition as the treated cells. The analysis shows clear separation between the treated and untreated controls. The data presented here is that of four biological repeats, the experiment was conducted using LC-MS, and the data generated were analysed using SIMCA software.

A general overview of the metabolome of the cells at the multivariate level revealed the identification of 422 metabolites (Table 4.1). Based on the number of significant metabolites, the effect of the two compounds on the extracellular metabolome was more pronounced than that on the intracellular composition. In terms of multivariate analysis, HDK20 had a stronger extracellular effect on the whole metabolome (422 metabolites) of treated trypanosomes

compared to its intracellular effect with predictive variability (0.443) higher than its orthogonal effect (0.35). HDK20 significantly altered 14 extracellular metabolites with highest predictive effect (0.862) and very low orthogonal variability (0.092) compared to HDK40. The effect of HDK20 and HDK40 appear to be weak intracellular compared to their extracellular effect.

The predictive variation in table 4.1 refers to between-groups variation, which is caused by the effect of the intervention (treatments) on the metabolites, while the orthogonal variation refers to variations within the group, caused by systematic effect on metabolites. Other statistical analyses used include the PCV ANOVA which is the p-value of cross validated analysis of variance between the two groups. From these analyses a good outcome will be having a higher predictive and a lower orthogonal variation and a significant CV ANOVA (<0.05). Hence, a model having an insignificant p-value and/or low predictive variation with a high orthogonal variation was regarded to be insignificant at multivariate level; however this would not be the case at the univariate level.

Table 4.1 General overview of the metabolome of treated cells at multivariate level.

		whole metabolome				Selected metabolites			
Cellular part	No. of metabolites	Comparison	Pred. var.	Ortho. var.	PCV-ANOVA	No. of metabolites	Pred. var.	Ortho. var.	PCV-ANOVA
Intra	422 (whole metabolome)	3C vs 5C	0.20	0.655	1.0	4	0.861	0.051	0.082
		4C vs 5C	0.13	0.766	0.945	7	0.779	0.028	0.033
Extra		3S vs 5S	0.357	0.485	0.949	14	0.862	0.092	0.0038
		4S vs 5S	0.443	0.35	0.952	15	0.751	0.186	0.043

Pred. var. = predictive variation = between groups variation, caused by the effect of intervention on metabolites; Ortho. Var. = orthogonal variation = within group variation, caused by systematic effect on metabolites; PCV ANOVA = p-value of cross validated Analysis of Variance between the two groups; the good model = higher predictive and lower orthogonal variation + significant CV ANOVA (<0.05). Insignificant p-value and/or low pred. var. and high Ortho. Var. = the model is insignificant at multivariate level, but this is not the case at univariate level.

An overview of the intracellular metabolome at the univariate level for the HDK20 (3C) treated cells compared to the intracellular metabolome of the untreated cells revealed the perturbation of four metabolites: Choline, and 3-(4-Hydroxyphenyl) lactate were slightly elevated, while L-

Tryptophan, and 2-oxobut-3-enanoate were moderately reduced in the intracellular extract (see table 4.2).

Table 4.2 Overview of differences in the intracellular metabolome after HDK20 or HDK40 treatment - univariate level

Putative Metabolite	Mass	*RT	3C/5C	p-value	**FDR	Putative Metabolite	Mass	RT	4C/5C	p-value	FDR
2-oxobut-3-Enanoate	100.0	14.4	0.54	0.04	0.67	(R)-2-Hydroxystearate	300.3	3.814	2.33	0.030	0.75
Choline	103.1	20.39	3.04	0.03	0.67	N3-hydroxyethylcytosine	155.1	17.51	0.53	0.041	0.77
L-Tryptophan	204.1	11.53	0.43	0.03	0.67	3-(4-Hydroxyphenyl)lactate	182.0	8.582	3.68	0.036	0.80
3-(4-Hydroxyphenyl) Lactate	182.1	8.582	1.91	0.03	0.67	N-Acetyl-beta-alanine	131.1	14.28	0.50	0.002	0.79
						L-Tryptophan	204.1	11.53	0.50	0.028	0.76
						Choline	103.0	20.39	3.17	0.043	0.78
						L-Histidine	155.0	14.77	0.47	0.019	0.80

3C and 4C are the intracellular metabolome of HDK20 or HDK40 treated trypanosomes respectively and it is here compared with 5C which is the intracellular metabolome of drug-free control cells in order to identify any changes in intracellular metabolism. *Retention time; **False discovery rate.

An overview of the intracellular metabolome at the univariate level for HDK40 (4C) compared to the intracellular metabolome of the untreated trypanosomes shows the perturbation of 7 metabolites namely: (R)-2-Hydroxystearate, 3-(4-Hydroxyphenyl) lactate, and Choline, all of which were moderately elevated in the extracellular medium, while N3-hydroxyethylcytosine, N-Acetyl-beta-alanine, L-Tryptophan, and L-Histidine were slightly depleted. Most of these are from the amino acid metabolic pool (see table 4.2).

An overview of the extracellular metabolome at the univariate level for the HDK20 and 40 treated trypanosomes (3S and 4S respectively) compared to the untreated control cells (5S) reveal the perturbation of 12 metabolites in the spent medium of the HDK20 treated cells (Table 4.3) while a total of 15 metabolites were observed to have changed in the extracellular metabolome (spent

medium) after HDK40 treatment, compared to that of the untreated trypanosomes (5S) (Table 4.4).

Table 4.3 Overview of the extracellular metabolome - univariate level (HDK20 treated cells)

Putative metabolite	Mass	*RT	3S/5S	p.value	**FDR
3-Oxo-5beta-cholanate	374.28	3.612	27.0912	0.010704	0.26991
Cholesterolsulfate	466.31	3.565	3.814068	0.002192	0.070549
Glycine	75.032	15.46	1.400403	0.038769	0.26991
Docosahexaenoicacid	328.24	3.698	1.288593	0.024936	0.26991
2-Oxoglutarate	146.02	14.96	1.668769	5.57E-04	0.019716
5S-hydroxy-12-keto-6Z,8E,10E,14Z-eicosatetraenoic acid	334.21	4.165	494.5669	1.88E-06	1.33E-04
13E-docosenoic acid	338.32	3.676	1.586402	0.023889	0.26991
1-octadecanoyl-2-nonadecanoyl-sn-glycero-3-phosphoserine	805.58	3.914	3.404562	0.011189	0.26991
AMP	347.06	13.31	387.5218	3.89E-07	3.44E-05
Adenine	135.05	9.549	2.405145	0.003438	0.10141
2-Methyl-3-oxopropanoate	102.03	14.84	1.582258	5.55E-04	0.019716

This table shows the result of the extracellular metabolomic perturbation of 3S - which is the average of 4 separate determinations of the spent medium of HDK20 treated trypanosomes, compared with the average of 4 separate determinations of 5S - which is the spent medium of the drug free control cells in order to see whether there is any changes in the extracellular metabolome. The sample preparation and analysis for the 3S and 5s samples were performed in parallel. *Retention time; **FDR = False discovery rate.

It could be clearly observed for both the HDK20 and HDK40 treated cells that all the metabolic changes observed in the extracellular medium (spent medium) i.e. 3S/5S and 4S/5S reflected elevated metabolite levels, largely from the glycerophospholipid metabolism (Tables 4.3 and 4.4).

Table 4.4 Overview of the extracellular metabolome - univariate level (HDK40 treated cells)

Putative metabolite	Mass	*RT	4S/5S	p.value	**FDR
1-Palmitoylglycerophosphocholine	495.33	4.604	843.4975	0.007954	0.23872
1-Oleoylglycerophosphocholine	521.35	4.495	5787.07	4.80E-06	5.34E-04
Ethyl (5Z,8Z,11Z,14Z)-icosa-5,8,11,14-tetraenoate	332.27	3.706	1.721136	0.015041	0.23872
Ethyl (5Z,8Z,11Z,14Z)-5,8,11,14-icosatetraenoate	434.24	4.55	186.0807	0.032151	0.23872
1-Oleoyl-glycero-3-phosphate	436.26	4.518	1821.768	2.74E-05	0.001584
1-Stearoyl-2-meadoyl-sn-glycero-3-phosphocholine	811.61	3.835	3.064126	0.040941	0.23872
(2R)-2-Acetoxy-3-(hexadecyloxy)propyl 2-(trimethylammonio)ethyl phosphate	523.36	4.461	10063.61	1.25E-06	4.34E-04
1-Stearoyl-2-arachidonoyl phosphatidylinositol	886.56	3.623	8.814194	0.043642	0.23872
1-Hexadecanoyl-2-(9Z-octadecenoyl)-sn-glycero-3-phospho-1'-myo-inositol.	836.54	3.629	8.640292	0.02004	0.23872
1-(1Z-octadecenyl)-2-oleoyl-sn-glycero-3-phosphoserine	773.56	3.626	12.35933	0.043039	0.23872
1-octadecyl-2-(6Z,9Z,12Z-octadecatrienoyl)-glycero-3-phosphoserine	771.54	3.622	12.65741	0.043017	0.23872
Adenine	135.05	9.549	1.48833	0.009708	0.23872
[ST dimethyl(5:0/3:0)] (5Z,7E,22E,24E)-(1S,3R)-26,27-dimethyl-24a-homo-9,10-seco-5,7,10(19),22,24-cholestapentaene-1,3,25-triol	454.34	3.887	3962.885	3.69E-05	0.00183
Reduced Vitamin K (phylloquinone)	470.38	3.966	441.9501	0.027529	0.23872

This table shows the result of the extracellular metabolomic perturbation of group 4S - which is the average of 4 separate determinations of the spent medium of HDK40 treated trypanosomes, compared with the average of 4 separate determinations of 5S - which is the spent medium of the drug free control cells in order to see whether there are any changes in the extracellular metabolome. The sample preparation and analysis for the 4S and 5S samples were performed in parallel. *Retention time; **FDR = False discovery rate.

4.3 Discussion

The structural diversity of natural compounds and the fact that they usually possess highly specific and selective biological activities based on their mode of action are the two main reasons why natural products are of immense interest to drug development. Two classical examples of these are the tubulin-assembly promotion activity of paclitaxel, and the HMG-CoA reductase inhibition displayed by statins such as lovastatin, neither of which would have been discovered and developed without the natural product leads and investigating their mode of action (Cragg and Newman, 2013). A complete knowledge of the interaction of a

drug lead with its biological target is particularly helpful for the process of drug development, because it allows the use of medicinal chemistry strategies for optimization of the compounds drug-like properties, and in some cases a more suitable design of clinical trial. This is crucial to the development of new and efficient chemotherapy that will replace the current inefficient ones.

It is very rare nowadays for a new chemotherapeutic agent to be licensed without prior knowledge of its MOA, hence understanding drug mode of action is of fundamental importance. Yet, of the five drugs currently in use against human African trypanosomiasis (HAT), convincing evidence on a specific mode of action has only been proposed for the polyamine pathway inhibitor eflornithine - which also is the most recently developed. Knowledge of the MOA of a novel anti-parasite inhibitor reduces the risk of unexpected toxicity and also allows synergism and resistance mechanisms to be predicted (Vincent *et al.*, 2012). Accordingly, the mode of action was studied for two of our purified compounds and the findings are discussed here.

Although the two purified compounds studied in this work were obtained from two distinct plants and these compounds belong to different class of compounds i.e. diterpenes (HDK20) and triterpenes (HDK40), they, surprisingly, displayed similar mode of action, however they both differ slightly in the extent to which they elicit their trypanocidal activity. Previously, the trypanocidal (mode of) action of some diterpenoids and triterpenoids has been studied and reported in the literature. For instance, Eleanolone, a diterpene isolated from the ethyl acetate extract of the marine alga *Bifurcaria bifurcata*, was reported to inhibit the growth of *Trypanosoma brucei rhodesiense in vitro* with an IC_{50} of 45.0 μ M (Galle *et al.*, 2013). The diterpene HDK20 reported in this work also induced a rapid, irreversible growth arrest of *Trypanosoma brucei* (Fig. 4.1), probably by inhibiting mitochondrial DNA replication, thereby preventing the initiation of the S-phase of the cell cycle and leading to accumulation of cells with 1 nucleus and 1 kinetoplast.

It follows also that the diterpene tested here is targeting a significant part of the trypanosome that once initiated, the trypanosomes lacks the machinery of reversing it, at least not within a short period of time following exposure.

A clerodane 16 α -hydroxycleroda-3,13(14)Z-dien-15,16-olide (i.e. HDK20), was previously purified from the ethanolic extract of the leaves of *Polyalthia longifolia* var. *pendula* (Annonaceae), and was tested against *Leishmania donovani* where it was reported to be potent, safe, and orally active (Misra *et al.*, 2010). This diterpene was active against the amastigote forms of the parasite *in vitro* (IC₅₀= 5.79 μ g/mL). The *in vivo* anti-leishmanial studies of this compound were performed in hamsters infected with *L. donovani*, at oral doses of 25, 50, 100 and 250 mg/kg/day (n= 6) for 5 consecutive days, showing potency from 50 mg/kg/day. *In vivo* survival studies of up to 6 months as well as *in vitro* cytotoxicity studies on macrophages indicated that this compound is safe (Misra *et al.*, 2010). This is consistent with our own finding that the clerodane, was not toxic to Human Embryonic Kidney cells at concentrations >400 μ g/mL (see section 3.2.6 of chapter 3). These findings present this clerodane as a potential lead for the discovery of a safe trypanocide that will replace the existing toxic ones.

It has previously been reported that clerodane selectively targets topoisomerase and thereby the DNA of pathogens including *Leishmania*. For instance, it has been shown that the clerodane 16 α -hydroxycleroda-3,13(14)Z-dien-15,16-olide (HDK20) inhibits DNA topoisomerases I of *L. donovani* (Misra *et al.*, 2010). It is thought that topoisomerase inhibitors block the ligation step of DNA replication, thereby generating single and double stranded breaks that eventually harm the integrity of the genome. Introduction of these breaks would subsequently lead to apoptosis and, inevitably, cell death. HDK20 was also shown to affect cell cycle progression in the work here presented (Fig. 4.4), and induced significant DNA breaks in trypanosomes after 12 hours of incubation (Fig. 4.6), a phenomenon that was also noticed with the DAPI microscopy (Fig. 4.5). Hence, the mechanism of DNA breaks observed in this work may be similar to the one that occurs through inhibition of DNA topoisomerases 1 reported in literature for this clerodane; this, however, was not directly confirmed with our data.

Triterpenes are C-30 terpenoids broadly distributed all over the plant kingdom. These compounds, have been reported to show a wide range of biological properties, and can be seen in their free form in so many cyclic skeletal types, or sometimes linked to sugar moieties (triterpene saponins). Triterpenes can also exist in modified forms owing to ring cleavage, oxidations and loss of carbon atoms (limonoids, nortriterpenoids, quassinoids). These latter

classes are often of particular interest with respect to their biological activity, and are limited to some families of plants, mostly of the order Sapindales, such as *Simaroubaceae*, *Rutaceae*, *Cneoraceae* or *Meliaceae* (Schmidt *et al.*, 2012). The most wide spread triterpenes commonly found in plant species are the oleanolic and ursolic acids, which have been reported as been active against various *Leishmania* species (Peixoto *et al.*, 2011; Schmidt *et al.*, 2012).

It was also observed in this work that both HDK20 and HDK40 depleted the mitochondrial membrane potential of trypanosomes and depleted their ATP concentration (Fig 4.7). From the timeline observed, it appears that the depolarisation of the mitochondrial membrane potential may occur first, and that ATP depletion is subsequently reduced as a result thereof. Such a link is consistent with current models of the functioning of the mitochondrion of BSF *T. brucei* (Alkhaldi *et al.*, 2016).

The kDNA of trypanosomatids is a structure that is highly organised, and is made up of tens of maxicircles and thousands of minicircles (Liu *et al.*, 2015, Alkhaldi *et al.*, 2016). To ensure that *T. brucei* daughter cells receive identical kDNA networks, the process of replication is highly synchronized with replication of the nuclear materials, prior to cell division; thus, the mitochondrial S phase for kDNA replication is initiated before the longer nuclear S-phase (Mckean, 2003; Jensen and England, 2012). Indeed, the initiation of mitochondrial division appears to be an essential checkpoint that must precede nuclear division, leading necessarily to the creation of 1N2K cells before the onset of mitosis and nuclear division (Chanez *et al.*, 2006). The here observed accumulation of 1N1K cells thus appears to indicate a failure either to initiate mitochondrial S-phase, or a failure of the mitochondrial S-phase, i.e. of kDNA replication. With the mitochondrial S-phase not being concluded, the nuclear S-phase would not commence, resulting in cell cycle arrest at 1N1K.

Replication of the kDNA is dependent on intracellular ATP and hundreds of mitochondrial proteins (Beck *et al.*, 2013), that are mobilized to the mitochondria (Schneider *et al.*, 2007) in what is, in BSF, is also an ATP-dependent process (Williams *et al.*, 2008). Thus it is reasonable to conjecture that the severe depletion of ATP and the decrease of the parasites' mitochondrial membrane potential interfered with the successful initiation or conclusion of kDNA replication, resulting in cell cycle arrest due to the failure of cells to progress from the

G1 phase, hence the reason why the cell population as observed in this study universally contain only a single nucleus and kinetoplast. Similar observations were also reported following RNAi knockdown of ATP/ADP carrier in procyclic forms of *T. brucei* cells, in which failure of the overall cell division machinery was linked to reduced cytosolic ATP levels (Gnipova *et al.*, 2015).

The above investigation thus gives rise to a model by which HDK20 and HDK40 rapidly depolarise the mitochondrial membrane, leading to a much-reduced cellular level of ATP, which in turn leads to cell cycle arrest at the stage of the mitochondrial S-phase. What remains unclear is what the primary target(s) might be, that by binding of either natural compound causes the collapse of Ψ_m . We considered that an analysis of biochemical pathways by metabolomics might give an indication as which protein(s) is/are targeted by the test compounds. There are two approaches to studying metabolomics-based mode of drug action; firstly, the alterations that ensued after drug induction are observed using a metabolic fingerprint, after which the metabolome is then compared with drugs whose mode-of-action is already known by using a multivariate statistical analysis (Yi *et al.*, 2007). Unfortunately, there are only a few trypanocides whose mode-of-action is known, even though examples subsist, such as the new N-myristoyltransferase (NMT) inhibitors and Eflornithine (Vincent *et al.*, 2012). However, it is unlikely that a novel compound with an unknown anti-trypanosome mode of action would precisely mimic the effects of either the NMT inhibitors or eflornithine. A higher probability of success would come with an unbiased approach, focusing on individual metabolite abundance changes that take place after addition of the drug (Le Roch *et al.*, 2008); this facilitates the discovery of new modes of action. Correspondingly a non-targeted metabolomic-based approach was used in this work to enable us to study pathways in response to the action of the isolated compounds with the aim of defining the mode of action of these trypanocides.

Metabolomic profiling of the effect of HDK20 and HDK40 on *Trypanosoma brucei* resulted in the identification of 422 metabolites using LC-MS. Based on the number of significantly changed metabolite levels, the effect of the two compounds on the extracellular medium (by modulation of export and/or import rates) was higher compared to their effects on the intracellular metabolite pools. In terms of multivariate analysis, HDK20 had better extracellular effect on the whole metabolome (422 metabolites) of treated trypanosomes

compared to its intracellular effect with predictive variability (0.443) higher than its orthogonal effect (0.35). HDK20 significantly altered 14 extracellular metabolites with highest predictive effect (0.862) and very low orthogonal variability (0.092) compared to HDK40. The effect of HDK20 and HDK40 appear to be weak intracellular compared to their extracellular effect.

Although the metabolomic assessments of *T. brucei* cells did not clearly reveal the targeting of any specific metabolic pathway, it appeared that these compounds may have some effects on the plasma membrane following 8 hours of incubation at concentrations around their EC₅₀. The results of the metabolomic profile of the extracellular metabolome may support this speculation as most of the few metabolites with increased concentration compared to the untreated control were found to be associated with glycerophospholipids metabolism. The perturbation of the plasma membrane integrity following hours of incubation which led to permeabilization of trypanosomes' plasma membrane and the corresponding increase in fluorescence brought about by the entry of propidium Iodide into the cells may also support the suspicion that loss of plasma membrane integrity may be a contributing factor. However this finding needs to be interpreted with caution as a total loss of cell membrane integrity would result in the wholesale release of cellular contents into the culture media, and this was certainly not observed. Any serious effects on plasma membrane integrity would therefore occur much later than the observed biochemical changes on Ψ_m and ATP levels, and even cell division.

In summary, the mode-of action of HDK20 and HDK40 appear to be similar and only differ in the extent of damage they inflict on trypanosomes, and in their metabolomic profile, although the interpretation of the metabolomic data is by no means straightforward. Hence their activity timeline can be summarised thus: (1) a fast and profound depolarisation of the parasites' mitochondrial membrane potential after 1 hour of incubation and this continued until a near complete depolarization was achieved after 12 hours. The mechanism causing this might be irreversible as shown by the experiment showing irreversibility of growth arrest after 1 h. (2) Intracellular ATP levels of the *T. brucei* were found to be depleted on a timescale closely following the loss of mitochondrial membrane potential. (3) Fluorescence microscopic assessment of DNA configuration revealed cell cycle defects after 8 hours of incubation with the natural compounds: DNA synthesis could not be initiated, leading to a

dramatic reduction of cells in the S phase. (4) DNA fragmentation became evident after 10 hours of incubation with compound HDK-20, visualised by flow cytometry and Terminal deoxynucleotidyl transferase dUTP Nick-End Labelling (TUNEL) assay, which revealed significant DNA fragmentation after 12 hours.

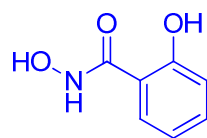
Further mode-of-action studies, Structure Activity Relationship (SAR) analysis of related compound libraries could improve the efficacies of these compounds, which would enable *in vivo* animal work to confirm their *in vivo* anti-parasite activity.

Chapter 5: Evaluation of mitochondrion-targeting lipophilic cation conjugates of Salicylhydroxamate and 2,4-Dihydroxybenzoate as potential drugs against African trypanosomes.

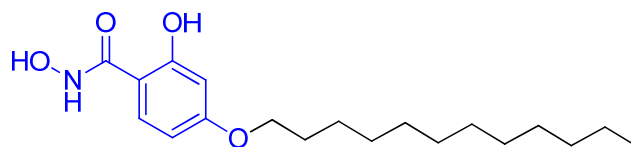
5.1 Introduction

In contrast to mammalian cells, which contain hundreds of mitochondria per cell, trypanosomes possess a single mitochondrion that is involved in vital cellular functions including maintenance and expression of genetic information, energy metabolism, RNA editing, Fe-S cluster biogenesis, etc, yet is biochemically very different from mitochondria in human cells (Verner *et al.*, 2016). Hence, this essential organelle represents a good chemotherapeutic target for the development of trypanocidal drugs (Lanteri *et al.*, 2008; Cortes *et al.*, 2015; Alkhaldi *et al.*, 2016). Among the many validated mitochondrial targets of *T. brucei* (e.g. kDNA and topoisomerases, tRNA import, fatty acid biosynthesis) (Fidalgo *et al.*, 2011), the mitochondrial respiration of the parasite is a particularly attractive target. In effect, during their life-cycle, trypanosomes adapt their energy metabolism to the availability of nutrients in their environment (Tielens and Van Hellemond, 1998). Hence, procyclic forms of *T. brucei* have a fully functional respiratory chain and synthesize ATP by oxidative phosphorylation in the mitochondrion. In contrast, bloodstream trypomastigotes of *T. brucei* (i.e. the human-infective form) rely exclusively on glycolysis for energy production as they have no oxidative phosphorylation, no cytochrome-mediated electron transport systems, and no tricarboxylic acid cycle (Verner *et al.*, 2016). Clarkson *et al* have shown that respiration of *T. b. brucei* trypomastigotes is dependent on a plant-like alternative oxidase known as the trypanosome alternative oxidase (TAO), which is localized in the inner mitochondrial membrane (Clarkson *et al.*, 1989). Because it is essential to the viability of bloodstream trypanosomes, and because it has no counterpart in the mammalian host, TAO is considered an excellent target for chemotherapy (Nihei *et al.*, 2002; Yabu *et al.*, 2006; Chaudhuri *et al.*, 2006; Nakamura *et al.*, 2010).

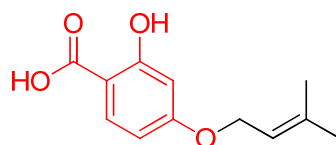
Earlier reports in the literature have shown that very simple chemical structures containing the 2,4-dihydroxybenzoate (2,4-DHB) and salicylhydroxamate (SHAM) scaffolds (Fig. 5.1) did inhibit TAO (Clarkson *et al.*, 1976; Grady *et al.*, 1986; Ott *et al.*, 2006) however, their trypanocidal activity proved disappointing because the inhibitors did not effectively cross the inner mitochondrial membrane to reach their target.



SHAM



p-n-dodecylsalicylhydroxamic acid



ACB41

Figure 5.1 Examples of 2,4-dihydroxybenzoate and salicylhydroxamate derivatives showing low micromolar activity against *T. brucei*.

In the present chapter, a strategy to enhance the antitrypanosomal potency of this class of compounds based on the conjugation of these trypanocides with a mitochondrion-targeting lipophilic cation (LC) (See Appendix C) (Madak and Neamati, 2015) was investigated. The triphenylphosphonium (TPP) cation is one of the most successful LC for mitochondria targeting (Smith *et al.*, 2003; 2008; 2011), and the use of the “TPP strategy” to deliver trypanocidal drugs to the mitochondrion of trypanosomes has recently been demonstrated (Long *et al.*, 2012; Cortes *et al.*, 2015). Lipophilic cations can cross lipid bilayers by non-carrier mediated transport and accumulate specifically into mitochondria driven by the plasma and mitochondrial transmembrane potentials (Ross *et al.*, 2006; Luque-Ortega *et al.*, 2010; Taladriz *et al.*, 2012; Dardonville *et al.*, 2015). The strong accumulation of dications by the charged mitochondria allows the inhibition of various essential functions with relatively low extracellular drug concentrations (Wilkes *et al.*, 1997; Ibrahim *et al.*, 2011; Alkhaldi *et al.*, 2016). In addition, LCs can cross the blood–brain barrier (BBB) and generate therapeutically effective concentrations in the brain (Smith *et al.*, 2003), which is particularly relevant for the treatment of late-stage sleeping sickness.

Accordingly, the activity of 3 series of LC conjugates based on the 2,4-DHB and SHAM

scaffolds (Figure 5.2) is been reported here. The compounds were evaluated *in vitro* against African trypanosome species (*T. b. brucei*, *T. congolense*), including wild-type and multi-drug resistant strains in order to assess their effects on the parasite's viability, their toxicity on mammalian cells, and to evaluate their structure activity relationship.

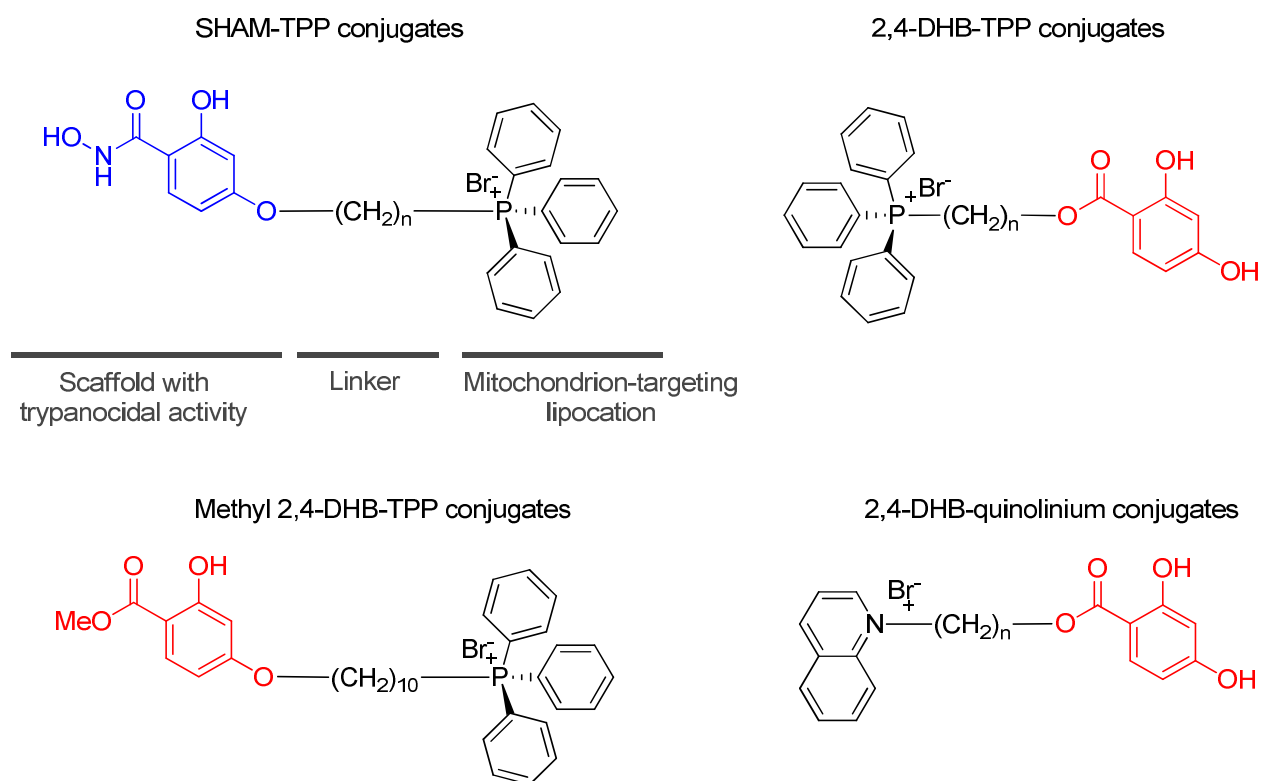


Figure 5.2 Design and general structure of the SHAM and 2,4-DHB conjugates.

5.2 Results

5.2.1 Assessment of trypanocidal activity of mitochondrion-targeting lipophilic cations on wild-type and multi-drug resistant trypanosome lines; determination of *in vitro* selectivity index.

Two different cationic groups were tested as mitochondrion targeting moieties: the bulky TPP cation and the flat heteroaromatic 1-quinolinium cation. Methylene spacers from 4 to 16 units were tested to find the optimal length between the LC carrier moieties and the trypanocidal scaffold.

As TAO is essential for parasite viability, inhibition of TAO should have a deleterious effect on parasite growth. Also the test compounds were tested on an *in vitro* culture of mammalian cell [Human Embryonic Kidney (HEK) cells, or Human Foreskin Fibroblast (HFF) cells], and the trypanocidal effect (EC_{50} *T. brucei*) was compared with the cytotoxicity effect on human cells (CC_{50} HEK or HFF) in order to determine the *in vitro* selectivity index of the test compounds.

5.2.1.1 *In vitro* activity of lipophilic cation–TAO inhibitors on *T. brucei* (Lister s427) and *T. congolense* (strain IL3000) bloodstream forms

In order to assess the trypanocidal activity of these mitochondrion-targeting lipophilic cations, drug-sensitive wild-type strains of *T. brucei* (Lister s427, and *T. congolense* (strain IL3000) were used, and this was done in parallel with the multi-drug resistant *T. b. brucei* line B48 which lacks both the *TbAT1/P2* transporter and the high affinity pentamidine transporter (HAPT), hence became highly resistance (>200 fold) to pentamidine, melarsoprol and diminazene. These experiments were performed *in vitro* using an Alamar blue-based assay (Table 5.1). The structures of all the TAO inhibitors can be found in Appendix C.

The result showed that SHAM and 2,4-DHB, the scaffolds used in the design of the new inhibitor series, were active in the micromolar range against bloodstream trypomastigotes of *T. b. brucei* s427 (WT). The cationic inhibitors were the most effective against *T. brucei* WT with EC_{50} values ranging from the outstanding 0.6 nM (TAO52) to 1.75 μ M (TAO46). The SHAM–TPP conjugates (i.e. TAO4, 5, and 6) and the 2,4-DHB-quinolinium conjugates (TAO - 23, 24, and 28) displayed submicromolar EC_{50} values (0.1 to 0.4 μ M) against this trypanosome strain. However, the 2,4-DHB-TPP derivatives (i.e. TAO – 7, 8, 9, 10, 25, and 27) were 10- to 66-times more active with low to mid-nanomolar EC_{50} values (0.0012 to 0.073 μ M) - in the same range as the reference drugs pentamidine and diminazene (Table 5.1). However, the TPP derivatives (TAO49, TAO47, TAO45) were >24-fold more potent than their respective quinolinium counterparts (TAO50, TAO48, TAO46), displaying single-digit nanomolar EC_{50} values. The 4-formyl-3-hydroxyphenoxy-based inhibitors (TAO45, TAO46) were the least active of these series, with EC_{50} values of 0.133 and 1.75 μ M, respectively.

Table 5.1 EC₅₀ values (μM) against Wild Type and Resistant Strains of *T. b. brucei*, *T. congolense*, and Cytotoxicity against Human Cells (CC₅₀, μM).

Cmpd	<i>T. brucei</i> WT ^a	SI ^b	<i>T. brucei</i> B48 ^c	RF ^d	<i>T. congolense</i> WT ^e	SI ^f	Human cells ^{g,h}
TAO 1	2.92 ± 0.70	46.92	Nd ⁱ		15.28 ± 2.23	8.97	137
TAO 2	0.30 ± 0.09	4396.7	Nd		4.62 ± 0.38	285.50	1319
TAO 3	2.42 ± 0.61	68.18	Nd		16.69 ± 2.29	9.89	165
TAO 4	0.40 ± 0.14	>1000	Nd		27.20	>14.7	>400 ^g
TAO 5	0.20 ± 0.04	>2043	Nd		Nd		>400 ^g
TAO 6	0.14 ± 0.01	>2857	Nd		46.40	8.6	>400 ^g
TAO 7	0.073 ± 0.003	106	0.359 ± 0.004	0.94	3.9 ± 2.7	2	7.73 ± 0.79 ^g
TAO 8	0.0059 ± 0.0025	789	0.056 ± 0.004	1.24	0.21 ± 0.16	21.9	4.68 ± 1.26 ^g
TAO 9	0.0013 ± 0.0010	1768	0.019 ± 0.002	0.86	0.19 ± 0.03	12.2	2.33 ± 0.53 ^g
TAO 10	0.0012 ± 0.0012	1334	0.021 ± 0.003	0.96	0.03±0.02	5.5	1.65 ± 0.42 ^g
TAO 16	135 ± 35	>3	Nd		>100	>4	>400 ^g
TAO 17	30.7 ± 3.8	>13	Nd		>100	>4	>400 ^g
TAO 18	> 100	>4	Nd		>100	>4	>400 ^f
TAO 19	32.72 ± 9.79	>12	Nd		55.48	>7	> 400 ^g
TAO 20	0.0018 ± 0.0004	3433	0.015 ± 0.001	0.7	0.95 ± 0.05	180	6.01 ± 1.47 ^g
TAO 21	0.06 ± 0.01	1966	0.19 ± 0.02	3	1.50 ± 0.29	59	118
TAO 22	32.94 ± 0.88	>63	33.63 ± 1.03	1.0	>100	>2	> 200 ^h
TAO 23	0.33 ± 0.01	609	0.347 ± 0.002	1.05	7.3 ± 0.3	34.1	202 ± 7 ^h
TAO 24	0.10 ± 0.01	1657	0.125 ± 0.015	1.21	3.6 ± 0.1	95.8	172 ± 14 ^h
TAO 25	0.0015 ± 0.0003	23378	0.0012±0.0001	0.78	Nd		59.7± 6.4 ^h
TAO 26	31.82 ± 0.93	869	22.11 ± 4.09	0.69	>100		26964
TAO27	0.009 ± 0.001	27714	0.008 ± 0.001	0.91	0.118 ± 0.007	>3384	249 ± 66 ^h
TAO28	0.14 ± 0.01	2410	0.14 ± 0.01	1.01	3.0 ± 0.2	>132	345 ± 24 ^h
TAO29	49.04 ± 7.79	>4	41.58 ± 5.51	0.85	>100	>2	> 200 ^h
TAO30	42.12 ± 2.85	>5	36.55 ± 0.88	0.87	>100	>2	> 200 ^h
TAO31	14.54 ± 0.97	>13	14.90 ± 1.02	0.98	52.09 ± 3.70	>4	> 200 ^h
TAO32	26.71 ± 5.52	>7	31.94 ± 7.99	1.19	>100	>2	> 200 ^h
TAO33	11.88 ± 1.60	>10	12.95 ± 3.71	1.09	>100	>2	> 200 ^h
TAO34	45.68 ± 1.52	>4	48.96 ± 0.64	1.07	>100	>2	> 200 ^h
TAO35	17.59 ± 0.55	>11	15.50 ± 0.78	0.88	42.62 ± 6.32	>5	> 200 ^h
TAO36	>400		>400		>400		> 200 ^h
TAO37	3.77 ± 0.12	>68	3.63 ± 0.18	1.0	>400		> 200 ^h

TAO38	14.40 ± 0.067	>15	14.40 ± 0.23	1.0	>400		> 200 ^h
TAO39	4.06 ± 0.091	>50	4.44 ± 0.02	1.1	>400		> 200 ^h
TAO40	>400		>400		>400		> 200 ^h
TAO41	17.70 ± 0.48	>11	20.50 ± 1.78	1.15	72.85 ± 22.49	>2.7	> 200 ^h
TAO42	>400		>400		51.58 ± 1.84	>4	> 200 ^h
TAO43	14.58 ± 0.22	>15	15.62 ± 0.21	1.07	>100	>2	> 200 ^h
TAO44	>400		>400		Nd		> 200 ^h
TAO45	0.13 ± 0.0033	1538	0.11 ± 0.02	0.9	0.27 ± 0.12	>740	> 200 ^h
TAO46	1.75 ± 0.013	>100	2.35 ± 0.15	1.3	2.11 ± 0.70	>100	> 200 ^h
TAO47	0.0024 ± 0.00080		0.0022 ± 1.2E-4	1.0	0.039 ± 0.015	>5128	> 200 ^h
TAO48	0.21 ± 0.023	>1000	0.30 ± 0.026	1.4	1.82 ± 0.45	>100	> 200 ^h
TAO49	0.0016 ± 0.00047		0.0019 ± 3.2E-4	0.9	0.005 ± 0.001	>40000	> 200 ^h
TAO50	0.032 ± 0.00058	>6666	0.089 ± 0.0010	2.7	Nd		> 200 ^h
TAO51	14.72 ± 0.14	>15	17.30 ± 0.19	1.17	>50	>4	> 200 ^h
TAO52	0.00058 ± 0.00001		0.00075 ± 4E-5	1.2	0.018 ± 0.005	>11111	> 200 ^h
TAO53	>400		>400		>400		> 200 ^h
DHB ^j	17.1 ± 1.0		Nd		Nd		Nd
PMD	0.0028 ± 0.0003		0.94 ± 0.03	98	Nd		Nd
SHAM ^k	38.7 ± 4.8		Nd		Nd		Nd
PAO ^l	0.0011 ± 0.00003		Nd		Nd		0.036 ± 0.004 ^g 0.29 ± 0.02 ^h
DMZ	0.065 ± 0.007		0.78 ± 0.04		0.15 ± 0.002		Nd

^aTrypomastigotes of *T. b. brucei* s427 (n ≥ 4). ^bSelectivity index (SI) = CC₅₀/EC₅₀ (*T. brucei* WT). ^c*T. b. brucei* strain resistant to pentamidine, diminazene, and melaminophenyl arsenicals. ^dResistance factor relative to WT. ^eTrypomastigotes of *T. congolense* IL3000. ^fSelectivity index (SI) = CC₅₀/EC₅₀ (*T. congolense* WT). ^gActivity on human embryonic kidney cells; ^hActivity on Human Foreskin Fibroblast (HFF) cells. ⁱNot determined. ^j2,4-Dihydroxybenzoate. ^kSalicylhydroxamate. ^lPhenylarsine oxide.

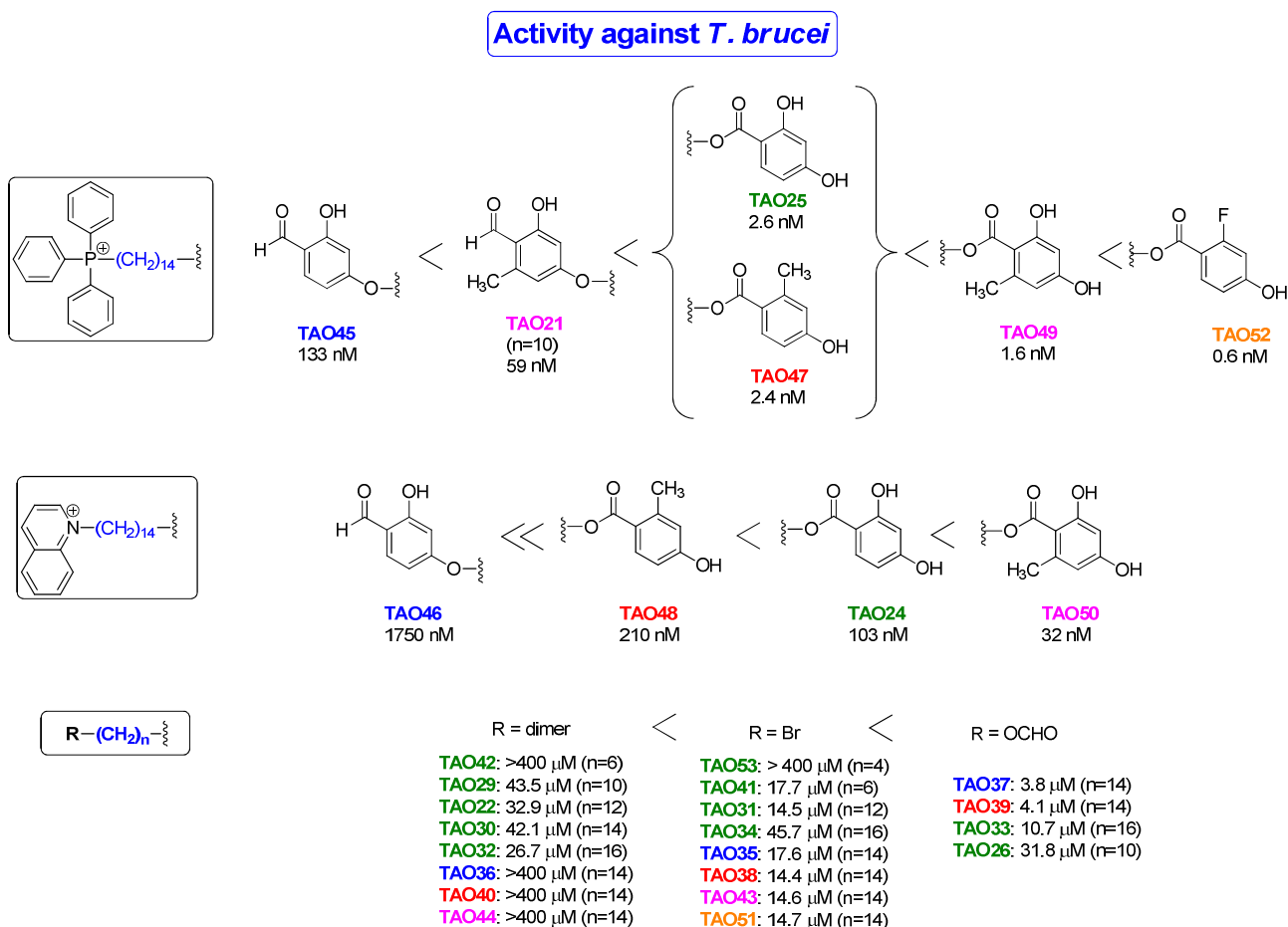


Figure 5.3 comparing the trypanocidal efficacies of the 2,4-DHB based inhibitors. This figure shows an abridged structure of the test compounds and their corresponding EC₅₀, as well as comparative analyses of the trypanosomal activity of the structures with regards to their trypanocidal activity. The direction of the arrow shows a decrease in activity from right to left for each series. The complete structures can be found in appendix C.

The non-cationic TAO inhibitors displayed much reduced activity against *T. brucei* with EC₅₀ values in the micromolar range (Figure 5.3). However, the formiate derivatives (TAO33, TAO39, TAO37) were approximately 3-times more potent than the bromo analogues (TAO34, TAO38, TAO35 respectively), whereas the dimer compounds (TAO22, TAO29, TAO30, TAO32, TAO36, TAO42, TAO44, TAO40) displayed very weak activity against *T. brucei* (IC₅₀ >25 μM). This result was not unexpected as these compounds do not have the lipocation mitochondrion-targeting group and the observed low activity probably results from poor uptake into the mitochondrion of the parasite.

There was no clear trend as regards to the influence of the spacer length on the activity against *T. brucei* but spacers with more than 8 methylene units seemed to be favoured: 12 > 10 > 8

methylene units for TAO – 4, 5, and 6 respectively; then $10 > 14 > 12 \approx 9 > 16 \gg 8$ methylene units for TAO - 7, 8, 9, 10, 25, and 27 respectively. Also, $14 > 16 > 12$ methylene units for TAO – 23, 24, and 28 respectively (See Table 5.1 and Appendix C). TAO18 and TAO16, lacking the TPP or 1-quinolinium cations, were mostly inactive showing that the LC-carrier moiety effectively enhances the trypanocidal activity of the compounds. Another interesting finding was the low activity displayed by the methyl ester analogue TAO17 (30.7 μM) compared to its benzoate counterpart TAO9 (0.0013 μM). This finding illustrates the importance of the 4-OH for higher activity in this series.

The compounds were generally less active against *T. congolense* strain IL3000 grown in culture (from 20- to 250-fold). However, with EC_{50} values for the best compounds (TAO- 8, 9, 10, 27, 45, 47, 49 and 52) in the submicromolar range (Table 5. 1), close to or better than that of the widely used (Giordani *et al.*, 2016) reference drug diminazene ($\text{EC}_{50} = 0.15 \mu\text{M}$), several compounds showed significant potential for use against this species.

5.2.1.2 Assessment of cross-resistance with current anti-trypanosome drugs

Strains that are resistant to current chemotherapies can be used as a model to study the possibility of cross-resistance between the existing chemotherapies, as already exists in the field, and any potential new trypanocides. Considering the current threat of trypanosomes' drug resistance, it is important that a potential trypanocide, whether for human or veterinary use, be tested for cross resistance, and this treatment should at least not be cross-resistant with the diamidine and arsenic-based drugs currently in use. Besides, the development of new drugs became a high priority exactly because of the high levels of resistance to these classes of drugs. It is for this reason that the compounds tested here were evaluated whether they would be effective against a well-characterised multi-resistant laboratory strain of *T. b. brucei*, which is resistant to the diamidines and melaminophenyl arsenicals.

In the present study, all experiments were carried out at least three times for each compound tested and each of these experiments included a positive control, pentamidine, and diminazene; drug-free incubations were used as negative controls. The fluorescence intensities obtained were analysed using the GraphPad Prism 5 software, and these data were plotted by non-linear regression to a sigmoid curve with variable slopes, in order to determine the EC_{50} values (The Effective Concentration that inhibits 50% of the maximal growth of trypanosomes).

The result showed that a very little difference in activity was observed between WT and B48 cell lines, with resistance factors (RF) consistently close to 1 (Table 5.1), showing that the known drug transporters TbAT1 and HAPT1 are not involved in their uptake.

Normally, a resistance factor >1 signifies cross resistance, while a resistance factor of <1 signifies increased sensitivity of the resistant strain to the test compound.

However a resistance factor of approximately 1 was observed for the majority of the test compounds reported in this assay (Table 5.1) and this signifies no *in vitro* cross resistance of these test compounds with the current diamidine and arsenical trypanocides.

5.2.1.3 Cytotoxic activity of lipophilic cation-TAO inhibitors on human cells and therapeutic index values

The high level of toxicity in the current sleeping sickness therapies is one of the main reasons for the efforts to develop a new trypanocide. Hence, the test compounds studied here were tested using the cell viability dye, Alamar blue, for their effects on human embryonic (HEK 293-T) cells or Human Foreskin Fibroblast (HFF) cells in order to assess whether the highly impressive anti-trypanosome activity of these test compounds (as listed in Table 5.1), is the result of a general toxicity or is selectively targeting trypanosomes.

The experiments were carried out at least three times for each compound tested and each of these experiments included a positive control, phenylarsine oxide – a known cytotoxic agent (Alkhaldi *et al.*, 2016), drug-free incubations were used as negative controls. The fluorescence intensities obtained were analysed using the GraphPad Prism 5 software, and these data were plotted by non-linear regression to a sigmoid curve with variable slopes, in order to determine the CC₅₀ values (the cytotoxic concentration that inhibits 50% of the maximal growth of HEK or HFF cells).

The results of the toxicity assays against the mammalian cells revealed that the test compounds that displayed the anti-trypanosome activity have a much lower activity, or in some cases, no effect on the growth and viability of these cells. The therapeutic index rates calculated as CC₅₀ of HEK or HFF cells / EC₅₀ of wild-type *T. b. brucei* are shown in Table 5.1.

In general, the compounds' cytotoxicity was low ($>200\ \mu\text{M}$), except for TAO – 7, 8, 9, 10, and 25 which displayed a cytostatic (as opposed to cytotoxic) effect in the low micromolar range. In most cases the selectivity indices (SI) were >200 , and TAO27 reached SI $>27,000$.

It is however worth mentioning here that in this experiment, the higher limit of the therapeutic index was not achieved as the highest concentration of the test compounds on HEK or HFF cells were $400\ \mu\text{M}$ and a large percentage of the test compounds did not affect the growth of these mammalian cells at this concentration. Whereas the results presented here appear to be highly promising, it is however acknowledged that the low *in vitro* toxicity may not necessarily translate to a low *in vivo* toxicity, given the complexity of whole organisms and the many varied tissues. Hence, a far more toxicological and pharmacological analyses of this test compounds need to be performed if this series of inhibitors are to be developed into genuine lead compounds for anti-trypanosomal drug development.

5.2.2 Analysis of structural determinants of the mitochondrial-targeting inhibitors contributing to their trypanocidal activity

The structural determinants for activity of the test compounds against TAO are similar to those previously found to be essential for anti-trypanosome activity of some trypanocides. For instance the presence of the 4-hydroxyl on the scaffold of the SHAM derivatives and the 2,4-dihydroxybenzoate derivatives were found to be a significant requirement for improved anti-trypanosome activity of these classes of inhibitors (See also Fig. 5.4). A hydroxyl substituted benzoate moiety was previously reported to be the basic structural requirement needed to inhibit the alternative oxidase activity in plants and trypanosomes as reported for Ascofuranone (AF) and its derivatives (Saimoto *et al.*, 2013). Saimoto and his fellow workers also identified the pharmacophore of ascofuranone that interacts with TAO base on structure-activity relationship. The comprehensive inhibitory profiles of these analogues implicated the 1-formyl and 6-hydroxyl groups on AF, as contributing to intramolecular hydrogen bonding and/or serving as donor for hydrogen-bonding, and that these were responsible for the direct interaction with TAO (Saimoto *et al.*, 2013).

Because the compounds tested in the present work are targeted at TAO, and the protein is located in the mitochondria, the hydroxyl requirement for increased activity may be similar to that already reported for SHAM and ascofuranone.

Another very important groups on the scaffolds that clearly contributed to the anti-trypanosome activity of these classes of inhibitor as observed in this assay is the presence of the lipophilic triphosphonium or a 1-quinolinium cations (Figure 5.4). For instance, TAO18 and TAO16, lacking the TPP or 1-quinolinium cations (See Table 1 and Appendix C), were mostly inactive showing that the LC-carrier moiety effectively enhances the trypanocidal activity of the compounds. This same observation has been reported for some tripanocidal triphosphonium salts (Alkhaldi *et al.*, 2016).

Another requirement for antitrypanosomal activity of this series of compounds is the number of methylene units (n). It was clearly observed that the trypanocidal activity decreases when the methylene units is less than 10 but increases when the number of methylene units is more than 10, up to when the number of methylene units is 12 for the SHAM derivatives. A similar observation was also made for the anti-trypanosomal effect of ascofuranone derivatives, where it was reported that the methylene group is contributory to the conformation of the TAO enzyme-bound molecule (Saimoto *et al.*, 2013).

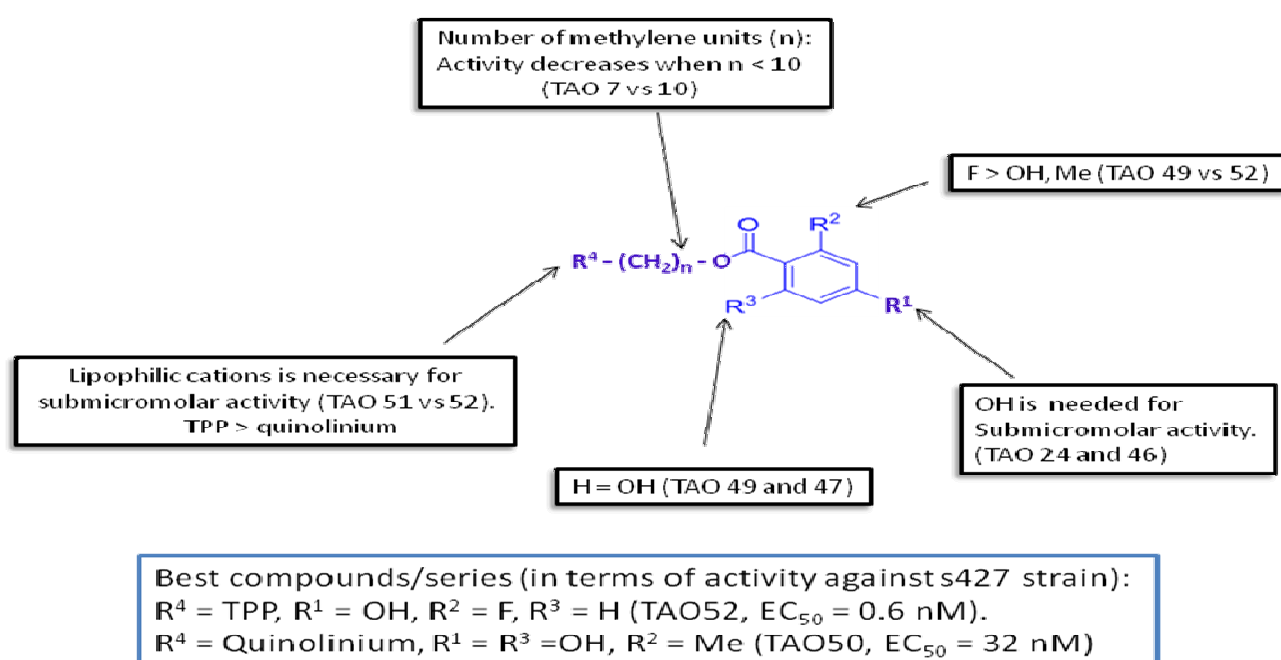


Figure 5.4 Summary SAR of DHA-based trypanocides with triphenylphosphonium or quinolinium lipophilic cations (LC); or its dimer, highlighting the unique structures on the scaffold that is responsible for the trypanocidal activity on wild-type s427 BSF trypanosomes.

Finally, the strategy that involves the use of triphenylphosphonium lipophilic cation conjugate is more effective at killing the parasites than that involving the use of quinolinium lipophilic cation.

5.2.3 Monitoring the rate of trypanosome lysis induced by test compounds, using propidium iodide

The purpose of this experiment was to monitor the speed of action of the test compounds, in order words, how fast these compounds act on trypanosomes in real time, and whether they also cause loss of membrane integrity, becoming permeable to propidium iodide across the cell membrane. The principle behind this assay is that trypanosomes become fluorescent when there is a breach in the plasma membrane integrity (i.e., loss of cellular integrity), allowing propidium iodide to enter the cell and bind to nucleic acids.

Various dilutions of the test compounds were used to study the dose dependence effect of the test compounds on cell viability during 6 hours of exposures. Digitonin was used as positive control, while untreated wells served as negative controls. The effects of two representative LC conjugates (i.e. TPP and quinolinium derivatives with the same linker and high activity/selectivity profile) were tested on *T. b. brucei* in real time. The effects of TAO25 and TAO24 on *T. brucei* s427 trypomastigotes was dose-dependent; at doses near their EC₅₀ values the compounds induced increased rate of PI influx only marginally compared with untreated control cells, over the 6 hours of the experiments. For both compounds, at ~3-fold of their EC₅₀ values (1.5 nM and 100 nM, respectively), killing of the trypanosomes was complete in approximately 4 hours (Figure 5.5). These results show that there is no immediate disruption of the plasma membrane from the administration of these nanomolar concentrations of LC conjugates.

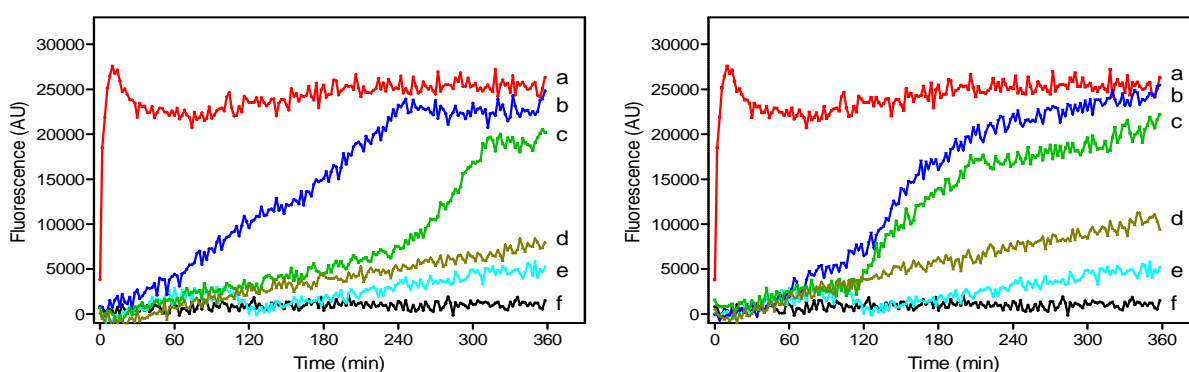


Figure 5.5 Viability assay for TAO24 and TAO25. Left panel: cells were incubated with 10 μ M digitonin (a) or with test compound TAO24 at 6 \times (b), 4 \times (c) or 2 \times EC₅₀ (d), or no test compound (e) in the presence of 9 μ M propidium iodide. Background fluorescence was recorded for wells containing media only (f). Right panel: parallel experiment with compound TAO25, at 3 \times (b), 2 \times (c) and 1 \times EC₅₀ (d). An increase in fluorescence recorded as arbitrary units (A.U.) correlates with increased permeability to propidium iodide, reflecting membrane integrity.

5.3 Discussion

The chemotherapy of HAT is still deficient despite recent efforts to discover new treatments effective for both stages of the illness (Eperon *et al.*, 2014). Besides, drugs against animal African trypanosomiasis (AAT, or nagana) are even more urgently needed than for the corresponding human condition (Giordani *et al.*, 2016). As current drugs are becoming ineffective due to drug resistance, cross-resistance between existing drugs and new ones is one of the most important issues that must be tackled early in the search for new antitrypanosomal agents (Rodenko *et al.*, 2013).

In this work, two trypanocidal scaffolds (i.e. 2,4-dihydroxybenzoate and salicylhydroxamate) known to interact with mitochondrial targets were conjugated with a mitochondrion-targeting lipophilic cation in order to boost their potency against trypanosomes. Their activities against WT and resistant *T. brucei*, and against a drug-sensitive *T. congolense* strain, were studied *in vitro*.

The first important result came from the low nanomolar range activities displayed by the 2,4-DHB–TPP derivatives (TAO- 7, 8, 9, 10, 25, and 27, 47, 49 and 52), and the submicromolar activities of the 2,4-DHB–quinolinium derivatives (TAO- 23, 24, and 28, 48 and 50), as compared with the mid-micromolar EC₅₀ values of the parent compound. In contrast, the SHAM–TPP derivatives displayed somewhat lower activities, even though this still represented an approximately 100-fold improvement in potency relative to SHAM. The superior antitrypanosomal activities observed with the TPP vs quinolinium conjugates is consistent with earlier studies on diphenyl cationic trypanocides (Dardonville *et al.*, 2015). It probably reflects the higher lipophilicity and charge dispersion around the phosphorus atom in the TPP cation, which is optimal for membrane permeation and accumulation in the mitochondrion.

Secondly, the insignificant differences in susceptibility between the WT and the multi-drug resistant B48 cell lines means that cross-resistance with existing first line HAT and AAT drugs, including pentamidine, diminazene, cymelarsan and melarsoprol, is highly unlikely to appear with these compounds, despite the diamidines, at least, also having mitochondrial targets (Lanteri *et al.*, 2008; de Macêdo *et al.*, 2015). Indeed, some compounds (e.g. TAO25) were, if anything, slightly more effective against the *T. brucei* B48 resistant line compared to WT, although this did not reach statistical significance. The lack of cross-resistance of 2,4-DHB and SHAM-LC conjugates with diamidines can be attributed to the fact that diamidine resistance in *T. brucei* is associated with loss of specific cell surface transporters (Baker *et al.*, 2013; Munday *et al.*, 2014), whereas the lipophilic LC conjugates are likely to diffuse across biological membranes. Also noteworthy is the submicromolar to nanomolar activity displayed by compounds TAO- 8, 9, 10 and 27, 45, 47, 49, and 50 against *T. congolense*, the principal etiological agent of AAT. Their EC₅₀ values are similar to, and in one case (i.e. TAO49), 30-fold more effective than the veterinary drug diminazene and their utility against AAT should be investigated further, as drugs against this condition are even more urgently needed than for the corresponding human condition (Giordani *et al.*, 2016).

In conclusion, in this chapter, several highly potent trypanocidal agents against *T. brucei* and *T. congolense* with very high selectivity indices up to >23,000 and no cross resistance with existing trypanocidal drugs were synthesized. We showed that the linking of a lipophilic cation to the 2,4-DHB or SHAM scaffold drastically improved the activity against trypanosomes *in vitro*. The 2,4-DHB scaffold gave the most potent compounds and the 14-methylene linker seemed optimal for trypanocidal action. Since the compounds described here were designed as potential mitochondrion-targeted molecules, more so that SHAM and 2,4-DHB are previously known to target TAO, the mechanism of their derivatives studied here might also be via inhibition of TAO. Hence their effects on parasite respiration need to be further investigated in order to know whether TAO might be involved in the observed antitrypanosomal activity.

Chapter 6: Investigation into the mode of action of mitochondria targeting lipophilic cations against *T. b. brucei* bloodstream form

6.1 Introduction

Respiration of bloodstream trypomastigotes of *Trypanosoma brucei* relies on a plant-like alternative oxidase known as the trypanosome alternative oxidase (TAO) (Nihei, *et al.*, 2002; Chaudhuri *et al.*, 2006; Yabu *et al.*, 2006; Nakamura *et al.*, 2010). This mitochondrial enzyme, which is essential to the viability of trypomastigotes and has no counterpart in the mammalian host, is a validated target for chemotherapy (Nihei, *et al.*, 2002; Ott *et al.*, 2006; Nakamura *et al.*, 2010). To boost the activity of a TAO inhibitor, 2,4-dihydroxybenzoate (DHB), and salicylhydroxamate (SHAM), which were hitherto fairly active against *T. brucei* in a whole cell assay, we investigated a chemical strategy consisting of the conjugation of these fairly active TAO inhibitors with lipophilic cations (LCs) that can cross lipid bilayers by non-carrier mediated transport, and thus accumulate specifically into mitochondria, driven by the plasma and mitochondrial transmembrane potentials. In chapter five it was reported that this design afforded three series of LC–TAO inhibitor conjugates active in the submicromolar (i.e. TAO- 4, 5, 6, 23, 24, and 28) to low nanomolar (i.e. TAO- 7, 8, 9, 10, 25, 28, 47, 49, and 52) range against wild type and resistant strains of African trypanosomes (*T. brucei brucei*, *T. congolense*). Selectivity over human cells was >200 and reached >23,000 for TAO25.

We therefore speculated in chapter 5 that the mechanism of their anti-parasitic effect is most likely via the intended target (TAO).

However, how easily enzyme inhibitors reach their target *in vivo* is determined by the accessibility of the enzyme (either intra- or extracellular) and the pharmacokinetics of the inhibitor. It is not uncommon that excellent enzyme inhibitors designed for intracellular targets are inactive when tested in whole cell assays because the compounds simply do not reach the requisite concentration at the target location (Gilbert *et al.*, 2013). In the case of antiparasitic compounds whose target is located inside the mitochondrion of the parasite, the compound must at a minimum cross the plasma and mitochondrial membranes to reach the enzyme target (Delespaux *et al.*, 2013); additional membranes will have to be crossed for intracellular parasites. Consequently, effective delivery strategies that exist to ensure proper access of a drug to its cellular target must be validated.

Hence, in this chapter, an attempt was made to study the effect of the compound series on some biochemical parameters including parasite respiration, mitochondrial membrane potential (Ψ_m)

and the cell cycle, in order to understand whether these compounds do indeed, as designed, effectively target TAO *in vitro*. We also aim to investigate whether the LC-carrier strategy developed herein had successfully delivered the specific antiparasitic agents to their mitochondrial target.

6.2 Results

6.2.1 Effects of TAO over-expression and aquaporin knockout in TAO activity against *T. b. brucei* bloodstream forms

TAO was over-expressed in wild type trypanosomes using pHD1336 as expression vector (Fig. 6.1A). The purpose was to study the effect of the over-expressed TAO gene on the tolerance of trypanosomes to the test inhibitors. Hence, we should be able to know whether these classes of inhibitors inhibit TAO activity in the mitochondria of trypanosomes.

The result of over expression of the TAO gene in the wild type trypomastigotes of *T. brucei* s427 is shown in Fig. 6.1B. Expression in clone 3 was approximately 80% higher than in the s427 WT and empty vector (controls), while expression in clone 2 was 60% higher than in the control cells. As expected, the expression levels in the two control strains (s427 WT vs Empty vector) were identical.

Thus, the introduction of the construct resulted in a moderate increase in the expression of the mRNA (Figure 6.1C).

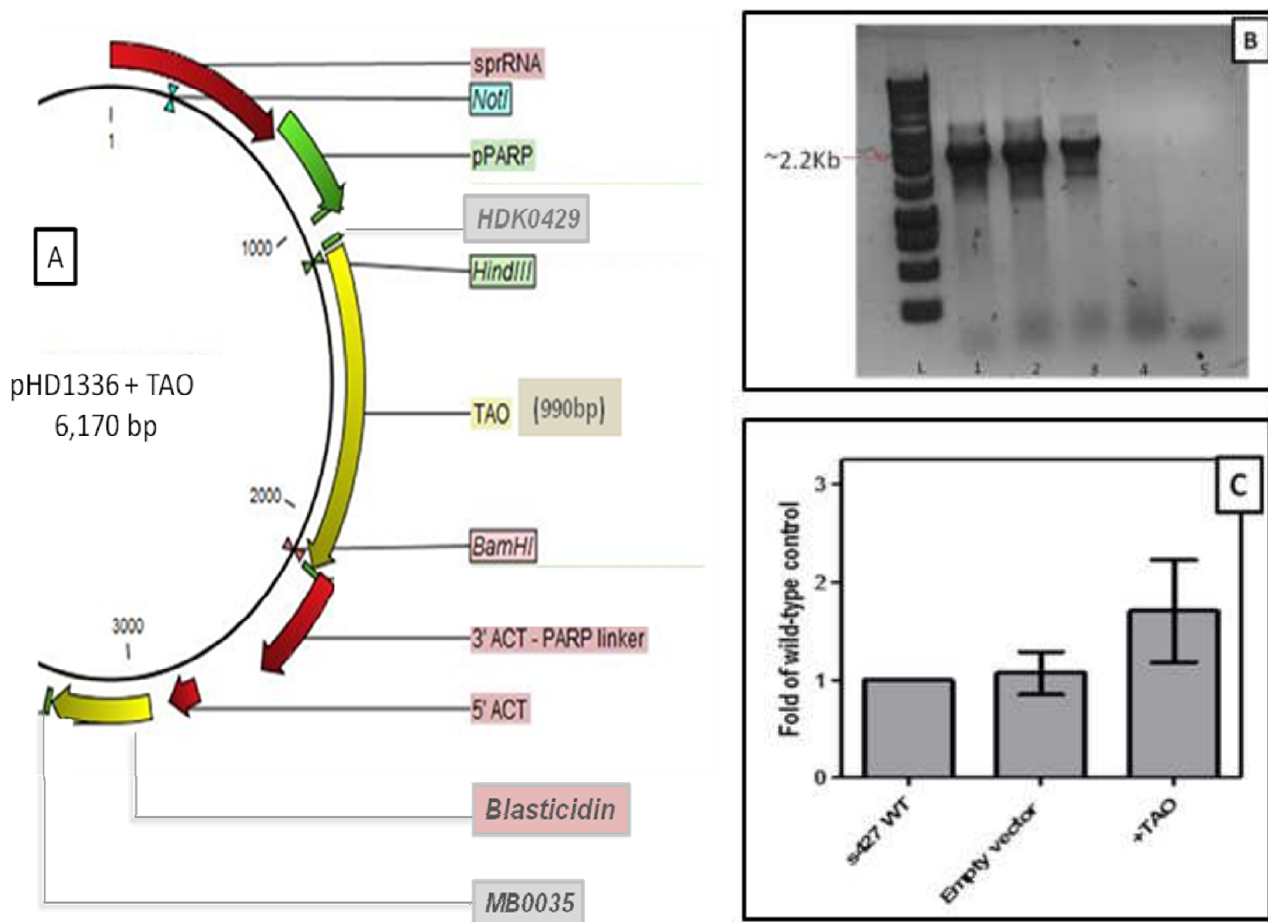


Figure 6.1 Expression of TAO in *T. b. brucei* trypomastigotes. Panel A: pHD1336 plasmid map showing strategy for TAO over-expression. Panel B: PCR confirmation/Agarose gel electrophoresis of TAO insert in BSF *T. brucei*, L=1kb DNA ladder (ThermoFisher Scientific), lanes 1-3 = TAO over-expressor clones 1-3, lane 4 = wild type *T. brucei*, lane 5 = water. Panel C: Relative levels of TAO expression were determined by qPCR in wild-type Lister 427, in the same cell line transfected with the 'empty vector' pHD1336 (no insert) and with the TAO open reading frame in pHD1336. HDK0429 and MB0035 are primers. Error bars are average and SEM of 6 determinations.

The *T. brucei* cell line over-expressing TAO (*TbTAO^{oe}*) was used in parallel with other strains to determine the EC_{50} of the test series and compared with the EC_{50} values of the wild type control. It was anticipated that genuine TAO inhibitors, acting principally on this protein, would display reduced activity against *TbTAO^{oe}*, whereas compounds that predominantly acted by another mechanism against the parasite, would display an unchanged activity against this strain.

Hence, some of the compounds were tested on a *T. b. brucei* cell line overexpressing TAO, as a further test for activity through inhibition of TAO, as it is not possible to delete the TAO gene, or even reduce its expression by RNAi (Helfert *et al.*, 2001; Schnaufera *et al.*, 2002).

The aquaporins are known to be directly involved in the export of glycerol, H₂O, urea, and other small molecules across the *T. brucei* cell membrane (Munday *et al.*, 2015). We therefore hypothesised that the export of glycerol would become essential for the survival of BSF *T. brucei* especially when there is a blockade of the aerobic respiration via TAO, with the attendant build-up of glycerol in the cell. Trypanosomes lacking the aquaglyceroporin (aquaporin) should die due to mass action of glycerol which builds up inside the cell and inhibits the anaerobic pathway of glycolysis that is the cell's only pathway to ATP when TAO is inhibited. Similarly this mass action effect should play-out if there is also glycerol build-up in the media in the presence of TAO inhibition (Yabu *et al.*, 1998). Accordingly, two strains: one lacking the aquaporin 2 and aquaporin 3 genes (aqp2/3 null) and the other lacking all three aquaporin genes (aqp1-3 null) were tested. Also, the compounds were tested against the wild type *T. brucei* BSF in the presence of 5 mM glycerol.

The result showed that there was no significant difference between the wild type and the TAO over-expressor lines, only a few of the inhibitors tested were only slightly less active against the *TbTAO^{oe}* line. However, TAO25 and SHAM were significantly less effective against this cell line than against the wild-type control, by 2.6 (P=0.0001) and 1.6-fold (P<0.01), respectively, indicating a possible involvement of TAO in the MOA of both compounds (table 6.1) but, the level of overexpression was really modest, as established by qPCR (Figure 6.1), owing to the already very high expression level of TAO in *T. brucei* trypomastigotes.

Table 6.1 EC₅₀ values (μM) of LC TAO inhibitors against BSF *T. b. b.* cell line over-expressing TAO, and glycerol (5 mM) potentiating effect on Wild type BSF *T. b. b.*

	s427 WT ^a		TAO-over-expressor ^b				TAO inhibitor + 5 mM glycerol on <i>T. b. b</i> s427 WT ^c			
COMPD	AVG ^d (μM)	SEM ^e (μM)	AVR (μM)	SEM	RF ^f	t-test ^g	AVG (μM)	SEM	RF	t-test
TAO 7	0.073	3.28E-03	0.081	2.20E-04	1.12	0.12	0.08	0.01	1.16	0.33
TAO 8	0.0059	2.50E-03	0.0062	1.99E-04	1.05	0.94	0.01	0.002	0.88	0.86
TAO 9	0.0013	1.03E-03	0.0012	2.19E-05	0.95	0.96	0.0017	1.1E-04	1.26	0.83
TAO 10	0.0012	1.17E-03	0.0012	3.58E-05	0.93	0.96	0.0012	3.4E-05	1.01	1.00
TAO 20	0.0018	3.55E-04	0.0019	1.23E-04	1.09	0.79	-	-	-	-
TAO 21	0.062	0.0054	0.061	0.0020	0.97	0.87	-	-	-	-
TAO 22	32.94	0.88	33.047	5.65	1.00	0.98	13.62	1.18	0.41	4.0E-05
TAO 23	0.33	0.014	0.37	0.024	1.11	0.21	0.23	0.01	0.69	2.7E-03
TAO 24	0.10	0.012	0.11	0.0021	1.07	0.63	0.08	0.01	0.75	0.19
TAO 25	0.0015	0.0002	0.0039	0.00014	2.60	1.35E-04	0.0008	6.7E-05	0.56	0.05
TAO 26	31.82	0.93	35.00	0.60	1.10	0.05	17.48	0.88	0.55	1.E-04
TAO 27	0.0092	0.0007	0.0077	1.05E-04	0.83	0.12	0.005	4.2E-05	0.54	3.7E-03
TAO 28	0.143	0.014	0.15	0.0041	1.07	0.59	0.09	0.003	0.62	0.02
TAO 29	49.04	7.79	44.64	1.12	0.91	0.71	12.25	0.61	0.25	0.01
TAO 30	42.12	2.85	50.88	2.24	1.21	0.07	15.88	1.48	0.38	7.5E-04
TAO 31	14.54	0.97	14.89	0.94	1.02	0.81	6.16	0.30	0.42	8.6E-04
TAO 32	26.71	5.52	32.18	0.34	1.21	0.44	12.41	0.30	0.46	0.08
TAO 33	11.88	1.60	10.92	0.53	0.92	0.70	5.14	0.52	0.43	0.02
TAO 34	45.68	1.52	50.70	1.96	1.11	0.09	11.08	0.65	0.24	8.6E-06

TAO 35	17.59	0.55	15.83	0.30	0.90	0.05	10.746	0.540	0.61	8.79E-04
TAO 37	3.77	0.12	4.17	0.087	1.11	0.05	1.798	0.011	0.48	7.19E-05
TAO 38	14.40	0.07	14.26	0.062	0.99	0.21	7.498	0.120	0.52	9.48E-07
TAO 39	4.06	0.09	4.17	0.054	1.03	0.36	7.800	0.392	1.92	7.50E-04
TAO 41	17.70	0.48	21.58	0.60	1.22	0.01	12.093	0.538	0.68	0.001
TAO 43	14.58	0.22	13.97	0.098	0.96	0.06	7.707	0.027	0.53	6.29E-06
TAO 45	0.13	0.003	0.075	0.0072	0.56	0.002	0.067	0.005	0.51	4.84E-04
TAO 46	1.75	0.01	1.36	0.18	0.78	0.09	1.229	0.077	0.70	0.003
TAO 47	0.0024	7.97E-04	0.0038	5.03E-04	1.56	0.22	0.003	0.0005	1.32	0.44
TAO 48	0.21	0.02	0.16	0.017	0.78	0.18	0.145	0.007	0.69	0.06
TAO 49	0.0016	4.70E-04	0.0023	8.82E-05	1.45	0.22	0.001	0.0001	0.92	0.81
TAO 50	0.03	0.001	0.056	0.010	1.76	0.07	0.071	0.002	2.22	2.07E-05
TAO 51	14.72	0.14	13.57	0.052	0.92	0.002	7.185	0.067	0.49	1.13E-06
TAO 52	0.001	1.20E-05	6.9E-04	1.22E-04	1.19	0.41	0.00039	0.00003	0.66	0.01
DHB ^h	17.06	1.08	nd	Nd	Nd	Nd	19.00	1.02	1.11	0.26
SHAM ⁱ	38.73	4.78	60.31	4.97	1.56	0.01	7.01	0.31	0.18	1.3E-11
PDM ^j	0.0028	2.70E-04	0.0031	2.88E-04	1.08	0.57	0.0037	5.6E-04	1.32	0.13
DMZ ^k	0.065	0.01	nd ^l	nd	nd	nd	0.06	2.1E-03	0.97	0.84
PAO ^m	0.0012	2.89E-05	0.0013	7.7E-05	1.14	0.12	nd	nd	nd	nd

^aTrypomastigotes of *T. b. brucei* s427 (n ≥ 4). ^b*T. brucei* over-expressing TAO. ^c*T. b. b* incubated with TAO inhibitors in the presence of 5mM glycerol.

^dAverage of at least 4 independent determinations. ^eStandard error of mean of all determinations. ^fResistance factor. ^gUnpaired Student's t-test comparing EC₅₀ value of WT against the various cell lines or determinations. ^h2,4-Dihydroxybenzoate. ⁱSalicylhydroxamate. ^jPentamidine and ^kdiminazene aceturate, both are known trypanocides. ^lNot determined. ^mPhenylarsine oxide, a known cytotoxic agent.

Table 6.2 EC₅₀ values (μM) of LC TAO inhibitors against BSF *T. b. b.* cell line with double or triple knockouts of the aquaporin genes.

	s427 WT ^a		aqp2/3-double null ^b				aqp1-3 triple null ^c			
COMPD	AVG ^d (μM)	SEM ^e (μM)	AVG (μM)	SEM	^f RF	^g t-test	AVG (μM)	SEM	RF	t-test
TAO 7	0.073	3.28E-03	0.073	0.0013	1.00	0.99	0.08	0.002	1.16	0.06
TAO 8	0.0059	2.50E-03	0.0044	8.6E-04	0.75	0.70	0.01	2.2E-04	1.06	0.92
TAO 9	0.0013	1.03E-03	0.0013	3.7E-05	0.98	0.99	0.001	4.5E-05	0.87	0.91
TAO 10	0.0012	1.17E-03	0.0016	2.0E-04	1.27	0.84	0.001	2.7E-05	0.86	0.91
TAO 20	0.0018	3.55E-04	0.0015	1.2E-04	0.87	0.70	0.0013	9.8E-05	0.76	0.49
TAO 21	0.062	0.0054	0.056	6.2E-04	0.89	0.47	0.06	2.2E-03	0.93	0.66
TAO 22	32.94	0.88	26.68	1.80	0.81	0.02	8.94	0.60	0.27	4.73E-06
TAO 23	0.33	0.014	0.26	0.021	0.78	0.03	0.12	0.01	0.38	8.13E-05
TAO 24	0.10	0.012	0.09	0.0012	0.89	0.44	0.04	0.01	0.37	0.01
TAO 25	0.0015	0.0002	0.0020	1.9E-05	1.36	0.09	0.0009	1.2E-05	0.61	0.06
TAO 26	31.82	0.93	27.43	0.67	0.86	0.02	15.64	0.38	0.49	3.26E-05
TAO 27	0.0092	0.0007	0.01	5.5E-04	0.92	0.49	0.01	1.5E-04	0.77	0.06
TAO 28	0.143	0.014	0.25	0.02	1.74	0.005	0.06	0.01	0.44	0.01
TAO 29	49.04	7.79	24.59	0.57	0.50	0.07	7.09	0.78	0.14	0.01
TAO 30	42.12	2.85	28.22	1.20	0.67	0.01	14.77	0.24	0.35	4.63E-04
TAO 31	14.54	0.97	10.04	0.09	0.69	0.01	4.69	0.33	0.32	4.14E-04
TAO 32	26.71	5.52	14.31	0.78	0.54	0.12	9.28	0.30	0.35	0.04
TAO 33	11.88	1.60	4.99	0.12	0.42	0.02	1.27	0.07	0.11	2.74E-03
TAO 34	45.68	1.52	14.52	0.72	0.32	1.52E-05	5.07	0.24	0.11	3.24E-06

TAO 35	17.59	0.55	8.397	0.24450	0.48	0.000085	7.8700	0.39793	0.45	0.000136
TAO 37	3.77	0.12	1.426	0.09300	0.38	0.000056	1.8170	0.02515	0.48	0.000080
TAO 38	14.40	0.07	7.084	0.20000	0.49	0.000001	7.1617	0.55037	0.50	0.000199
TAO 39	4.06	0.09	1.396	0.04350	0.34	0.000014	1.8463	0.16086	0.45	0.000284
TAO 41	17.70	0.48	11.550	0.62000	0.65	0.000919	12.0700	0.14364	0.68	0.000367
TAO 43	14.58	0.22	7.302	0.00800	0.50	0.000005	6.7843	0.27070	0.47	0.000023
TAO 45	0.13	0.003	0.042	0.00549	0.32	0.000612	0.0531	0.00635	0.40	0.000364
TAO 46	1.75	0.01	0.954	0.02885	0.54	0.000474	1.0843	0.02700	0.62	0.000024
TAO 47	0.0024	7.97E-04	0.002	0.00012	0.92	0.835686	0.0049	0.00308	2.01	0.483710
TAO 48	0.21	0.02	0.098	0.01064	0.47	0.017224	0.0861	0.00472	0.41	0.006264
TAO 49	0.0016	4.70E-04	0.001	0.00016	0.51	0.259280	0.0014	0.00013	0.89	0.744033
TAO 50	0.03	0.001	0.035	0.00258	1.11	0.116814	0.0277	0.01012	0.87	0.693984
TAO 51	14.72	0.14	6.752	0.07900	0.46	0.000001	6.9927	0.19160	0.48	0.000005
TAO 52	0.001	1.20E-05	0.0002	0.00013	0.43	0.011882	0.00037	0.00005	0.64	0.016516
DHB ^h	17.06	1.08	nd	nd	nd	nd	16.59	0.88	0.96	0.44
SHAM ⁱ	38.73	4.78	31.86	0.95	0.82	0.36	8.91	0.35	0.23	0.0043
PDM ^j	0.0028	2.70E-04	0.049	0.004	17.34	8.54E-08	0.07	5.6E-04	26.04	5.5E-16
DMZ ^k	0.065	0.01	nd ^l	nd	nd	nd	nd	nd	nd	nd
PAO ^m	0.0012	2.89E-05	0.0013	4.2E-05	1.17	0.02	0.0013	3.1E-05	1.11	0.04

^aTrypomastigotes of *T. b. brucei* s427 (n ≥ 4). ^bAquaporin2/3 double knockout and ^caquaporin1-3 triple knockout BSF *T. brucei*. ^dAverage of at least 4 independent determinations. ^eStandard error of mean of all determinations. ^fResistance factor. ^gUnpaired Student's t-test comparing EC₅₀ value of WT against the various cell lines or determinations. ^h2,4-Dihydroxybenzoate. ⁱSalicylhydroxamate. ^jPentamidine and ^kdiminazene aceturate, both are known trypanocides. ^lNot determined. ^mPhenylarsine oxide, a known cytotoxic agent. It should be noted that the experiments reported in tables 6.1 and 6.2 were performed in parallel, there have the same controls and experimental conditions.

Co-incubation with glycerol, which inhibits the *T. brucei* anaerobic ATP production pathway (Brohn and Clarkson, 1978), significantly ($P < 0.05$) increased the trypanocidal activities of most of the compounds and SHAM, whereas it had no effect on the efficacy of TAO-39, 47 and 50 and the control drugs pentamidine and diminazene (Table 6.1). These results are consistent with the aerobic glycolytic pathway being a target of these compounds which is expected for compounds inhibiting TAO. Meanwhile, TAO20 which lacks either a SHAM or a 2,4-DHB group for binding to TAO, displayed no differential effects against *T. b. brucei* in the presence of 5 mM glycerol, or against the AOX-OE line, indicating that indeed it was not an inhibitor of TAO. However, with an EC_{50} of just 1.8 ± 0.4 nM and a selectivity >3000 reported for it in chapter five, it might be worth investigating its mode of action separately.

Similarly, most of the inhibitors were significantly more effective against the *T. brucei* cell lines from which both aquaporins AQP2 and AQP3 (aqp2/3 null) or all aquaporins (aqp1-3 null) were knocked out (Table 6.2). The effect of the compounds on the AQP knockout lines may be explained by a shift in metabolism of trypanosomes in the presence of the TAO inhibitors. Inhibition of TAO forces the parasite to produce glycerol in large quantity to survive via the anaerobic ATP-production pathway. In the absence of aquaglyceroporins, trypanosomes are not able to efficiently dispose of that glycerol, resulting in higher susceptibility to the TAO inhibitors.

6.2.2 Lipophilic cation–TAO inhibitors strongly affect the mitochondrial membrane potential (Ψ_m)

If the lipophilic cations are, as designed, accumulating in the *T. brucei* mitochondrion, then it is expected that this will impact on the mitochondrial membrane potential Ψ_m , as a result of (1) the accumulation of cations in the mitochondrial matrix, and (2) disruption of mitochondrial functions involved in maintaining the ion gradients. Similar effects have been shown for various diamidines, choline-derived dications and bisphosphonium compounds (Lanteri *et al.*, 2008; Ibrahim *et al.*, 2011; Alkhaldi *et al.*, 2016). Thus in this section, we show the result of the Ψ_m of two representative molecules (TAO25 and TAO33) from our series of compounds.

Fluorescence Activated Cell Sorting technology (FACS) was employed for the determination of the change in mitochondrial membrane potential (MMP) due to exposure of trypanosomes to

TAO25 or TAO33 by using tetramethylrhodamine ethyl ester (TMRE) (Denninger *et al.*, 2007), using a cell density of 1×10^6 cells/mL with and without test compounds for the start of the experiment. 1 mL of these samples were transferred at each time point into a microfuge tube and centrifuged at 4500 rpm for 10 min at 4 °C. The pellet was re-suspended in 1 mL PBS containing 200 nM of TMRE, followed by incubation at 37 °C for 30 min. The suspension was placed on ice for at least 30 minutes before analysis by a Becton Dickinson FACS Calibur using a FL2-height detector and CellQuest and FlowJo software (Ibrahim *et al.*, 2011). Valinomycin (100 nM) and troglitazone (10 µM) were employed as negative (mitochondrial membrane depolarisation) and positive (mitochondrial membrane hyperpolarisation) controls respectively (Denninger *et al.*, 2007). Mitochondrial membrane potential was determined at 0, 1, 4, 8 and 12 h.

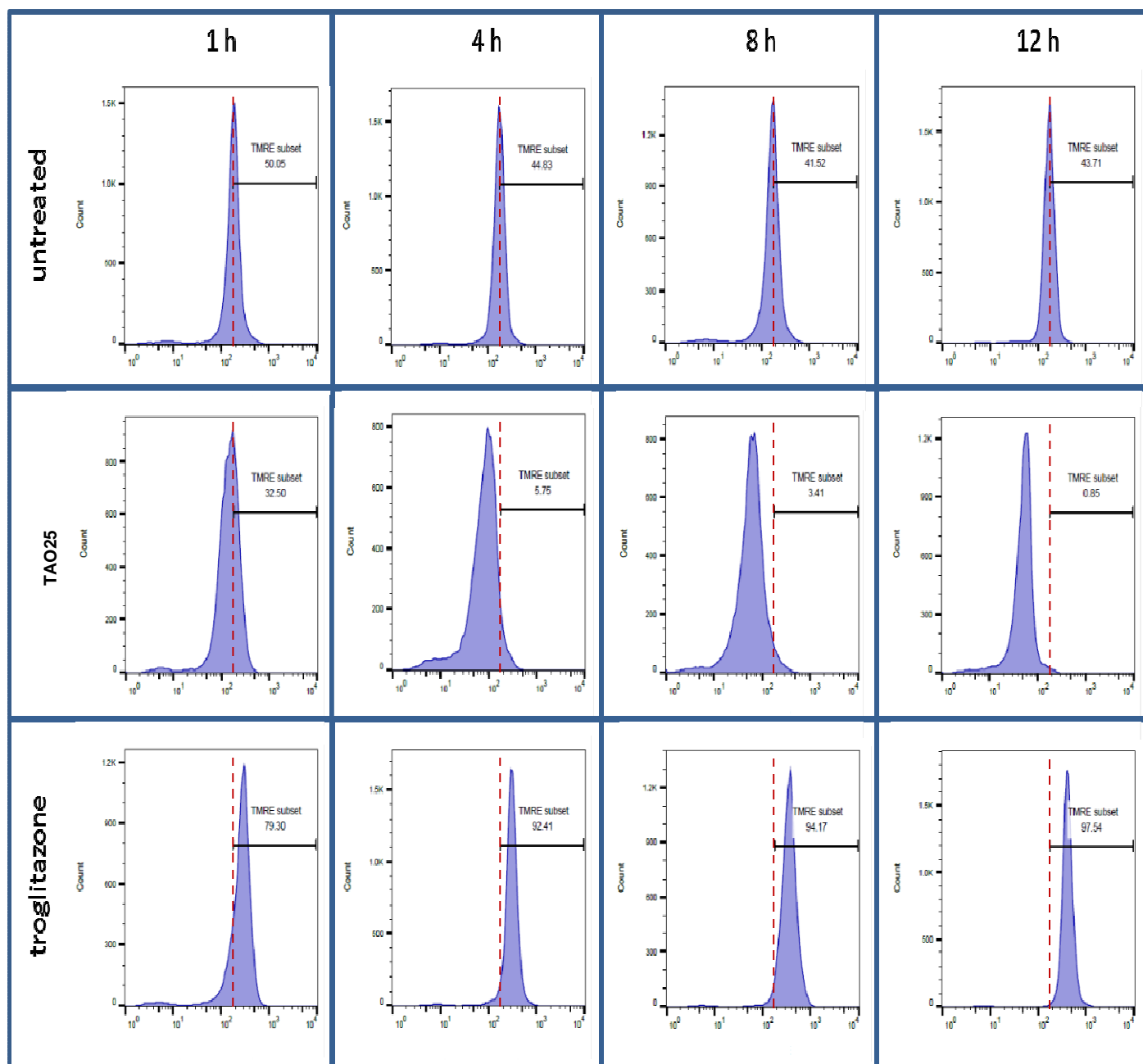


Figure 6.2 Histograms of TMRE fluorescence in populations of *T. b. brucei* trypomastigotes incubated with 0.005 μM TAO25, Valinomycin (100 nM) (see appendix F), 10 μM troglitazone, or no test compound for the indicated duration. Y-axis shows the number of cells (count) with a particular intensity of fluorescence as shown on the X-axis in artificial units (A.U.). A shift of the TMRE fluorescence to the left indicate depolarization while a shift to the right indicates hyperpolarization of the mitochondria membrane potential.

The histograms above (Figure 6.2) are an extract from the results of the histograms for TMRE in the FL2H channel. The histogram results for other test compounds are presented in Appendix F.

This assay was performed three times and the average was plotted using the GraphPad prism 5 software as shown in figure 6.3.

The result showed that TAO25 and TAO33 indeed rapidly depolarized the mitochondrial membrane, as measured by the fluorescent probe TMRE (figure 6.3).

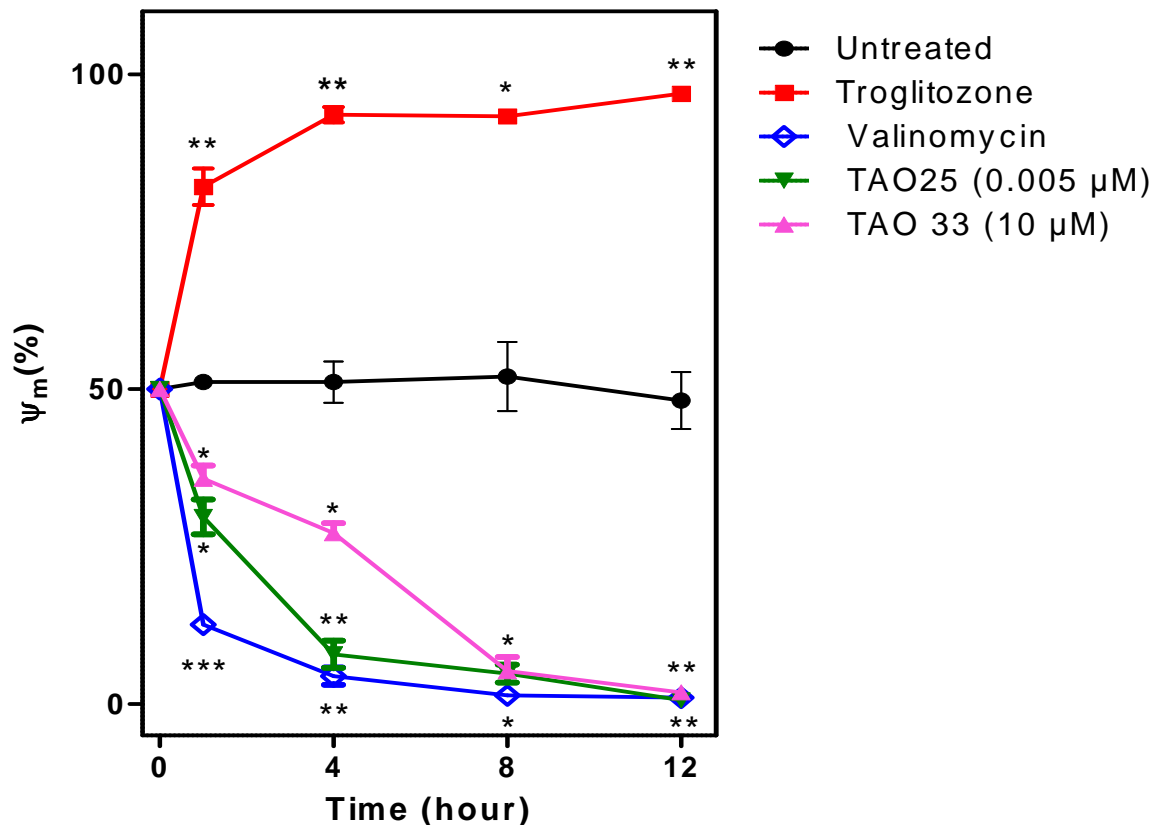


Figure 6.3 Mitochondrial membrane potential (Ψ_m) of treated and untreated *T. b. brucei* s427 WT cells. Data points represent average and SEM of flow cytometric determinations of TMRE fluorescence and are expressed as the percentage of cells that exhibit >200 artificial units of fluorescence intensity in the analyzed populations. Valinomycin and Troglitazone were used as controls for depolarization and hyperpolarization, respectively. Statistically significant differences from untreated control populations were assessed using an unpaired Student's t-test; * $P < 0.05$; ** $P < 0.01$; *** $P < 0.001$.

Figure 6.3 shows the percentage of cells in the population that accumulated >200 artificial units of TMRE fluorescence, which was set at 50% for the 0 time point of untreated cells; any increase in fluorescence such as induced by troglitazone signifies a hyperpolarization of the mitochondrial membrane and a decrease in fluorescence such as induced by valinomycin indicates depolarization. It is thus clear that TAO- 25 and 33 rapidly decreases *T. brucei* Ψ_m , although not

as rapidly as the potassium ionophore valinomycin (Figure 6.3). The reduced fluorescence is not simply the result of cells dying, as can be seen from the histograms of TMRE fluorescence for the individual determinations (Figure 6.2 and Appendix F).

6.2.3 Effects of lipophilic cation-TAO inhibitors on ATP levels in *T. b. brucei*

As mentioned in the last section, these compound series have a strong effect on trypanosomes' mitochondrial function by depolarizing the mitochondrial membrane potential (Ψ_m).

It is well acknowledged that the oligomycin-sensitive ATP synthase located in the mitochondrial membrane of bloodstream form (BSF) *T. b. b.* maintains its mitochondrial membrane potential, and it has been reported that there is a direct link between the mitochondrial membrane potential and ATP synthesis in BSF trypanosomes (Brown *et al.*, 2006). Meanwhile, ATP is an essential source of energy for trypanosome and it obtains this from glycolysis; many trypanosome enzymes and functions directly depend on ATP for their metabolic function (Alkhaldi *et al.*, 2016). Therefore, measurement of intracellular ATP level is fundamental to understanding cellular metabolism of trypanosomes in the presence and absence of the test compounds. Accordingly, these compounds were tested at the same concentrations as that of the mitochondrial membrane potential above in order to study their effect on ATP production.

The intracellular ATP levels were measured using an ATP Determination Kit (Invitrogen) following the manufacturer protocol. ATP was determined using recombinant firefly luciferase and its substrate D-luciferin. This assay is based on luciferase activity which requires ATP as a co-factor in an enzymatic reaction to produce a luminescent light (emission maximum was approximately 560 nm at pH 7.8). Known amounts of an ATP standard (provided by the kit), prepared as a serial dilution were made and used to plot a standard curve which was eventually used to quantify *in vivo* ATP levels (Figure 6.4, panel A).

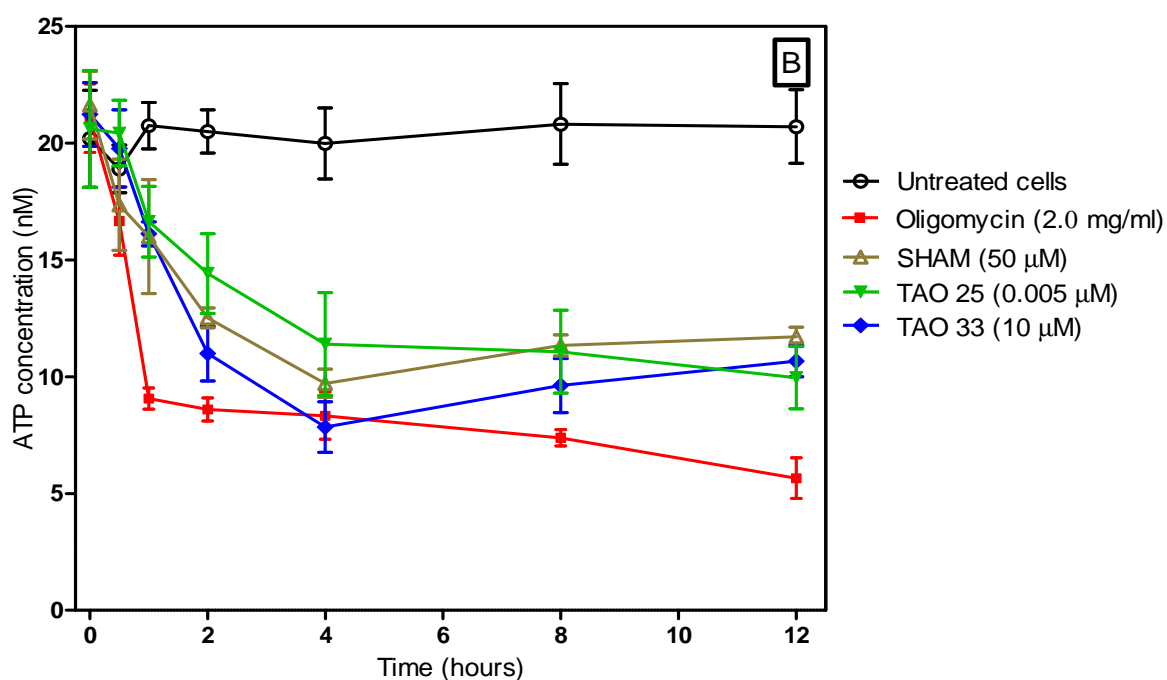
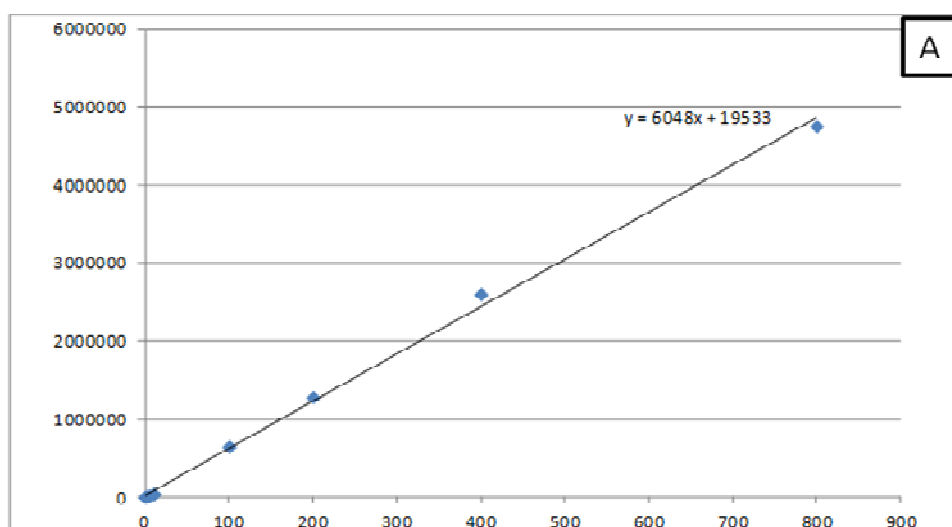


Figure 6.4 ATP concentrations in 10^7 *T. b. brucei*. Panel A: ATP standard curve done in parallel and under the same assay condition as that of the test samples, the luminescence gotten expressed as artificial units were plotted against ATP concentrations (10 nM – 800 nM) to generate an equation for a straight line from which the ATP concentrations in the test samples were extrapolated by fitting their luminescence to this equation; Panel B: ATP concentrations in treated and untreated 10^7 *T. b. brucei* cells using 50 mL extraction buffer. Incubation was for a period of 12 hours with samples taken at each time point. The results shown here are the averages of four independent experiments; and the error bars represent standard errors of 4 determinations.

The result shown in figure 6.4B shows the effects of TAO25, and TAO33 (at 0.005 μ M, and 10 μ M, respectively) on intracellular ATP levels of *T. b. brucei*. It was clear from the result that these compounds depleted the intracellular ATP after one hour by at least 20%. This decline in intracellular ATP level tended to persist with time, and after 12 hours of incubation, the ATP levels went down to about 50% for both TAO inhibitors. Interestingly, there is a positive correlation between depolarisation of the mitochondrial membrane potential and intracellular ATP concentrations.

6.2.4 Effects of lipophilic cation-TAO inhibitors on oxygen consumption rate in *T. b. brucei*

The BSF trypanosomes require oxygen for respiration which is their only means of generating ATP via the glycerol-3-phosphate oxidase system which comprises TAO as the only terminal oxidase. Consequently, the oxygen consumption rate (OCR) of trypanosomes is a key indicator of their normal cellular function mediated by TAO. It therefore follows that trypanosomes with dysfunctional mitochondria, caused by treatment with a test compound targeting mitochondrial function, will show a reduced oxygen consumption rate when compared to untreated cells.

Accordingly, the effects of selected lipophilic cation-TAO inhibitors on OCR were determined using the Oxygen Consumption Rate Assay Kit (Cayman chemicals, Ann Arbor MI, USA). This method was designed to measure extracellular oxygen consumption in mammalian cells but was adapted to trypanosomes following manufacturer's protocol with substantial modifications (See section 2.8 of chapter 2).

The result of the oxygen consumption rate assay in wild type *T. brucei* s427 BSF revealed that the various LC-TAO inhibitors tested, at concentrations close to their EC₅₀, inhibited oxygen consumption when compared to the untreated control. SHAM, a known inhibitor of TAO also had a similar effect on the OCR of these trypanosomes (Figure 6.5).

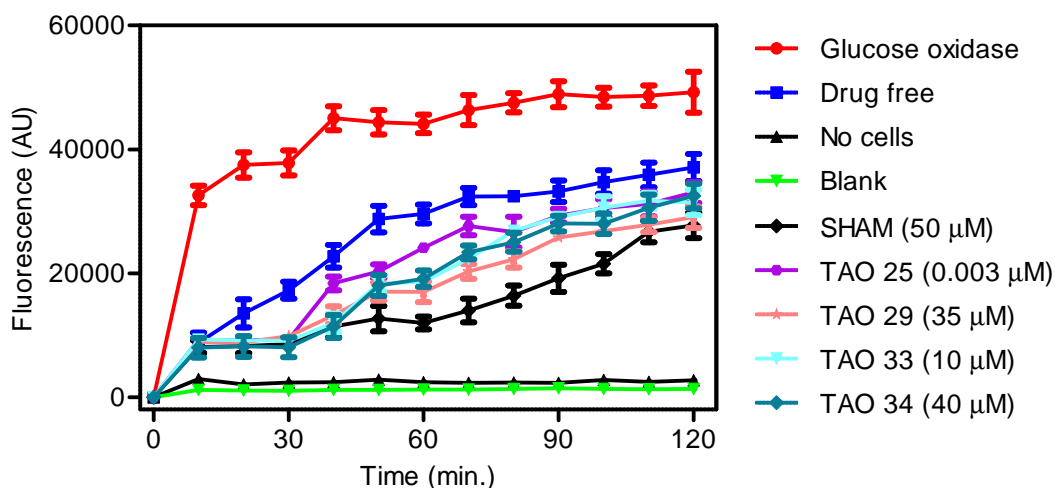


Figure 6.5 Oxygen consumption assay of selected TAO inhibitors on *T. b. bs427* following 2 hours of incubation of the cells with the respective compounds at the indicated concentration, using the MitoXpress®-Xtra HS kit (Cambridge Bioscience), which generates a fluorescence signal inversely proportional to the oxygen concentration. SHAM, No cells, Drug free and Glucose oxidase wells were used as controls. Blank wells were used to check background fluorescence.

Following the reduction in oxygen consumption brought about by the incubation of the various test compounds (Fig. 6.5), it was then necessary to do a dose-dependency assay with a few of these compounds.

The dose-dependent effects of TAO25 and TAO29 on oxygen consumption by *T. b. brucei* bloodstream trypomastigotes were tested using the same fluorescent oxygen reporter probe and it was found that both test compounds inhibit oxygen consumption of WT trypanosomes in a dose-dependent manner. The dose dependence pattern of inhibition of our test compounds correspond well with a similar trend observed with the known TAO inhibitor, SHAM (Figure 6.6). These results clearly indicate a dose dependent effect of TAO25 and TAO29 on the respiration of *T. brucei* trypomastigotes.

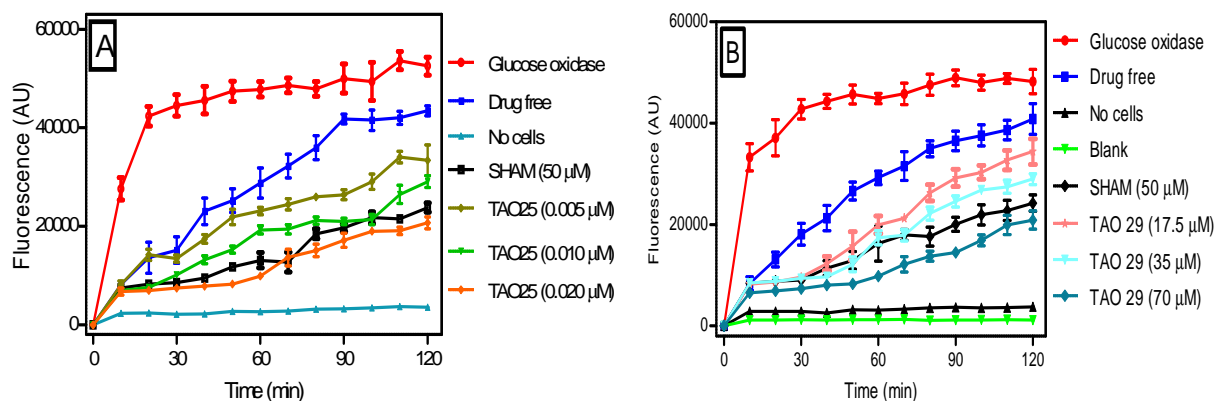


Figure 6.6 Dose dependent oxygen consumption assay of TAO25 (Panel A) and TAO 29 (Panel B) on *T. b. b* s427, using the MitoXpress®-Xtra HS kit (Cambridge Bioscience), which generates a fluorescence signal inversely proportional to the oxygen concentration. Glucose oxidase was used to rapidly deplete the cell suspension of oxygen over 2 hours, generating a maximum signal for reference, whereas wells without cells were used to establish a null/background fluorescence level. Trypanosomes nearly depleted the medium of oxygen in approximately 90 min (drug free control), a rate that was dose-dependently reduced by TAO25 and TAO 29, and also by SHAM. Symbols represent the average and SEM of 4 determinations.

We decided to carry-out this assay on the Aquaporin 1-3 triple null trypanosome cell line (*aqp1-3* null) in order to further confirm whether the increased susceptibility of this strain to the TAO inhibitors reported for this strain (Table 6.2) is related to a reduction in OCR. In Chapter 5, we have shown that the *aqp1-3* null strain is more susceptible to the inhibition of TAO mediated respiration by the test compounds.

These compounds were tested at concentrations close to the EC_{50} of these compounds on the trypanosome *aqp1-3* null cell line, which are lower than those used on the wild-type cells in order to allow the parasites to survive the period of incubation. However, it was found that despite this reduced concentration the effect of the test compounds on the OCR of *aqp1-3* null cell line were found to be more profound (figure 6.7, Panel A) than that observed for the wild-type trypanosomes (figure 6.5).

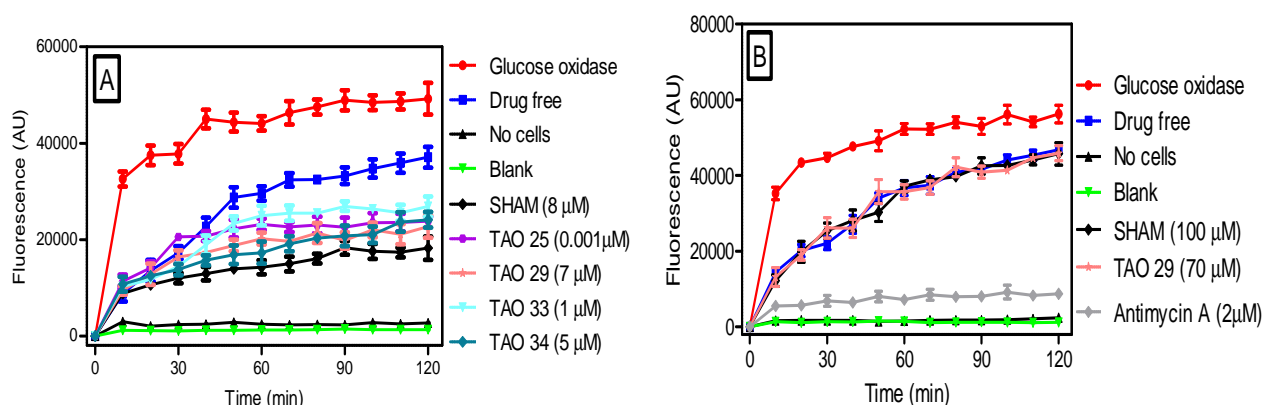


Figure 6.7 oxygen consumption assay of TAO inhibitors on aqp1-3 triple null trypanosomes (panel A), and on Mammalian cells (HFF-T25) (panel B), using the MitoXpress®-Xtra HS kit (Cambridge Bioscience), which generates a fluorescence signal inversely proportional to the oxygen concentration. SHAM or Antimycin-A wells were used as positive control (Panels A and B respectively) while Drug free and Glucose oxidase wells were used as negative control. Blank wells were used to check background fluorescence. SHAM and TAO29 had no effect on mammalian respiration (Panel B) over the 2 hours of incubation.

Also because mammalian cells lack the TAO but rather depend on a cytochrome system for their respiration, and considering the high selectivity index obtained by our TAO inhibitors in chapter 5, we decided to test these compounds on a mammalian cell line (Human Foreskin Fibroblast, HFF-T25) to further confirm this observation.

The result showed that TAO29 and SHAM at a high concentration of 70 μ M and 100 μ M respectively did not inhibit the mammalian cells from respiring (figure 6.7, panel B). However, the well-known respiratory toxin antimycin A was used as a positive control. Antimycin A is known to bind to the Qi site of cytochrome c reductase, inhibiting the oxidation of ubiquinone and disrupting the electron transport chain between cytochrome b and c of the oxidative phosphorylation, which in turn leads to a cessation of respiration. Accordingly, the Antimycin A used in this assay fully inhibited oxygen consumption in the mammalian cells (figure 6.7, panel B). These results underscore the reduced toxicity/increased selectivity and safety of our TAO inhibitors and implicate TAO-mediated parasite respiration as the possible target.

6.2.5 Cell cycle analysis of lipophilic cation–TAO inhibitor exposed cells

It has recently been shown that the treatment of *T. b. brucei* trypomastigotes with a different class of lipophilic cations, consisting of symmetrical bisphosphonium compounds, led to a rapid inhibition of the cell cycle by preventing initiation of S-phase; these compounds were shown to inhibit the mitochondrial F₀F₁ ATPase (Alkhaldi *et al.*, 2016). We thus investigated whether the lipophilic cation-TAO inhibitors might have a similar effect on cell cycle progression. In order to establish this, the DNA content was measured over a 24 hour period.

Fluorescence Activated Cell Sorting Technology (FACS) was used to study the effects of the test compounds on DNA content in BSF *T. b. b. s427* WT. Cell density was adjusted to 1×10^7 cells/mL with and without test compounds for the duration of the experiment. 1 mL of sample was transferred at each time point into microfuge tubes and centrifuged at $1620 \times g$ for 10 min at 4 °C, washed once in PBS containing 5 mM EDTA and re-suspended, then fixed in 1 mL of 70% methanol and 30% PBS/EDTA. The tube with the cells was left at 4 °C overnight in the dark, and the samples were subsequently washed once with 1 mL PBS/EDTA, re-suspended in 1 mL PBS/EDTA containing 10 µg/mL propidium iodide and incubated at 37 °C for 45 minutes. RNase A (10 µg/mL) was added before the samples were analysed by a Becton Dickinson FACSCalibur using the FL2-Area detector and CellQuest software. The data obtained were analysed using flowJo software (Flowjo LLC, Ashland, OR, USA).

Figure 6.8 shows that TAO25 did not inhibit progress through the cell cycle, as 0.005 µM of TAO25 had no effect on the percentage of cells in G1, S or G2 phase after as much as 24 h, while the lipophilic bisphosphonium compounds CD38 and AHI-9 earlier reported in literature significantly reduced the percentage of S-phase cells after 8 and 12 h of incubation, respectively (Alkhaldi *et al.*, 2016).

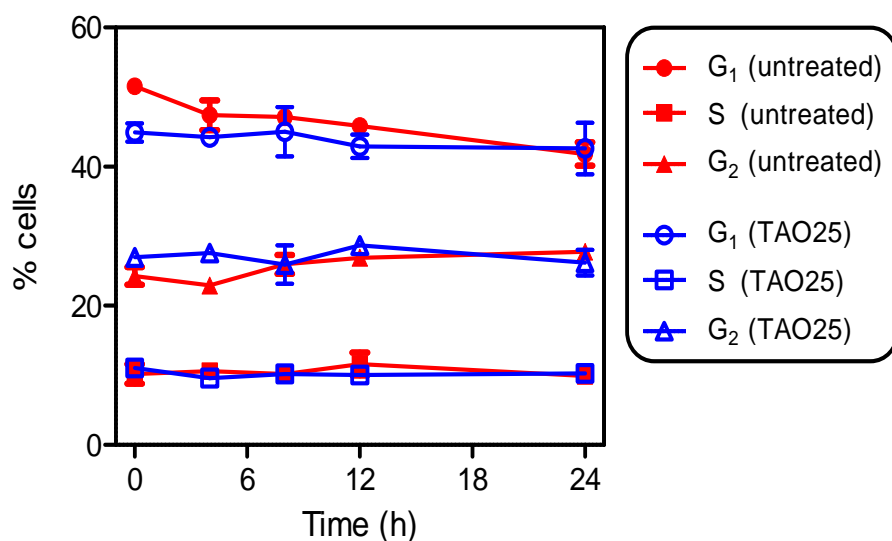


Figure 6.8 Percentage of cells at various cell division stages in populations treated or not treated with 0.005 μ M of TAO25 over a 24 hour period. The percentages are the average of three independent determinations and SEM, obtained using flow cytometry after cell permeabilization and staining with propidium iodide.

It is however possible that a higher concentration of the inhibitor would impact on the cell cycle or a longer incubation time would have changed the dynamics of the action of the compound tested on the cell cycle. Though this was not further tested and there is no report in the literature to support this, nevertheless, this observation which is the first of its kind as far as TAO inhibition is concerned, might be correct.

6.3 Discussion

Our preliminary study of the MOA of these compounds showed that, contrary to the report that bisphosphonium salt derivatives inhibit the mitochondrial F_0F_1 ATPase (Alkhaldi *et al.*, 2016), these compounds, although also lipophilic cations, do not appear to inhibit progression through the cell cycle. Since the compounds described here were designed as potential mitochondrion-targeted molecules, we studied their effect on parasite respiration and investigated whether TAO might be involved in the observed antitrypanosomal activity.

It has been previously reported that glycerol, whether generated endogenously or added exogenously, is capable of inhibiting the anaerobic glycolysis sufficiently to result in *in vitro* or *in vivo* cell death of BSF *T. brucei*. In some reports, the concomitant administration of SHAM and

glycerol to rats infected with *T. b. b* resulted in a rapid clearance of parasitaemia in rats (Clarkson and Brohn, 1976; Brohn and Clarkson, 1978; Yabu *et al.*, 1998).

Glycerol is known to inhibit anaerobic glycolysis and ATP generation that takes place in the glycosome of the BSF *T. brucei* by mass action. More recently, glycerol was reported to potentiate ascofuranone by together completely blocking the parasite's energy production, therefore inhibited the *in vitro* growth of the trypanosome (Yabu *et al.*, 1999). However, the combination of ascofuranone and the large volume of glycerol required to cure sleeping sickness is pharmacologically impracticable.

The effects of our test compounds in combination with glycerol on the *in vitro* cell growth were also examined in this work, and it was clear that glycerol did potentiate the trypanocidal activity of our test compounds (Table 6.1). Earlier *in vitro* reports also revealed that inhibitors of TAO are trypanocidal when combined with the mass action of glycerol, which suppresses a glycerol-producing pathway (Hammond *et al.*, 1985; Kiara and Njogu, 1989). This is because this combination would simultaneously inhibit both the anaerobic glycolytic pathway and the aerobic respiration, thus leading to a total inhibition of energy production (ATP) by the trypanosomes. The anaerobic respiratory pathway is mediated by the reverse action of glycerol kinase. In fact, the trypanosome glycerol kinase under physiologic condition does not play a crucial role in the trypanosome's metabolism, and is therefore regarded as a sub-optimal drug target for trypanosomiasis, but it becomes essential when TAO is disabled (Verlinde *et al.*, 2001). However, we observed that some of our test compounds had a strong inhibitory effect on the *in vitro* growth of trypanosomes, in the lower nanomolar range, even without glycerol.

The combination of 5 mM glycerol with TAO inhibitors such as SHAM and our synthesized TAO inhibitors also increased the trypanocidal activity in most cases. SHAM is a well known iron chelator that binds iron in the di-iron centre of the TAO active site and acts as an inhibitor of this metallo enzyme (Grady *et al.*, 1993; Yabu *et al.*, 1999). However our compound was designed to specifically bind to TAO and avoid iron containing molecules in the biological system. It therefore follows that our test compounds block aerobic respiration via TAO inhibition while glycerol potentiated the trypanocidal activities of our test compounds by blocking the anaerobic respiration via a blockade of the reverse action of glycerol kinase. Indeed, most of the TAO inhibitors tested herein and the control, SHAM, were significantly more active against *T. brucei*

when co-administered with glycerol *in vitro*, indicating that the aerobic energy metabolic pathway may be a target of these compounds.

Following the interesting result obtained from the co-administration of our compounds with glycerol *in vitro*, we decided to further test them on trypanosomes lacking the ability to export glycerol out of their cell (Aquaporin knockout cells). We reported some relatively small but significant differences using a cell line from which both AQP2 and AQP3 were knocked out – several compounds were significantly more effective against that cell line. Knockout of all aquaporins (*aqp1-3* null) made the cells clearly even more susceptible to the TAO inhibitors: more compounds displayed a significantly lower EC₅₀ value, and by a larger margin. The explanation for the effect of the AQP knockout lines is that inhibition of TAO causes a shift in metabolism from TAO-mediated aerobic respiration to anaerobic respiration via the reverse action of glycerol kinase, thereby producing glycerol in large quantities. We speculated that trypomastigotes of *T. brucei* without aquaglyceroporins would not be able to efficiently dispose of that glycerol, and our observations are consistent with that hypothesis.

The observation that our test compounds (TAO inhibitors) are more active against the aquaporin knockout trypanosomes is a positive development for an anti-trypanosomal strategy, as pentamidine and melarsoprol resistance in field isolates has been attributed to the loss of TbAQP2 function (Graf *et al.*, 2013). Wild-type AQP2 was reported to be absent in field isolates of *T. b. gambiense*, correlating with the poor outcome of melarsoprol treatment, but expression of a wild-type copy of *TbAQP2* gene in the most resistant strain completely reversed melarsoprol resistance and re-introduced the High Affinity Pentamidine Transporter (HAPT1) function and transport kinetics (Munday *et al.*, 2015), demonstrating the importance of the aquaporins in the transport, effectiveness and resistance of key trypanocides such as pentamidine and melarsoprol. Therefore any drug that can specifically target this resistant strain will be a solution to the problem of drug resistance in trypanosomiasis caused by *T. brucei*. However, we did not test the effect of deleting only TbAQP2 on the effectiveness of TAO inhibitors, and expect that the impact of this will be limited, given the continued expression of TbAQP1 and TbAQP3.

As TAO is essential for the respiration of bloodstream form trypanosomes we investigated whether some of the compounds were actually inhibitors of TAO mediated respiration. Several of the inhibitors were tested for effects on oxygen consumption using a fluorescent oxygen reporter

probe (kit); the compounds tested did inhibit oxygen consumption in a similar way as SHAM, and lower concentrations gave similar effects on the AQP knockout line. A dose-response with a few of the test compounds was also achieved, showing that indeed the reduced oxygen consumption is most likely the result of the effect of the test compounds on oxygen consumption, and the fact that the compounds did not affect oxygen consumption in mammalian cells clearly points to the major difference between BSF trypanosomes respiration and mammalian cell respiration. This difference is the presence of TAO in trypanosomes and its role as the sole terminal oxidase, and the absence of TAO in mammalian cells. Considering that TAO catalyses the reaction using oxygen in trypanosomes, inhibiting it therefore stood out, exactly as observed in the oxygen consumption assay.

From our data, we can conclude at this point that the excellent anti-trypanosomal activity displayed by our compounds, as reported in chapter 5, is indeed via TAO inhibition. However, a direct inhibitory study with purified recombinant TAO (rTAO) and a study of its kinetics in the presence of the inhibitors would be necessary to confirm these findings. This work will be presented in Chapter 7.

**Chapter 7: Direct inhibition studies with purified recombinant
TAO lacking a mitochondria targeting signal.**

7.1 Introduction

Alternative oxidases (AOXs), which are found across a broad range of organisms, including plants, nematodes, algae, yeast and certain disease-causing microorganisms including *Trypanosoma brucei*, are mitochondrial, cyanide-insensitive membrane-bound proteins that catalyse the oxidation of ubiquinol and the four-electron reduction of oxygen to water (Young *et al.*, 2013). In *T. brucei*, a parasite that causes African trypanosomiasis in humans (sleeping sickness) and livestock (nagana) throughout sub-Saharan Africa, the trypanosome alternative oxidase (TAO) is unique and essential for the respiration of bloodstream form (BSF) parasites. In effect, in BSF trypanosomes, TAO is the sole terminal oxidase enzyme, and required to ultimately re-oxidize the NADH that is produced during glycolysis. As TAO has no counterpart in mammals and it is conserved among *T. brucei* subspecies (Yabu *et al.*, 2010), it has been validated as a promising target for the chemotherapy of African trypanosomiasis (Yabu *et al.*, 2003; Yabu *et al.*, 2006; Menzies *et al.*, 2016).

TAO is a cyanide-resistant and cytochrome-independent ubiquinol oxidase, formerly known as glycerol-3-phosphate oxidase, which is sensitive to the specific inhibitors salicylhydroxamic acid (SHAM) and ascofuranone (AF) (Grant and Sargent, 1960; Evans and Brown, 1973; Clarkson *et al.*, 1989; Minagawa *et al.*, 1997). The AOX gene in trypanosomes contains 990 nucleotides encoding the 330 amino acids full length protein, including the N-terminal 25 amino acid residue “Mitochondrial Targeting Signal” (MTS) (Appendix G). As the MTS is usually cleaved after transportation of the protein to the mitochondrion, the physiologically functional and relevant form of TAO is lacking the MTS sequence (Hamilton *et al.*, 2014). However, only the full length protein has been overexpressed and studied (Shiba *et al.*, 2012; Kido *et al.*, 2010) so far, in spite of the difficulties associated with its reduced stability, poor solubility and low yield.

Because the full length TAO is not physiologically active in trypanosomes, it is imperative to target the physiological form of TAO and carry out direct inhibitory studies with potential inhibitors. It was hypothesized that rTAO without the MTS (Δ MTS rTAO) would be more active, and more soluble, resulting in higher yield, and that this could also increase the stability and resolution of the protein. In addition, it was proposed that performing direct inhibitory studies of the Δ MTS rTAO with potential TAO inhibitors would give a clearer evidence for their *in vivo*

inhibition and kinetics than when using the full length protein, and that this could result in the discovery of more potent inhibitors that specifically targets the physiological form of TAO.

In addition, it was reported in chapter 5 that the newly designed mitochondrion-targeted LC-TAO inhibitors significantly improved the activity of 2,4-dihydroxybenzoate and salicylhydroxamate (SHAM) against *T. brucei* and *T. congolense* strains in the lower micromolar to nanomolar range, and in chapter 6 that the mechanism of their antiparasite activities suggested inhibition of the parasites' respiration, most likely via inhibition of TAO. Consequently in this chapter a direct inhibitory study has been carried out on Δ MTS rTAO to confirm whether this promising anti-trypanosome activity is via TAO inhibition. We have used the computer program mitoprot (<http://www.expasy.org/tools/>) to predict the MTS to be 23 to 25 amino acids long and decided to try to produce pure TAO without the N-terminal 25 amino acids (Δ MTS rTAO).

Hence, in the present study, we report for the first time the production of a more active physiologic rTAO enzyme lacking the MTS sequence (Δ MTS rTAO). We also report the novel use of a SUMO expression system (Appendix G) to optimise the production of rTAO. This Δ MTS rTAO enzyme was used to study the activity of our new TAO inhibitors based on the 4-hydroxybenzoate and 4-alkoxy benzaldehyde scaffolds (Figure 7.1). The results of rTAO inhibition and trypanocidal activity against several wild type and drug-resistant strains of trypanosomes will allow the production of structure-activity relationships (SAR) with these potent TAO inhibitors.

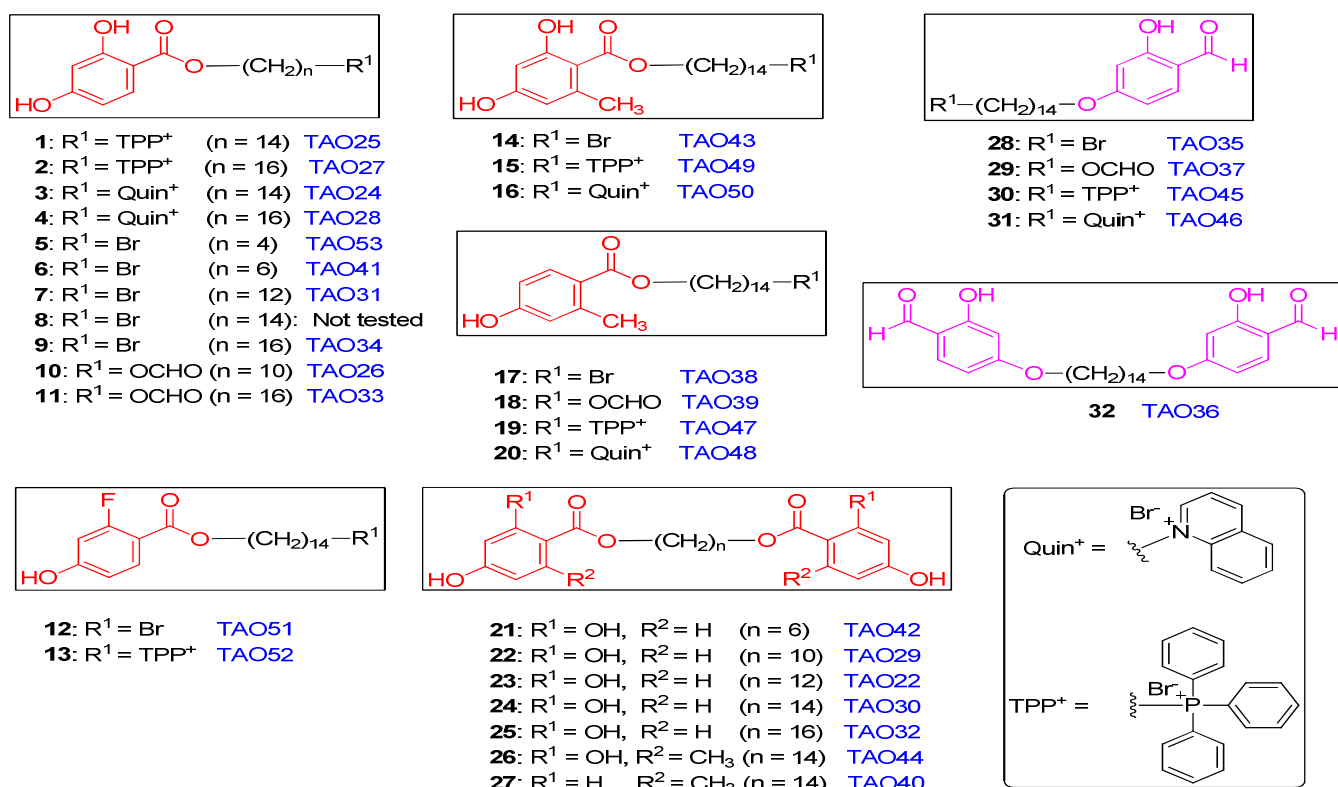


Figure 7.1 Summarized structures of the TAO inhibitors. Detailed full list of structures can be found in appendix C.

7.2 Results

7.2.1 Complementation by rTAO of FN102 *E.coli* lacking a terminal oxidase

Haem is a cofactor of enzymes such as peroxidases, catalases, sensor molecules, and cytochromes of the P450 class. Four terminal oxidases including the quinol oxidases: cytochrome bo, and cytochrome bd have previously been identified in *E.coli* cell membranes (Shiba *et al.*, 2012; Kido *et al.*, 2010). These four proteins catalyze similar reactions to TAO, which makes it difficult to measure the activity of TAO in *E.coli* that is engineered to express TAO. Haem is critical for the synthesis of all *E.coli*'s quinol oxidases but is not required for TAO activity. The synthesis of the first committed compound, 5-Aminolevulinic acid (ALA), is known to take place via two separate routes (Nihei *et al.*, 2003; Shiba *et al.*, 2012). The first is condensation of glycine and succinyl-CoA (C-4 pathway), which occurs in fungi, and animals. The second is the conversion of glutamate to ALA (C-5 pathway), occurs in Archaea, plants, and most bacteria. *E.coli* is an

organism which synthesises ALA, being the first committed compound in haem biosynthesis, from glutamate (C-5 pathway) (Kido *et al.*, 2010).

Therefore, to remove all quinol oxidase activity of the haem-containing cytochrome complexes completely from the host *E.coli* strain, a haem-deficient *E.coli* strain FN102 was used for the overproduction of TAO. This *E. coli* strain was previously described by Nihei *et al.* (2003) and Elliott *et al.* (2014), and involved the introduction of the $\Delta\text{hemA}::\text{Km}^R$ mutation into strain BL21(DE3) by P1 transduction. Because the hemA-deficient mutant lacks the enzyme glutamyl-tRNA reductase which is needed to catalyze the first committed step of haem biosynthesis in *E.coli*, the mutant would not grow aerobically without ALA, which is a precursor for protohaem IX biosynthesis (but does grow anaerobically). Nevertheless, the FN102 haem-deficient *E.coli* strain that was transformed with a pETSUMO plasmid vector (Figure 7.2) containing the ΔMTS rTAO sequence showed similar aerobic growth comparable to the wild-type even without ALA (Figure 7.3, panels C and D).



Figure 7.2 Plasmid map showing the point of insertion of fl or ΔMTS -TAO in pETSUMO expression vector via the T – A cloning.

The pET SUMO expression system (ThermoFisher Scientific) was used in this experiment with the aim of producing highly soluble protein in haem-deficient *E. coli*. It utilizes fusion with a small ubiquitin-related modifier (SUMO), which belongs to the growing family of ubiquitin-related proteins, to enhance the solubility of expressed fusion proteins. In contrast to ubiquitin,

SUMO is involved in the stabilization and localization of proteins *in vivo*. After expression, the 11 kD SUMO moiety was cleaved by the ULP-1 (Ubiquitin-like-specific protease 1) protease at the carboxyl terminal, producing the native TAO protein. The TA cloning - a subcloning technique which does not require the use of restriction enzymes - was used following the manufacturer's instructions and it was easier and quicker than traditional subcloning. The technique depends on the ability of adenine (A) and thymine (T) on different DNA fragments to hybridize and become ligated together in the presence of a ligase (the T4 ligase was used in this experiment). PCR products were amplified using Taq DNA polymerase which favourably adds an adenine to the 3' end of the PCR product. The PCR-amplified insert was then cloned into pETSUMO, which is a linearized vector having a complementary 3' thymine (T) overhang.

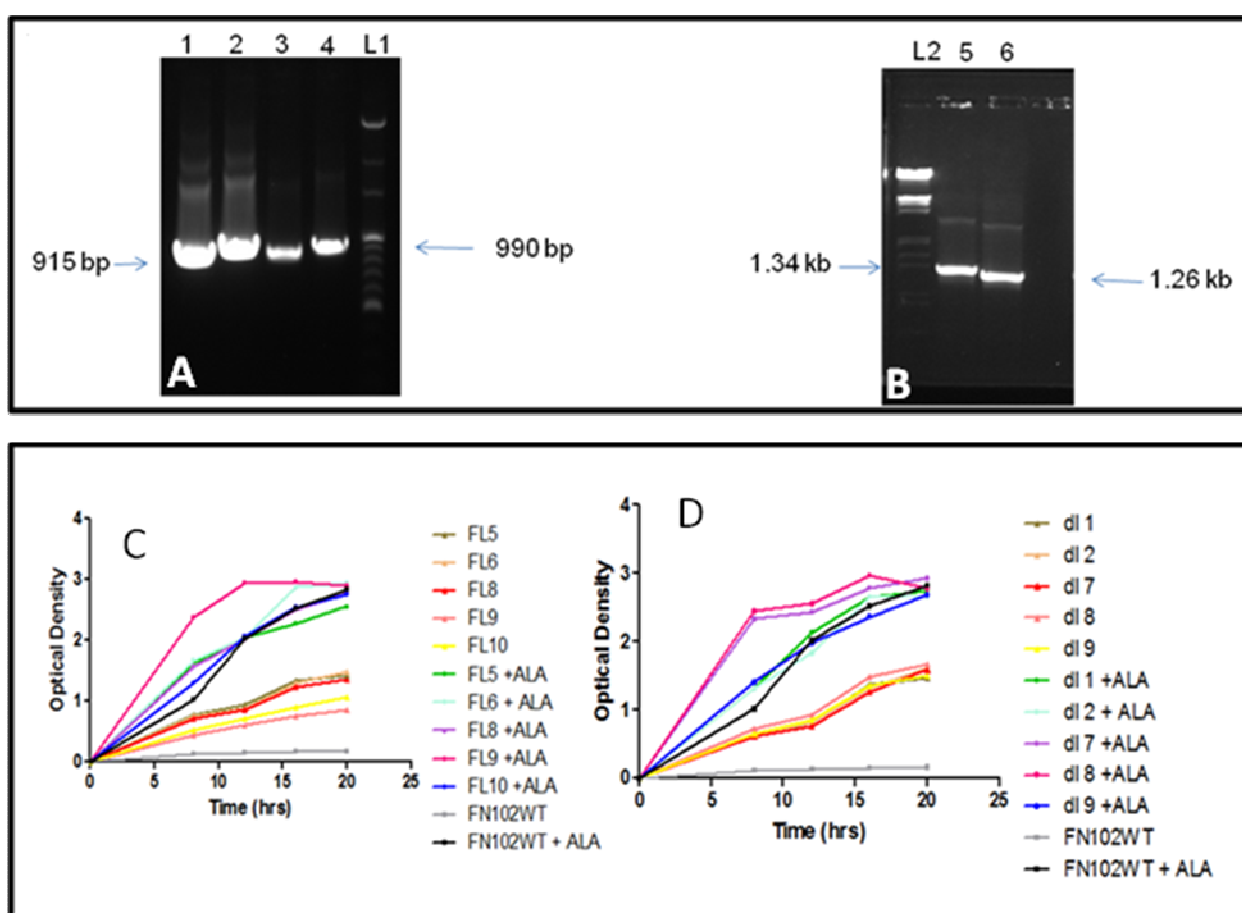


Figure 7.3 Comparative studies of the complementation of haem deficient FN102 *E. coli* by full-length (fl) and Δ MTS-TAO. Panel A shows the PCR confirmation of Δ MTS-rTAO (lanes 1 and 3 = 915 bp), and fl-rTAO (lanes 2 and 4 = 990 bp), while panel B is the PCR confirmation of these TAO genes in the plasmid (pET101) vector; NHis₆SUMO- Δ MTS-TAO (lane 6 = 1.26 kb), and NHis₆SUMO-fl-TAO (lane 5 = 1.34 kb). L1= BRG-100-02 DNA ladder; L2 = M2 DNA ladder (BIO-RAD)

Panel C is a growth curve of selected clones of haem deficient FN102 *E. coli* with the fl-rTAO gene; while panel D is for clones having the Δ MTS-rTAO. Wild type (haem deficient) FN102 *E. coli* were simultaneously grown in plus or minus 50 μ g/ml ALA media and were used as controls.

As expected, the result showed that terminal oxidase activity of the haem deficient FN102 *E. coli* was restored in all native FN102 colonies having the NHis₆SUMO-pET 101 plasmid with the TAO insert. There was no visible aerobic growth in the native FN102 (FN102 WT) in the absence of ALA or NHis₆SUMO-pET 101 with TAO insert (Figure 7.3).

It was also observed that cultures of colonies having the TAO insert plasmid plus 50 μ g/ml ALA displayed a better growth pattern than those having the TAO insert plasmid but without ALA and also better than the native FN102 cultures with 50 μ g/ml ALA. This observation could be due to TAO restoring the terminal oxidase activities in the native FN102 cells but in addition boost the terminal oxidase activities in native FN102 when the normal haem synthesis pathway was restored in the presence of ALA (see figure 7.3).

However, there were no significant observable difference in the growth pattern of the FN102 *E. coli* having the first 75 nucleotide sequence of TAO open reading frame deleted when compared with the clones having the full length TAO (fl rTAO) gene, showing that Δ MTS-TAO is fully active as terminal oxidase. This is consistent with the fact that the MTS is cleaved off upon transportation to the mitochondria in trypanosomes. This is to our knowledge the first direct evidence that the trypanosome alternative oxidase 75 nucleotide Mitochondrial targeting signal is not essential for TAO activity.

Hence, this result showed recombinant TAO functioned as a terminal oxidase in the respiratory chain of the haem deficient FN102 *E. coli* complementing the function of the deleted quinol oxidases.

7.2.2 SDS-PAGE analysis of purified rTAO at various stages of purification and purification table for Δ MTS-TAO/fl-TAO.

SDS-PAGE analysis of rTAO from various stages of purification was carried out. FN102 lysate, membrane fraction, flow-through, and peak fractions from TALON column were subjected to a discontinuous SDS-PAGE using Bio-rad protein size marker alongside (Figure 7.4). As expected, a band corresponding to 48 kD which is the correct size for full length TAO (NHis₆SUMO-fl-TAO) was observed in lanes 9 and 10 (duplicate). Upon cleavage of the NHis₆SUMO (11 kD) with the highly efficient SUMO (ULP-1) protease produces the native TAO protein of interest with a band corresponding to 37 kD seen in lanes 12 and 13 (Figure 7.4), which is the exact size of full length TAO (TAO having MTS). On panel 'A', Lane 4 shows a band corresponding to 45 kD, which is the size of NHis₆SUMO- Δ MTS-TAO. But upon cleavage of the NHis₆SUMO (11 kD) with SUMO (ULP-1) protease, a band equal to approximately 34 kD was observed in lanes 6 and 7 (duplicate). This is the size of TAO without MTS.

Overall, a physiologically active TAO without the Mitochondrial Targeting Signal was successfully purified.

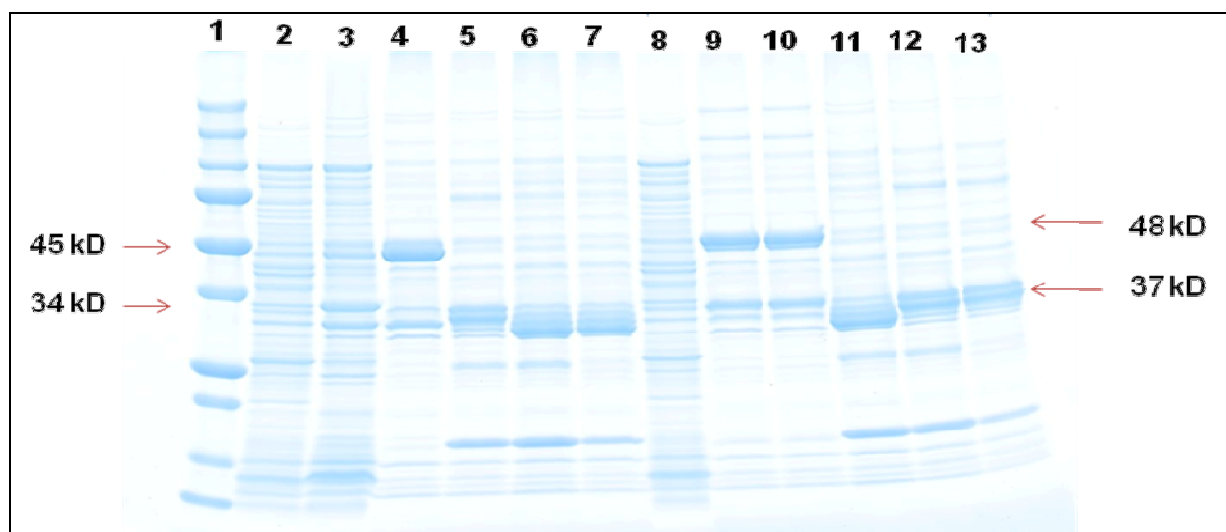


Figure 7.4 SDS-PAGE for the various purification steps involved in the purification of rTAO from FN102 *E. coli* mitochondria membrane. Purification process of Δ MTS-TAO and full length (fl) TAO. Lane: 1 = Marker protein (Bio-rad). 2 = Lysed FN102/ NHis₆SUMO- Δ MTS-TAO cells. 3 = membrane fraction. 4 = NHis₆SUMO- Δ MTS-TAO. 6, 7, and 11 = Δ MTS-TAO (NHis₆SUMO is cleaved). 8 = Lysed FN102/NHis₆SUMO-fl-TAO cells. 10 = NHis₆SUMO-fl-TAO. 5, 12, and 13 = fl-TAO (NHis₆SUMO is cleaved)

Purified Δ MTS-TAO obtained from the column was clear while that of the fl-TAO was slightly turbid; this may be because the MTS is known to be slightly hydrophobic (Shiba *et al.*, 2013). In addition, although the two forms of purified TAO were very active, the purified Δ MTS-TAO was more active than fl-TAO, and was found to be higher in total and specific activity, and yield (Table 7.1).

Also, the purified Δ MTS-TAO exhibited a better specific activity, activity recovery, and fold of purification (392.24 μ mol/min/mg, 1.27%, and 7.91 respectively) than the fl-TAO (195.74 μ mol/min/mg, 0.33, and 7.91 respectively) (Table 7.1).

Table 7.1 Purification and activity table for rTAO

Purification step.		Total activity (μ mol /min)	Total protein (mg)	Specific activity (μ mol/min/mg)	Activity recovery (%)	Purification (x fold)
Lysate	Δ MTS TAO	142409	3690	38.59	100.00	1.00
	Fl TAO	60900	2460	24.76	100.00	1.00
Membrane	Δ MTS TAO	18492	310	59.65	12.99	1.55
	Fl TAO	7600.04	179.80	42.27	12.48	1.71
Co – column	Δ MTS TAO	2211.20	8.60	257.09	1.55	6.66
	Fl TAO	335.01	2.20	152.27	0.55	6.15
Cleaved	Δ MTS TAO	1802.11	4.60	392.24	1.27	10.16
	Fl TAO	203.02	1.0368	195.79	0.33	7.91

7.2.3 Direct inhibitory studies with Δ MTS TAO: SAR studies with cationic and non-cationic inhibitors.

The TAO inhibitors were tested for their direct inhibitory effect on physiological TAO (i.e. Δ MTS). These compounds were specifically made to fit into the TAO binding pocket and prevent the binding of Ubiquinol-1, which is the physiological substrate of TAO. The samples were dissolved in DMSO to make a stock solution of 10 mM, which was stored at -20 °C and used for the assay. Ascofuranone and salicylhydroxamic acid (SHAM), two known TAO inhibitors were

used as positive controls in the assay while an equal volume of DMSO was used as negative control. The DMSO had no effect on TAO activity (result not shown). Control experiments were also carried out. In one of the control experiments, auto-oxidation of Ubiquinol-1 was carried out using the same protocol but without TAO. This was to check the quality of Ubiquinol-1, which can be re-oxidized to Ubiquinone in the presence of molecular oxygen. No auto-oxidation was observed. In another control experiment, the quality of the purified rTAO was tested in the presence of 1 mM ascofuranone which completely inhibited the conversion of Ubiquinol-1 to Ubiquinone-1. This result (not shown) indicates that no other oxidase was purified together with TAO.

We are aware that some of these compounds, because of their chemical structures, may complex with the di-iron in the catalytic site of TAO thereby chelating it and rendering it ineffective, creating the possibility that these compounds also non-specifically bind with other haem-containing proteins (*in vivo*) in mammalian cells, or indeed form complexes with metals in solution. It was because of this possibility that we decided to conduct a control assay where we pre-incubate 1 mM iron (II) chloride (FeCl_2) and 250 nM purified rTAO for 2 minutes before using it for the TAO inhibition assay. This result was compared with that of TAO without incubation with FeCl_2 under the same assay condition. There was no difference in TAO activity with or without FeCl_2 . This observation rules out the possibility for the assumption that the mechanism of inhibition might be via chelating of the di-iron in TAO catalytic site.

Table 7.2 EC₅₀ values (μM) against *T. b. brucei* WT and IC₅₀ values of inhibition of rTAO (μM)

Compound	EC ₅₀ (μM) <i>T. b. brucei</i> ^a	IC ₅₀ (μM) rTAO ^b
TAO18	>100	1.9 ± 0.015 ^c
TAO22	32.94 ± 0.88	0.007 ± 0.00011
TAO24	0.1 ± 0.012	1.36 ± 0.064
TAO25	0.0015 ± 0.0002	1.46 ± 0.008
TAO26	31.82 ± 0.93	0.15 ± 0.0051
TAO29	49.04 ± 7.79	0.0069 ± 0.00012
TAO30	42.12 ± 2.85	0.0157 ± 0.0013
TAO31	14.54 ± 0.97	0.0174 ± 0.0018
TAO32	26.71 ± 5.52	0.0123 ± 0.0041
TAO33	11.88 ± 1.6	0.0144 ± 0.012
TAO34	45.68 ± 1.52	0.0124 ± 0.003
TAO35	17.59 ± 0.55	0.0728 ± 0.011
TAO36	>200	0.2403 ± 0.020
TAO37	3.77 ± 0.12	0.327 ± 0.23
TAO38	14.4 ± 0.07	0.0072 ± 0.003
TAO39	4.06 ± 0.09	0.0011 ± 0.0002
TAO40	>200	0.0125 ± 0.0028
TAO41	17.7 ± 0.48	0.241 ± 0.023
TAO42	>200	0.0565 ± 0.010
TAO43	14.58 ± 0.22	0.0065 ± 0.001
TAO44	>200	0.011 ± 0.011
TAO45	0.13 ± 0.003	0.221 ± 0.012
TAO46	1.75 ± 0.01	1.23 ± 0.018
TAO47	0.0024 ± 7.97E-04	0.081 ± 0.009
TAO48	0.21 ± 0.02	0.0295 ± 0.029
TAO49	0.0016 ± 4.70E-04	0.0883 ± 0.013
TAO50	0.03 ± 0.001	0.1043 ± 0.011
TAO51	14.72 ± 0.14	0.0295 ± 0.003
TAO52	0.001 ± 1.20E-05	0.0303 ± 0.003
TAO53	>200	0.45 ± 0.008
ASF ^d	ND	0.002 ± 0.004
SHAM ^e	38.73 ± 4.78	5.93 ± 0.13

^aTrypomastigotes of *T. b. brucei* (n = 3). ^bPurified recombinant trypanosome alternative oxidase (n = 4).

^cStandard Error of Mean (SEM). ^dAscofuranone, and ^eSalicylhydroxamic acid were used as controls for TAO inhibition. Only the compounds showing some level of activity (<5 μM) against rTAO are shown in this table.

Most of the compounds tested against rTAO (25 out of 30) displayed submicromolar inhibition (Table 7.2). Among these, one compound (TAO39) was twice as potent as the reference drug ascofuranone ($IC_{50} = 2$ nM), four inhibited TAO with $IC_{50} < 10$ nM (TAO- 22, 29, 38 and 43), and thirteen displayed 2-digit nanomolar IC_{50} values (Table 7.2). The 2,4-dihydroxybenzoates inhibited TAO in the low nanomolar (non-cationic derivatives: TAO- 26, 31, 33, 34, 41, and 53) to low micromolar range (cationic compounds: TAO- 24, 25, 27, 28) (Table 7.2).

With the non-cationic derivatives, a correlation between inhibitory activity and methylene linker length was observed, the longest linkers giving the best, low nanomolar, inhibitors ($C16 > C12 >> C10 > C6 > C4$). For the C16 linker, little difference in activity was observed when changing the R^1 group from a bromine (TAO34) to a formiate group (TAO33). However, the introduction of a lipocation such as TPP (TAO27) or quinolinium (TAO28) in this position was highly detrimental to TAO inhibition (>500 -fold decrease in potency). As regards to cationic inhibitors, a linker with 14 methylene units was preferred (compare TAO -25/27 and TAO- 24/28). Hence, this linker was chosen to design the rest of inhibitors for the SAR studies.

The effect on TAO inhibition of the modification of the phenyl ring substituents R^2 and R^3 is shown in Table 7.2. The introduction of a methyl group in R^3 was favourable as shown by the 16- and 13-fold increase in inhibition of TAO49 and TAO50 compared to TAO25 and TAO24, respectively. In fact, the presence of a methyl group alone in R^3 (i.e. without OH group in R^2) was sufficient to get nanomolar range inhibitors (TAO- 38, 39, 47 and 48) of similar potencies (compare TAO- 43/38, 49/47, 50/48) indicating that the 2-OH group is not essential for binding to TAO. Replacement of the methyl group in R^3 by a fluorine atom was favourable for the cationic TPP derivative (TAO52 is 2.7-fold more potent than TAO47) whereas it was unfavourable for the non-cationic bromo analogue (TAO51 is 4-fold less potent than TAO38).

The 4-formyl-3-hydroxyphenoxy-based inhibitors TAO- 35, 37, 45 and 46 were somewhat less potent than the 4-hydroxybenzoate derivatives (compare TAO35 with TAO51/43/38, 37 vs 39, and 45 vs 25/52/49/47) with the following order of inhibitory potency: $R^1 = Br > ^+PPh_3 > OCHO >> \text{quinolinium}$. Interestingly, the cationic TPP analogue TAO45 was 5-fold more potent than the quinolinium counterpart TAO46.

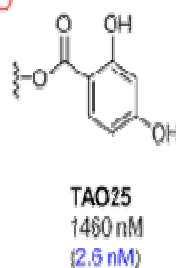
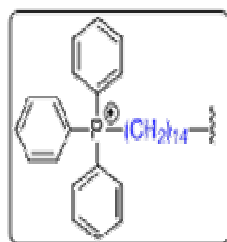
The 4-hydroxybenzoate dimers (TAO- 22, 29, 30, 32, 40, and 44) inhibited TAO in the low nanomolar range (11–15.7 nM) whereas the 4-formyl-3-hydroxyphenoxy-based dimer TAO36

was approximately 21-times less potent inhibitor ($IC_{50} = 240$ nM) (Table 7.2). For the dimer series, a linker of 10 to 12 methylene units seemed to be favoured (compare TAO- 29/22 vs TAO- 30/32) whereas the nature of R^1 and R^2 was less influential (compare TAO30 with TAO- 44/40). Importantly, for the 2-fluoro-4-hydroxybenzoate (TAO52), 2,4-dihydroxy-6-methylbenzoate (TAO- 49 and 50), and 4-hydroxy-2-methylbenzoate (TAO- 47 and 48) series, the addition of a mitochondrion-targeting lipocation in R^1 hardly affected their inhibitory potency against TAO showing that the lipocation does not participate in the interaction with the binding pocket (or, at the very least, does not interfere with binding to TAO).

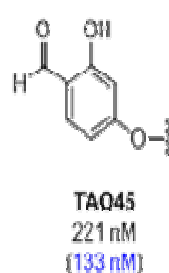
A comparative summary of the structure activity relationship with respect to these compounds' activities against *T. brucei* and rTAO is given in figure 7.5 (Panel A). Unfortunately panel B of figure 7.5 gave a negative correlation between the *in vitro* trypanocidal activity and inhibition of rTAO, partly because optimisation for mitochondrial targeting does not necessarily run parallel with optimisation of protein binding

A

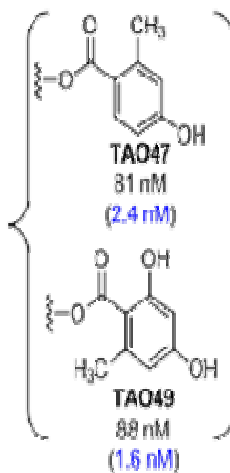
Inhibition of rTAO (EC₅₀ against *T. brucei* WT)



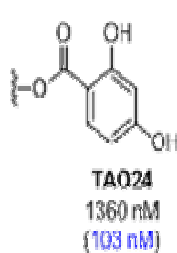
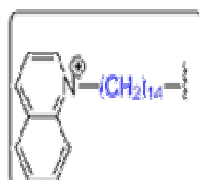
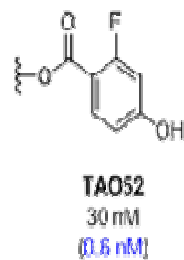
<



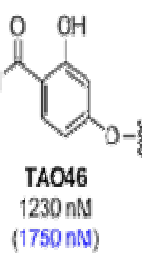
<



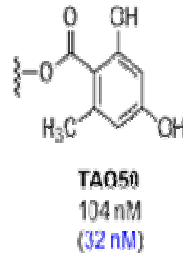
<



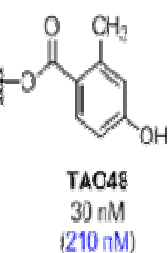
<



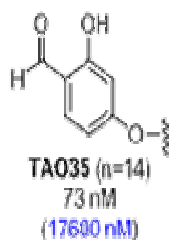
<<



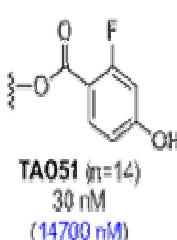
<



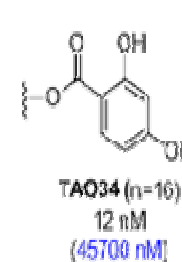
Br-(CH₂)_n-



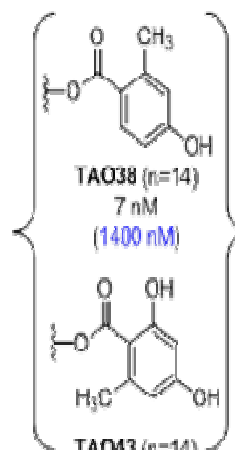
<



<



<



Influence of methylene chain length: **TAO53** (n=4) < **TAO41** (n=6) < **TAO31** (n=12) < **TAO34** (n=16)

450 nM < 240 nM < 17 nM < 12 nM

(NE, > 400 μM) (17700 nM) (14500 nM) (45700 nM)

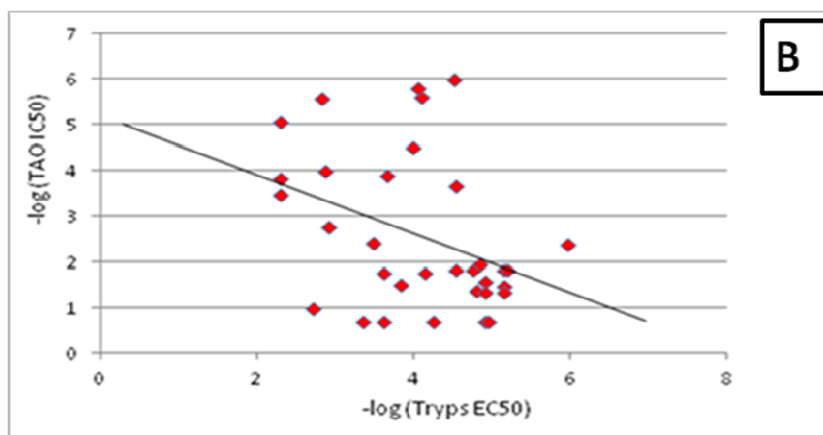
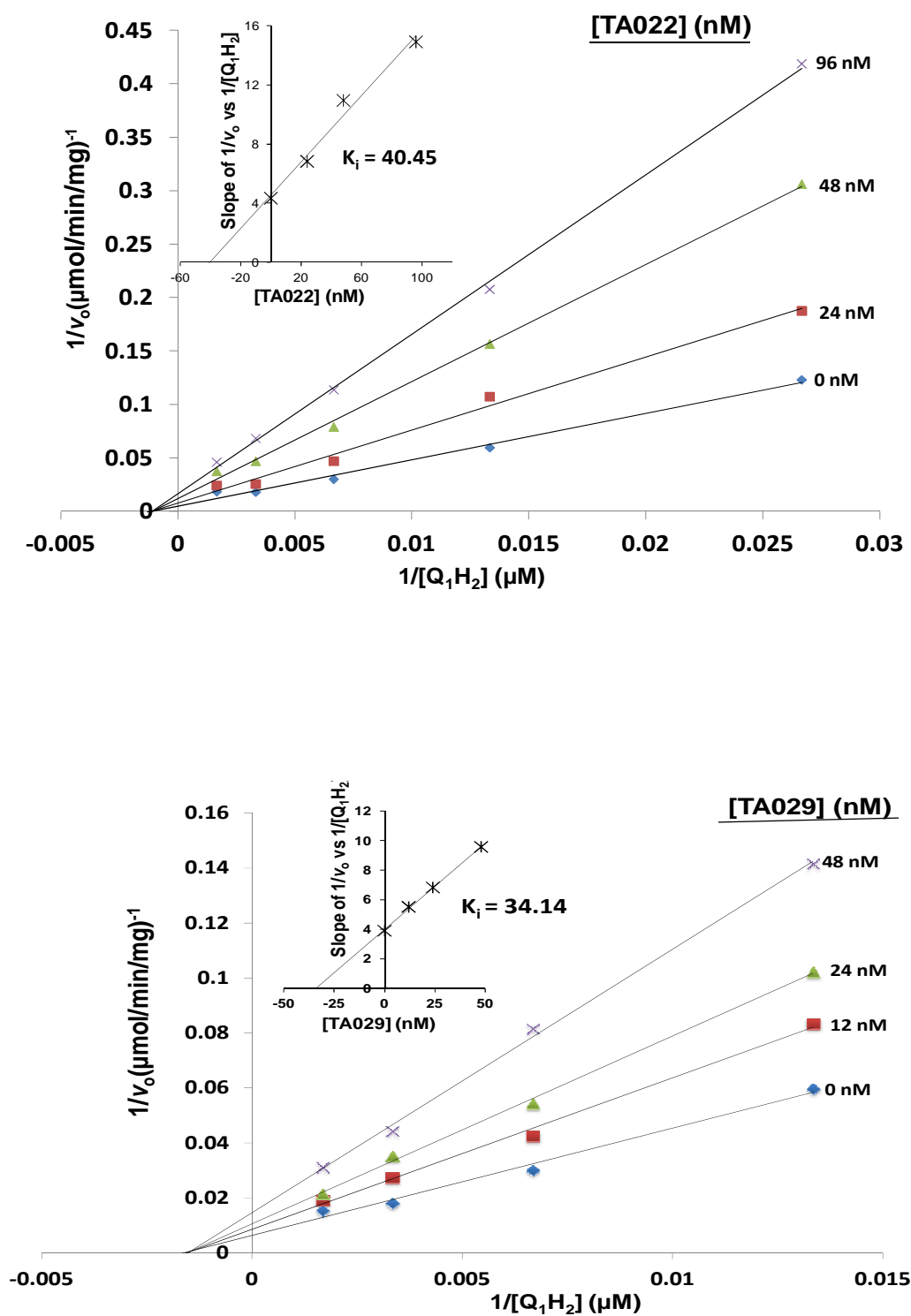


Figure 7.5 Comparative analysis of test compounds on rTAO inhibition. Panel A is a comparative summary of the structure activity relationship with respect to the test compounds' activities against *T. brucei* and rTAO. Panel B is A scattered plot showing negative correlation between IC₅₀ and EC₅₀ of TAO inhibitors, where the log of minimum inhibitory concentration (IC₅₀) for rTAO inhibition [-log (TAO IC₅₀)] was plotted against the effective concentration that brought about 50% of the maximal effect on trypanosomes (EC₅₀) on the -log(Tryps EC₅₀) axis.

7.2.4 Michaelis-Menten kinetics and double reciprocal Lineweaver-Burk plots for TAO inhibitors

Some of the TAO inhibitors were used for TAO kinetics assay. Briefly, 5 μ l of a 50 ng/ μ l of Δ MTS-rTAO prepared in 0.5 M Tris-HCl buffer (pH 7.3) was used, this gave a 250 nM TAO in the 1 ml reaction mix. The inhibitor concentration was varied and 2 μ l of the inhibitor was taken each time. The reaction was in a total reaction volume of 1 ml 0.5 M Tris-HCl buffer (pH 7.3), and in a 1 cm path length cuvette. The contents of the cuvette was well mixed and quickly transferred to the UV- 300 double beam spectrophotometer (Shimadzu, Japan) set at 278 nm wavelength, λ scale (2 cm/min), scan speed 2(5), temperature was 25 °C. The background activity was measured for at least 1 minute before the introduction of Ubiquinol-1 to initiate the reaction. Activity was measure for 2 minutes, and was recorded as units of absorbance per minutes. The data obtained were fitted for the Michaelis Menten plot, which were then transformed to double-reciprocal plots for estimation of kinetic parameters. The reciprocals of the specific activity against that of the Ubiquinol concentration gave the double-reciprocal/Lineweaver-Burk plot. The enzyme inhibition constant K_i was also determined and presented below.

The K_i of TAO- 22, 29, 32, 33 were determined to be 41, 34, 32, and 71 μM , respectively. The Lineweaver–Burk analysis indicated that, similarly to SHAM (Ott et al., 2006), the compounds inhibit TAO non-competitively (Figure 7.6).



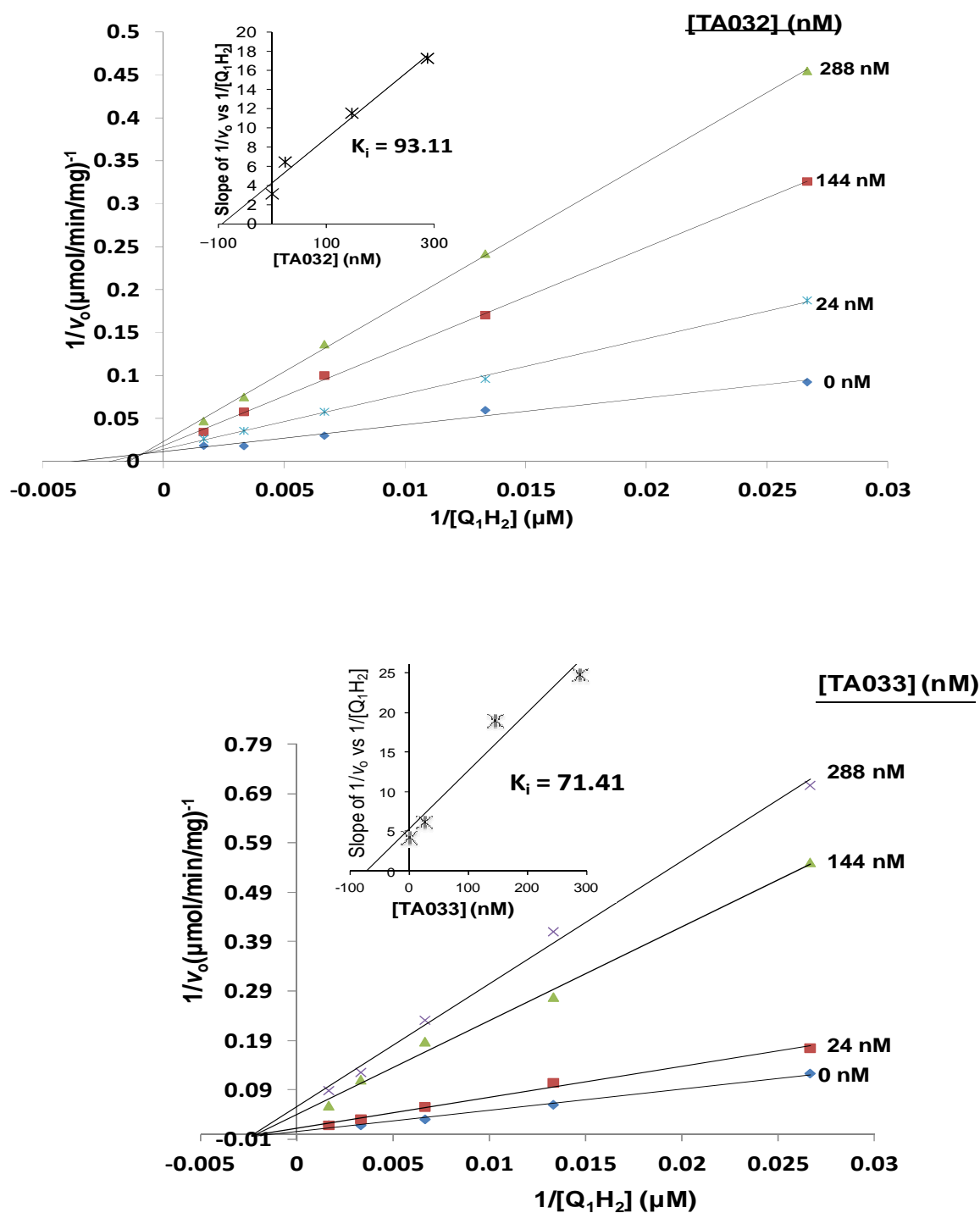


Figure 7.6 TAO kinetic determinations in the presence of varying concentrations of inhibitors and substrate concentration (Q_1H_2) (0 – 600 μM), with 250 ng TAO in a 1 ml (0.5 M Tris-HCl buffer, pH 7.3) reaction mix. The figure shows the Lineweaver-Burk plots (main figures) for the test compounds (TAO- 22, 29, 32 and 33) as well as their corresponding K_i determinations (inset figures). All test compounds revealed a non-competitive (mixed) type inhibition.

While IC_{50} and K_i are both ways of determining an inhibitor's ability to inhibit the action of an enzyme, however they are not the same. The K_i value, is the true equilibrium constant, and is regarded as a better measure, considering that the K_i of an enzyme-inhibitor complex is always a constant. IC_{50} value on the other hand will vary depending on substrate concentration. Consequently, the K_i values were determined and reported in this work (inserts of figure 7. 6). The result showed the IC_{50} values of the compounds tested correlate well with the K_i determinations for each compounds, so that the lower the IC_{50} the lower the K_i . All the inhibitors reported here behaved as a non-competitive inhibitor (mixed type) with respect to Q_1H_2 .

7.2.5 Binding affinity of lipophilic cation–TAO inhibitor to TAO revealed by Surface Plasmon Resonance (Biacore) spectrometry.

It was reported in the previous section that some of the inhibitors tested for their direct inhibitory activities on purified rTAO have a very good inhibition in the nanomolar range; also their affinities for rTAO were determined in terms of inhibition constants (K_i). However the direct inhibitory studies alone are insufficient in highlighting how tightly bound the inhibitors are to the rTAO, *i.e.* the constant of association (K_a), or their ease of dissociation from the rTAO once they are bound to it, *i.e.* constant of dissociation (K_d).

It is more and more acknowledged that the rates at which drugs associate and dissociate from a receptor (the binding kinetics) directly affect drug efficacy and safety (Pan *et al.*, 2013). This would, however, be important for the rational optimisation of kinetics during lead optimization of these inhibitors (Copeland *et al.*, 2006; Lu and Tonge, 2010).

Consequently, surface plasmon resonance (SPR) binding analysis was used to study the molecular interactions that exist between the test compounds and rTAO, following the method described in Drescher *et al.* (2009). SPR is an optical technique used for detecting the interaction between two different molecules where one is mobile and the other one is fixed on a thin gold film (Schuck, 1997). In the work described here, using a single-cycle kinetics method, purified rTAO (10 mg/ml in 10 mM acetate buffer pH 5.5) was immobilized onto a sensor chip by an amine-coupling reaction (Biacore, Piscataway, NJ, USA) and it was inserted into the flow chamber of a Biacore T200 instrument (Biacore, Uppsala, Sweden). The Running Buffer used was made up of 10 mM HEPES pH 7.4, 300 mM NaCl, 0.05% Tween 20, 0.2% DMSO. The flow rate was 10 ml/min,

and a final response of 17914 RU, where RU is response unit, and one RU represents the binding of 1 pg of protein per square mm.

The detection limit was $10^3 - 5 \times 10^7$ (1/Ms) for K_a and $10^{-5} - 1$ (1/s) for K_d .

The addition of the test compounds (0.5, 1, 2, 4 and 8 μ M in running buffer), which is the flow-through analyte, into the chamber resulted in binding of the test compound to the immobilized rTAO. This produced a small change in refractive index at the gold surface, which was quantified with exactitude. The binding affinities were then obtained from the ratio of the rate constants obtained, which gave a straightforward characterization of TAO-inhibitor interaction.

The compounds tested had an unusually high bulk contribution that made the sensorgram shift down during the injection and shifting up during wash steps, however it did not drastically affect the determined K_{on} (K_a), K_{off} (K_d) and K_D (K_{off}/K_{on}).

Initially, an attempt was made to determine the K_D s of the test compounds by fitting the sensorgram to a 1:1 binding model. However, the sensorgram from these compounds were fitting much better when using a heterogeneous ligand model (such heterogeneity may have come from a distinct binding site to TAO or from the immobilization procedure considering that the amine coupling method was used to immobilize TAO). Consequently two sets of K_{on} , K_{off} and K_D were calculated (for comparison, data from both models are reported here).

In addition, another justification for using the heterogeneous ligand model is that recently the co-crystal structure of TAO29 with TAO was obtained (still under refinement), and surprisingly, TAO29 seems not to bind to the active site of the rTAO but to a different site supposed to interact with membrane lipids. Although, the possibility of their binding to the active site in addition to a second site cannot be completely ruled out, it therefore provides a "convenient" explanation to the heterogeneity response seen in the SPR analysis. The determined K_D s varied from 0.1 to 1 μ M.

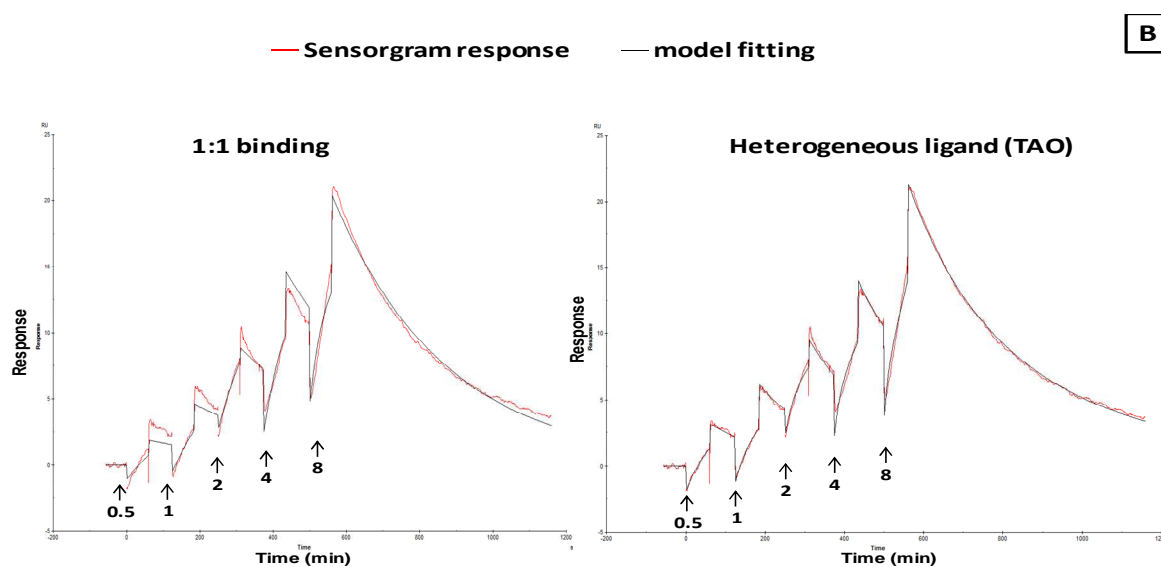
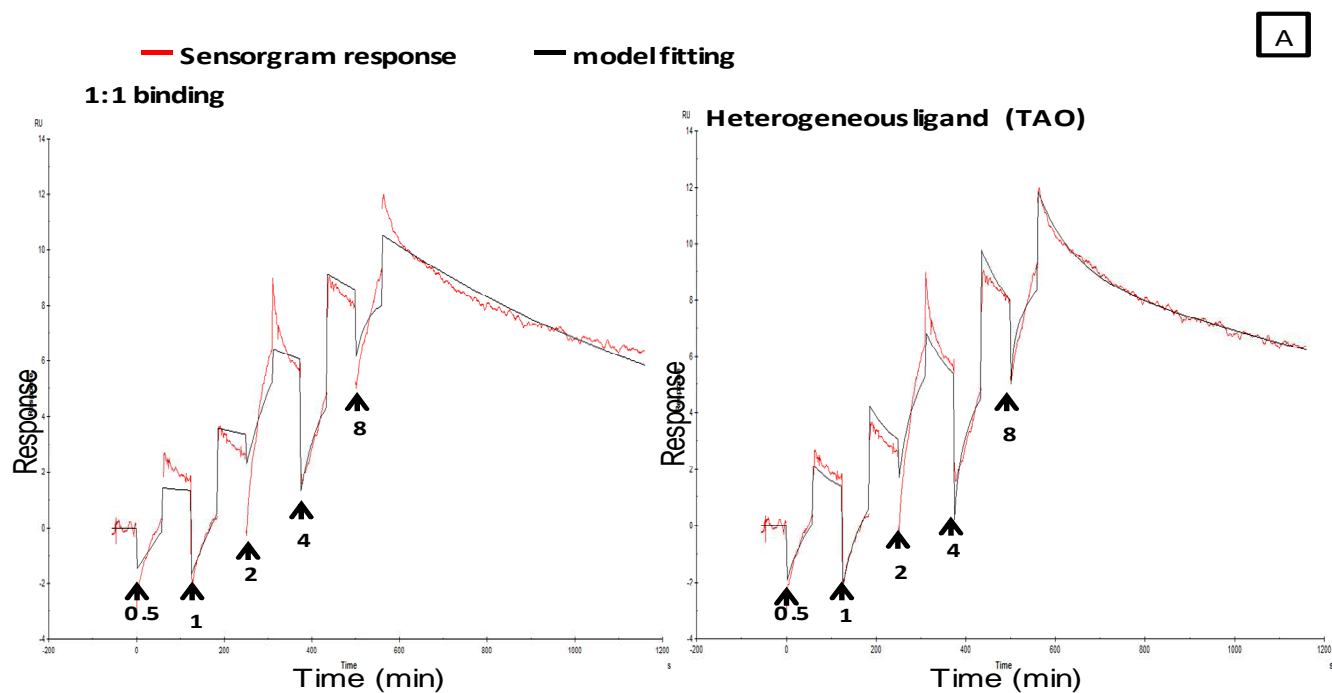


Figure 7.7 Binding kinetics of TAO22 and TAO29 (Panels A and B respectively) into rTAO. The models used were a 1:1 binding (left) and heterogeneous ligand (right) models. Method: Single-cycle kinetics; Running buffer: 10 mM HEPES pH 7.4, 300 mM NaCl, 0.05% Tween 20, 0.2% DMSO; Analyte concentrations: (0.5, 1, 2, 4 and 8 mM) in running buffer; Detection limit: $K_a = 10^3 - 5 \times 10^7$ (1/Ms) and $K_d = 10^{-5} - 1$ (1/s). The full result including other test compounds is summarised in table 7.3

Table 7.3 Summary table for TAO inhibitors' binding kinetics as revealed by SPR (BIAcore) experiments.

	Model	K _a 1 (1/Ms)	K _d 1(1/s)	K _D 1 (nM)	K _a 2 (1/Ms)	K _d 2 (1/s)	K _D 2 (nM)	Chi ² (RU ²)	U- value
TAO22	1:1 binding	4.72E+03	9.84E-04	208.6				0.225	2
	Heterogeneous ligand	3.07E+03	6.42E-04	208.7	3.05E+04	1.34E-02	439.7	0.128	N/A
TAO29	1:1 binding	2.68E+03	3.21E-03	1200				0.393	1
	Heterogeneous ligand	1.73E+04	6.92E-03	399.9	4.94E+01	2.44E-03	49360	0.117	N/A
TAO30	1:1 binding	8.06E+03	2.27E-03	280.9				0.183	2
	Heterogeneous ligand	1.99E+04	5.85E-03	293.8	4.58E+02	2.66E-06	5.812	0.117	N/A
TAO31	1:1 binding	4.87E+03	8.74E-03	1795				0.431	2
	Heterogeneous ligand	1.09E+04	9.69E-03	888.9	1.29E+01	2.77E-03	215400	0.197	N/A
TAO32	1:1 binding	3.96E+03	2.32E-03	584.9				0.413	2
	Heterogeneous ligand	2.80E+04	9.83E-03	350.6	1.58E+02	3.56E-04	2256	0.0856	N/A
TAO33	1:1 binding	7.56E+03	1.26E-03	166.4				0.128	2
	Heterogeneous ligand	2.19E+04	2.79E-03	126.3	9.24E+02	3.65E-04	395.4	0.0337	N/A
TAO34	1:1 binding	2.02E+04	1.81E-03	89.45				0.0856	5
	Heterogeneous ligand	2.77E+03	4.26E-06	1.54	4.83E+04	8.31E-03	172	0.0446	N/A

The chi-square value is a quantitative measure which shows the closeness of fit, so that in an ideal situation it will approximate to the square of the short-term noise level. The U-value was obtained using the 1:1 binding model fitting, and it is also an additional indicator of the parameter significance. This is a parameter that represents the distinctiveness of the calculated rate constants and R_{max} (RU), where R_{max} corresponds to the analyte binding capacity of the surface, and this parameter is determined by testing the dependence of fitting on correlated variations between selected variables. Lower values indicate greater confidence in the results. A high value (above about 25) indicates that the reported kinetic constants contain no useful information (Ndao *et al.*, 2014).

K_a = constant of association (on rate); K_d = constant of dissociation (off rate); RU = response unit; K_D = equilibrium dissociation constant. N/A = not applicable.

On-Off rate map of TAO inhibitors

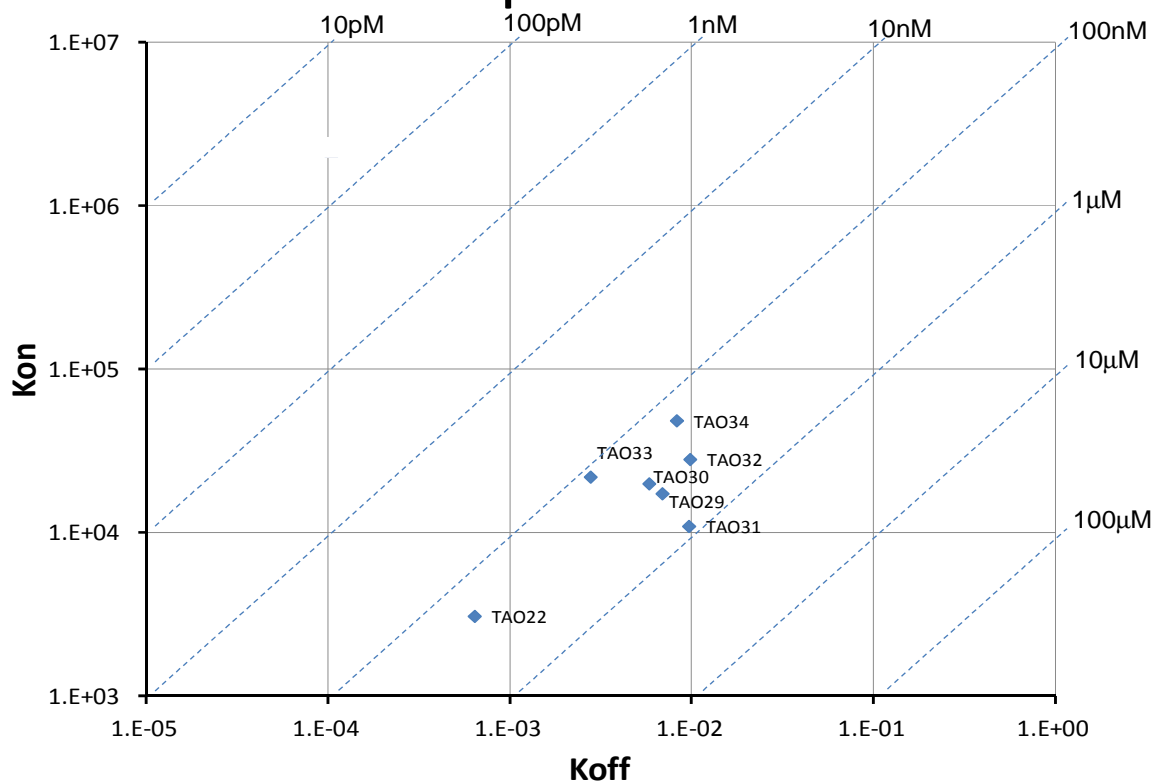


Figure 7.8 On-Off rate map of TAO inhibitors. This map shows a pictorial view of the K_{on} and K_{off} for all the test compounds. It shows that apart from TAO 22, the compounds clustered closely, indicating how close their constants of association (K_{on}) and dissociation (K_{off}) is from one another.

7.3 Discussion

At the moment, neglected tropical diseases (NTDs) still remain a serious health emergency requiring a serious effort in the investigation of new drugs to fight them, the WHO's ambition of eliminating African trypanosomiasis as a public health problem (Simarro *et al.*, 2015), and the United Nations' goal of reducing poverty, obviously will be advanced by developing a new drug that is affordable, safe and very effective for the treatment of both human and animal African trypanosomiasis. However, these road maps are still very far from realization. In fact, the drug development pipeline in the field of NTDs is almost dry, except for developments with fexinidazole and the Scynexis oxaborole presently in clinical trials for late stage sleeping

sickness (Jones *et al.*, 2015). Therefore specific targeting strategies should be exploited in order to identify new classes of possible drug candidates.

However, it is very important when developing an efficient anti-parasitic drug to identify molecular targets in the parasite, one that should be critical for growth and survival of the parasite. Ideally this target should be absent or not important in humans or animals, and if at all present in humans/animal, it should be structurally distinct. We have identified an important target protein in African trypanosome which is important for their energy (ATP) generation and survival in the human host; this protein is called trypanosome alternative oxidase (TAO).

We developed an integrated strategy to specifically target TAO using parallel synthesis that will generate compound libraries, combined with phenotypic assays that allow testing of compounds in a rational period of time. This strategy provides new hit compounds that can be progressed further to hit-to-lead, followed by the lead optimization steps in the drug discovery process. The target-based approach is at present regarded to be very efficient (Gilbert *et al.*, 2011). However, as stated earlier, in order to rationally carry out this process of target-based drug discovery that will target TAO, it is of paramount importance to have significant information on the molecular target (TAO), and on the hit-target binding mode (TAO-inhibitor complex), so that modification on the hit scaffold can be reasonably guided by a combination of biophysical, biochemical, and computational methods. For this reason, having identified some of our molecules to be promising by means of various cell-based experiments, it was therefore essential to verify the potential target(s) using the available bioanalytical approaches.

We have previously reported (Chapter 6) that in a whole-cell assay with the parasite, more than a half of all the test compounds were significantly more active against *T. brucei* when co-administered with glycerol, or when tested against the aquaporin knockout cell lines; the compounds in addition also inhibited parasite respiration in an *in vitro* assay. A similar result was obtained with the TAO inhibitor SHAM (but not with control drugs that do not act on TAO), indicating that the test compounds are most probably acting on parasite respiration through TAO inhibition. This was further investigated, and confirmed, with our test compounds, which inhibited oxygen consumption of *T. brucei* WT, in a similar dose-dependent manner as SHAM, rapidly depolarized the mitochondrial membrane, and displayed reduced activity against a trypanosome line over-expressing TAO.

As a whole, these data are consistent with TAO being the primary target of these inhibitors in the parasite which led us to carryout direct inhibitory assay and study the kinetics of rTAO, which is reported here.

The TAO gene contains 990 nucleotides encoding 330 amino acids full length protein, including the N-terminal 25 amino acid residue Mitochondrial Targeting Signal (MTS). For the majority of mitochondrial proteins, their transport into the mitochondria relies on two key fundamentals: (i) the presence of an MTS within the protein and (ii) the presence of some specific translocators within the mitochondrial membrane domain which recognize the specific signals (Bauer *et al.*, 2000). Basically, three types of MTS have been reported to be found in proteins that are intended for delivery into the mitochondria: A stop-transfer or sorting signal, an internal signal, and the N-terminal signals (Neupert and Herrmann, 2007). The N-terminal targeting sequence, also called pre-sequence, is an amphipathic helix containing both hydrophobic and basic amino acid residues (Hamilton *et al.*, 2014).

Of the three MTS, only the N-terminal signal is usually cleaved after transportation of the protein to the mitochondria (Hamilton *et al.*, 2014). Consequently, the physiological and functional TAO is without MTS (Bauer *et al.*, 2000). Despite this phenomenon, only the full length protein has been over-expressed and studied to date. Yet, the problems of reduced stability, poor solubility and yield, and poor X-ray diffraction resolution of crystals of the recombinant AOX are thought to be due to the presence of the MTS (Shiba *et al.*, 2013). Because the full length TAO is not physiologically active in BSF *T. brucei*, it is important to target the physiological form of the TAO when developing inhibitors that would target TAO and study the kinetics of the inhibitor- Δ MTS TAO complex, mimicking what would actually happen *in vivo*.

We have reported the expression and purification of the physiological form of the alternative oxidase from *Trypanosoma brucei* (TAO) without its N-terminal 25 amino acid mitochondrial targeting sequence (Δ MTS rTAO), and discovered that it was more soluble, stable, active, and was produced in a higher yield (Table 7.1). This physiologically relevant rTAO enzyme was used to characterize the inhibitory efficacy of 32 cationic and non-cationic compounds and develop structure-activity relationships with these series of 4-hydroxybenzoate and 4-alkoxybenzaldehyde derivatives.

Interestingly, the lipophilic cation (LC) compounds with C-14 methylene linker which seemed optimal for trypanocidal action reported in chapter five also provided improved inhibitory activity against the pure recombinant TAO enzyme compared to SHAM. However, the correlation between inhibition of purified rTAO and the trypanocidal effects of the reported LC conjugates is much complicated by the fact that the local concentration of the test compounds in functional, charged mitochondria remains unknowable for the moment. As intended, this makes the apparent EC₅₀ concentration *in vitro* much lower than the IC₅₀ concentration against the isolated enzyme, exactly as recently reported for the inhibition of the *T. brucei* F₁F₀ ATPase by lipophilic bisphosphonium compounds (Alkhaldi *et al.*, 2016). Although the evidence suggests that some of the LC conjugates have sufficiently low IC₅₀ values to act principally through inhibition of mitochondrial TAO, the possibility that (some of) the compounds also impact on other mitochondrial functions cannot be excluded.

The kinetics of binding to TAO determined by Lineweaver-Burk plot analysis and Surface Plasmon Resonance (SPR) experiments indicated a non-competitive inhibition. Some of the inhibitors showed nanomolar IC₅₀ values against Δ MTS rTAO in the same range as ascofuranone (IC₅₀ = 2 nM) (Table 7.2). Ascofuranone has been found to be a good inhibitor of TAO (Suzuki *et al.*, 2004). However, it was observed that perfect killing of the parasites can only be achieved when ascofuranone is given along with 5 mM glycerol *in vitro*. Ascofuranone, which is a prenylphenol antibiotic that was previously obtained from *Ascochyta visiae* - a phytopathogenic fungus, was reported to strongly inhibit both the glycerol-3-phosphate-dependent mitochondrial O₂ consumption and glucose-dependent cellular respiration of BSF *T. b. b.* This inhibition was thought to be due to the blockade of the mitochondrial electron-transport system of the trypanosome, which is composed of glycerol-3-phosphate dehydrogenase (EC 1.1.99.5) including the alternative oxidase (TAO) (Suzuki *et al.*, 2004, Shiba *et al.*, 2013).

Ascofuranone was also reported to noncompetitively inhibit the reduced coenzyme Q1-dependent O₂ consumption of the *T. b. b.* mitochondria with regards to ubiquinol (K_i = 2.38 nM) (Suzuki *et al.*, 2004). Consequently, the susceptible site was the trypanosomes' ubiquinone redox machinery that links the activities of the two enzymes. We also carried out some kinetics studies on some of our compounds and discovered that they did have the same non-competitive mode of TAO inhibition as ascofuranone.

Salicylic hydroxamic acid (SHAM) is a known inhibitor of TAO, which non-specifically chelates the iron in the di-iron centre of TAO. SHAM has been comprehensively studied as an inhibitor of the cyanide-insensitive alternative oxidase present in the respiratory system of plants, and more recently it was reported to inhibit TAO, and also displayed a non-competitive (mixed type) mode of inhibition similar to the one reported for our compounds (Yabu *et al.*, 1998).

In conclusion, we have used the target-based approach to synthesize a number of mitochondrion-targeted LC inhibitors of TAO, which are based on SHAM and DHB conjugated with triphenylphosphonium or quinolinium cations. Our initial data on this are highly encouraging, and revealed a great prospect for developing an effective, nontoxic inhibitor against African trypanosomes. In fact one of the advantages of these inhibitors/strategy is that unlike the non-specific iron chelators such as SHAM, and 3,4-dihydroxybenzoate, our LC-TAO inhibitors are specifically targeting TAO as shown by their very low toxicity to mammalian cells, and we showed previously that they did not affect the respiration of mammalian cells. Therefore the strategy for delivering these inhibitors across biological membranes as reported in this work is safe, and is a strategy that can be easily used for delivering other drugs across biological membranes to their targets, thereby reducing the risk of drug toxicity due to off-target effects. Considering our available data as reported in this work, we conclude at this point that the mechanism of action of these inhibitors is indeed via TAO inhibition. Therefore strategies to optimize the trypanocidal activity of these promising compounds should be given top priority.

Chapter 8: General Discussion

The burden of parasitic disease (both human and veterinary) is still disappointingly high, particularly in resource-poor communities found in many less developed countries, notwithstanding the enormous efforts and resources put into various measures targeted at reducing this global burden by some organisation including the World Health Organization, UNICEF, the Food and Agriculture Organization of the United Nations (FAO), the Medicines for Malaria Venture (MMV), DNDi, Medecins-sans-Frontiers, the Consortium for Parasitic Drug Development, and the Bill & Melinda Gates Foundation, not leaving out the huge efforts generated by the Millennium Goals.

These parasitic diseases include some of the most neglected tropical diseases, such as leishmaniasis, caused by more than 20 species of *Leishmania*, which affects approximately 200 million people living in areas including Africa, Asia, South and Central America, and southern Europe (Barrett, and Croft, 2012).

African trypanosomiasis on the other hand is a major health challenge facing the sub-Saharan African region, and is both a human disease (sleeping sickness) and a veterinary condition in livestock, including wildlife (nagana). The disease is caused by infection of humans and animals with parasites called trypanosomes, usually through the bite of infected tsetse flies. The agricultural losses alone attributed to this infection are estimated at USD 4.75 billion by the FAO, and threaten food security for millions of people (FAO, 2016).

The disease could be fatal unless adequately treated with one of the few drugs available, as there is no vaccine or prophylactic medication, and insect vector control is barely effective given the enormous areas that are tsetse habitat. Several efforts have been made in order to control this disease, including the use of drugs. However, HAT is particularly problematic to treat due to the unacceptable toxicity and the complicated administration of the chemotherapies presently available for treatment. Besides, resistance to current drugs by trypanosomes is another threat to chemotherapy (Munday *et al.*, 2014).

A few drugs are at the moment registered for use in treating HAT: pentamidine, melarsoprol, suramin, eflornithine, and Nifurtimox Eflornithine Combination Therapy (NECT). NECT is the current recommended treatment for late stage *T. b. gambiense* HAT (Giordani *et al.*, 2016).

However, none of these drugs are absolutely safe as all of them have certain degree of toxicity. Pentamidine and suramin are used in the first or early stage of *T. b. gambiense* and *T. b. rhodesiense* infections respectively.

Meanwhile three key drugs are used to treat AAT: diminazene aceturate (DA), homidium salts (chloride or bromide), and isometamidium chloride (ISM). However, many problems are associated with the few available treatment options, these includes parenteral administration requiring long term hospitalization. Another challenge is the lack of guaranteed supply and high cost of drug in the resource-poor communities where the disease is concentrated. For instance, between 2002 and 2010, the average cost to treat a second-stage *T. b. gambiense* HAT patient with DMFO rose from €28 to €336 (Simarrøt *et al.*, 2012), while 400 USD/treatment was spent on amphotericin B (AmBisome) for a patient infected with visceral leishmaniasis in Sudan (Salih *et al.*, 2014). Moreover, the current drugs are very old, as most of them were discovered in the early-to-mid-twentieth century and are becoming ineffective due to drug resistance; meanwhile investment in new drug development for this most neglected disease has been almost non-existent for decades (Barrett, 1999; Rodenko *et al.*, 2015).

Toxicity of some of these trypanocides is still a serious challenge; for instance, melarsoprol, a drug used for treating the second stage of HAT, is so toxic that it was reported to cause deaths in patient at an unacceptable rate of 10% due to a fatal reactive encephalopathy (Barrett 1999, Fairlamb *et al.*, 1992; Burri, 2010). Other side effects include vomiting and nausea (Jannin and Cattand, 2004; Garcia, 2007).

A major challenge facing chemotherapies of these two neglected tropical diseases is the issue of resistance to the current chemotherapies. For instance, melarsoprol (Delespaulx and de Koning, 2007; Graf *et al.*, 2013) and eflornithine resistance (Vincent *et al.*, 2010) for late stage HAT, and pentavalent antimonials for leishmaniasis (Sundar *et al.*, 2008) have all been reported, this further reduces the available treatment options.

As a result of the limitations facing existing chemotherapies, there is an urgent need for the development of new drugs that will replace the existing inefficient ones and that will be used for treating the most neglected tropical diseases, such as trypanosomiasis and leishmaniasis. However, it is important that the development of new anti-trypanosomiasis/leishmaniasis drugs should be targeted at a reasonable price, and this should lead to a significant reduction in

treatment costs, considering that these diseases affect mostly poor communities. Such solutions with the right cost/benefit balance could well include natural products research, although the search for new anti-trypanosomiasis/leishmaniasis drugs should by no means be limited to this strategy alone. However, the momentum to make new compounds from natural products, such as that from plant sources is considerable (Newman & Cragg, 2007).

There is strong evidence in literature that medicinal plants are a rich source of drug candidates and leads, and, like synthetic compounds, could be exploited as anti-protozoan agents that could solve the present problem of drug inefficiencies (Schmidt *et al.*, 2012). Some of the drugs in use today were originally from plants traditionally used for treating the same infection as now their isolated compounds do (Maya *et al.*, 2007). The success story of the alkaloid artemisinin from the Chinese anti-malarial wormwood plant (*Artemisia annua*), and quinine from the bark of cinchona trees (*Cinchona officinalis*) are classic examples. Several plant-derived natural products from diverse structural classes including various flavonoids, alkaloids, quinonoids and terpenoids have been studied as anti-kinetoplastid candidates against some parasite specific metabolic pathways such as nucleic acid biosynthesis, biomembranes, and cytoskeletal proteins and enzymes (Wink, 2012).

In search of improved and non-toxic active antiprotozoal principles that are not cross-resistant with current anti-parasitics, seven plants used locally in Nigeria to treat trypanosomiasis and other tropical fevers were obtained and extracted with hexane, ethyl acetate and methanol. The plants were evaluated for activity against selected kinetoplastid parasites. Active principles were isolated by bioassay-led fractionation, testing for trypanocidal activity, and identified using NMR and mass spectrometry. The extracts and their purified compounds of three out of the seven plants were active *in vitro* against *T. brucei*, *T. congolense*, and *L. mexicana*.

The result shows that crude extracts and isolated active compounds from *Polyalthia longifolia* and *Eucalyptus maculata*, in particular, display promising activity against drug-sensitive and multi-drug resistant *T. brucei*. In addition, these compounds were active against a veterinary trypanosome species, *T. congolense*, and against *L. mexicana*. This observation validates the folkloric claims that extracts of the plants from which there were isolated have activity against protozoan parasites. None of the isolated compounds displayed toxicity towards Human

Embryonic Kidney cells at concentrations up to 400 µg/mL. This is not surprising as these plants have been used for treating infectious disease for many years without any known side effects.

Two of the isolated compounds (a diterpene and a triterpene, HDK20 and HDK40 respectively) were studied for their mechanism of action against a model organism, *T. brucei* s427 WT. It was observed that fluorescence microscopic assessment of DNA configuration revealed cell cycle defects after 8 hours of incubation with the natural compounds: DNA synthesis could not be initiated, leading to a dramatic increase of cells with 1 nucleus and 1 kinetoplast (1N1K). This shows that these compounds both affect cell cycle progression and their effect may be on the G1 phase of the cell cycle. Nuclear DNA fragmentation also became evident after 10 hours of incubation with compound HDK-20 when visualised by flow cytometry.

In an additional investigation into the mode of action of the HDK20 and HDK40, we tested whether these compounds cause DNA fragmentation via the induction of programmed cell death (PCD or apoptosis) in the trypanosomes. Terminal deoxynucleotidyl transferase dUTP Nick-End Labelling (TUNEL) assay was therefore used, revealing an increase in DNA fragmentation after 12 hours. This may indicate that a prolonged inability to progress the cell cycle could lead to the breakdown of DNA duplication machinery and the initiation of apoptotic process and subsequent nuclear DNA fragmentation. However, a conclusion of apoptosis would require substantial additional evidence and it is possible that these compounds interfere with some part of DNA replication, so as to introduce errors and breaks. Also the use of TUNEL assay to measure DNA fragmentation in kinetoplastids needs to be backed up with fluorescent microscopic examinations of the nuclear DNA and kDNA as it is also possible for normal replicating kDNA to be label by this method.

Compounds HDK-20 and HDK-40 also induced a fast and profound depolarisation of the parasites' mitochondrial membrane potential after 1 hour of incubation and this continued until a near complete depolarization was achieved after 12 hours, indicating that membrane depolarization is likely the first event in the entire process that lead to cell death. This explanation is likely so as it was also observed that intracellular ATP levels of *T. brucei* were found to be reduced shortly after depolarization of the membrane, indicating a direct link between mitochondria membrane potential and ATP generation. It thus appears that the mitochondria may be the primary target of the compounds, leading to reduced ATP generation and the inability to

initiate replication of kDNA, the essential first step in the trypanosome's cell cycle - causing cell cycle arrest.

Metabolomic assessment is a pointer to metabolic perturbations in the parasite and should give us a clue if there were any of such perturbations involved in the mode-of-action of the test compounds. However, metabolomic assessments of *T. brucei* cells incubated with HDK20 or HDK40 did not reveal the targeting of any specific metabolic pathway. Since the isolated compounds have almost no toxicity against human cells but are very active *in vitro* against multidrug-resistant trypanosomes, these compounds could serve as lead compounds towards the identification of more efficient anti-trypanosome drugs.

Another way to develop safer and more effective drugs that will overcome the issues of toxicity and resistance is to have a well-defined target in the parasite, with a clear mechanism of action. To accomplish this, highly selective compounds that affect unique and essential molecular targets in the parasites should be developed. Accordingly, energy metabolism and the respiratory pathways of these parasites have been identified. The parasite specific cyanide-insensitive Trypanosome Alternative Oxidase (TAO) has been validated as a drug target in *T. brucei* (Yabu *et al.*, 1998; 2003; 2006; Nakamura *et al.*, 2010). TAO is considered a good chemotherapeutic target for drug development because this unique oxidase is very essential for the parasite's respiration and survival since it re-oxidises cytosolic NADH, and because this protein is not found in the mammalian host but present in many obligate parasites (Nakamura *et al.*, 2010). Earlier reports in the literature have shown that very simple chemical structures containing the 2,4-dihydroxybenzoate (2,4-DHB) and salicylhydroxamate (SHAM) scaffolds did inhibit TAO (Clarkson *et al.*, 1989; Grady *et al.*, 1986; Ott *et al.*, 2006). However, their trypanocidal activity proved disappointing because the inhibitors did not effectively cross the highly negatively charged inner mitochondrial membrane to reach their target. Hence in the second aspect of this thesis, a strategy to enhance the antitrypanosomal potency of these classes of TAO inhibitors based on their conjugation with a mitochondrion-targeting lipophilic cation (LC) using quinolinium or triphenylphosphonium (TPP) was developed and investigated.

Their activities against WT and resistant *T. brucei* and *T. congolense* strains were studied *in vitro*. The first important result came from the low nanomolar range activities displayed by some of the 2,4-DHB-TPP derivatives, and the submicromolar activities of the 2,4-DHB-quinolinium

derivatives, as compared with the micromolar EC₅₀ values of the parent compound. In contrast, the SHAM–TPP derivatives displayed somewhat lower activities, even though this still represented an approximately 100-fold improvement in potency relative to SHAM. Superior antitrypanosomal activities were observed with the TPP vs quinolinium conjugates, which is consistent with earlier studies on diphenyl cationic trypanocides (Dardonville *et al.*, 2015). It probably reflects the higher lipophilicity and charge dispersion around the phosphorus atom in the TPP cation, which is optimal for membrane permeation and accumulation in the mitochondrion. In some cases, these compounds were more active, than clinical drugs like pentamidine *in vitro*. Also noteworthy is the submicromolar activity displayed by some of the test compounds against *T. congolense*, the principal etiological agent of AAT. Their EC₅₀ values were similar to the veterinary drug diminazene and their utility against AAT would be interesting to investigate further, as drugs against this condition are even more urgently needed than for the corresponding human condition (Giordani *et al.*, 2016).

A major issue for existing antiparasitic agents is drug resistance. Accordingly, resistant strains were used in this study as a model to determine cross-resistance between existing classes of trypanocides and the test compounds. This includes a multi-drug resistant strain, B48, which lacks both the *Trypanosoma brucei* aminopurine transporter TbAT1/P2 and the high affinity pentamidine transporter (HAPT1). There were no significant differences in susceptibility between the WT and both of these resistant strains, which means that cross-resistance with existing first line HAT and AAT drugs, including pentamidine, diminazene, cymelarsan and melarsoprol, is highly unlikely to appear with these compounds, despite the diamidines, at least, also having mitochondrial targets (Lanteri *et al.*, 2008; de Macedo *et al.*, 2015).

Considering that resistance to these important trypanocides such as the diamidines has been previously linked to the loss of specific cell surface transporters such as the P2/TbAT1 and HAPT drug transporters (Matovu *et al.*, 2003; Bridges *et al.*, 2007), it therefore follows that these specific surface transporters are not associated with the internalisation of these test compounds, rather there are more likely to diffuse across biological membranes, ruling out any possibility for cross resistance. Lipophilic cations can cross lipid bilayers by non-carrier mediated transport and accumulate specifically into mitochondria driven by the plasma- and mitochondrial transmembrane potentials (Taladriz *et al.*, 2012; Ross *et al.*, 2006; Luque-Ortega *et al.*, 2010; Dardonville *et al.*, 2015). The strong accumulation of dications by the charged mitochondria

allows the inhibition of various essential functions with relatively low extracellular drug concentrations (Wilkes *et al.*, 1997; Ibrahim *et al.*, 2011; Alkhalidi *et al.*, 2016). In addition, LCs can cross the blood–brain barrier (BBB) and generate therapeutically effective concentrations in the brain (Smith *et al.*, 2003), which is particularly relevant for the treatment of late-stage sleeping sickness.

As stated before, it is imperative when developing new chemotherapy that the new chemotherapeutic agent should not be toxic to human cells; therefore, their efficacy against the target parasites should be optimised whilst toxicity is reduced to an acceptable level, with increased selectivity index (SI). Consequently, the toxicity levels for the LC inhibitors tested in this work were determined *in vitro* using mammalian cells such as Human Embryonic Kidney (HEK) cells or Human Foreskin Fibroblast (HFF). The results show that all of the compounds were lower in toxicity on HEK cells, and in some cases not toxic at a concentration of up to 400 μ M *in vitro*. With many of them displaying an SI >200-fold.

The low toxicity of the LCs tested here is similar to that reported in literature. For instance, a mitochondria-targeting antioxidant mitoquinone (MitoQ) comprising the lipophilic triphenylphosphonium (TPP) cation covalently linked to ubiquinone was developed and was reported to be safe and protective in animal models (Barry *et al.*, 2010). MitoQ was also used in a phase 1 human clinical trial to investigate whether it could act as a disease-modifying agent in untreated patients with Parkinson's disease. It was reported to be safe and well tolerated by those who took part in the clinical trial, further highlighting the safety of TPP-LC conjugates (Barry *et al.*, 2010).

The trypanocidal activity of our mitochondrion-targeting LC-TAO inhibitors, which inhibited trypanosome growth with EC₅₀ in the low nanomolar range, was further enhanced in the presence of glycerol, and also showed enhanced activity against aqp2/3, and aqp1-3 KO trypanosomes, and inhibited parasite respiration dose-dependently, confirming that TAO is the cellular target of this compound. Consequently, these compounds were tested in a direct inhibitory assay with purified rTAO. More than 50% of these inhibitors effectively inhibited rTAO at concentrations as low as 1 nM - further confirmation that TAO is the cellular target of these compounds.

The relationship between the biological activity of a compound and its structure is known as the Structure Activity Relationship (SAR). SAR analysis was performed on our library of mitochondrion-targeting LC compounds in order to determine the key functional groups of the pharmacophore responsible for its anti-trypanosome activity, this is an important tool in the further optimisation of the scaffold. The structural determinants for activity of the test compounds against TAO were similar to those previously found to be essential for TAO inhibition of some trypanocides. For instance the presence of the 4-hydroxyl group on the scaffold of the SHAM derivatives and the 2,4-dihydroxybenzoic acid derivatives were found to be a significant requirement for improved activity of these classes of inhibitors. A hydroxyl substituted benzoic acid moiety was previously reported to be the basic structural requirement needed to inhibit the alternative oxidase activity in plants and trypanosomes as reported for Ascofuranone and its derivatives (Saimoto *et al.*, 2013).

Another very important group on the scaffolds that clearly contributed to the anti-trypanosome activity of these classes of inhibitor as observed in this assay is the presence of the lipophilic triphosphonium or a quinolinium cations, as those lacking it were mostly inactive showing that the LC-carrier moiety effectively enhances the trypanocidal activity of the compounds. This same observation has been reported for some triphosphonium salts as trypanocides (Alkhaldi *et al.*, 2016).

The number of methylene units was another key requirement for rTAO inhibition and antitrypanosome activity of the series of test compounds reported in this work. Because of the large size of the TPP cation, long spacers (14 to 16 methylene units) are needed to accommodate the pharmacophore in the enzyme binding-site, leaving the cationic moiety outside of the active site cavity. In contrast, the flat quinolinium cation seems to tolerate somewhat shorter linkers (14 > 16 \approx 12 methylene units) even though the tetradecane linker was optimum with both series.

To investigate the mode of action of the LC - TAO compounds, various methods were employed. A preliminary investigation into the cellular actions of some of the compounds was performed using various strategies such as cell cycle progression, mitochondrial membrane potential, ATP content of cells, oxygen consumption assay, and DNA fragmentation. It was discovered that all LC-TAO inhibitors tested in this work led to a rapid reduction of *T. b. brucei* Ψ m after 1 hour of incubation with the test compounds and also decreased the intracellular ATP level soon after.

These findings are very consistent with the mitochondria being the target of these compounds. It was because of these findings that the cell cycle was also studied. However, the compounds did not significantly affect the cell cycle at the test concentration and incubation period.

In conclusion, we have successfully developed potential drug leads for the treatment of African trypanosomiasis. We are therefore confident that the findings from this work significantly enhance existing knowledge on trypanocidal strategies, with the identified hit compounds acting as a structural guide, and contributing to the on-going drug development against trypanosomiasis. We also hope that the strategies used in this work will gain application in the treatment of other parasitic diseases. Further work including lead optimization and *in vivo* assays with the most promising inhibitors is in progress.

Appendices

Appendix A: List of selected medicinal plants used in this research



Plant- A: *Centrosema pubescens* Benth. (Family *Fabaceae*)



Plant-B: *Moringa oleifera* Lam (Family *Moringaceae*)



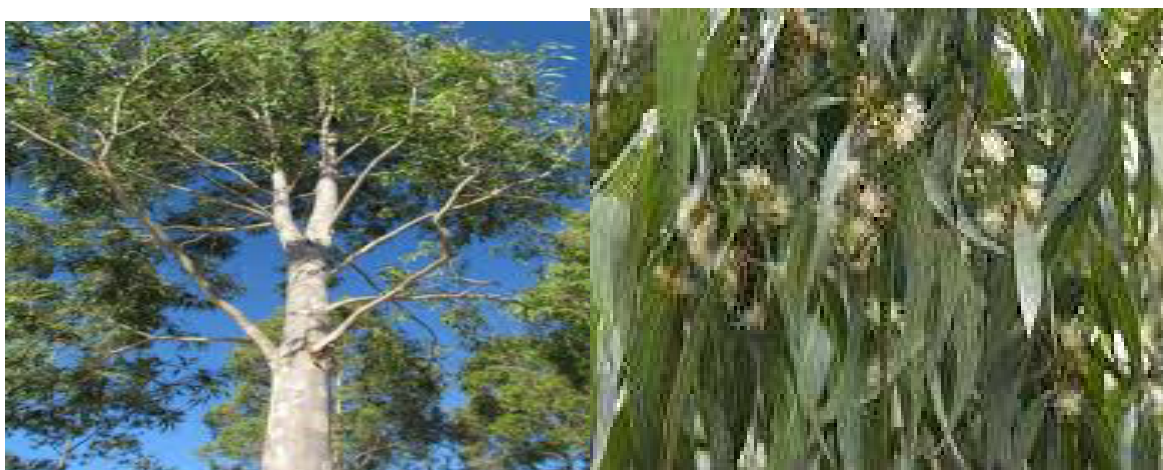
Plant C: *Tridax procumbens* (L.) L. (Family *Compositae*)



Plant D: *Polyalthia longifolia* (Sonn.) Thwaites (Family *Annonaceae*)



Plant E: *Newbouldia laevis* (P.Beauv.) Seem. (Family *Bignoniaceae*)

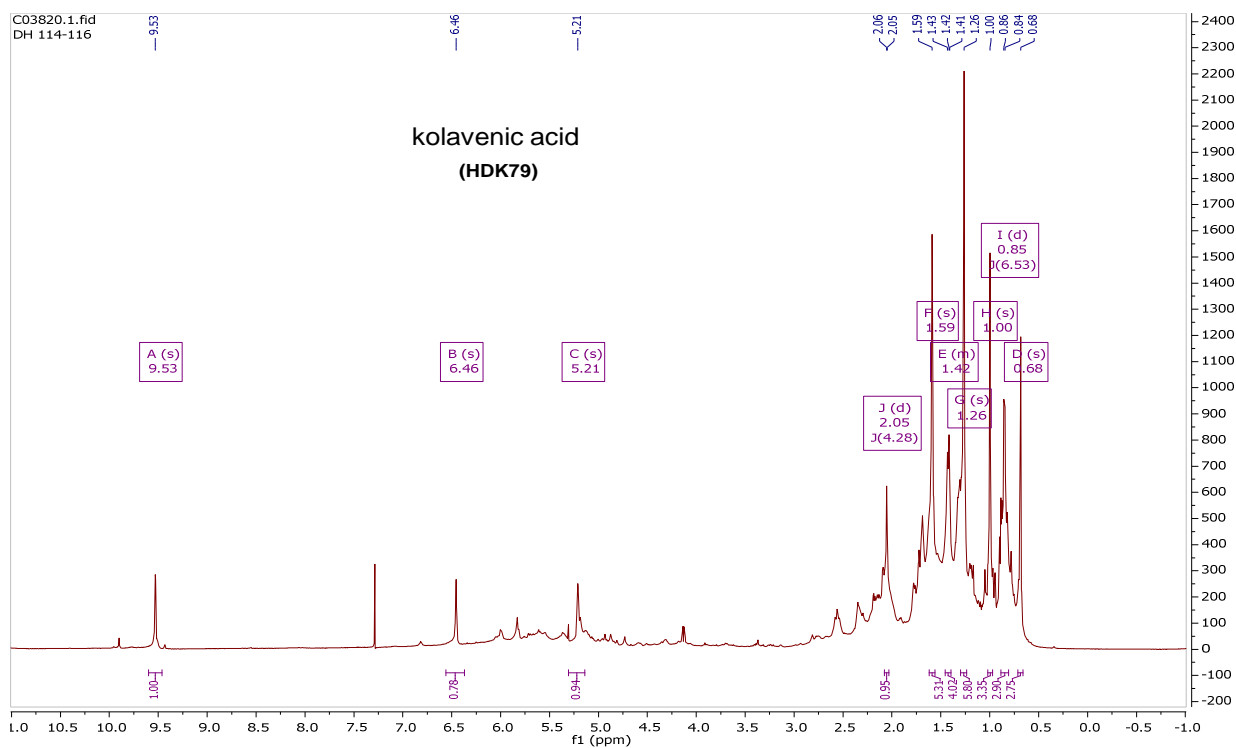
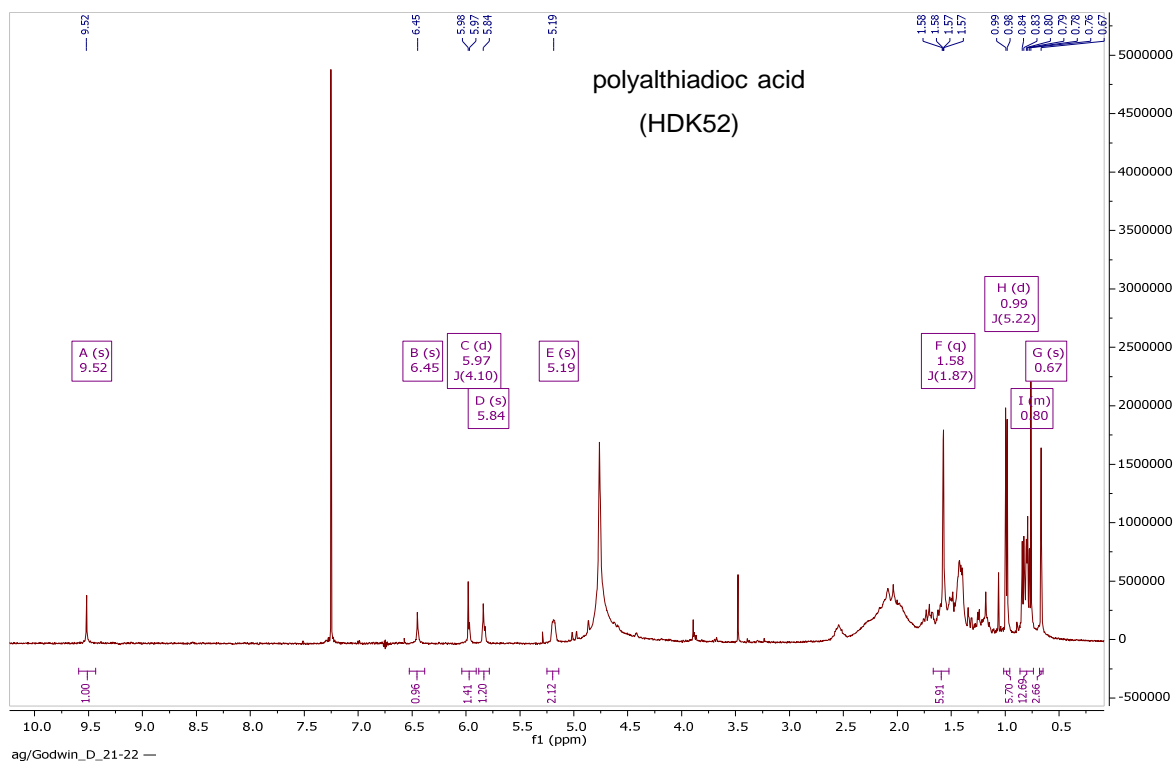


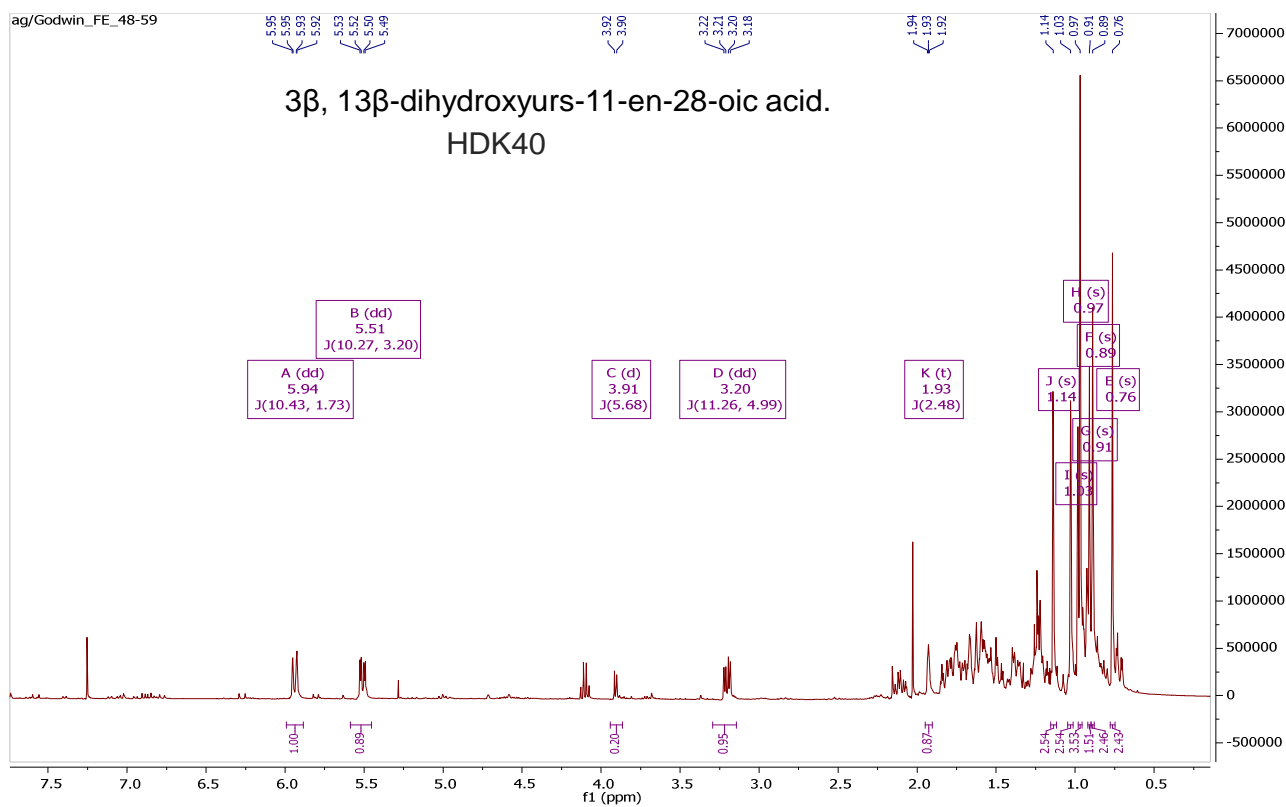
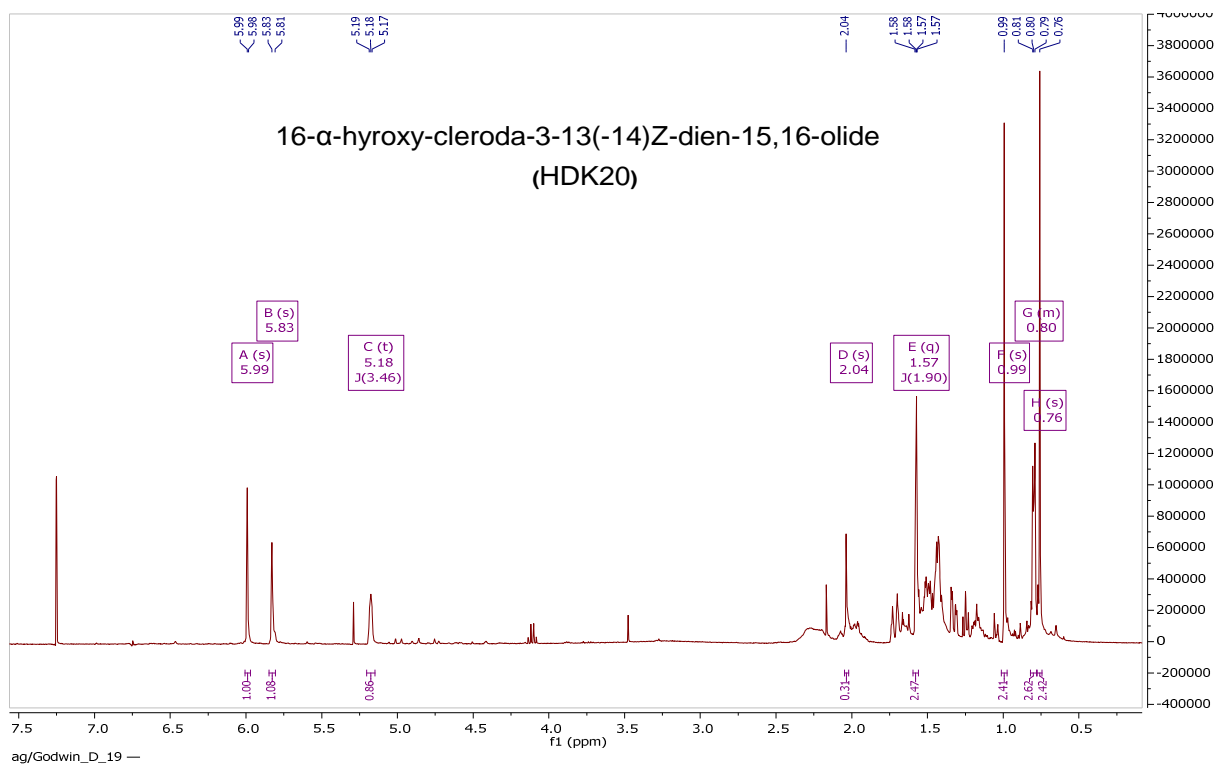
Plant F: *Eucalyptus maculata* Hook. (Family *Myrtaceae*)

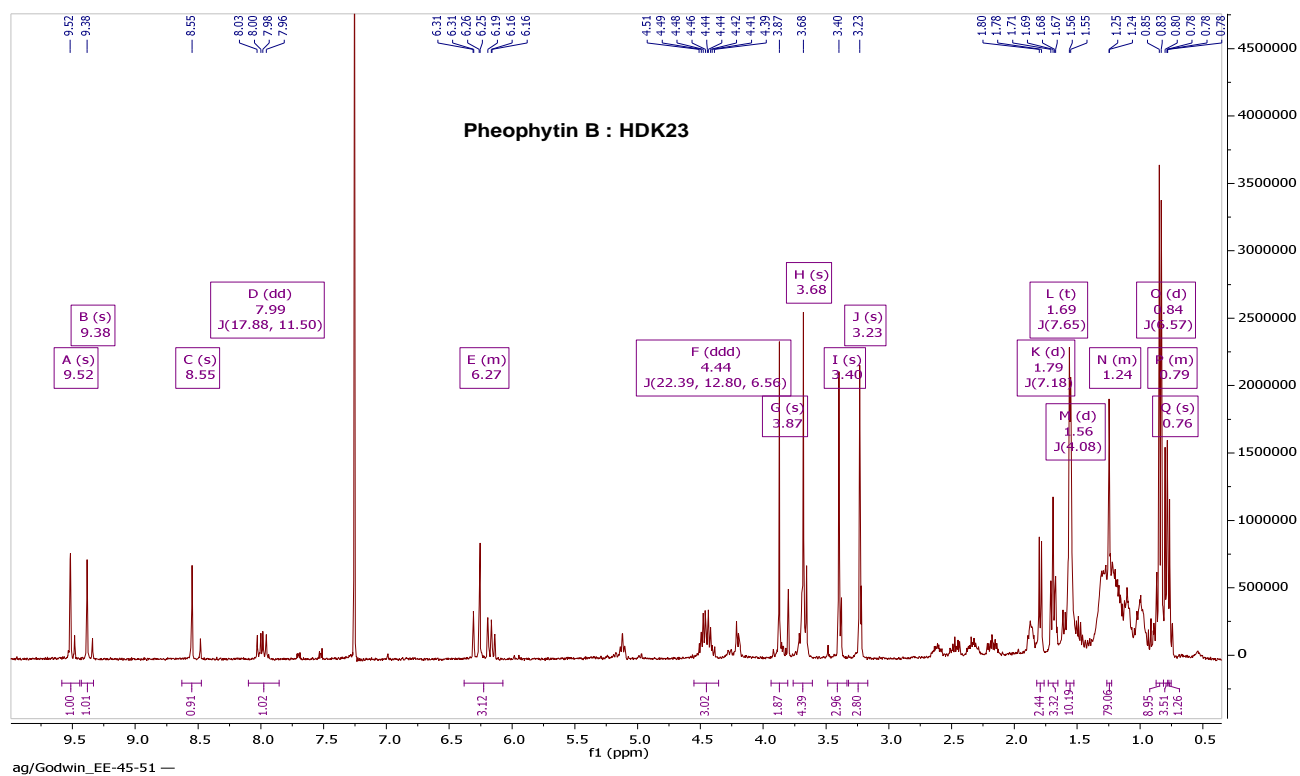
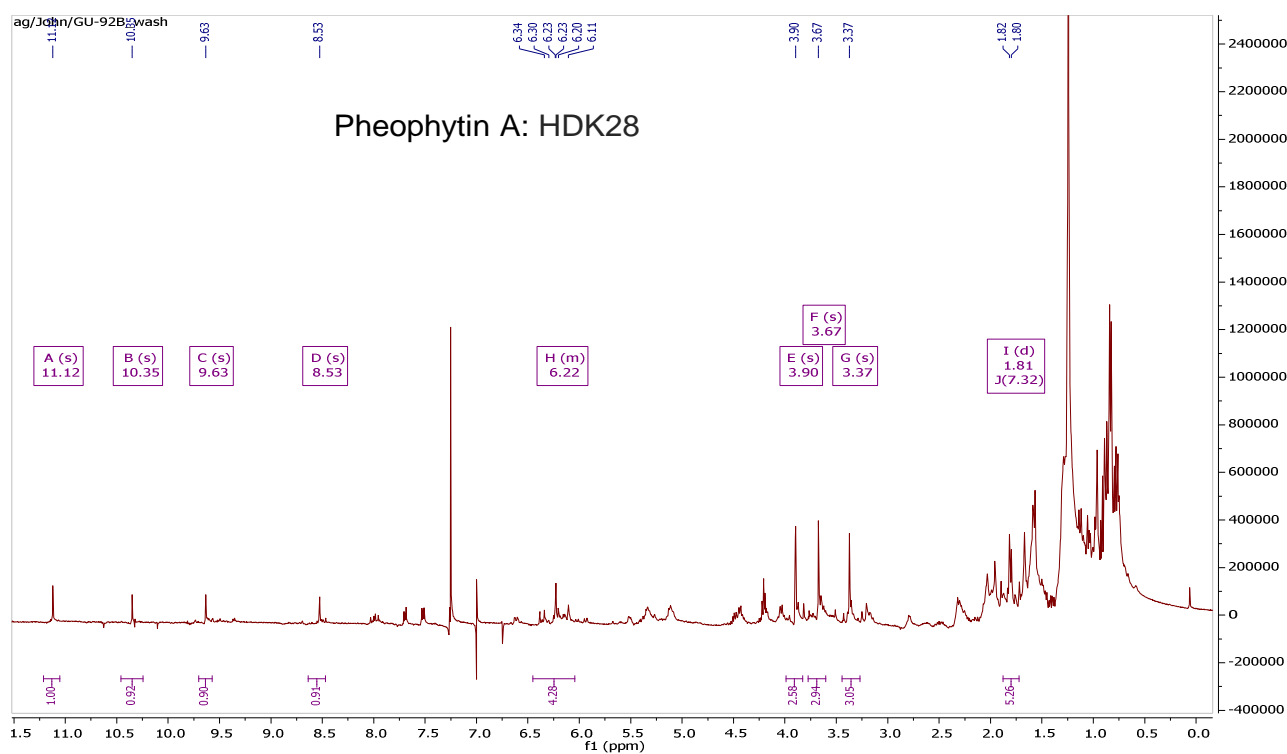


Plant G: *Jatropha tanjorensis* J.L.Ellis & Saroja (Family *Euphorbiaceae*)

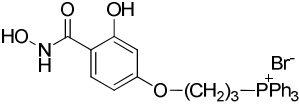
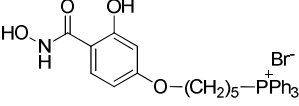
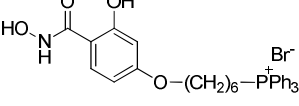
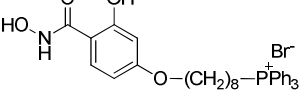
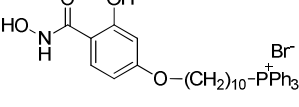
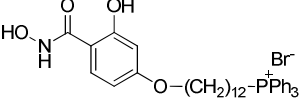
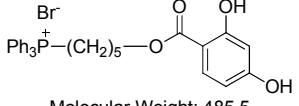
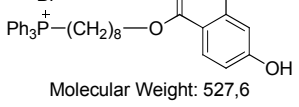
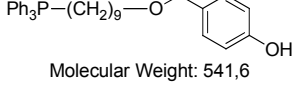
Appendix B: Proton NMR of purified natural compounds.

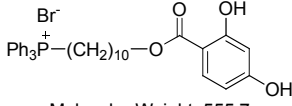
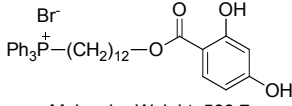
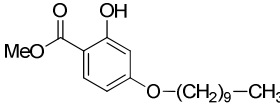
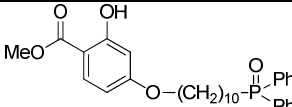
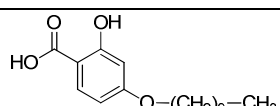
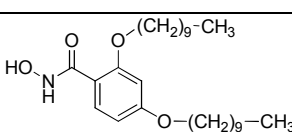
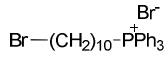
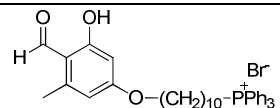
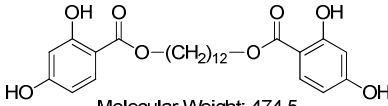
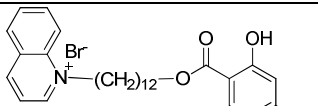
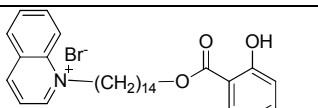


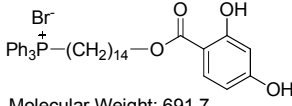
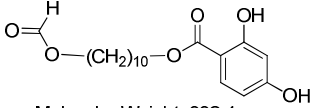
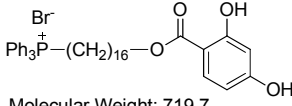
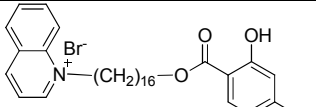
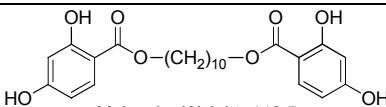
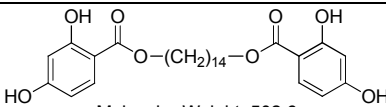
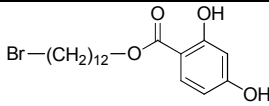
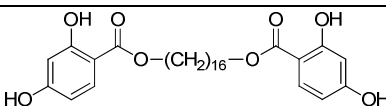
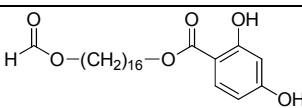
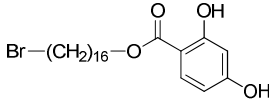
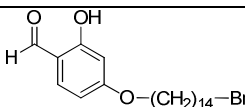


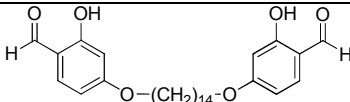
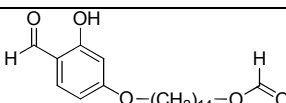
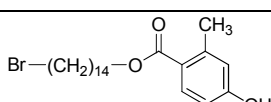
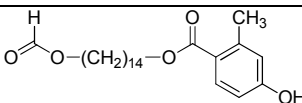
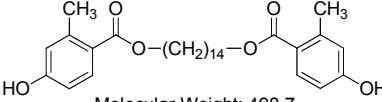
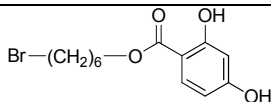
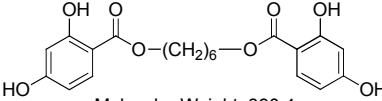
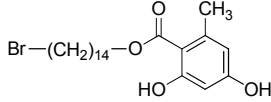
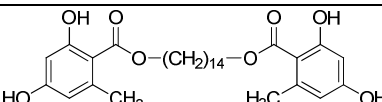
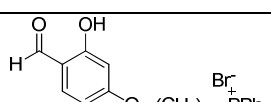
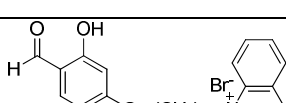


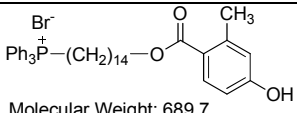
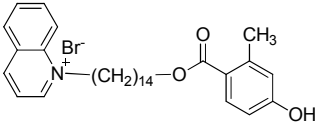
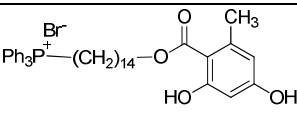
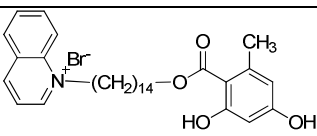
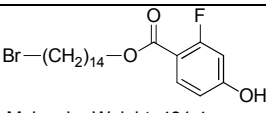
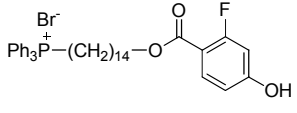
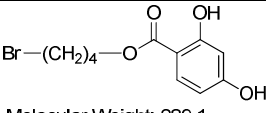
Appendix C: Structure of synthesized TAO inhibitors

Cmpounds	Reference Number	Structure
TAO1	PFG64 1-3	 <p>Molecular Weight: 552,4</p>
TAO2	PFG53 1-5	 <p>Molecular Weight: 580,4</p>
TAO3	PFG64 1-6	 <p>Molecular Weight: 594,5</p>
TAO4	PFG59 1-8	 <p>Molecular Weight: 622,5</p>
TAO5	PFG64 1-10 CDVI25	 <p>Molecular Weight: 650,6</p>
TAO6	PFG64 1-12 CIGI11	 <p>Molecular Weight: 678,6</p>
	CDVI20	 <p>Molecular Weight: 485,5</p>
TAO7	PFG63 1-8	 <p>Molecular Weight: 527,6</p>
TAO8	PFG63 1-9	 <p>Molecular Weight: 541,6</p>

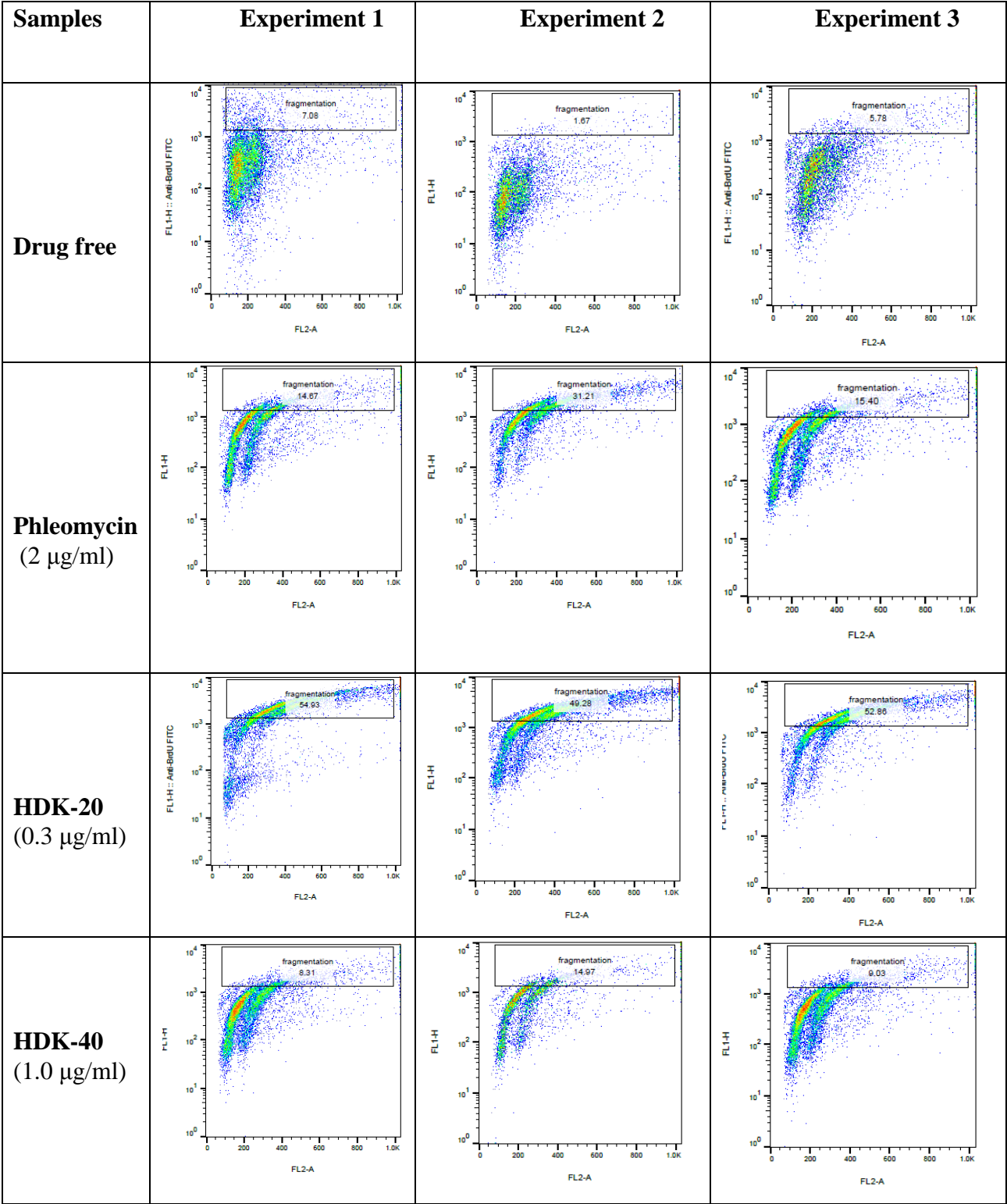
TAO9	PFG63 1-10	 <p>Molecular Weight: 555,7</p>
TAO10	PFG63 1-12 CDVI19	 <p>Molecular Weight: 583,7</p>
TAO16	PFG80	 <p>Molecular Weight: 308,4</p>
TAO17	PFG82	 <p>Molecular Weight: 508,6</p>
TAO18	PFG83	 <p>Molecular Weight: 294,4</p>
TAO19	PFG86	 <p>Molecular Weight: 294,4</p>
TAO20	PFG76	 <p>Molecular Weight: 555,7</p>
TAO21	PFG95	 <p>Molecular Weight: 555,7</p>
TAO22	CDVI24/F3	 <p>Molecular Weight: 474,5</p>
TAO23	CIGI 2	 <p>Molecular Weight: 530,5</p>
TAO24	CIGI 4	 <p>Molecular Weight: 558,5</p>

TAO25	CIGI 5	 <p>Molecular Weight: 691,7</p>
TAO26	CIGI 1/F2	 <p>Molecular Weight: 338,4</p>
TAO27	VBI 3	 <p>Molecular Weight: 719,7</p>
TAO28	CIGI 6	 <p>Molecular Weight: 586,6</p>
TAO29	CIGI 1/F3	 <p>Molecular Weight: 446,5</p>
TAO30	CIGI 3/F3	 <p>Molecular Weight: 502,6</p>
TAO31	CDVI24/F1	 <p>Molecular Weight: 401,3</p>
TAO32	VBI 1/F3	 <p>Molecular Weight: 530,6</p>
TAO33	VBI 1/F2	 <p>Molecular Weight: 422,6</p>
TAO34	VBI 1/F1	 <p>Molecular Weight: 457,4</p>
TAO35	TDI 5/F3	 <p>Molecular Weight: 413,4</p>

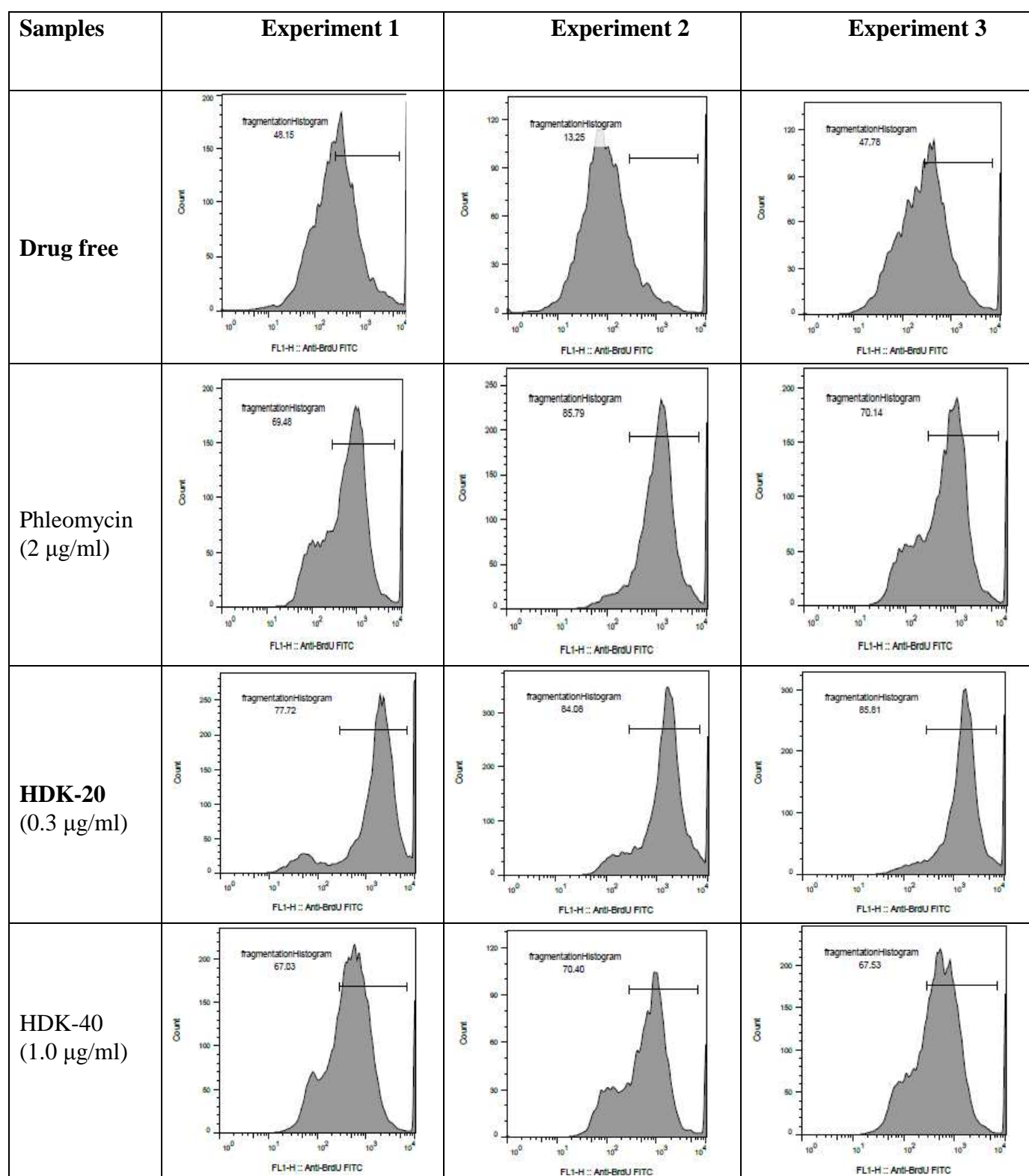
TAO36	TDI 5/F5	 <p>Molecular Weight: 470,6</p>
TAO37	TDI 5/F4	 <p>Molecular Weight: 378,5</p>
TAO38	TDI 7/F4	 <p>Molecular Weight: 427,4</p>
TAO39	TDI 7/F5	 <p>Molecular Weight: 392,5</p>
TAO40	TDI 11/F5	 <p>Molecular Weight: 498,7</p>
TAO41	TDI 9/F3	 <p>Molecular Weight: 317,2</p>
TAO42	TDI 9/F5	 <p>Molecular Weight: 390,4</p>
TAO43	TDI 13/F1	 <p>Molecular Weight: 443,4</p>
TAO44	TDI13/F3	 <p>Molecular Weight: 530,6</p>
TAO45	TDI 15	 <p>Molecular Weight: 675,7</p>
TAO46	TDI 16	 <p>Molecular Weight: 542,5</p>

TAO47	TDI 17	 <p>Molecular Weight: 689,7</p>
TAO48	TDI 18	 <p>Molecular Weight: 556,6</p>
TAO49	TDI 20	 <p>Molecular Weight: 705,7</p>
TAO50	TDI 21	 <p>Molecular Weight: 572,6</p>
TAO51	TDI 19/F2	 <p>Molecular Weight: 431,4</p>
TAO52	TDI 26	 <p>Molecular Weight: 693,7</p>
TAO53	LAGI 1	 <p>Molecular Weight: 289,1</p>

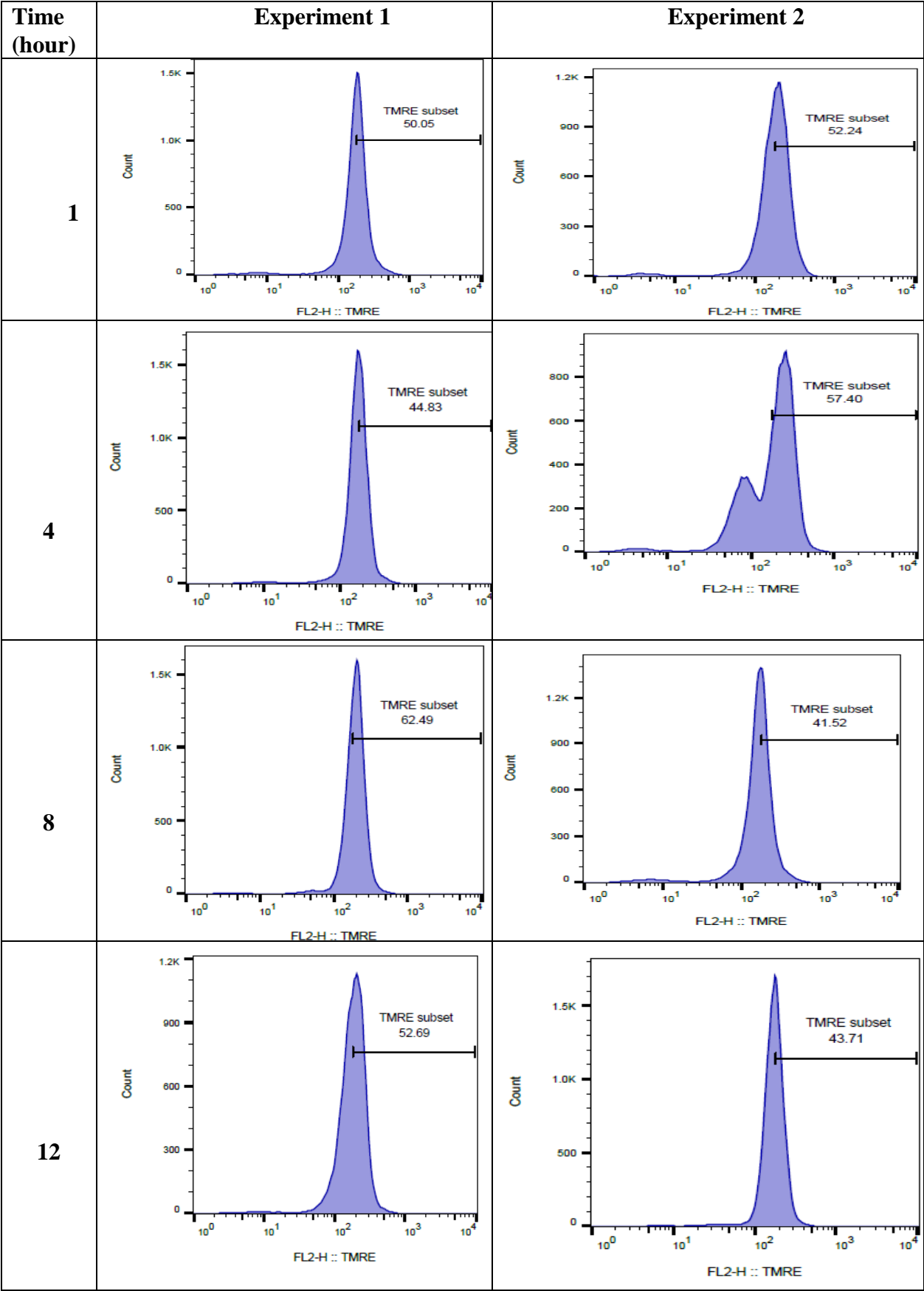
Appendix D: TUNEL assay dot plot of treated and untreated *T. brucei* s427 WT cells



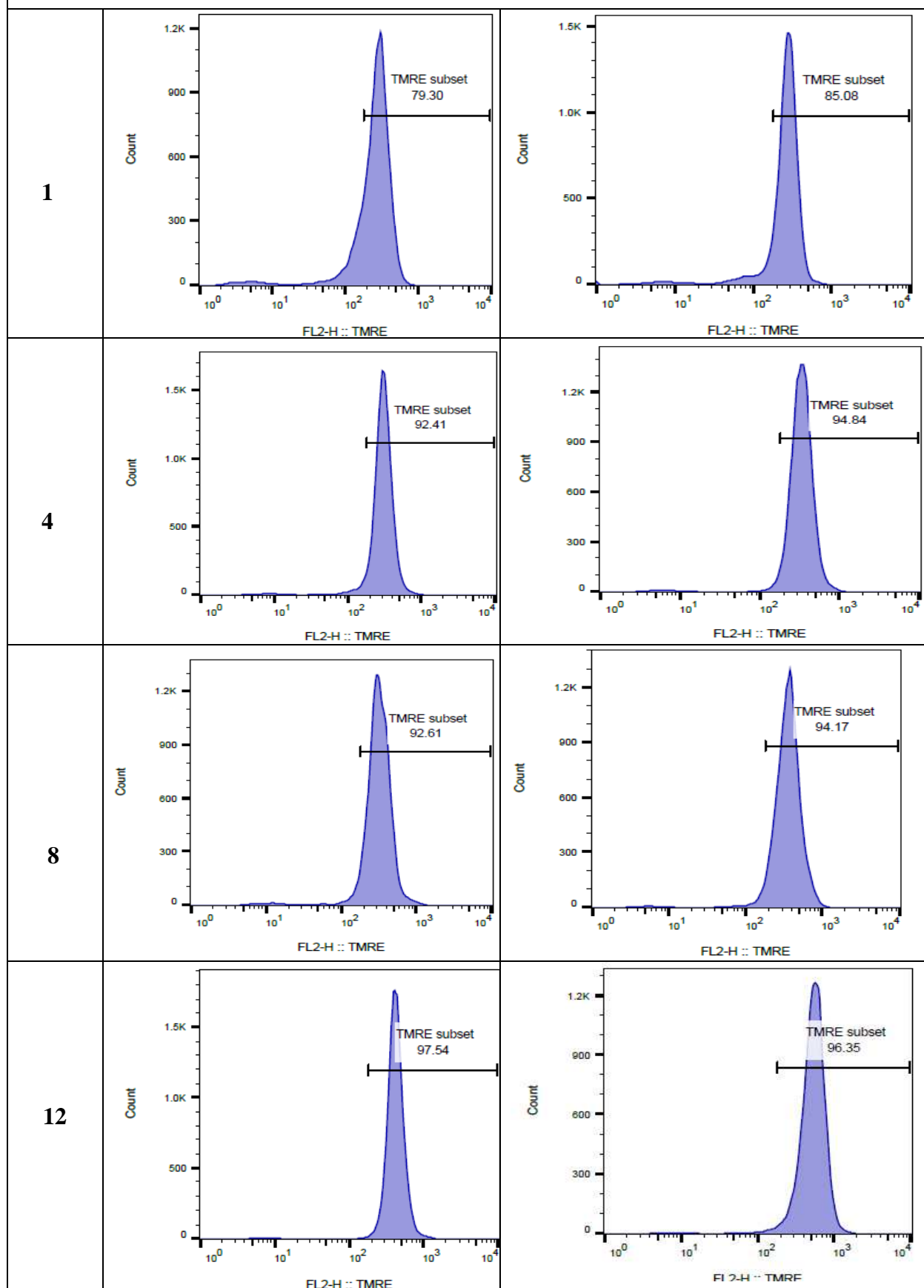
Appendix E: TUNEL assay histogram plot of treated and untreated *T. brucei* s427 wt cells



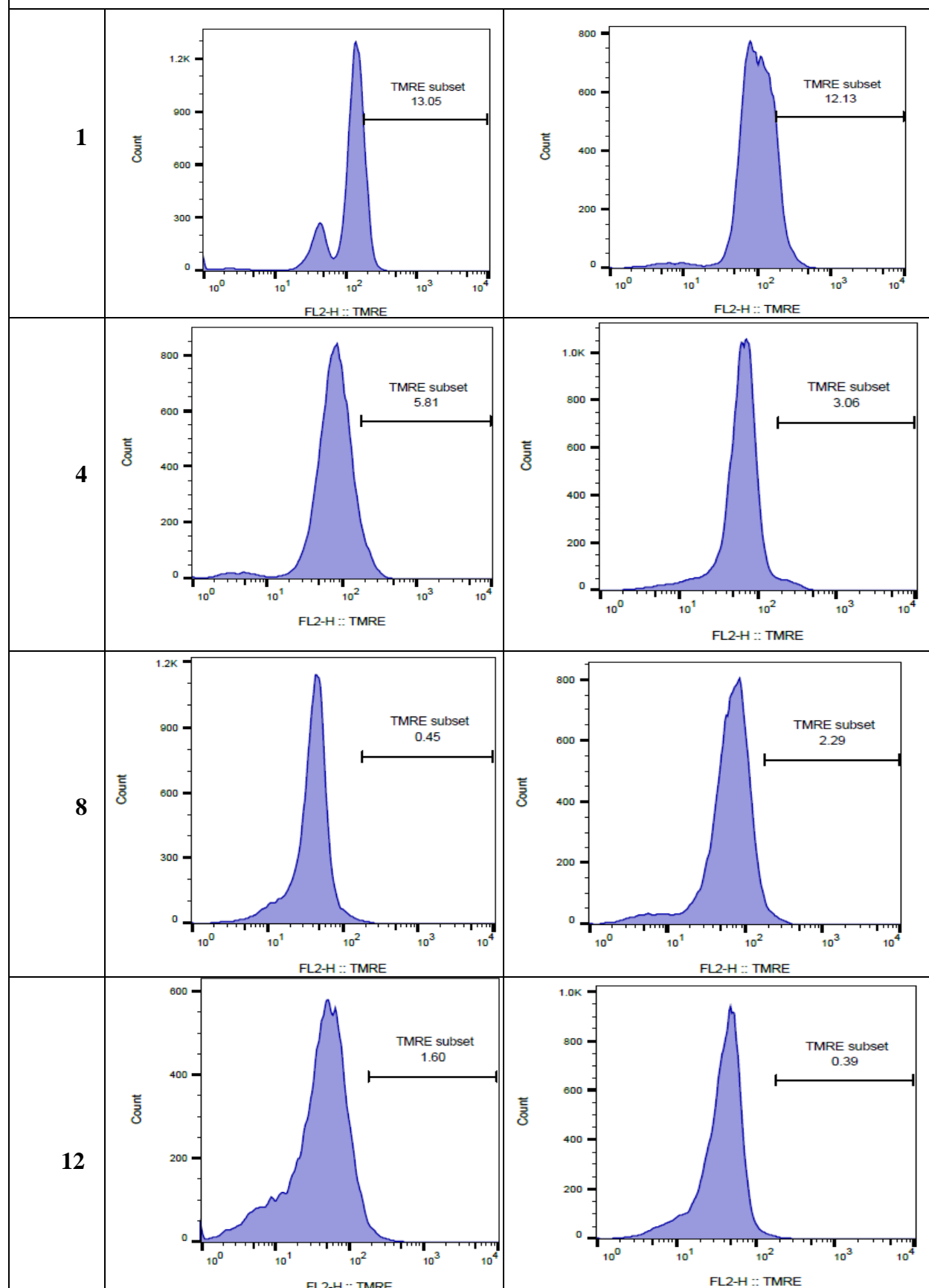
Appendix F: Mitochondrial membrane potential (% Ψ_m) of untreated *T.b.b* s427 WT cells



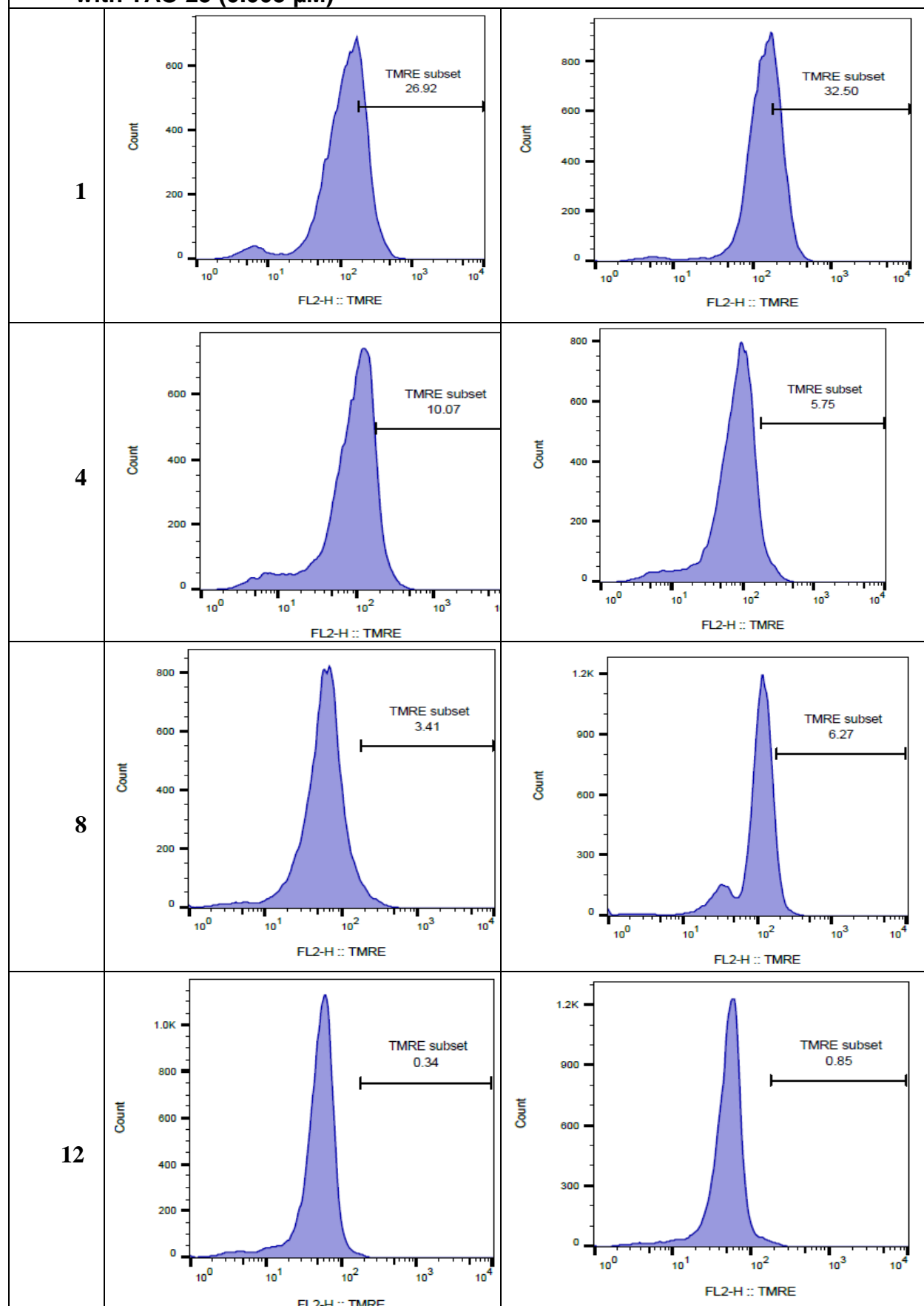
Mitochondrial membrane potential (% Ψ_m) of treated *T.b.b* s427 WT cells with Troglitazone (10 μ M).



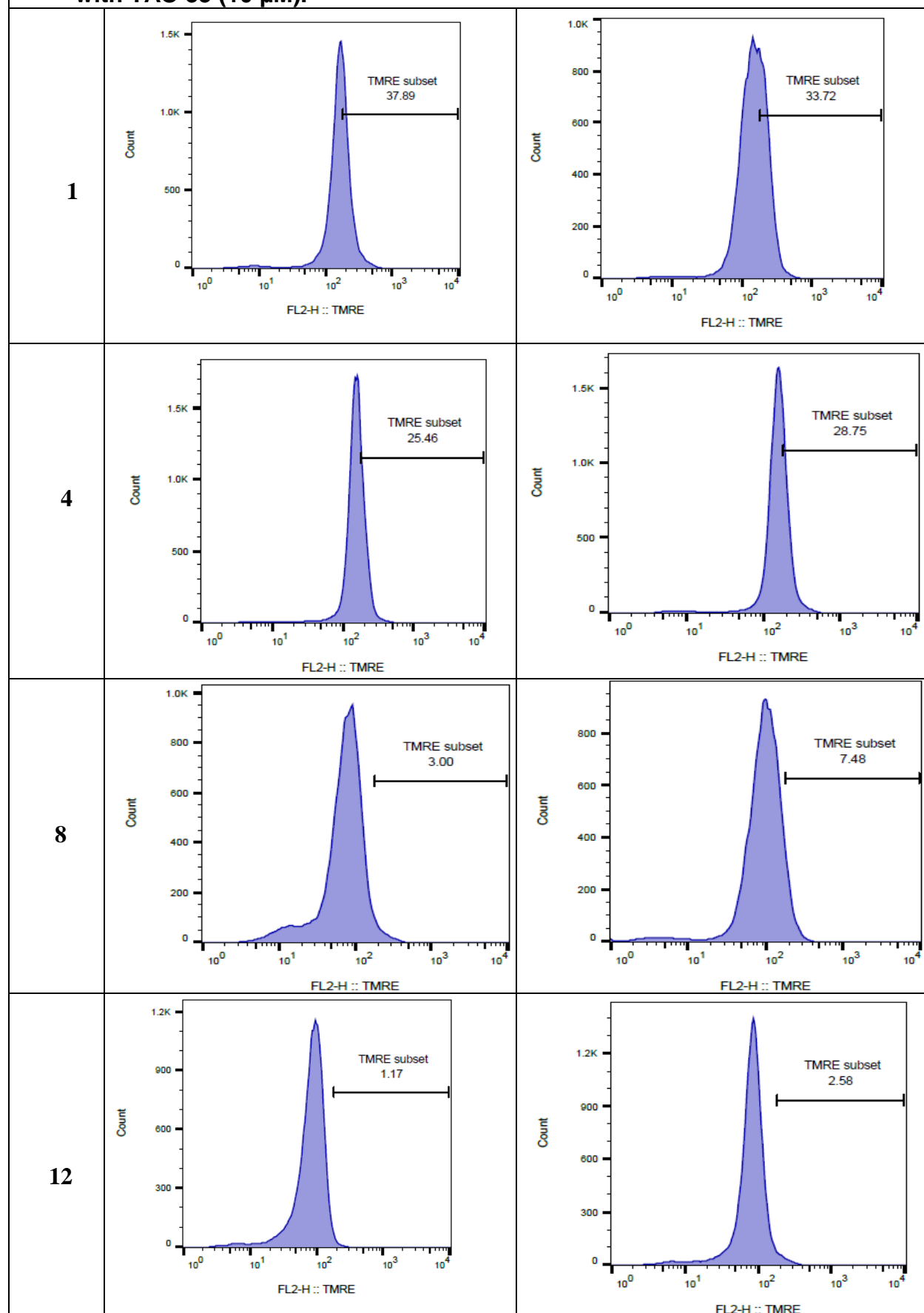
Mitochondrial membrane potential (% Ψ_m) of treated *T.b.b* s427 WT cells with Valinomycin (100 nM).



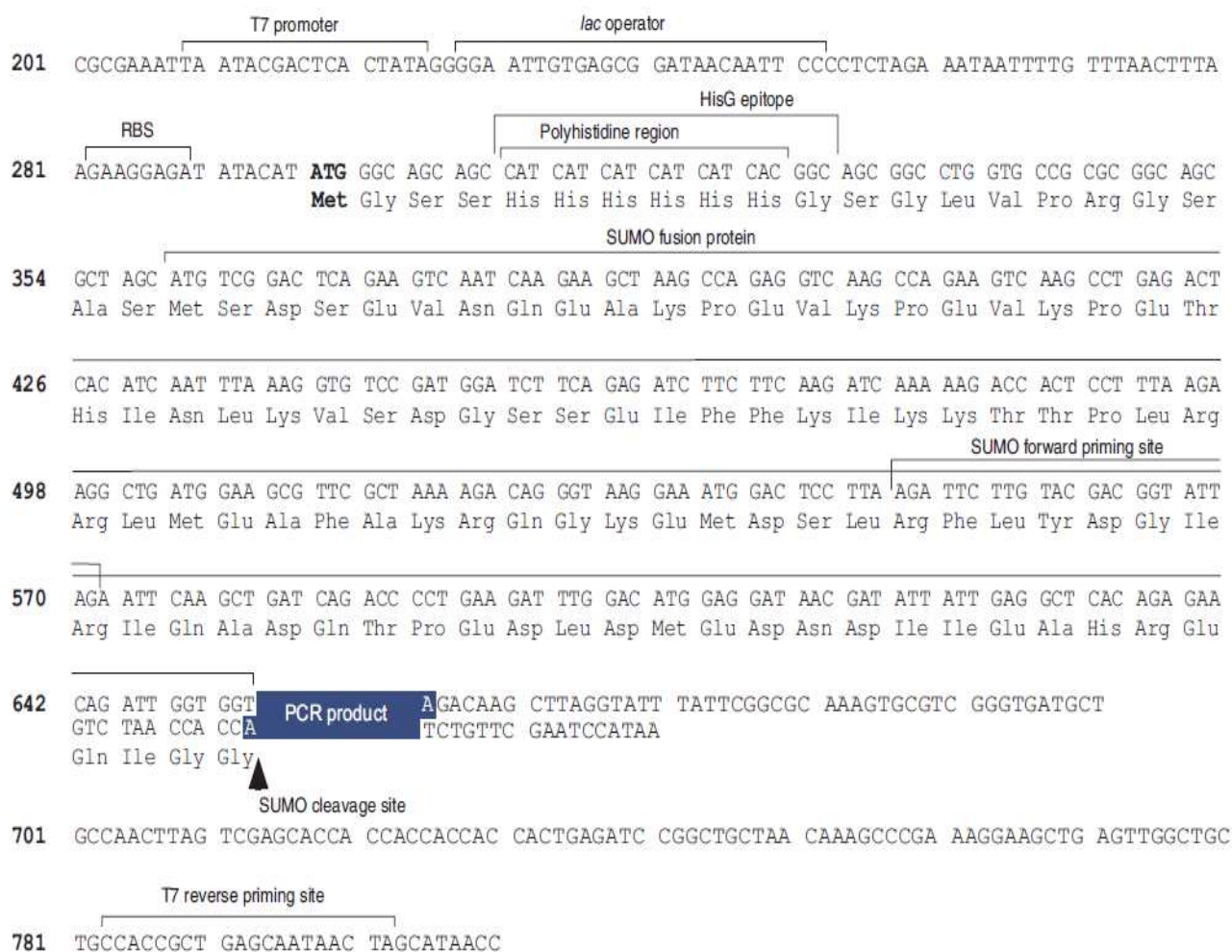
Mitochondrial membrane potential (% Ψ_m) of treated *T.b.b* s427 WT cells with TAO 25 (0.005 μ M)



Mitochondrial membrane potential (Ψ_m) of treated *T.b.b* s427 WT cells with TAO 33 (10 μ M).



Appendix G: TAO cloning in pET SUMO showing the SUMO cleavage site.



Appendix H: Gene sequences and Primer design

Full length (FL) TAO

ATGTTTCGTAACCACGCATCGAGGATCACTGCCGCAGCTGCGCCTTGGGTGCTCCGGACGGCTTGCCGCCA
GAAGTCTGACGCCAAAAACACCTGTGTGGGGACACACTCAACTGAACCGTCTCAGTTTTTTGGAAACCGTGC
CTGTCGTTCCCTTTGCGTGTTTCCGATGAAAGCAGTGAGGACCGCCCCACCTGGAGCCTTCCCGATATTGAGA
ATGTGGCCATAACGCACAAGAAGCCAAACGGCCTCGTTGATACACTCGCCTACCGCAGCGTCCGCACCTGC
CGCTGGTTATTTGACACATTCTCTCTACCGTTTCGGTTCCATCACGGAGAGCAAAGTCATCAGCCGCTGC
CTTTTCTTGAAACTGTTGCCGGTGTCCTGGGATGGTCCGTGGAATGTTGCGCCACCTTTCATCATTGCGG
TACATGACGCGCGACAAGGGTTGGATTAACACTCTTCTTGTGGAAGCAGAGAATGAGCGCATGCACCTCAT
GACGTTTCATTGAACTTCGCCAACCAGGGCTCCCCCTACGCGTTTCCATCATTATTACGCAAGCCATTATGTA
CCTCTTCCCTCCTGGTCGCCTATGTGATTTCCTTGTACACCGCTTGTGCGTTACCTTGAAGAGGAA
GCCGTCATTACATACACCGGCGTTATGAGAGCAATTGACGAAGGAAGGCTGCGCCCTACCAAAAAATGATGT
TCCCGAAGTGGCTCGCGTGTACTGGAACCTCAGCAAAAATGCCACATTCGCGACCTCATCAACGTGATCC
GAGCTGACGAGGCGGAGACCGTGTCTTAACACACATTTGCTGACATGCACGAAAAACGCTGCAAAA
CAGTGTCAACCCCTTCGTTGTTCTGAAGAAGAACCAGAGGAAATGTACTCCAACCAACCAAGTGGTAAGA
CAAGGACGGATTTTGAAGCGAAGGCGCCAAAACACTGCGAGTAATGTAAACAAACACGTGTAA

One letter amino acid sequence for full length TAO.

MFRNHASRITAAAAPWVLR**TACRQK**SDAKTPVWGHTQLNRLSFLETVPVVPLRVSDASSE
DRPTWSLPDIENVAITHKKPNGLVDTLAYRSVRTCRWLFDTFSLYRFGSITESKVISRCL
FLETVAGVPGMVGGMLRHLSSLRYMTRDKGWINTLLVEAENERMHLMTFIELRQPGLPLR
VSIITQAIMYLFLLVAYVISPRFVHRFVGYLEEEAVITYTGVMMRAIDEGRLRPTKNDVP
EVARVYWNLSKNATFRDLINVIRADEAEHRVVNHTFADMHEKRLQNSVNPFFVLKKNPEE
MYSNQPSGKTRTDFGSEGAKTASNVNKHV

ΔMTS TAO sequence (915 bp)

TCTGACGCCAAAACACCTGTGTGGGGACACACTCAACTGAACCGTCTCAGTTTGGAAACCGTGCCTGTCGTTCCCTTTCGGT
GTTTCCGATGAAAGCAGTGAGGACCGCCCCACCTGGAGCCTTCCCGATATTGAGAATGTGGCCATAACGCACAAGAAGCCAA
ACGGCCTCGTTGATACACTCGCTACCGCAGCGTCCGCACCTGCCGCTGGTTATTTGACACATTCTCTCTACCGTTTCGGTT
CCATCACGGAGAGCAAAGTCATCAGCCGCTGCCTTTTCTTGAAACTGTTGCCGGTGTCGCGGGGATGGTCGGTGGAATGTTG
CGCCACCTTTCATCATTGCGGTACATGACGCGCGACAAGGGTGGATTAACACTCTT**CTTGTTGAAGCAGAGAATGAGCGC**AT
GCACCTCATGACGTTTCATTGAACCTTCGCCAACCAGGGCTCCCCCTACGCGTTTCCATCATTATTACGCAAGCCATTATGTACCT
CTTCCTCGTGGTGCCTATGTGATTTCCCCCGTTTGTACACCGCTTTGTCGGTTACCTTGAAGAGGAAGCCGTCATTACATAC
ACCGCGTTATGAGAGCAATTGACGAAGGAAGGCTGCGCCCTACCAAAAATGATGTTCCCGAAGTGGCTCGCGTGTACTGGA
ACCTCAGCAAAAATGCCACATTCCGCGACCTCATCAACGTGATCCGAGCTGACGAGGCGGAGCACCCTGTCGTTAACCACAC
ATTTGCTGACATGCACGAAAAACGCTGCAAAACAGTGTCAACCCCTTCGTTGTTCTGAAGAAGAACCCAGAGGAAATGTACT
CCAACCAACCAAGTGGTAAGACAAGGACGATTTTGGAAGCGAAGGCGCCAAAACCTGC**GAGTAATGTAAACAAACACGT**

Primers design for rTAO production using SUMO vector.

SUMO-TbAOX-DL-25-F1: **AGCGACGCCAAAACACCTGTGTGGG**

SUMO-TbAOX-FL-F1: **AGCCGTAACCACGCATCGAGG**

TbAOX-F2: **CTTGTTGAAGCAGAGAATGAGCGC**

SUMO-TbAOX-Rv: **TTACACGTGTTTGTTTACATTACTC**

His6-SUMO-TbAOX-FW: **CACCATGGGCAGCAGCCATCATCATC**

Primers design for TAO over-expression in BSF *T. brucei* s427WT

Forward- HDK559 GCGC **AAGCTT** ATGTTTCGTAACCACG

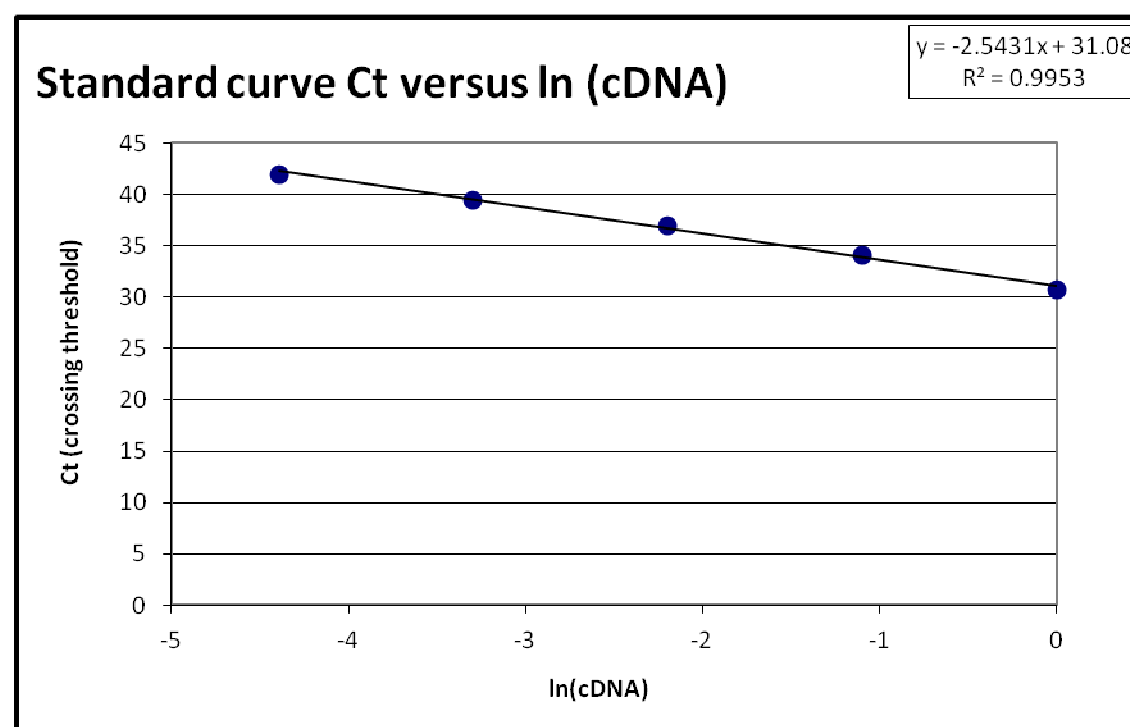
Reverse-HDK560: GC**GGATCC** TACACATGTTTGTTTACATT

Primers design for qRT-PCR

Forward-HDK637: CGAAGTGGCTCGCGTGTA

Reverse-HDK638: TGATGAGGTCGCGGAATGT

APPENDIX I: PCR analysis of TAO overexpression, showing amplification, standard curve and PCR primer Efficiency.



Reference

- Abubakar, A., Ogbadoyi, E.O., Okogun, J.I., Gbodi, T.I., Ibikunle, G.F. (2012). The identification of putative antitrypanosomal compounds in *Tridax procumbens* extracts. *Int. J. Med. Aromat. Plants.* 2, 185–194.
- Abubakar, A., Sabo, H.M., Onaolapo, A.Y., Abdullahi, S.S., Kabir, H.M., Danladi, I.O. (2016). The metabolism of african trypanosomes in relation to pathogenic mechanisms A Review. *Journal of Pharmacy and Biological Sciences.* 11, 68 – 72.
- Acha, P. N., Szyfres, B. (2003). Zoonoses and communicable diseases common to man and animals (Vol. 3). Pan American Health Org.
- Aksoy, S. (2003). Control of tsetse flies and trypanosomes using molecular genetics. *Vet. Parasitol.* 115, 125–145.
- Albert, M.A., Haanstra, J.R., Hannaert, V., Van Roy, J., Opperdoes, F.R., Bakker, B.M., Michels, P.A. (2005). Experimental and in silico analyses of glycolytic flux control in bloodstream form *Trypanosoma brucei*. *J. Biol. Chem.* 280, 28306–28315.
- Albright, J.W., Albright, J.F. (1981). Basis of the Specificity of Rodent Trypanosomes for Their Natural Hosts. 33, 355-363.
- Ali, J.A.M., Tagoe, D.N.A., Munday, J.C., Donachie, A., Morrison, L.J., de Koning, H.P. (2013) Pyrimidine biosynthesis is not an essential function for trypanosoma brucei bloodstream forms. *PLoS ONE* 8, e58034.
- Ali, J.A.M., Creek, D.J., Burgess, K., Allison, H.C., Field, M.C., Mäser, P., De Koning, H.P. (2013). Pyrimidine salvage in *Trypanosoma brucei* bloodstream forms and the trypanocidal action of halogenated pyrimidines. *Mol Pharmacol.* 83, 439-453
- Alli, L.A. Okochi, V.I. Adesokan, A.A. (2011). Anti-trypanosomal activity and haematological effects of aqueous extract of leaves of *Morinda lucida* on *Trypanosoma brucei brucei* infected rats. *Asian J. Pharm. Health Sci.* 1, 111–115.
- Alkhalidi, A.A.M, Creek, D.J., Ibrahim, H., Kim, D.H., Quashie, N.B., Burgess, K.E., Changtam, C., Barrett, M.P., Suksamrarn, A., de Koning, H.P. (2015). Potent trypanocidal curcumin analogs bearing a monoene linker motif act on *Trypanosoma brucei* by forming an adduct with trypanothione. *Mol Pharmacol.* 87, 451-464
- Alkhalidi, A.A.M., Martinek, J., Panicucci, B., Dardonville, C., Zíková, A., de Koning, H.P. (2016). Trypanocidal action of bisphosphonium salts through a mitochondrial target in bloodstream form *Trypanosoma brucei*. *Int. J. Parasitol. Drugs Drug Resist.* 6, 23-34.

- Alsford, S., Eckert, S., Baker, N., Glover, L., Sanchez-Flores, A., Leung, K.F., Turner, D.J., Field, M.C., Berriman, M., Horn, D. (2012). High-throughput decoding of antitrypanosomal drug efficacy and resistance. *Nature*. 482, 232-6.
- Alvarez-Miranda, M., Rodriguez-Gonzalez, A., Ptero, G., Lacal, J.C. (2003). Characterization of the mechanism of action of ES-285, a novel antitumor drug from *Mactomeris polynyma*. *Clin. Cancer Res.* 9, 17.
- Asbeck, K., Kurath, U., Roditi, I., Gibson, W. (2004). *Trypanosoma (Nannomonas) simiae* and *T. (N.) godfreyi* have genes encoding glutamic acid and alanine-rich proteins. *Mol. Biochem. Parasitol.* 134, 159-62.
- Ashour, H.M. (2008). Antibacterial, antifungal, and anticancer activities of volatile oils and extracts from stems, leaves, and flowers of *Eucalyptus sideroxylon* and *Eucalyptus torquata*, *Cancer Biol. Ther.* 7, 399-403.
- Atouguia, J.L.M., Kennedy, P.G.E. (2000). Neurological aspects of human African trypanosomiasis. In infectious diseases of the nervous system. L.E. Davis and P.G.E. Kennedy, editors. Butterworth-Heinemann. Oxford, United Kingdom. 321-372.
- Bacchi, C.J., Yarlett, N. (1993). Effects of antagonists of polyamine metabolism on African trypanosomes. *Acta Trop.* 54, 225–236.
- Baker, N., Glover, L., Munday, J. C., Aguinaga, A.D., Barrett, M. P., de Koning, H.P., Horn, D. (2012). Aquaglyceroporin 2 controls susceptibility to melarsoprol and pentamidine in African trypanosomes. *Proc. Natl. Acad. Sci. U.S.A.* 109, 10996–11001.
- Baker, N., de Koning, H.P., Mäser, P., Horn, D. (2013). Drug resistance in African trypanosomiasis: the melarsoprol and pentamidine story. *Trends Parasitol.* 29, 110-118.
- Bankole, A.E., Adekunle, A.A., Sowemimo, A.A., Umebese, C.E., Abiodun, O., Gbotosho, G. O. (2016). Phytochemical screening and in vivo antimalarial activity of extracts from three medicinal plants used in malaria treatment in Nigeria. *Parasitol Res.* 115, 299–305.
- Barreto-de-Albuquerque, J., Silva-dos-Santos, D., Pérez, A.R., Berbert, L.R., Santana-van-Vliet, E., Farias-de-Oliveira, D.A. (2015). *Trypanosoma cruzi* Infection through the oral route promotes a severe infection in mice: New disease form from an old infection? *PLoS Negl. Trop. Dis.* 9, e0003849.
- Barrett, M.P., Bakker, B.M., Breitling, R. (2010.) Metabolomic systems biology of trypanosomes. *Parasitology.* 137, 1285–90.
- Barrett, M.P., Boykin, D.W., Brun, R., Tidwell, R.R. (2007). Human African trypanosomiasis: pharmacological re-engagement with a neglected disease. *British Journal of Pharmacology.* 152, 1155–1171.
- Barrett, M.P., Burchmore, R.J., Stich, A. (2003). The trypanosomiases. *Lancet.* 362, 1469-80.

- Barrett, M.P., Croft, S.L. (2012). Management of trypanosomiasis and leishmaniasis. *British medical bulletin*. 104, 175–96.
- Barrett, M.P. (1999). The fall and rise of sleeping sickness. *Lancet*. 353, 1113–1114.
- Barry, J.S., Fiona, L.R., Michelle, M.L., Christopher, M.F., John, D.O., Victor, F., Robin, A.J.S., Michael, P.M., Kenneth, M.T., Taylor, K.M. (2010). A double-blind, placebo-controlled study to assess the mitochondria-targeted antioxidant mitoq as a disease-modifying therapy in parkinson's disease. *Movement Disorders*. 25, 1670–1674.
- Bates, P.A. (2007). Transmission of *Leishmania* metacyclic promastigotes by phlebotomine sand flies. *Int. J. Parasitol.* 37, 1097–1106.
- Batista, J.S., Oliveira, A.F., Rodrigues, C.M., Damasceno, C.A., Oliveira, I.R., Alves, H.M., Paiva, E.S., Brito, P.D., Medeiros, J.M., Rodrigues, A.C., Teixeira, M.M. (2009). Infection by *Trypanosoma vivax* in goats and sheep in the Brazilian semiarid region: From acute disease outbreak to chronic cryptic infection. *Vet. Parasitol.* 28, 131–5.
- Bauer, M.F, Hofmann, S., Neupert, W., Brunner, M. (2000). Protein translocation into mitochondria: the role of TIM complexes. *Trends Cell Biol.* 10, 25–31.
- Beck, K., Acestor, N., Schulfer, A., Anupama, A., Carnes, J., Panigrahi, A.K., Stuart, K. (2013). *Trypanosoma brucei* Tb927.2.6100 is an essential protein associated with kinetoplast DNA. *Eukaryot. Cell*. 12, 970–978.
- Bellofatto, V., Fairlamb, A.H., Henderson, G.B., Cross, G.A. (1987). Biochemical changes associated with alpha-difluoromethylornithine uptake and resistance in *Trypanosoma brucei*. *Mol. Biochem. Parasitol.* 25, 227–238.
- Berger, B.J., Carter, N.S., Fairlamb, A.H. (1995). Characterisation of pentamidine-resistant *Trypanosoma brucei brucei*. *Mol. Biochem. Parasitol.* 69, 289–298.
- Besteiro, S., Williams, R.A.M., Coombs, G.H., Mottram, J.C. (2007). Protein turnover and differentiation in *Leishmania*. *International journal for parasitology*. 37, 1063–1075.
- Bitonti, A.J., Dumont, J.A., McCann, P.P. (1986). Characterization of *Trypanosoma brucei brucei* S-adenosylmethionine decarboxylase and its inhibition by Berenil, pentamidine and methylglyoxal bis (guanyldrazone). *Biochem. J.* 237, 685–689.
- Bonner, W.D., Clarke, S.D., Rich, P.R. (1986). Partial purification and characterization of the quinol oxidase activity of *Arum maculatum* mitochondria. *Plant Physiol.* 80, 838–42
- Bridges, D.J., Gould, M.K., Nerima, B., Maser, P., Burchmore, R.J., de Koning, H.P. (2007). Loss of the high-affinity pentamidine transporter is responsible for high levels of cross-resistance between arsenical and diamidine drugs in African trypanosomes. *Mol Pharmacol.* 71, 1098–1108.

- Bringaud, F., Barrett, M.P., Zilberstein, D. (2012). Multiple roles of proline transport and metabolism in trypanosomatids. *Front. Biosci.* 17, 349- 74.
- Brohn, F.H., Clarkson, A.B. Jr. (1978). Quantitative effects of salicylhydroxamic acid and glycerol on *Trypanosoma brucei* glycolysis *in vitro* and *in vivo*. *Acta Trop.* 35, 23-33.
- Brown, C. (2008). Trypanosomiasis, African. In: Foreign animal diseases. 7th edition. Boca Raton, FL: United States Animal Health Association. p. 405-9.
- Brown, S.V., Hosking, P., Li, J., Williams, N. (2006). ATP synthase is responsible for maintaining mitochondrial membrane potential in bloodstream form *Trypanosoma brucei*. *Eukaryotic Eukaryot. Cell.* 5, 45-53.
- Brun, R., Blum, J., Chappuis, F., Burri, C. (2010). Human African Trypanosomiasis. *The Lancet.* 357, 148-159.
- Burgess, K.E., Creek, D., Dewsbury, P., Cook, K., Barrett, M.P. (2011). Semi-targeted analysis of metabolites using capillary-flow ion chromatography coupled to high resolution mass spectrometry. *Rapid Commun. Mass Spectrom.* 22, 3447–52.
- Burri, C. (2010). Chemotherapy against human African trypanosomiasis: is there a road to success? *Parasitology*, 137, 1987-1994.
- Butler, M.S. (2004). The role of natural product in chemistry in drug discovery. *J. Nat. Prod.* 67, 2141–2153.
- Caceres, A.J., Michels, P.A., Hannaert, V. (2010). Genetic validation of aldolase and glyceraldehyde-3-phosphate dehydrogenase as drug targets in *Trypanosoma brucei*. *Mol Biochem Parasitol.* 169, 50–54.
- Campos, M.C., Leon, L.L., Taylor, M.C., Kelly, J.M. (2014). Benznidazole-resistance in *Trypanosoma cruzi*: evidence that distinct mechanisms can act in concert. *Mol. Biochem. Parasitol.* 193, 17-9.
- Capewell, P., Veitch, N.J., Turner, C.M.R., Raper, J., Berriman, M., Hajduk, S.L., MacLeod, A. (2011). Differences between *Trypanosoma brucei gambiense* Groups 1 and 2 in their resistance to killing by trypanolytic factor 1. *PLoS Negl. Trop. Dis.* 5, e1287
- Carter, N.S., Berger, B.J., Fairlamb, A.H. (1995). Uptake of diamidine drugs by the P2 nucleoside transporter in melarsen-sensitive and -resistant *Trypanosoma brucei brucei*. *J. Biol. Chem.* 270, 28153–28157.
- Carter, N.S., Fairlamb, A.H. (1993). Arsenical-resistant trypanosomes lack an unusual adenosine transporter. *Nature.* 361, 173–175.

- Cecchi, G., Courtin, F., Paone, M., Diarra, A., Franco, J.R., Mattioli, R.C., Simarro, P.P. (2009). Mapping sleeping sickness in Western Africa in a context of demographic transition and climate change. *Parasite*. 16, 99-106.
- Chanda, S., Nair, R., (2010). Antimicrobial activity of *Polyalthia longifolia* (Sonn.) thw. var. *Pendula* leaf extracts against 91 clinically important pathogenic microbial strains. *Chinese Medicine*. 1, 31-38.
- Chanez, A.L., Hehl, A.B., Engstler, M., Schneider, A. (2006) Ablation of the single dynamin of *T. brucei* blocks mitochondrial fission and endocytosis and leads to a precise cytokinesis arrest. *J. Cell Sci*. 119, 2968-2974.
- Chaudhuri, M., Ott, R.D., Hill, G.C. (2006). Trypanosome alternative oxidase: from molecule to function. *Trends Parasitol*. 22, 484-91.
- Chowdhury, Arnab Roy, Rahul Bakshi, Jianyang Wang, Gokben Yildirim, Beiyu Liu, Valeria Pappas-Brown, Gökhan Tolun *et al.* (2010) "The killing of African trypanosomes by ethidium bromide." *PLoS Pathog* 6, e1001226.
- Chris, J.P., Jay, D.K. (2014). Semi-synthetic artemisinin: a model for the use of synthetic biology in pharmaceutical development. *Nature reviews microbiology*. 12, 355 – 367.
- Clarkson, A.B., Jr., Bienen, E.J., Pollakis, G., Grady, R.W. (1989). Respiration of bloodstream forms of the parasite *Trypanosoma brucei brucei* is dependent on a plant-like alternative oxidase. *J. Biol. Chem*. 264, 17770-17776.
- Clarkson, A.B., Jr., Bohn, F.H. (1976). Trypanosomiasis: an approach to chemotherapy by the inhibition of carbohydrate catabolism. *Science*. 194, 204-206.
- Colegate, S.M., Molyneux, R.J. (2008). *Bioactive Natural Products: Detection, isolation and structure determination*; CRC Press: Boca Raton, FL, USA. 421 – 437.
- Copeland, R.A., Pompliano, D.L., Meek, T.D. (2006). Drug–target residence time and its implications for lead optimization. *Nat. Rev. Drug Discov*. 5, 730–739.
- Corson, T.W., Crews, C.M. (2007). Molecular understanding and modern application of traditional medicines: triumphs and trials. *Cell*. 130,769–774.
- Cortes, L.A., Castro, L., Pesce, B., Maya, J.D., Ferreira, J., Castro-Castillo, V., Parra, E., Jara, J. A., López-Muñoz, R. (2015). Novel Gallate triphenylphosphonium derivatives with potent antichagasic activity. *PLoS ONE*. 10, e0136852.
- Coustou, V., Guegan, F., Plazolles, N., Baltz, T. (2010). Complete in vitro life cycle of *Trypanosoma congolense*: development of genetic tools. *PLoS Negl. Trop. Dis*. 4, e618.
- Cox, F.E. (2004). History of sleeping sickness (African trypanosomiasis). *Infect. Dis. Clin. N. Am*. 2, 231-45.

- Cragg, G.M., Newman, D.J. (2005). Biodiversity: A continuing source of novel drug leads. *Pure Appl. Chem.* 77, 7–24.
- Cragg, G.M., Newman, D.J. (2013). Natural products: A continuing source of novel drug leads. *Biochimica et Biophysica Acta.* 1830, 3670–3695.
- Creek, D.J., Anderson, J., McConville, M.J., Barrett, M.P. (2012). Metabolomic analysis of trypanosomatid protozoa. *Mol Biochem Parasitol.* 181, 73–84
- Creek, D.J., Jankevics, A., Breitling, R., Watson, D.G., Barrett, M.P., Burgess, K.E. (2011). Towards Global Metabolomics Analysis with Liquid Chromatography-Mass Spectrometry: Improved metabolite identification by retention time prediction. *Anal. Chem.* 83, 8703–10.
- Croft, S.L, Barret, M.P, Urbina, J.A. (2005). Chemotherapy of trypanosomiasis and leishmaniasis. *Trends Parasitol.* 21, 508–512.
- Croft, S.L, Yardley, V., Kendrick, H. (2002). Drug sensitivity of *Leishmania* species: some unresolved problems. *Trans. R. Soc. Trop. Med. Hyg.* 96, 127–9.
- Cuadros, R., Montejó G.E., Wandosell, F., Faircloth, G., Fernandez-Sousa, J.M., Avila, J. (2000). The marine compound spisulosine, an inhibitor of cell proliferation, promotes the disassembly of actin stress fibers. *Cancer Lett.* 152, 23.
- Dardonville, C., Alkhaldi, A.A.M., De Koning, H.P. (2015). SAR Studies of Diphenyl Cationic Trypanocides: Superior Activity of Phosphonium over Ammonium Salts. *ACS Med. Chem. Lett.* 6, 151–155.
- Davila, A.M., Silva, R.A. (2009). Animal trypanosomiasis in South America. Current status, partnership, and information technology. *Ann N Y Acad Sci.* 916, 199–212.
- de Araújo, M.V., de Souza, P.S., de Queiroz, A.C., da Matta, C.B., Leite, A.B., da Silva, A.E., de França, J.A., Silva, T., Camara, C.A. and Alexandre-Moreira, M.S. (2014). Synthesis, leishmanicidal activity and theoretical evaluations of a series of substituted bis-2-hydroxy-1, 4-naphthoquinones. *Molecules.* 19, 15180–15195.
- de Koning, H.P. (2001). Uptake of pentamidine in *Trypanosoma brucei* is mediated by three distinct transporters: implications for cross-resistance with arsenicals. *Mol. Pharmacol.* 59, 586–592.
- de Koning, H.P., Jarvis, S.M. (1997a). Hypoxanthine uptake through a purine-selective nucleobase transporter in *Trypanosoma brucei brucei* procyclic cells is driven by proton-motive force. *Eur. J. Biochem.* 247, 1102–1110.
- de Koning, H.P., Jarvis, S.M. (1997b). Purine nucleobase transport in bloodstream forms of *Trypanosoma brucei brucei* is mediated by two novel transporters. *Mol. Biochem. Parasitol.* 89, 245–258.

- de Koning, H.P., Jarvis, S.M., (1999). Adenosine transporters in bloodstream forms of *Trypanosoma brucei brucei*: substrate recognition motifs and affinity for trypanocidal drugs. *Mol. Pharmacol.* 56, 1162–1170.
- de Koning, H.P., Watson, C.J., Jarvis, S.M. (1998). Characterization of a nucleoside/proton symporter in procyclic *Trypanosoma brucei brucei*. *J. Biol. Chem.* 273, 9486–9494.
- de Macêdo, J. P., Schumann Burkard, G., Niemann, M., Barrett, M.P., Vial, H., Mäser, P., Roditi, I., Schneider, A., Bütikofer, P. (2015). An Atypical Mitochondrial Carrier That Mediates Drug Action in *Trypanosoma brucei*. *PLoS Pathog.* 11, e1004875.
- de Macedo-Silva, S.T., Urbina, J.A., de Souza, W., Rodrigues, J.C.F. (2013). *In Vitro* Activity of the Antifungal Azoles Itraconazole and Posaconazole against *Leishmania amazonensis*. *PLoS ONE* 8, e83247.
- Delespaux, V., de Koning, H.P., Jäger, T., Koch, O., Flohé, L. (2013). Transporters in anti-parasitic drug development and resistance. *Trypanosomatid diseases: molecular routes to drug discovery*, 335-350.
- Delespaux, V., De Koning, H.P. (2007). Drugs and drug resistance in African trypanosomiasis. *Drug Resist. Update.* 10, 30–50.
- Delespaux, V., Geysen, D., Van den Bossche, P., Geerts, S. (2008). Molecular tools for the rapid detection of drug resistance in animal trypanosomes. *Trends in Parasitology.* 24, 236-242
- Denninger, V., Figarella, K., Schonfeld, C., Brems, S., Busold, C., Lang, F., Hoheisel, J., Duszenko, M. (2007). Troglitazone induces differentiation in *Trypanosoma brucei*. *Exp Cell Res.* 313, 1805-1819.
- Desquesnes, M., Dia, M.L. (2004). Mechanical transmission of *Trypanosoma vivax* in cattle by the African tabanid *Atylotus fuscipes*. *Vet Parasitol.* 119, 9-19.
- Dewick, P.M. (2002). *Medicinal Natural Products: A Biosynthetic Approach*, 2nd ed. John Wiley and Son. West Sussex, UK. p. 520.
- Dias, D.A., Urban, S., Roessner, U. (2012). A Historical Overview of Natural Products in Drug Discovery. *Metabolites.* 2, 303-336.
- Dietmar, S. (2008). The history of African trypanosomiasis. *Parasites & Vectors.* 1, 3.
- Dike, V.T., Vihiiior, B., Bosha, J.A., Yin, T.M., Ebiloma, G.E., De Koning, H.P., Igoli, J.O., Gray, A.I. (2016). Antitrypanosomal activity of a novel taccalonolide from the tubers of *Tacca leontopetaloides*. *Phytochem. Anal.* 27, 217–221.
- Ding, N., Yahara, S., Nohara, T. (1992). Structure of mimengoside A, and B, new triterpenoid glycosides from *Buddlejae Flos* produced from China. *Chem. Pharm. Bull.*, 40, 780-782.

- Docampo, R., Moreno, S. N. J. (2002). Current chemotherapy of human African trypanosomiasis. *Parasitology Research*. 90, 10 - 13.
- Doko, A., Verhulst, A., Pandey, V.S., Van der Stuyft, P. (1997). Artificially induced *Trypanosoma brucei brucei* infection in Lagune and Borgou cattle in Benin. *Vet Parasitol*. 69, 151-7.
- Dolan, R.B., Okech, G., Alushula, H., Mutugi, M., Stevenson, P., Sayer, P.D., Njogu, A.R. (1990). Homidium bromide as a chemoprophylactic for cattle trypanosomiasis in Kenya. *Acta Tropica*. 47, 137-144.
- Doua, F., Boa, F.Y., Schechter, P.J., Miezian, T.W., Diali, D., Sanon, S.R. (1987). Treatment of human late stage gambiense trypanosomiasis with alpha-difluoromethylornithine (eflornithine): efficacy and tolerance in 14 cases in Cote d'Ivoire. *Am. J. Trop. Med. Hyg.* 37, 525-33.
- Drescher, D. G., Drescher, M. J., Ramakrishnan, N. A. (2009). Surface plasmon resonance (SPR) analysis of binding interactions of proteins in inner-ear sensory epithelia. *Auditory and Vestibular Research: Methods and Protocols*, 323-343.
- Dua, V. K., Verma, G., Agarwal, D.D., Kaiser, M., Brun, R. (2011). Antiprotozoal activities of traditional medicinal plants from the Garhwal region of North West Himalaya, India. *Journal of Ethnopharmacology*. 136, 123–128.
- Edmundo, C.G. (2002). Salivaria or Stercoraria? The *Trypanosoma rangeli* dilemma. *Kinetoplastid Biology and Disease*. 1, 5.
- Ehrlich, P. (1907). Chemotherapeutische Trypanosomen-Studien. *Berliner klinische Wochenschrift*. 11, 310–314.
- El Sayed, K.A., Dunbar, D.C., Perry, T.L., Wilkins, S.P., Hamann, M.T., Greenplate, J.T. (1997). Marine natural products as prototype insecticidal agents. *J. Agric. Food Chem.* 45, 2735–2739.
- Ene, A.C., Atawodi, S.E., Apeh, Y.E.O. (2014). *In vitro* and *In vivo* antitrypanosomal effects of petroleum ether, chloroform and methanol extracts of *Artemisia maritime* Linn. *Brit. J. Pharm. Res.* 4, 751-58.
- Engstler, M., Pfohl, T., Herminghaus, S. (2007). Hydrodynamic flow mediated protein sorting on the cell surface of trypanosomes. *Cell*. 131, 505-15.
- Eperon, G., Balasegaram, M., Potet, J., Mowbray, C., Valverde, O., Chappuis, F. (2014). Treatment options for second-stage gambiense human African trypanosomiasis. *Exp. Rev. Anti-infect. Ther.* 12, 1407-1417.
- Evans, D.A., Brown, R.C. (1973). The inhibitory effects of aromatic hydroxamic acids on the cyanide-insensitive terminal oxidase of *Trypanosoma brucei*. *Trans R Soc Trop Med Hyg.* 67, 258.

- Evans, D.A., Brightman, C.A. (1980). Pleomorphism and the problem of recrudescence parasitaemia following treatment with salicylhydroxamic acid (SHAM) in African trypanosomiasis. *Trans. R. Soc. Trop. Med. Hyg.* 74, 601-604.
- Eze, A.A., Gould, M.K., Munday, J.C., Tagoe, D.N.A., Stelmanis, V., Schnauffer, A., De Koning, H.P. (2016). Loss of mitochondrial membrane potential is a late adaptation of *Trypanosoma brucei brucei* to Isometamidium preceded by mutations in the γ Subunit of the F_1F_0 -ATPase. *PLoS Negl Trop Dis.* 10, e0004791
- Eze, C.O., Nworu, C.S., Esimone, C.O., Okore, V.C. (2014). Immunomodulatory activities of methanol extract of the whole aerial part of *Phyllanthus niruri* L. *J. Pharmacognosy Phytother.* 6, 41-46.
- Fabbretti, A., Gualerzi, C.O., Brandi, L. (2011). How to cope with the quest for new antibiotics. *FEBS Lett.* 585, 1673–1681.
- Fairlamb, A.H., Henderson, G.B., Cerami, A. (1989). Trypanothione is the primary target for arsenical drugs against African trypanosomes. *Proc. Natl. Acad. Sci.* 86, 2607-2611.
- Fairlamb, A.H. (1990). Future prospects for the chemotherapy of human trypanosomiasis. 1. Novel approaches to the chemotherapy of trypanosomiasis. *Trans. R. Soc. Trop. Med. Hyg.* 84, 613–617.
- Fairlamb, A.H., Blackburn, P., Ulrich, P., Chait, B., Cerami, A. (1985). Trypanothione: a novel bis (glutathionyl) spermidine cofactor for glutathione reductase in trypanosomatids. *Science.* 22, 1485–1487.
- Fairlamb, A.H., Carter, N.S., Cunningham, M., Smith, K. (1992). Characterisation of melarsen-resistant *Trypanosoma brucei brucei* with respect to cross-resistance to other drugs and trypanothione metabolism. *Mol. Biochem. Parasitol.* 53, 213–222.
- Fairlamb, A.H., Gow, N.A., Matthews, K.R., Waters, A.P. (2016). Drug resistance in eukaryotic microorganisms. *Nat. Microbiol.* 1, 16092.
- Fairlamb, A.H., Smith, K., Hunter, K.J. (1992). The interaction of arsenical drugs with dihydrolipoamide and dihydrolipoamide dehydrogenase from arsenical resistant and sensitive strains of *Trypanosoma brucei brucei*. *Mol. Biochem. Parasitol.* 53, 223–232.
- FAO (2016). <http://www.fao.org/ag/againfo/programmes/en/paat/disease.html>
- Fenn, K., Matthews K.R. (2007). The cell biology of *Trypanosoma brucei* differentiation. *Curr. Opin. Microbiol.* 10, 539–546.
- Ferrante, A., Allison, A.C. (1989). Alternative pathway activation of complement by African trypanosomes lacking a glycoprotein coat. *Parasite Immunol.* 5, 491-8.

- Fidalgo, L. M., Gille, L. (2011). Mitochondria and trypanosomatids: Targets and drugs. *Pharm. Res.* 28, 2758-2770.
- Fish, W.R., Looker, D.L., Marr, J.J., Berens, R.L. (1982). Purine metabolism in the bloodstream forms of *Trypanosoma gambiense* and *Trypanosoma rhodesiense*. *Biochim. Biophys. Acta* 719, 223–231.
- Franco, J.R., Simarro, P.P., Diarra, A., Ruiz-Postigo, J.A., Samo, M., Jannin, J.G. (2012). Monitoring the use of nifurtimox-eflornithine combination therapy (NECT) in the treatment of second stage gambiense human African trypanosomiasis. *Research and Reports in Tropical Medicine.* 3, 93–101.
- Galle, J., Attioua, B., Kaiser, M., Rusig, A., Lobstein, A., Vonthron-Senecheau, C. (2013). Eleganolone, a Diterpene from the French Marine Alga *Bifurcaria bifurcata* inhibits growth of the human pathogens trypanosoma brucei and Plasmodium falciparum. *Mar. Drugs.* 11, 599-610.
- Garcia, L.S. (2007). *Diagnostic Medical Parasitology*. Vol 2, 5th edn. ASM Press, Washington D. C, pp 771–812
- Garcia-Granados, A., Linan, E., Martínez, A., Rivas, F., Mesa-Valle, C. M., Castilla-Calvente, J. J., Osuna, A. J. (1997). *In vitro* action of ent-manoyl oxydes against Leishmania donovani. *Nat. Prod.* 60, 13-16.
- Georghiou, G.P. (1990). Overview of insecticide resistance. In: *Managing Resistance to Agrochemicals: From Fundamental Research to Practical Strategies*. Green, M.B., Le Baron, H.M., Moberg, W.K., Eds. ACS Symp. Ser. 421. Am. Chem. Soc. Washington, DC, USA. 18–41.
- Gerasimos, L., Kent, L.H. (2014). Motility and more: the flagellum of Trypanosoma brucei. *Nat. Rev. Microbiol.* 12, 505–518.
- Gerencser, L., Rinyu, L., Laszlo Kalman, L., Takahashi, E., Wraight, C.A., Maroti, P. (2004). Competitive binding of quinone and antibiotic stigmatellin to reaction centers of photosynthetic bacteria. *Acta Biologica Szegediensis.* 48, 25-33.
- Gibson, W.C., Stevens, J.R., Mwendia, C.M., Ngotho, J.N., Ndungu, J.M. (2001). Unravelling the phylogenetic relationships of African trypanosomes of suids. *Parasitology.* 122, 625-31.
- Gilbert, I.H. (2013). *Drug Discovery for Neglected Diseases: Molecular Target-Based and Phenotypic Approaches*. *J. Med. Chem.* 56, 7719-7726.
- Gilbert, I.H., Leroy, D., Frearson, J.A. (2011). Finding new hits in neglected disease projects: target or phenotypic based screening? *Curr Top Med Chem.* 11, 1284– 1291.

- Gile, G.H., Moog, D., Slamovits, C.H., Maier, U.G., Archibald, J.M. (2015). Dual Organellar Targeting of Aminoacyl-tRNA Synthetases in Diatoms and Cryptophytes. *Genome Biol. Evol.* 7, 1728–1742.
- Giordani, F., Morrison, L. J., Rowan, T., De Koning, H.P., Barrett, M.P. (2016). The animal trypanosomiasis and their chemotherapy - a review. *Parasitol. Int.* 143, 1862-1889.
- Gnipova, A., Subrtova, K., Panicucci, B., Horvath, A., Lukes, J., Zikova, A. (2015). The ADP/ATP carrier and its relationship to OXPHOS in an ancestral protist *Trypanosoma brucei*. *Eukaryot. Cell.* 14, 297–310.
- Goldberg, B., Rattendi, D., Lloyd, D., Sufrin, J.R., Bacchi, C.J. (1998). Effects of intermediates of methionine metabolism and nucleoside analogs on S-adenosylmethionine transport by *Trypanosoma brucei brucei* and a drug-resistant *Trypanosoma brucei rhodesiense*. *Biochem. Pharmacol.* 56, 95-103.
- Gould, M. K., Vu, X. L., Seebeck, T., de Koning, H.P. (2008). Propidium iodide-based methods for monitoring drug action in the kinetoplastidae: Comparison with the Alamar Blue assay. *Anal. Biochem.* 382, 87-93.
- Gould, M.K., Bachmaier, S., Ali, J.A.M., Alsford, S., Tagoe, D.N.A., Munday, J.C., Schnauffer, A.C., Horn, D., Boshart, M., De Koning, H.P. (2013). Cyclic AMP effectors in African trypanosomes revealed by genome-scale RNAi library screening for resistance to the phosphodiesterase inhibitor Cpd A. *Antimicrob. Agents Chemother.* 57, 4882-4893.
- Gould, M.K., De Koning, H.P. (2011). Cyclic nucleotide signalling in protozoa. *FEMS Microbiol. Rev.* 35, 515-541.
- Gow, A.G., Simpson, J.W., Picozzi, K. (2007). First report of canine African trypanosomosis in the UK. *J. Small. Anim. Pract.* 48, 658-61.
- Grady, R.W., Bienen, E.J., Clarkson, A.B., Jr. (1986). p-Alkyloxybenzhydroxamic acids, effective inhibitors of the trypanosome glycerol-3-phosphate oxidase. *Mol. Biochem. Parasitol.* 19, 231-240.
- Grady, R.W., Bienen, E.J., Clarkson, A.B., Jr. (1986). p-Alkyloxybenzhydroxamic acids, effective inhibitors of the trypanosome glycerol-3-phosphate oxidase. *Molecular and biochemical parasitology.* 19, 231-240
- Grady, R.W., Bienen, E.J., Dieck, H.A., Saric, M. And Clarkson, A.B., Jr. (1993). N-n-Alkyl-3, 4-dihydroqbenzamides as inhibitors of the trypanosome alternative oxidase: activity *in vitro* and *in vivo*. *Antimicrob. Agents Chemother.* 37, 1082-1085.
- Graf, F. E., Ludin, P., Wenzler, T., Kaiser, M., Brun, R., Pyana, P. P., Büscher, P., Koning, H.P., Horn, D., Maser, P. (2013). Aquaporin 2 mutations in *Trypanosoma brucei gambiense* field isolates correlate with decreased susceptibility to pentamidine and melarsoprol. *PLoS Negl. Trop. Dis.* 7, e2475.

- Graf, F.E., Baker, N., Munday, J.C., De Koning, H.P., Horn, D., Mäser, P. (2015). Chimerization at the AQP2-AQP3 locus is the genetic basis of melarsoprol-pentamidine cross-resistance in clinical *Trypanosoma brucei gambiense* isolates. *Int J Parasitol Drugs Drug Res.* 5, 65-68.
- Graf, F.E., Ludin, P., Wenzler, T., Kaiser, M., Brun, R., Pyana, P.P., Buscher P., de Koning, H.P., Horn, D., Maser, P. (2013). Aquaporin 2 Mutations in *Trypanosoma brucei gambiense* Field Isolates Correlate with Decreased Susceptibility to Pentamidine and Melarsoprol. *PLoS Negl. Trop. Dis.* 7: e2475.
- Grant, P.T., Sargent, J.R. (1960). Properties of L-alpha-glycerophosphate oxidase and its role in the respiration of *Trypanosoma rhodesiense*. *Biochem. J.* 76, 229-37.
- Grewal, A.S., Pandita, D., Bhardwaj, S., Lather, V. (2016). Recent Updates on Development of Drug Molecules for Human African Trypanosomiasis. *Curr Top Med Chem.* 16, 2245-65.
- Gurib-Fakim, A. (2006). Medicinal plants: traditions of yesterday and drugs of tomorrow. *Mol. Aspects Med.* 27, 1–93.
- Gustave, S., Pierre, F., Oumarou, F., Prosper, I.N., Judith, T., Flobert N., Tazoacha A. (2015). Trypanosome infection rates in tsetse flies in the “silent” sleeping sickness focus of Bafia in the Centre Region in Cameroon. *Parasites & Vectors.* 8, 528.
- Gutierrez, C., Corbera, J.A., Morales, M., Büscher, P. (2006). Trypanosomosis in goats: current status. *Ann. N Y Acad. Sci.* 1081, 300-10.
- Haanstra, J.R., Van, T.A, Kessler, P., Reijnders, W., Michels, P.A., Westerhoff, H.V., Parsons, M., Bakker, B.M. (2008). Compartmentation prevents a lethal turbo-explosion of glycolysis in trypanosomes. *Proc Natl Acad Sci U S A.* 105, 17718-17723.
- Hamilton, P.B., Adams, E.R, Malele, I.I, Gibson, W.C. (2008). A novel, high-throughput technique for species identification reveals a new species of tsetse-transmitted trypanosome related to the *Trypanosoma brucei* subgenus, Trypanozoon. *Infect. Genet. Evol.* 8, 26–33.
- Hamilton, V., Singha, U.K., Smith, J.T., Weems, E., Chaudhuri, M. (2014). Trypanosome Alternative Oxidase Possesses both an N-Terminal and Internal Mitochondrial Targeting Signal. *Eukaryot. Cell.* 13, 539-547.
- Hammond, D.J., Aman, R.A., Wang, C.C. (1985). The role of compartmentation and glycerol kinase in the synthesis of ATP within the glycosome of *Trypanosoma brucei*. *J. Biol. Chem.* 260, 15646- 15654.
- Hannaert, V. (2011). Sleeping Sickness Pathogen (*Trypanosoma brucei*) and Natural Products: Therapeutic Targets and Screening Systems. *Planta Med.* 77, 586–597.
- Hassani, S., Asghari, G., Yousefi, H., Kazemian, A., Rafieiean, M., Darani, H.Y. (2013). Effects of different extracts of *Eucalyptus camaldulensis* on *Trichomonas vaginalis* parasite in culture medium. *Adv. Biomed. Res.* 2, 47.

- Hawking, F. (1936). The absorption of arsenical compounds and tartar emetic by normal and resistant trypanosomes and its relation to drugresistance. *J. Pharm. Exp. Therap.* 59, 123–156.
- Helfert, S., Estevez, A.M., Bakker, B., Michels, P., Clayton, C. (2001). Roles of triosephosphate isomerase and aerobic metabolism in *Trypanosoma brucei*. *Biochem. J.* 357, 117–25.
- Higgins, C.F. (1992). ABC transporters: from microorganisms to man. *Annu. Rev. Cell Biol.* 8, 67–113.
- Ibrahim, H.M.S., Al-Salabi, M.I., Sabbagh, N.E., Quashie, N.B., Alkhaldi, A.A.M., Escale, R., Smith, T.K., Vial, H.J., De Koning, H.P. (2011). Symmetrical choline-derived dications display strong anti-kinetoplastid activity. *J. Antimicrob. Chemother.* 66, 111-125.
- Igoli, J.O., Gray, A.I., Clements, C.J., Mouad, H.A. (2011). Antitrypanosomal activity and cytotoxicity of some compounds and extracts from Nigerian medicinal plants. In: *Phytochemicals – Bioactivities and Impact on Health*, Iraj Rasooli, Ed. InTech, pp. 375-88.
- Ilboudo, H., Bras-Gonçalves, R., Camara, M., Flori, L., Camara, O., Sakande, H., Leno, M., Petitdidier, E., Jamonneau, V., Bucheton, B. (2014). Unravelling human trypanotolerance: IL8 is associated with infection control whereas IL10 and TNF α are associated with subsequent disease development. *PLoS Pathog.* 10, e1004469.
- Imamura, H., Downing, T., Van den Broeck, F., Sanders, M.J., Rijal, S., Sundar, S., Mannaert, A., Vanaerschot, M., Berg, M., De Muylder, G., Dumetz, F. (2016). Evolutionary genomics of epidemic visceral leishmaniasis in the Indian subcontinent. *Elife.* 5, e12613.
- Ingrid, S., Zdenek, V., Frederic, B., Pete, F., Julius, L., Anton, H. (2013). Characterization of Two Mitochondrial Flavin Adenine Dinucleotide-Dependent Glycerol-3-Phosphate Dehydrogenases in *Trypanosoma brucei*. *Eukaryotic Cell.* 12, 1664.
- Jacobs, R.T., Nare, B., Wring, S.A., Orr, M.D., Chen, D., Sligar, J.M., Jenks, M.X., Noe, R.A., Bowling, T.S., Mercer, L.T., Rewerts, C. (2011). SCYX-7158, an orally-active benzoxaborole for the treatment of stage 2 human African trypanosomiasis. *PLoS Negl Trop Dis.* 5, e1151.
- Jamonneau, V., Ilboudo, H., Kaboré, J., Kaba, D., Koffi, M., Solano, P., Garcia, A., Courtin, D., Laveissière, C., Lingue, K., Büscher, P., Bucheton, B. (2012). Untreated human infections by *Trypanosoma brucei gambiense* are not 100% fatal *PLoS. Negl. Trop. Dis.* 6, e1691.
- Jannin, J, Cattand, P. (2004). Treatment and control of human African trypanosomiasis. *Curr Opin Infect Dis.* 17, 565-571.
- Jensen, R.E., Englund, P.T. (2012). Network news: the replication of kinetoplast DNA. *Annu. Rev. Microbiol.* 66, 473–491.
- Jones, D.C., Foth, B.J., Urbaniak, M.D., Patterson, S., Ong, H.B., Berriman, M., Fairlamb, A.H. (2015). Genomic and Proteomic Studies on the Mode of Action of Oxaboroles against the African Trypanosome. *PLoS Negl Trop Dis.* 9, e0004299

- Jones, T.W., Davila, A.M. (2001). *Trypanosoma vivax* out of Africa. Trends Parasitol. 17, 99-101.
- Juszczuk, M.I., Rychter A.M. (2003). Alternative oxidase in higher plants. Acta Biochemica Polonica. 50, 1257–1271.
- Kaiser, M., Bray, M.A., Cal, M., Trunz, B.B., Torreele, E., Brun, R. (2011). Antitrypanosomal Activity of Fexinidazole, a New Oral Nitroimidazole Drug Candidate for Treatment of Sleeping Sickness. Antimicrobial agents and chemotherapy. 55, 5602–5608
- Kaminsky, R., Zweggarth, E. (1989). Feeder layer-free in vitro assay for screening antitrypanosomal compounds against *Trypanosoma brucei brucei* and *T. b. evansi*. Antimicrob. Agents Chemother. 33, 881–885.
- Kamleh, A., Barrett, M.P., Wildridge, D., Burchmore, R.J., Scheltema, R.A. (2008). Metabolomic profiling using Orbitrap Fourier transform mass spectrometry with hydrophilic interaction chromatography: a method with wide applicability to analysis of biomolecules. Rapid Commun Mass Spectrom 22, 1912–1918.
- Keiser, J., Burri, C. (2000). Physico-chemical properties of the trypanocidal drug melarsoprol. Acta Trop. 74, 101–104.
- Kennedy, P.G. (2006). Diagnostic and neuropathogenesis issues in human African trypanosomiasis. Int. J. Parasitol. 36, 505-12.
- Kennedy, P.G.E. (2004). Human African trypanosomiasis of the CNS: current issues and challenges. J. Clin. Invest. 113, 496-504.
- Kiara, J.K., Njogu, R.M. (1989). Evidence for glycerol 3- phosphate:~lu~ose transphosphorylase activity in bloodstream *Trypanosoma brucei brucei*. Int. J. Biochem. 21, 839-845.
- Kido, Y., Sakamoto, K., Nakamura, K., Harada, M., Suzuki, T., Yabu, Y., Saimoto, H., Yamakura, F., Ohmori, D., Moore, A., Harada, S., Kita, K. (2010). Purification and kinetic characterization of recombinant alternative oxidase from *Trypanosoma brucei brucei*. Biochim. Biophys. Acta, Bioenerg. 1797, 443-450.
- Kido, Y., Shiba, T., Inaoka, D. K., Sakamoto, K., Nara, T., Aoki, T., Honma, T., Tanaka, A., Inoue, M., Matsuoka, S., Moore, A., Harada, S., Kita, K. (2010). Crystallization and preliminary crystallographic analysis of cyanide-insensitive alternative oxidase from *Trypanosoma brucei brucei*. Acta Crystallogr. Sect. F Struct. Biol. Cryst. Commun. 66, 275-278.
- Kolawole, O. T., Akanji, M. A., (2013). Inhibitory effect of leaf extract of *Newbouldia laevis* on the metabolic activities of α -glucosidase and α -amylase. Bangladesh J. Pharmacol. 8, 371-377.
- Kuzoe, F.A. (1993). Current situation of African trypanosomiasis. Acta Trop. 54, 153-162.

- La Greca, F., Magez, S. (2011). Vaccination against trypanosomiasis: can it be done or is the trypanosome truly the ultimate immune destroyer and escape artist? *Hum. Vaccin.* 7, 1225-1233.
- Lai, D.H., Hashimi, H., Lun, Z.R., Ayala, F.J., Lukes, J. (2008). Adaptations of *Trypanosoma brucei* to gradual loss of kinetoplast DNA: *Trypanosoma equiperdum* and *Trypanosoma evansi* are petite mutants of *T. brucei*. *Proc. Natl. Acad. Sci.* 105, 1999-2004.
- Lamour, N., Riviere, L., Coustou, V., Coombs G.H., Barrett, M.P., Bringaud, F. (2005). Proline metabolism in procyclic *Trypanosoma brucei* is down-regulated in the presence of glucose. *J. Biol. Chem.* 280, 11902-10.
- Lanteri, C.A., Tidwell, R.R., Meshnick, S.R. (2008). The mitochondrion is a site of trypanocidal action of the aromatic diamidine DB75 in bloodstream forms of *Trypanosoma brucei*. *Antimicrob. Agents Chemother.* 52, 875-882.
- Lanteri, C. A., Tidwell, R. R., Meshnick, S. R. (2008). The mitochondrion is a site of trypanocidal action of the aromatic diamidine DB75 in bloodstream forms of *Trypanosoma brucei*. *Antimicrob. Agents Chemother.* 52, 875-882
- Le Roch, K.G., Johnson, J.R., Ahiboh, H., Chung, D.W., Prudhomme, J., Plouffe, D., Henson, K., Zhou, Y., Witola, W., Yates, J.R., Mamoun, C.B., Winzeler, E.A., Vial, H. (2008). A systematic approach to understand the mechanism of action of the bisthiazolium compound T4 on the human malaria parasite, *Plasmodium falciparum*. *BMC Genomics.* 9, 513.
- Legros, D., Evans, S., Maiso, F., Enyaru, J.C.K., Mbulamberi, D. (1994). Risk factors for treatment failure after melarsoprol for *Trypanosoma brucei gambiense* trypanosomiasis in Uganda. *Trans. R. Soc. Trop. Med. Hyg.* 93, 439-442.
- Legros, D., Ollivier, G., Gastellu-Etchegorry, M., Paquet, C., Burri, C., Jannin, J., Buscher, P. (2002). Treatment of human African trypanosomiasis — present situation and needs for research and development. *Lancet Infect. Dis.* 2, 437-440.
- Lillico, S., Field, M.C., Blundell, P., Coombs, G.H., Mottram, J.C. (2003). Essential roles for GPI-anchored proteins in African trypanosomes revealed using mutants deficient in GPI8. *Mol. Biol. Cell.* 14, 1182-1194.
- Liu, B., Liu, Y., Motyka, S.A., Agbo, E.E., Englund, P.T. (2005). Fellowship of the rings: the replication of kinetoplast DNA. *Trends Parasitol.* 21, 363-369.
- Loiseau, P.M., Cojean, S., Schrevel, J. (2011). sitamaquine as a putative antileishmanial drug candidate: from the mechanism of action to the risk of drug resistance. *Parasite.* 18, 115-119.
- Long, T. E., Lu, X., Galizzi, M., Docampo, R., Gut, J., Rosenthal, P. J. (2012). Phosphonium lipocations as antiparasitic agents. *Bioorg. Med. Chem. Lett.* 22, 2976-2979.

- Lorenzen, K., Anke, T. (1996). Basidiomycetes as a source for new bioactive natural products. *Curr. Org. Chem.* 2, 329–364.
- Lu, H., Tonge, P.J. (2010). Drug-Target Residence Time: Critical Information for Lead Optimization. *Curr. Opin. Chem. Biol.* 14, 467–474.
- Lukeš, J., Hashimi, H., Zikova, A. (2005). Unexplained complexity of the mitochondrial genome and transcriptome in kinetoplastid flagellates. *Current genetics.* 48, 277-299.
- Luque-Ortega, J.R., Reuther, P., Rivas, L., Dardonville, C. (2010). New benzophenone-derived bisphosphonium salts as leishmanicidal leads targeting mitochondria through inhibition of respiratory complex II. *J. Med. Chem.* 53, 1788-1798.
- Madak, J.T., Neamati, N. (2015). Membrane Permeable Lipophilic Cations as Mitochondrial Directing Groups. *Curr. Topics Med. Chem.* 15, 745-766.
- Magona, J.W., Walubengo, J., Odimin, J.T. (2008). Acute haemorrhagic syndrome of bovine trypanosomosis in Uganda. *Acta Trop.* 107, 186-91.
- Mamani-Matsuda, M., Rambert, J., Malvy, D., Lejoly-Boisseau, H., Daulouede, S., Thiolat, D., Coves, S., Courtois, P., Vincendeau, P., Mossalayi, M.D. (2004). Quercetin induces apoptosis of *Trypanosoma brucei gambiense* and decreases the proinflammatory response of human macrophages. *Antimicrobial agents and chemotherapy.* 48, 924-929.
- Mansfield, J.M. (1994). T-cell responses to the trypanosome variant surface glycoprotein: a new paradigm? *Parasitol Today.* 10, 267-70.
- Maplestone, R.A., Stone, M.J., Williams, D.H. (1992). The evolutionary role of secondary metabolites - A review. *Gene.* 115, 151–157.
- Martinez, S., Gonzalez, M., Vernaza, M.E. (1997). Treatment of Cutaneous Leishmaniasis with Allopurinol and Stibogluconate. *Clinical Infectious Diseases.* 24, 165-169.
- Marty, P., Rosenthal, E. (2002). Treatment of visceral leishmaniasis: a review of current treatment practices. *Expert Opin Pharmacother.* 3, 1101-8.
- Maser, P., Luscher, A., Kaminsky, R. (2003). Drug transport and drug resistance in African trypanosomes. *Drug resistance updates.* 6, 281-290.
- Maser, P., Kaminsky, R. (1998). Identification of three ABC transporter genes in *Trypanosoma brucei* spp. *Parasitol. Res.* 84, 106–111.
- Matovu, E., Stewart, M., Geiser, F., Brun, R., Maser, P., Wallace, L., Buschmore, R., Enyaru, J., Barrett, M., Kaminsky, R., Seebeck, T., De Koning, H. (2003). Mechanism of arsenical and diamidines uptake and resistance in *Trypanosoma brucei*. *Eukaryotic Cell.* 2, 1003-1008.

- Matovu, E., Iten, M., Enyaru, J.C., Schmid, C., Lubega, G.W., Brun, R. Kaminsky, R. (1997). Susceptibility of Ugandan *Trypanosoma brucei rhodesiense* isolated from man and animal reservoirs to diminazene, isometamidium and melarsoprol. *Trop.Med.Int.Health.* 2, 13-18.
- Maya, J.D., Cassels, B.K., Iturriaga-Vásquez, P., Ferreira, J., Faúndez, M., Galanti, N., Ferreira, A., Morello, A. (2007). Mode of action of natural and synthetic drugs against *Trypanosoma cruzi* and their interaction with the mammalian host. *Comparative Biochemistry and Physiology Part A. Molecular & Integrative Physiology*, 146, 601-620.
- McKean, P.G. (2003). Coordination of cell cycle and cytokinesis in *Trypanosoma brucei*. *Curr. Opin. Microbiol.* 6, 600-607.
- Mejia, A.M., Hall, B.S., Taylor MC, Gómez-Palacio A, Wilkinson SR, Triana-Chávez O, Kelly JM. (2012). Benznidazole-resistance in *Trypanosoma cruzi* is a readily acquired trait that can arise independently in a single population. *J Infect Dis.* 206, 220-8.
- Menzies, S. K., Tulloch, L. B., Florence, G. J., Smith, T. K. (2016). The trypanosome alternative oxidase: a potential drug target? *Parasitology.* 1-9.
- Minagawa, N., Yabu, Y., Kita, K., Nagai, K., Ohta, N., Meguro, K., Sakajo, S., Yoshimoto, A. (1997). An antibiotic, ascofuranone, specifically inhibits respiration and in vitro growth of long slender bloodstream forms of *Trypanosoma brucei brucei*. *Mol. Biochem. Parasitol.* 84, 271-280.
- Misra, P., Sashidhara, K.V., Singh, S.P., Kumar, A., Gupta, R., Chaudhaery, S.S., Gupta, S.S., Majumder, H.K., Saxena, A.K., Dube, A. (2010). 16a-Hydroxycyclopropano-3,13 (14)Z-dien-15,16-olide from *Polyalthia longifolia*: a safe and orally active antileishmanial agent. *British Journal of Pharmacology.* 159, 1143–1150.
- Moyo, P., Botha, M.E., Nondaba, S., Niemand, J., Maharaj, V.J., Eloff, J.N., Louw, A.I., Birkholtz, L., 2016. *In vitro* inhibition of *Plasmodium falciparum* early and late stage gametocyte viability by extracts from eight traditionally used South African plant species. *J. Ethnopharmacol.* 185, 235–242.
- Munday, J. C., Eze, A. A., Baker, N., Glover, L., Clucas, C., Aguinaga Andrés, D., Natto, M. J., Teka, I. A., McDonald, J., Lee, R. S.; Graf, F. E., Ludin, P., Burchmore, R. J. S., Turner, C. M. R., Tait, A., MacLeod, A., Mäser, P., Barrett, M. P., Horn, D., De Koning, H. P. (2014). *Trypanosoma brucei* aquaglyceroporin 2 is a high-affinity transporter for pentamidine and melaminophenyl arsenic drugs and the main genetic determinant of resistance to these drugs. *J Antimicrob. Chemother.* 69, 651-663.
- Munday, J.C., Settimo, L., de Koning, H.P. (2015). Transport proteins determine drug sensitivity and resistance in a protozoan parasite, *Trypanosoma brucei*. *Front Pharmacol.* 6, 32.

- Muzitano, M. F., Tinoco, L. W., Guette, C., Kaiser, C. R., Rossi-Bergmann, B., Costa, S. S. (2006). The antileishmanial activity assessment of unusual flavonoids from *Kalanchoe pinnata*. *Phytochemistry*. 67, 2071-2077.
- Nakamura, K., Fujioka, S., Fukumoto, S., Inoue, N., Sakamoto, K., Hirata, H., Kido, Y., Yabu, Y., Suzuki, T., Watanabe, Y., Saimoto, H., Akiyama, H., Kita, K. (2010). Trypanosome alternative oxidase, a potential therapeutic target for sleeping sickness, is conserved among *Trypanosoma brucei* subspecies. *Parasitol. Int.* 59, 560-564.
- Ndao, D.M., Hickman, D.T., López-Deber, M.P., Davranche, A., Andrea Pfeifer, A., Muhs, A. (2014). Binding Affinity Measurement of Antibodies from Crude Hybridoma Samples by SPR. *Bio-protocol*. 4, e1276.
- Ndjakou Lenta, B., Vonthron-Sénécheau, C., Fongang Soh, R., Tantangmo, F., Ngouela, S., Kaiser, M., Tsamo, E., Anton, R., Weniger, B. (2007). *In vitro* antiprotozoal activities and cytotoxicity of some selected Cameroonian medicinal plants. *J. Ethnopharmacol.* 20, 8–12.
- Neupert, W., Herrmann, J.M. (2007). Translocation of proteins into mitochondria. *Annu. Rev. Biochem.* 76, 723–749.
- Newman, D.J., Cragg, G.M., Snader, K.M. (2003). Natural products as source of new drugs over the period 1981-2002. *J. Nat. Prod.* 66, 1022-1037.
- Newman, D.J., Cragg, G.M. (2007). Natural products as sources of new drugs over the last 25 years. *J. Nat. Prod.* 70, 461-77.
- Nihei, C., Fukai, Y., Kawai, K., Osanai, A., Yabu, Y., Suzuki, T., Ohta, N., Minagawa, N., Nagai, K., Kita, K. (2003). Purification of active recombinant trypanosome alternative oxidase. *FEBS Letters*. 538, 35 –40.
- Nihei, C., Fukai, Y., Kita, K. (2002). Trypanosome alternative oxidase as a target of chemotherapy. *Biochim. Biophys. Acta*. 1587, 234-239.
- Njiokoua, F., Simoa, G., Nkinina S.W., Laveissiere, C., Herder C. (2004). Infection rate of *Trypanosoma brucei s.l.*, *T. vivax*, *T. congolense* “forest type”, and *T. simiae* in small wild vertebrates in south Cameroon. *Acta Tropica* 92, 139–146.
- Nour, A.M., Khalid, S.A., Kaiser, M., Brun, R., Abdallah, W.E., Schmidt, T.J., (2009). The antiprotozoal activity of sixteen Asteraceae species native to Sudan and bioactivity-guided isolation of Xanthanolides from *Xanthium brasiliicum*. *Planta Med.* 75, 1363–1368.
- Nwodo, N.J., Ibezim, A., Ntie-Kang, F., Adikwu, M.U., Mbah, C.J. (2015). Anti-trypanosomal activity of Nigerian plants and their constituents. *Molecules*. 20, 7750-7771.
- Ohashi-Suzuki, M., Yabu, Y., Ohshima, S., Nakamura, K., Kido, Y., Sakamoto, K., Kita, K., Ohta, N., Suzuki, T. (2011). Differential kinetic activities of glycerol kinase among African trypanosome species: phylogenetic and therapeutic implications. *J. Vet. Med. Sci.* 73, 615-21.

- Olifiers, N., Jansen, A.M., Herrera, H.M., Bianchi R.C., D'Andrea P.S., Mourao G.M., Gompper M.E. (2015). Co-Infection and Wild Animal Health: Effects of Trypanosomatids and Gastrointestinal Parasites on Coatis of the Brazilian Pantanal. PLoS One. 14, e0143997.
- Omar, R.M.K., Igoli, J., Gray, A.I., Ebiloma, G.U, Clements, C., Fearnley, J., Ebel, R.A.E., Zhang, T., De Koning H.P., Watson D.G, 2015. Chemical characterisation of Nigerian red propolis and its biological activity against *Trypanosoma brucei*. Phytochem. Anal. 27, 107–115.
- Opperdoes F.R., Aarsen, P.N., van der Meer, C., Borst, P. (1976). *Trypanosoma brucei*: An evaluation of salicylhydroxamic acid as a trypanocidal drug. Experimental Parasitology. 40, 198 – 205.
- Opperdoes, F.R. (1985). Biochemical peculiarities of trypanosomes, African and South American. Br. Med. Bull. 41, 130–136.
- Opperdoes, F.R., Borst, P. (1977). Localization of nine glycolytic enzymes in a microbody-like organelle in *Trypanosoma brucei*: the glycosome. FEBS Lett. 80, 360–364.
- Ordóñez-Gutiérrez, L., Espada-Fernández, R., Dea-Ayuela, M.A., Torrado, J.J., Bola, S., Fernández, F., Alunda, J.M. (2007). *In vitro* effect of new formulations of amphotericin B on amastigote and promastigote forms of *Leishmania infantum*. Int. J. Antimicrob Agents. 30, 325–329.
- Oredsson, S., Anehus, S., Heby, O. (1980). Inhibition of cell proliferation by DL-a-difluoromethylornithine, a catalytic irreversible inhibitor of ornithine decarboxylase. Acta Chem. Scand. 34,457–458.
- Orsi, M., Essex, J.W. (2010). Passive permeation across lipid bilayers: a literature review, in: Sansom, M.S.P., Biggin, P.C. (Eds). Molecular simulations and biomembranes: from biophysics to function. Royal Society of Chemistry, Cambridge, pp. 76-90.
- Osorio, E., Arango, G.J., Jiménez, N., Alzate, F., Ruiz, G., Gutiérrez, D., Paco, M.A., Giménez, A., Robledo, S. (2007). Antiprotozoal and cytotoxic activities in vitro of Colombian Annonaceae. J. Ethnopharmacol. 22, 630–635.
- Ott, R., Chibale, K., Anderson, S., Chipeleme, A., Chaudhuri, M., Guerrah, A., Colowick, N., Hill, G.C. (2006). Novel inhibitors of the trypanosome alternative oxidase inhibit *Trypanosoma brucei* growth and respiration. Acta Trop. 100, 172-184.
- Pal, D., Bhattacharya, S., Baidya, P., Bijay, K.D., Pandey, J.N., Biswas, M. (2011). Antileishmanial activity of *Polyalthia longifolia* leaf extract on the *in vitro* growth of *Leishmania donovani* promastigote. Global J. Pharmacol. 5, 97-100.
- Pan, A.C., Borhani, D.W., Dror, R.O., Shaw, D.E. (2013). Molecular determinants of drug–receptor binding kinetics. Drug Discovery Today. 18, 667-672.

- Panigrahi, A.K., Zikova, A., Dalley, R.A., Acestor, N., Ogata, Y., Anupama, A., Myler, P.J., Stuart, K.D. (2008). Mitochondrial complexes in *Trypanosoma brucei*: a novel complex and a unique oxidoreductase complex. *Mol. Cell Proteomics*. 7, 534-45.
- Pattaraporn, B., Preecha, P., Chanpen, C. (2014). Antibacterial Activity of a Cardanol from Thai *Apis mellifera Propolis*. *Int. J. Med. Sci.* 11, 327-336.
- Peixoto, J.A., Silva, M.L.A., Crotti, A.E.M., Veneziani, R.C.S., Gimenez, V.M.M., Januário, A.H., Groppo, M., Magalhaes, L.G., Santos, F.F., Albuquerque, S., Silva-Filho, A.A., Cunha, W.R. (2011). Antileishmanial activity of the hydroalcoholic extract of *Miconia langsdorffii*, isolated compounds, and semi-synthetic derivatives. *Molecules*. 16, 1825-1833.
- Penketh, P.G., Klein, R.A. (1986). Hydrogen peroxide metabolism in *Trypanosoma brucei*. *Mol. Biochem. Parasitol.* 20, 111–121.
- Pepin, J., and Milord, F. (1994). The treatment of human African trypanosomiasis. *Adv. Parasitol.* 33, 1–47.
- Pepin, J., Milord, F., Guern, C., Schechter, P.J. (1987). Difluoromethylornithine for arseno-resistant *Trypanosoma brucei gambiense* sleeping sickness. *Lancet*. 2, 1431-3.
- Peregrine, A. S., Mamman, M. (1993). "Pharmacology of diminazene: A review". *Acta tropica*. 54, 3–4.
- Phadnis, A.P., Patwardhan, S.A., Dhaneshwar, N.N., Tavale, S.S., Guru Row, T. N. (1988). Clerodane diterpenoids from *Polyalthia longifolia*. *Phytochemistry* 27, 2899-2901.
- Phillips, M.A., Wang, C.C. (1987). A *Trypanosoma brucei* mutant resistant to alpha-difluoromethylornithine. *Mol. Biochem. Parasitol.* 22, 9–17.
- Picozzi, K., Carrington, M., Welburn, S.C. (2008). A multiplex PCR that discriminates between *Trypanosoma brucei brucei* and zoonotic *T. b. rhodesiense*. *Exp Parasitol.* 118, 41-6.
- Pieretti, S., Haanstra, J.R., Mazet, M., Perozzo, R., Bergamini, C., Prati, F., Fato, R., Lenaz, G., Capranico, G., Brun, R., Bakker, B.M., Michels, P.A.M., Scapozza, L., Bolognesi, M.L., Cavalli, A. (2012). Naphthoquinone Derivatives Exert Their Antitrypanosomal Activity via a Multi-Target Mechanism. *PLoS Negl. Trop. Dis.* 7, e2012.
- Pimenta, P.F., Pinto, P., Rangarajan, D., Smith, D.F., Sacks, D.L. (1994). Leishmania major: association of the differentially expressed gene B protein and the surface lipophosphoglycan as revealed by membrane capping. *Exp. Parasitol.* 79, 468-79.
- Pinchbeck, G.L., Morrison, L.J., Tait, A., Langford, J., Meehan, L., Jallow, S., Jallow, J., Jallow, A., Christley, R.M. (2008). Trypanosomiasis in The Gambia: prevalence in working horses and donkeys detected by whole genome amplification and PCR, and evidence for interactions between trypanosome species. *BMC Vet. Res.* 20, 4-7.

- Pospichal, H., Brun, R., Kaminsky, R., Jenni, L. (1994). Induction of resistance to melarsenoxide cysteamine (Mel Cy) in *Trypanosoma brucei brucei*. *Acta Trop.* 58, 187–197.
- Purvis, W. (2000). Lichens; Natural History Museum, London/Smithsonian Institution: Washington D.C., USA, p. 112.
- Raper, J., Portela, M.P., Lugli, E., Frevert, U., Tomlinson, S. (2001). Trypanosome lytic factors: novel mediators of human innate immunity. *Curr. Opin. Microbiol.* 4, 402-8.
- Rios Martinez, C.H., Nue Martinez, J.J., Ebiloma, G.U., de Koning, H. P., Alkorta, I., Dardonville, C. (2015). Lowering the pKa of a bisimidazoline lead with halogen atoms results in improved activity and selectivity against *Trypanosoma brucei* in vitro. *Eur. J. Med. Chem.* 101, 806-817.
- Rodenko, B., Wanner, M.J., Alkhaldi, A.A.M., Ebiloma, G.U., Barnes, R.L., Kaiser, M., Brun, R., McCulloch, R., Koomen, G., de Koning, H.P. (2015). Targeting the parasite's DNA with methyltriazenyl purine analogs is a safe, selective, and efficacious antitrypanosomal strategy. *Antimicrob. Agents Chemother.* 59, 6708 –6716.
- Rodenko, B., de Koning, H. P., Jäger, T., Koch, O., Flohé, L. (2013). Rational selection of antimicrobial drug targets: unique or conserved? Trypanosomatid diseases: molecular routes to drug discovery, 279-296.
- Ross, M. F., Da Ros, T., Blaikie, F. H., Prime, T. A., Porteous, C. M., Severina, I. I., Skulachev, V. P., Kjaergaard, H. G., Smith, R. A. J., Murphy, M. P. (2006). Accumulation of lipophilic dications by mitochondria and cells. *Biochem. J.* 400, 199-208.
- Saimoto, H., Kido, Y., Haga, Y., Sakamoto, K., Kita, K. (2013). Pharmacophore identification of ascofuranone, potent inhibitor of cyanide-insensitive alternative oxidase of *Trypanosoma brucei*. *J. Biochem.* 153, 267–273.
- Sakajo, S., Minagawa, N., Yoshimoto, A. (1993). Characterization of the alternative oxidase protein in the yeast *Hansenula anomala*. *FEBS Lett.* 318, 310–312.
- Salcedo, M., Cuevas, C., Otero, G., Sanchez-Puelles, J.M., Fernandez-Sousa, J.M., Avila, J., Salem, M.M., Werbovetz, K.A. (2006). Natural products from plants as drug candidates and lead compounds against leishmaniasis and trypanosomiasis. *Curr. Med. Chem.* 13, 2571-2598.
- Salih, N.A., van Griensven, J., Chappuis, F., Antierens, A., Mumina, A., Hammam, O., Boulle, P., Alirol, E., Alnour, M., Elhag, M.S., Manzi, M., Kizito, W., Zachariah, R. (2014). Liposomal amphotericin B for complicated visceral leishmaniasis (kala-azar) in eastern Sudan: how effective is treatment for this neglected disease? *Trop. Med. Int. Health.* 19, 146-52.
- Salim, B., Bakheit, M.A., Kamau, J., Nakamura, I., Sugimoto, C. (2011). Molecular epidemiology of camel trypanosomiasis based on ITS1 rDNA and RoTat 1.2 VSG gene in the Sudan. *Parasites & Vectors.* 4, 31.

- Sarker, S.D., Latif, Z., Gray, A.I. (2006). Methods in Biotechnology: Natural Product Isolation. Satyajit D., Ed.; Human Press Inc: Totowa, NJ, USA. p. 528.
- Schmidt, T.J., Khalid, S.A., Romanha, A.J., Alves, T.M.A., Biavatti, M.W., Brun, R., Da Costa, F.B., de Castro, S.L., Ferreira, V.F., de Lacerda, M.V.G., Lago, J.H.G., Leon, L.L., Lopes, N.P., das Neves Amorim, R.C., Niehues, M., Ogungbe, I.V., Pohlit, A.M., Scotti, M.T., Setzer, W.N., Soeiro, M.D.C., Steindel, M., Tempone, A.G. (2012). The potential of secondary metabolites from plants as drugs or leads against protozoan neglected diseases – Part I. Current Medicinal Chemistry. 19, 2128-2175.
- Schnauffer, A., Clark-Walker G.D., Steinberg, A.G., Stuart, K. (2005). The F₁-ATP synthase complex in bloodstream stage trypanosomes has an unusual and essential function. EMBO J. 24, 4029–4040.
- Schnauffer, A., Domingos, G.J., Stuart, K. (2002). Natural and induced dyskinetoplastic trypanosomatids: how to live without mitochondrial DNA. International Journal for Parasitology 32, 1071–1084.
- Schneider A., Bursac, D., Lithgow, T. (2007). The direct route: a simplified pathway for protein import into the mitochondrion of trypanosomes. Trends Cell Biol. 18, 12-18.
- Schneider, A. (2001). Unique aspects of mitochondrial biogenesis in trypanosomatids. Int. J. Parasitol. 31, 1403-15.
- Schneider, A., Bouzaidi-tiali, N., Chanez, A. I., Bulliard, I. (2007). ATP production in isolated mitochondria of procyclic *Trypanosoma brucei*. Methods Mol. Biol. 372, 379-87.
- Schuck, P. (1997). Use of surface plasmon resonance to probe the equilibrium and dynamic aspects of interactions between biological macromolecules. Annu. Rev. Biophys. Struct. 26, 541–566.
- Sekoni, V.O. (1994). Reproductive disorders caused by animal trypanosomiasis: a review. Theriogenology. 42, 557-70.
- Shakur, Y., De Koning, H.P., Ke, H., Kambayashi, J., Seebeck, T. (2011). Therapeutic potential of PDE inhibitors in parasitic diseases. Handb. Exp. Pharmacol. 204, 487-510.
- Shakya, N., Bajpai, P., Gupta, S. (2011). Therapeutic switching in leishmania chemotherapy: a distinct approach towards unsatisfied treatment needs. J. Parasit. Dis. 35, 104–112.
- Shapiro, T.A., Englund, P.T. (1995). The structure and replication of kinetoplast DNA. Annu. Rev. Microbiol. 49, 117–143.
- Sherma, J., Fried, F. (2006). Handbook of Thin Layer Chromatography. 2nd Edition. New York.
- Shiba H., Kidoa, Y., Sakamotoa, K., Inaokaa, D.K., Tsugea, C., Tatsumia, R., Takahashib, G., Baloguna, E.O., Narad, T., Aokid, T., Honmae, T., Tanakae, A., Inouef, M., Matsuokaf, S.,

- Saimotog, H., Mooreh, A.L., Harada, S., Kita, A. (2013). Structure of the trypanosome cyanide-insensitive alternative oxidase. *PNAS*. 110, 4580–4585.
- Shiba, T., Kido, Y., Sakamoto, K., Inaoka, D. K., Balogun, E. O., Nara, T., Aoki, T., Honma, T., Tanaka, A., Inoue, M., Matsuoka, S., Saimoto, H., Harada, S., Kita, K., Moore, A. L. (2012). Crystal structure of the alternative oxidases: New insights into the catalytic cycle. *Biochim. Biophys. Acta (BBA) – Bioenergetics*. 1817, Supplement, S102-S103.
- Siheri, W., Zhang, T., Ebiloma, G.U., Biddau, M., Woods, N., Hussain, M.Y., Clements, C.J., Fearnley, J., Ebel, R.E., Paget, T., Muller, S., Carter, K.C., Ferro, V.A., De Koning, H.P., Watson, D.G. (2016). Chemical and biological profiling of propolis from different regions within Libya. *PloS One*. 11, e0155355.
- Simarro, P.P., Cecchi, G., Franco, J.R., Paone, M., Diarra, A., Priotto, G., Mattioli, R.C Jannin, J.G. (2015). Monitoring the Progress towards the Elimination of Gambiense Human African Trypanosomiasis. *PLoS Negl Trop Dis*. 9, e0003785.
- Simarro, P.P., Cecchi, G., Paone, M. (2009). Towards the Atlas of human African trypanosomiasis. *Int. J. Health Geogr*. 8, 15.
- Simarro, P.P., Franco, J., Diarra, A., Postigo, J.A., Jannin, J. (2012). Update on field use of the available drugs for the chemotherapy of human African trypanosomiasis. *Parasitology*. 139, 842-846.
- Simpson, L., Sbicego, S., Aphasizhev, R. (2003). Uridine insertion/deletion RNA editing in trypanosome mitochondria: A complex business. *RNA*. 9, 265–276.
- Sindermann, H., Engel, J. (2006). Development of miltefosine as an oral treatment for leishmaniasis. *Trans. R. Soc. Trop. Med. Hyg*. 100, 17–20.
- Singh, O.P., Hasker, E., Sacks D., Boelaert, M., Sundar, S. (2014). Asymptomatic *Leishmania* Infection: A New Challenge for *Leishmania* Control. *Clin. Infect. Dis*. 15, 1424–1429.
- Singh, N., Kumar, R., Gupta, S., Dube, A., Lakshmi, V. (2008). Antileishmanial activity *in vitro* and *in vivo* of constituents of sea cucumber *Actinopyga lecanora*. *Parasitol. Res*. 103, 351-354.
- Sleigh, M.J. (1976). The mechanism of DNA breakage by phleomycin *in vitro*. *Nucleic Acids Res*. 3, 891-901.
- Smith, R.A. J., Adlam, V. J., Blaikie, F.H., Manas, A.R.B., Porteous, C.M., James, A.M., Ross, M. F., Logan, A., Cochem, H.M., Trnka, J., Prime, T.A., Abakumova, I., Jones, B.A., Filipovska, A., Murphy, M.P. (2008). Mitochondria-targeted antioxidants in the treatment of disease. *Ann. N. Y. Acad. Sci*. 1147, 105-111.
- Smith, R.A.J., Hartley, R.C., Murphy, M.P. (2011). Mitochondria-targeted small molecule therapeutics and probes. *Antioxidants & Redox Signaling*. 15, 3021-3038.

- Smith, R.A.J., Porteous, C.M., Gane, A. M., Murphy, M.P. (2003). Delivery of bioactive molecules to mitochondria *in vivo*. Proc. Nat. Acad. Sci. 100, 5407-5412.
- Soeiro, M.N., de Castro, S.L., de Souza, E.M., Batista, D.G., Silva, C.F., Boykin, D.W. (2008). Diamidine activity against trypanosomes: the state of the art. Curr. Mol. Pharmacol. 1, 151–161.
- Sokesi, T., Songolo, P., Masaninga, F., Babaniyi, O. (2016). Human African Trypanosomiasis: Challenges in the Diagnosis of Trypanosoma Brucei Rhodesiense – Case Report. Epidemiology (Sunnyvale). 6, 258.
- Sternberg, J.M. (2004). Human African trypanosomiasis: clinical presentation and immune response. Parasite Immunol. 26, 469-76.
- Stevenson, P., Sones, K.R., Gicheru, M.M., Mwangi, E.K. (1995). Comparison of isometamidium chloride and homidium bromide as prophylactic drugs for trypanosomiasis in cattle at Nguruman, Kenya. Acta Trop. 59, 257–258.
- Steverding, D. (2010). The development of drugs for treatment of sleeping sickness: a historical review. Parasit Vectors. 3, 15.
- Stewart, M.L., Krishna, S., Burchmore, R.J.S., Brun, R., De Koning, H.P., Boykin, D.W., Tidwell, R.R., Hall, J.E., Barrett, M.P. (2005). Detection of arsenical drug resistance in *Trypanosoma brucei* using a simple fluorescence test. Lancet. 366, 486-487
- Stuart, K., Brun, R., Croft, S. (2008). Kinetoplastids: related protozoan pathogens, different diseases. J. Clin. Invest. 118, 1301-10.
- Sundar, S., Rai, M., Chakravarty, J., Agarwal, D., Agrawal, N., Vaillant, M., Oliaro, P., Murray, H.W. (2008). New treatment approach in Indian visceral leishmaniasis: single-dose liposomal amphotericin B followed by short-course oral miltefosine. Clin Infect Dis. 47, 1000-1006.
- Sutherland, I.A., Peregrine, A.S., Lonsdale-Eccles, J.D., Holmes, P.H. (1991). Reduced accumulation of isometamidium by drug-resistant *Trypanosoma congolense*. Parasitology. 103, 245–251.
- Takahashi, M., Fuchino, H., Sekita, S., Satake, M. (2004). *In vitro* leishmanicidal activity of some scarce natural products. Phytother. Res. 18, 573-578.
- Takahashi, T., Kokubo, R., Sakaino, M., (2004). Antimicrobial activities of eucalyptus leaf extracts and flavonoids from *Eucalyptus maculata*. Lett. Appl. Microbiol. 39, 60-4.
- Taladriz, A., Healy, A., Flores Pérez, E. J., Herrero García, V., Ríos Martínez, C., Alkhaldi, A. A. M., Eze, A.A., Kaiser, M., De Koning, H.P., Chana, A., Dardonville, C. (2012). Synthesis and structure-activity analysis of new phosphonium salts with potent activity against African trypanosomes. J. Med. Chem. 55, 2606-2622.

- Tan, R.X., and Zou, W.X. (2001). Endophytes: A rich source of functional metabolites (1987 to 2000). *Nat. Prod. Rep.* 18, 448–459.
- Teka I., Kazibwe A., El-Sabbagh N., Al-Salabi M., Ward C., Eze A., Munday J., Maser P., Matovu E., Barrett M., de Koning H. (2011). The Diamidine Diminazene Aceturate is a substrate for the highaffinity pertamidine transporter: Implications for the development of high resistance levels in trypanosomes. *Molecular Pharmacology*. 80, 110- 116.
- Thumbi, S.M., Bronsvoort, B.M., Poole, E.J., Kiara, H., Toye, P.G. (2014) Parasite co-infections and their impact on survival of indigenous cattle. *PLoS ONE*. 9, e76324.
- Tielens, A.G.M., Van Hellemond J.J. (1998). Differences in energy metabolism between Trypanosomatidae. *Parasitol. Today*. 14, 265-271.
- Truc, P., Lejon, V., Magnus, E., Jamonneau, V., Nangouma, A., Verloo, D., Penchenier, L., Büscher P. (2002). Evaluation of the micro-CATT, CATT/*Trypanosoma brucei gambiense*, and LATEX/T. *b. gambiense* methods for serodiagnosis and surveillance of human African trypanosomiasis in West and Central Africa. *Bull. World Health Organ*. 80, 882–886.
- Tu, Y. (2011). The discovery of artemisinin (qinghaosu) and gifts from Chinese medicine. *Nat. Med.* 17, 1217–1220.
- Usman, H., Osuji, J.C. (2007). Phytochemical and in vitro antimicrobial assay of the leaf extract of *Newbouldia laevis*. *Afr. J. Tradit. Complement. Altern. Med.* 4, 476 – 480.
- Usta, J., Kreydiyyeh, S., Knio, K., Barnabe, P., Bou-Moughlabay, Y., Dagher, S. (2009). Linalool decreases HepG2 viability by inhibiting mitochondrial complexes I and II, increasing reactive oxygen species and decreasing ATP and GSH levels. *Biol. Interact.* 180, 39-46.
- Van hellemond, J. J., Opperdoes, F. R., Tielens, A. G. (2005). The extraordinary mitochondrion and unusual citric acid cycle in *Trypanosoma brucei*. *Biochem. Soc. Trans.* 33, 967-71.
- Vercesi, A.E., Moreno, S.N., Docampo, R. (1994). $\text{Ca}^{2+}/\text{H}^{+}$ exchange in acidic vacuoles of *Trypanosoma brucei*. *Biochem. J.* 304 (Pt 1), 227– 233.
- Verlinde, C.L.M., Hannaert, V., Blonski, C., Willson, M., Perie, J.J. (2001). Glycolysis as a target for the design of new anti-trypanosome drugs. *Drug Resistance Updates* 4, 50–65.
- Verner, Z., Basu, S., Benz, C., Dixit, S., Dobakova, E., Faktorova, D., Hashimi, H., Horakova, E., Huang, Z., Paris, Z., Pena-Diaz, P., Ridlon, L., Tyc, J., Wildridge, D., Zikova, A., Lukes, J. (2016). Malleable mitochondrion of *Trypanosoma brucei*. *Int. Rev. Cell Mol. Biol.* 315, 73-151.
- Vincent, I.M., Creek, D., Watson., D.G., Kamleh, M.A., Woods, D.J., Wong, P.E., Burchmore, R.J. Barrett, M.P. (2010). A molecular mechanism for eflornithine resistance in African trypanosomes. *PLoS Pathog*, 6, e1001204.

- Vincent, I.M., Creek, D.J., Burgess, K., Woods, D.J., Burchmore, R.J.S., Barrett, M.P. (2012) Untargeted metabolomics reveals a lack of synergy between Nifurtimox and Eflornithine against *Trypanosoma brucei*. PLoS Negl Trop Dis .6, e1618.
- Wandosell, F. (2003). The marine antitumor compound ES 285 activates EGD receptors. Clin. Cancer Res. 9, 24.
- Wang, S.Y., Tseng, C.P., Tsai, K.C., Lin, C.F., Wen, C.Y., Tsay, H.S., Sakamoto, N., Tseng, C.H., Cheng, J.C., 2009. Bioactivity-guided screening identifies pheophytin a as a potent anti-hepatitis C virus compound from *Lonicera hypoglauca* Miq. Biochem. Biophys. Res. Commun. 385, 230–235.
- Ward, C.P., Wong, P.E., Burchmore, R.J., De Koning, H.P., Barrett, M.P. (2011). Trypanocidal furamidine analogues: influence of pyridine nitrogens on trypanocidal activity, transport kinetics and resistance patterns. Antimicrob Agents Chemother. 55, 2352-2361.
- Wells, T.N., 2011. Natural products as starting points for future anti-malarial therapies: going back to our roots. Malar. J. 10 (Suppl. 1), S3.
- WHO 2016. <http://www.who.int/mediacentre/factsheets/fs259/en/>
- Wilkes, J.M., Mulugeta, W., Wells, C., Peregrine, A.S. (1997). Modulation of mitochondrial electrical potential: a candidate mechanism for drug resistance in African trypanosomes. Biochem J. 326, 755-761.
- Wilkinson, S.R., Taylor, M.C., Horn, D, Kelly, J.M., Cheeseman, I. (2008). A mechanism for cross-resistance to nifurtimox and benznidazole in trypanosomes. Proc Natl Acad Sci USA. 105, 5022-7.
- Willcox, M. (2011). Improved traditional phytomedicines in current use for the clinical treatment of malaria. Planta Med. 77, 662–671.
- Williams, B.I. (1996). African trypanosomiasis. In The Wellcome Trust illustrated history of tropical diseases. F.E.A.G. Cox, editor. The Wellcome Trust. London, United Kingdom. 178-191.
- Williams, S., Saha, L., Singha, U.K., Chaudhuri, M. (2008). *Trypanosoma brucei*: differential requirement of membrane potential for import of proteins into mitochondria in two developmental stages. Exp. Parasitol. 118, 420–433.
- Wink, M. (2007). Molecular modes of action of cytotoxic alkaloids- From DNA intercalation, spindle poisoning, topoisomerase inhibition to apoptosis and multiple drug resistance. Alkaloids. 64, 1–48.
- Wink, M., (2008). Evolutionary advantage and molecular modes of action of multi-component mixtures used in phytomedicine. Curr. Drug Metab. 9, 996–1009.

- Wink, M. (2012). Medicinal plants: a source of anti-parasitic secondary metabolites. *Molecules*. 17, 12771-12791.
- Wu, T.H., Cheng, Y.Y., Chen, C.J., Ng, L.T., Chou, L.C., Huang, L.J., Chen, Y.H., Kuo, S.C., El-Shazly, M., Wu, Y.C., Chang, F.R., Liaw, C.C., (2014). Three new clerodane diterpenes from *Polyalthia longifolia* var. *pendula*. *Molecules* 19, 2049-2060.
- Xiao, Y., McCloskey, D.E, Phillips, M.A. (2009). RNA interference-mediated silencing of ornithine decarboxylase and spermidine synthase genes in *Trypanosoma brucei* provides insight into regulation of polyamine biosynthesis. *Eukaryot Cell*. 8, 747-755.
- Yabu, Y., Minagawa, N., Kita, K., Nagai, K., Honma, M., Sakajo, S., Koide, T., Ohta, N. (1998). Oral and intraperitoneal treatment of *Trypanosoma brucei brucei* with a combination of ascofuranone and glycerol in mice. *Parasitol. Int.* 47,131-137.
- Yabu, Y., Suzuki, T., Nihei, C., Minagawa, N., Hosokawa, T., Nagai, K., Kita, K., Ohta, N. (2006). Chemotherapeutic efficacy of ascofuranone in *Trypanosoma vivax*-infected mice without glycerol. *Parasitol. Int.* 55, 39-43.
- Yabu, Y., Yoshida, A., Suzuki, T., Nihei, C., Kawai, K., Minagawa, N., Hosokawa, T., Nagai, K., Kita, K., Ohta, N. (2003). The efficacy of ascofuranone in a consecutive treatment on *Trypanosoma brucei brucei* in mice. *Parasitol Int.* 52, 155-64.
- Yang, G., Zhu, W., Kim, K., Byun, S.Y., Choi, G., Wang, K., Cha, J.S., Cho, H.S., Oldfield, E., No, J.H. (2015). *In vitro* and *in vivo* investigation of the inhibition of *Trypanosoma brucei* cell growth by lipophilic bisphosphonates. *Antimicrob Agents Chemother* 59, 7530 –7539.
- Yaro, M., Munyard, K.A., Stear, M.J, Groth, D.M. (2016). Combatting African Animal Trypanosomiasis (AAT) in livestock: The potential role of trypanotolerance. *Vet. Parasitol.* 225, 43-52.
- Yesilova, Y., Surucu, H.A., Ardic, N., Aksoy, M., Yesilova, A., Oghumu, S., Satoskar, A.R. (2016). Meglumine antimoniate is more effective than sodium stibogluconate in the treatment of cutaneous leishmaniasis. *J. Dermatolog. Treat.* 27, 83-7.
- Yi, Z.B., Yan, Y., Liang, Y.Z., Bao, Z. (2007). Evaluation of the antimicrobial mode of berberine by LC/ESI-MS combined with principal component analysis. *J. Pharm. Biomed. Anal.* 44, 301-304.
- Young, L., Shiba, T., Harada, S., Kita, K., Albury, M. S., Moore, A. L. (2013). The alternative oxidases: Simple oxidoreductase proteins with complex functions. *Biochem. Soc. Trans.* 41, 1305-1311.
- Yun, O., Priotto, G., Tong, J., Flevaud, L., Chappuis, F. (2010). NECT is next: implementing the new drug combination therapy for *Trypanosoma brucei gambiense* sleeping sickness. *PLoS Negl. Trop. Dis.* 4, e720.

- Zjawiony, J.K. (2004). Biologically active compounds from aphylllophorales (Polypore) fungi. *J. Nat. Prod.* 67, 300–310.
- Zoltner, M., Horn, D., De Koning, H.P., Field, M.C. (2016). Exploiting the Achilles' heel of membrane trafficking in trypanosomes. *Curr Opin Microbiol.* 34, 97-103.